UNIVERSITY OF SOUTHAMPTON

FACULTY OF MATHEMATICAL STUDIES

MATHEMATICAL MODELS FOR FRICTION WELDING

by

Andrew Francis

This thesis is submitted for the degree of
Doctor of Philosophy at the University of Southampton
June, 1983

UNIVERSITY OF SOUTHAMPTON

ABSTRACT

FACULTY OF MATHEMATICAL STUDIES

Doctor of Philosophy

MATHEMATICAL MODELS FOR FRICTION WELDING

by Andrew Francis

Extensive experimental investigations have been made into friction welding but very few relevant mathematical models have been produced. In this thesis several possible models are developed which describe the various phases of the frictioning stage.

Attention has been focussed, in particular, on the modelling of the softened layer of material which develops close to the weld interface. Solutions have been derived for the thickness of this layer, the reacted torque and the temperature distributions for the cases where the layer is modelled by either a viscous fluid or a Bingham substance. The solutions have largely been obtained using the heat balance integral method and their accuracy has been assessed with the aid of various asymptotic solutions.

Although this work has mainly been concerned with phase II of the frictioning stage, the equilibrium and deceleration phases have been examined.

The more specialised friction welding processes of orbital and inertial welding have also been considered.

An interesting feature of a friction weld is the upset collar which is formed by material expelled from the softened zone and a model to describe the shape of this extruded material has tentatively been put forward.

ACKNOWLEDGEMENTS

I would like to thank my supervisors Dr. R.E. Craine and Dr. J.G. Andrews for their help and direction in producing this thesis.

I am also indebted to Dr. A.P. Bennett for his help in establishing some of the physics involved and for his encouragement in times of despair.

I also give my thanks to Mrs. Hazel Paul and Miss Debbie Clark for their time and effort spent typing this text.

CONTENTS

CHAPTER 4 (continued)

CHAPTER 6 (continued)

CHAPTER 1

INTRODUCTION

1.1 The Origins of Friction Welding

The idea of welding using frictional heat as the heat source was first patented here in Britain during the early 1940's. After that time it received little attention in this country but it was reported that thermoplastics were being friction welded in Germany during World War II. In 1956 fresh interest was aroused by A.I. Chudikov who again suggested the use of friction as a heat source for welding metals and this led to an extensive study of friction welding in the U.S.S.R. under V.I. Vill [1]. It is believed that work also commenced at about the same time in the U.S.A. leading to the inertia technique of friction welding which was developed by the Caterpillar Tractor Company [2] in 1962. Friction welding was reintroduced in Britain in 1960 when the Welding Institute, formerly the B.W.R.A., constructed its first friction-welding machine based on Russian published data [3].

Friction welding is now exploited throughout the world as a reliable and efficient automated welding process.

1.2 Friction Welding Techniques

Although there are now several different friction welding techniques, the basic process remains the same. In the friction welding process the two components to be joined are forced to rub against each other thereby generating heat at the rubbing interface. Subsequently, the material on either side of the weld interface softens and a shortening

of the components takes place in the direction of the applied load. The rubbing is then terminated and the two components are forged together to form a weld [4]. Under normal conditions no melting at the interface occurs and the joint is produced by solid phase bonding [4,5,6].

There are four main methods of friction welding, namely, conventional or continuous drive friction welding [3,4,7], inertia-welding [2,8], orbital welding [9,10] and radial welding [11]. Certain aspects of the continuous drive process are examined extensively in this thesis but the other techniques are only briefly considered. A short description of the four main techniques is given below.

1.2.1 Continuous Drive Friction Welding

The continuous drive friction welding method is used for joining two components, at least one of which must be circular. In this case, the necessarily circular component is held in the headstock (or rotating) chuck of the friction welding machine whilst the other is held in the tailstock (or stationary chuck), both chucks being in axial alignment [7]. The basic principles of the technique are illustrated schematically in Figure 1.1. The headstock chuck is rotated at a given angular speed while the tailstock one is held stationary Figure 1.1(a). The tailstock chuck is then driven towards the headstock chuck by a hydraulic ram until the two specimens make contact. The load is maintained so the two components rub against each other at the interface [Figure 1.1(b)]. The heat generated by this rubbing causes the material on either side of the interface to soften and this softened material then begins to flow radially outwards forming an'upset collar' [Figure 1.1(c)]. The rubbing of the interface is continued until a

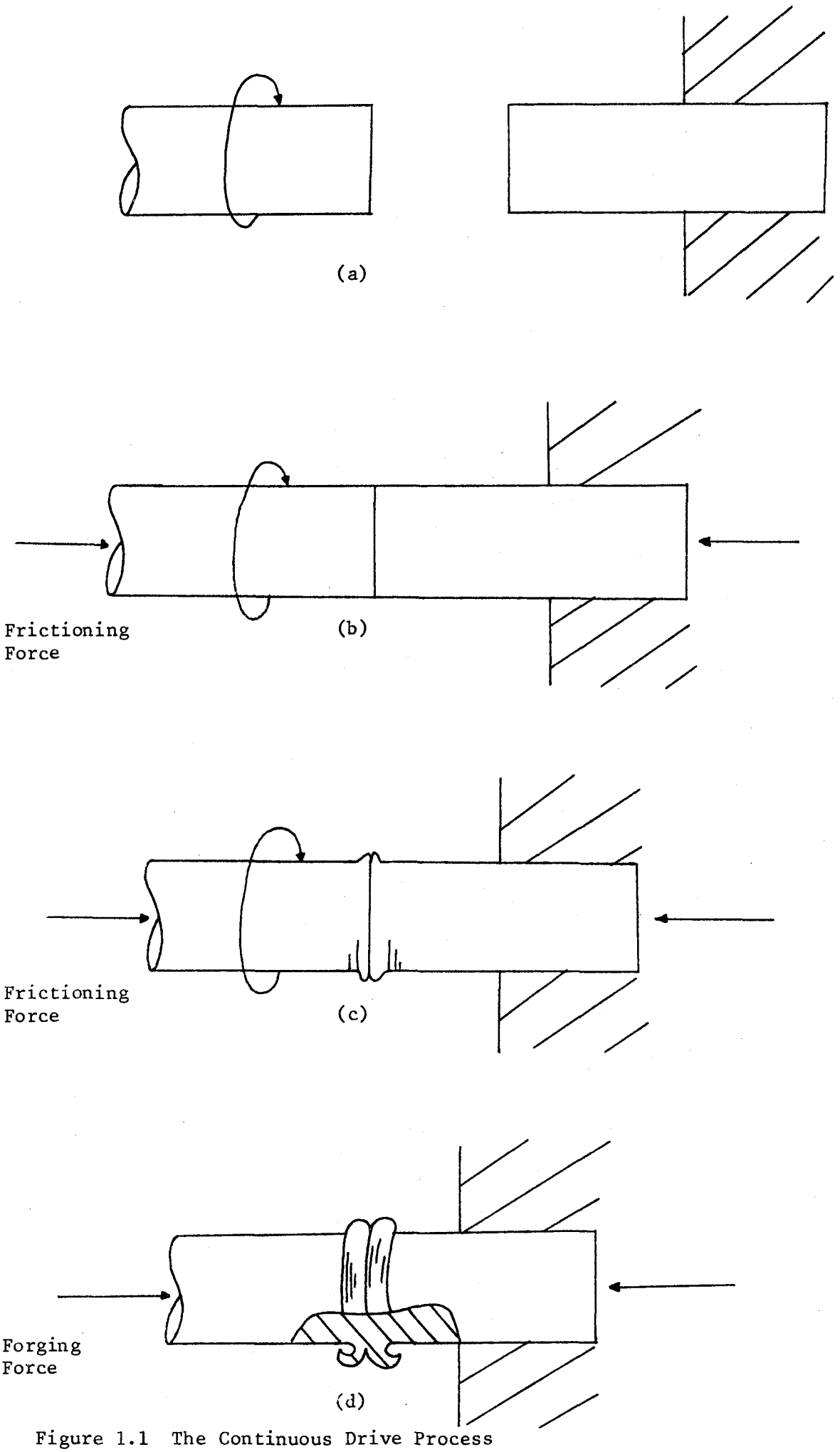

Figure 1.1 The Continuous Drive Process

prescribed amount of axial shortening (also called burnoff or upset) of the specimens has taken place or a certain time (weld time) has elapsed; the rotating component is then brought rapidly to rest. The axial force is maintained at the same value, or even increased, (forging pressure) for a short period of time afterthe rotation has stopped [Figure 1.1(d)]. In this forging stage the metal cools and the weld is consolidated.

When welding solid bars, the upset collar shown in section in Figure 1.1(d), produces no problem since it can be easily machined away. However, for the case of hollow tubes, a second collar is formed internally. This is a considerable nuisance if the tubes are long since it cannot be machined away and thus obstructs the tube. Thus this method of friction welding is not desirable for welding tubes which must carry oil, gas etc.

The main control variables in the continuous drive process are the rubbing speed, the applied load (which in turn controls the rate of upset) and the weld time or amount of axial shortening. These parameters control both the amount of heat that is put into the weld and the rate at which heat is generated, the latter being also depedent on time.

Figure 1.2 shows ideal ised traces of the variations with time of the speed of rotation, torque, applied load and axial shortening during a typical weld cycle using the continuous drive technique. It is convenient to divide the weld cycle into two stages: the frictioning stage (rotation continuing) and the forging state (rotation stopped) as shown in Figure 1.2. The frictioning stage can be divided further into the following four phases [3,4,7]:

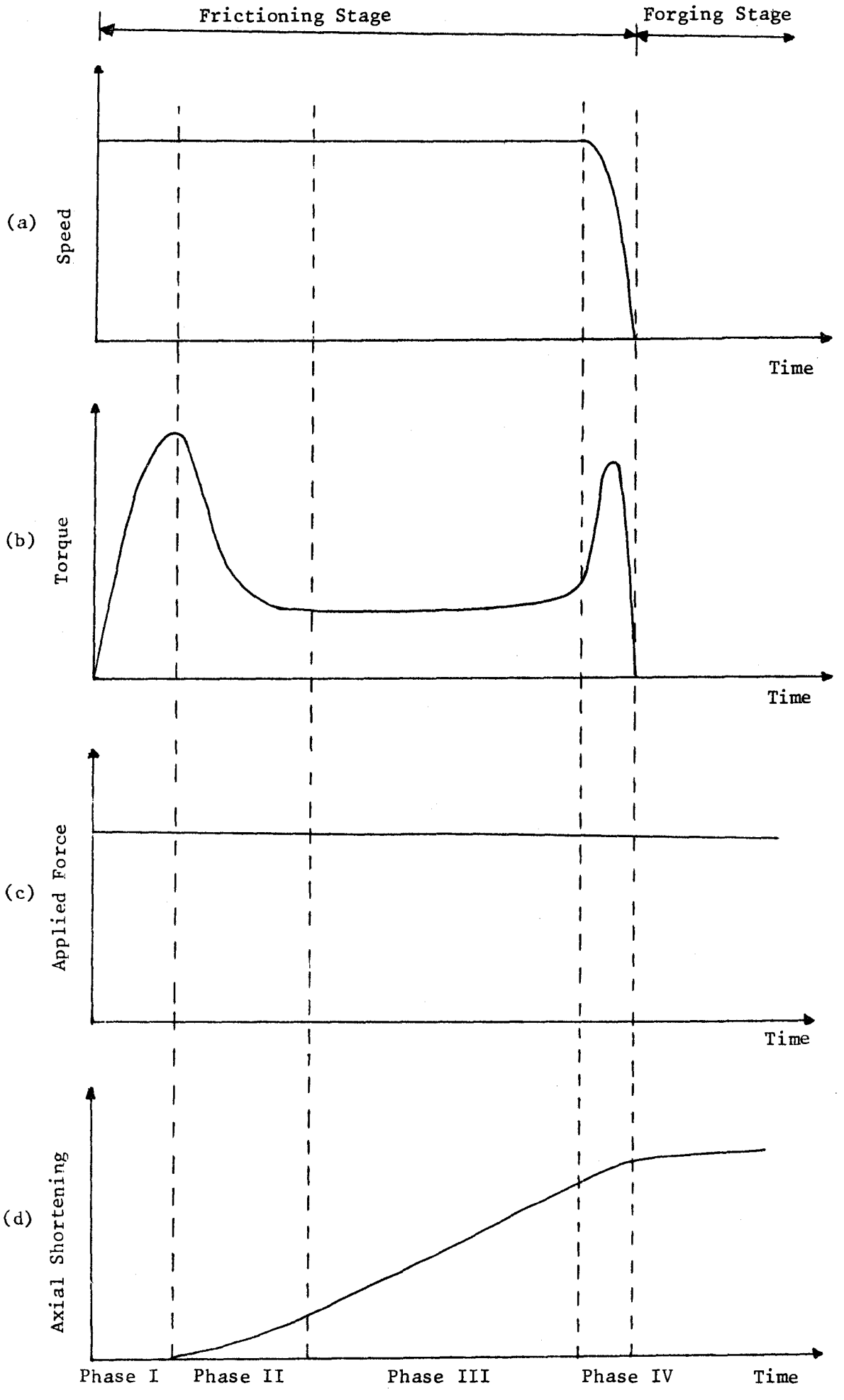

Figure 1.2 Idealised Traces of (a) Speed, (b) Torque, (c) Applied Force and (d) Axial Shortening for the Continuous Process.

Phase I.

This phase (sometimes called the conditioning phase) starts when the two components come into contact and rub against each other. As seen in Figure 1.2 the torque rises rapidly to a peak called the initial peak torque. During this initial transient phase the interface temperature rises to about 700°C , when welding mild steel, but no axial shortening takes place. The reaching of the initial peak torque marks the end of phase I.

Phase II.

This phase begins when the torque starts to fall from its initial peak and ends when equilibrium conditions have been reached. Again this is a transient phase in which the interface rises to a value close to the melting temperature, but does not actually attain it. The increase in temperature causes the material close to the interface to soften and axial shortening takes place. Subsequently there is a radial flow of material and the upset collar begins to form.

Phase III.

This is the equilibrium phase, during which the torque, temperature distribution and rate of axial shortening remain virtually constant. Under normal conditions most of the axial shortening takes place during this phase.

Phase IV.

This is called the deceleration phase; it starts when the hydraulic brake is applied to slow down the rotating specimen, and ends when the

rotation actually stops. As soon as the speed of rotation starts to decrease, the torque begins to increase, until it reaches a peak, called the terminal peak torque. The value of the torque then falls and reaches zero when the rotation ceases. However, axial shortening still continues until the end of the forging stage, which follows the deceleration phase (see Figure 1.2).

1.2.2 Inertia-Welding

The inertia (or flywheel) welding technique is a method for joining two specimens; again, at least one of which must be circular.

In this technique the specimens are again mounted in the machine in the same configuration as for the continuous drive case (see Figure 1.3) but this time instead of having a continuous drive to the headstack chuck, the latter is mounted on a flywheel [2,8]. The flywheels assembly is spun under power to a predetermined speed, thus storing a known amount of energy [Figure 1.3(a)]. The drive to the flywheel is then declutched and the tailstock chuck is driven towards the rotating headstock chuck by a hydraulic ram until the specimens make contact. [Figure 1.3(b)]. The energy stored in the flywheel is then used to generate heat at the rubbing interface. The consequent increase in temperature causes the material close to the interface to soften, axial shortening takes place and an upset collar begins to form Figure 1.3(c) . As rubbing proceeds, the resisting torque causes the speed of rotation to decrease until eventually the rotating component comes to rest. The axial force is maintained until the joint cools and consolidates. The process is in a transient state over the entire weld cycle and no equilibrium phase exists.

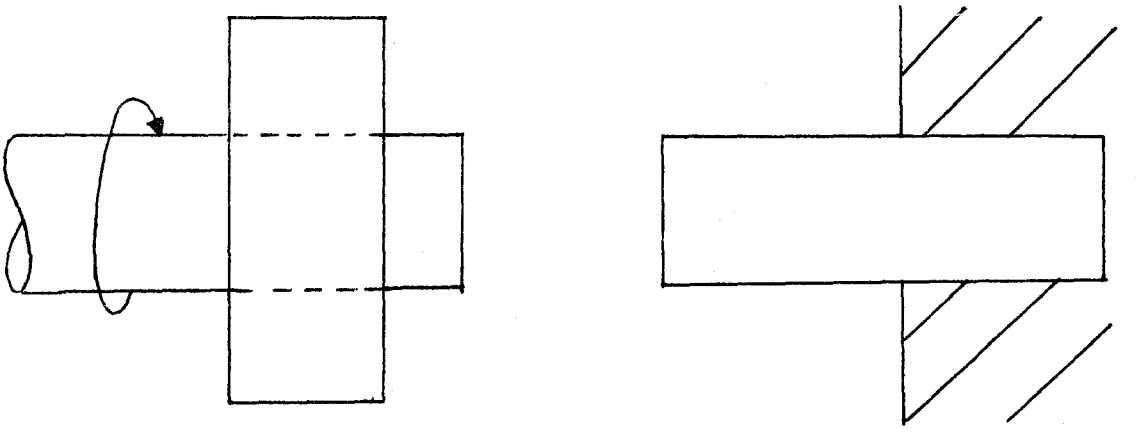

(a)

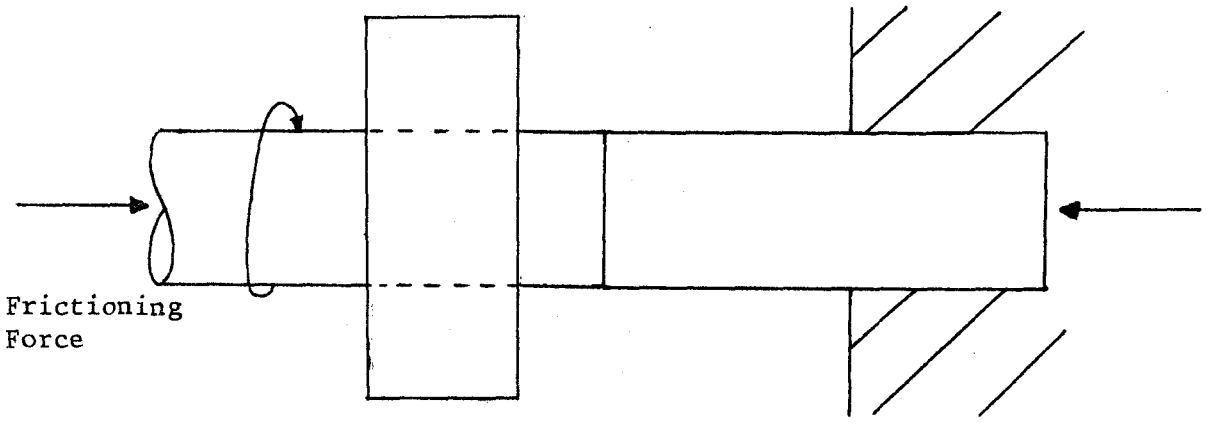

(b)

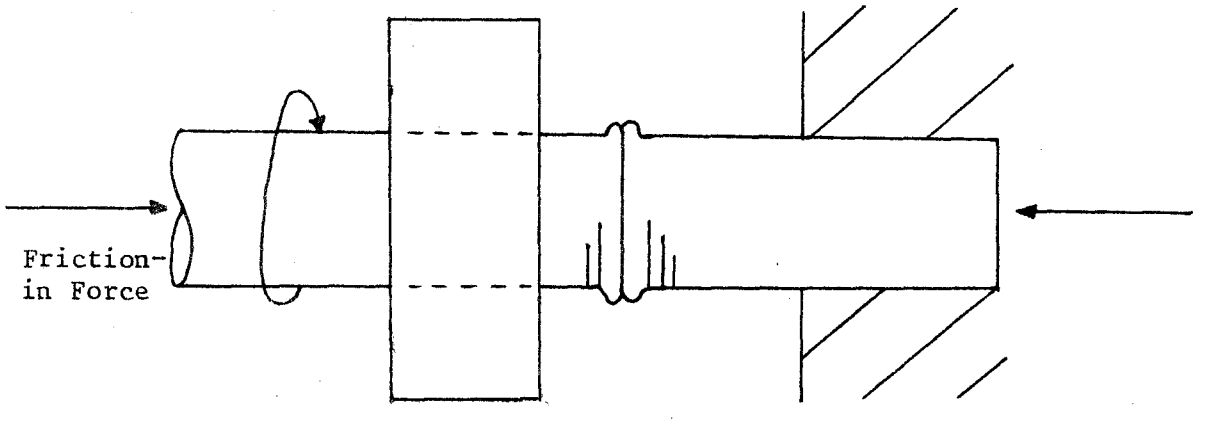

(c)

Figure 1.3 The Inertia Process

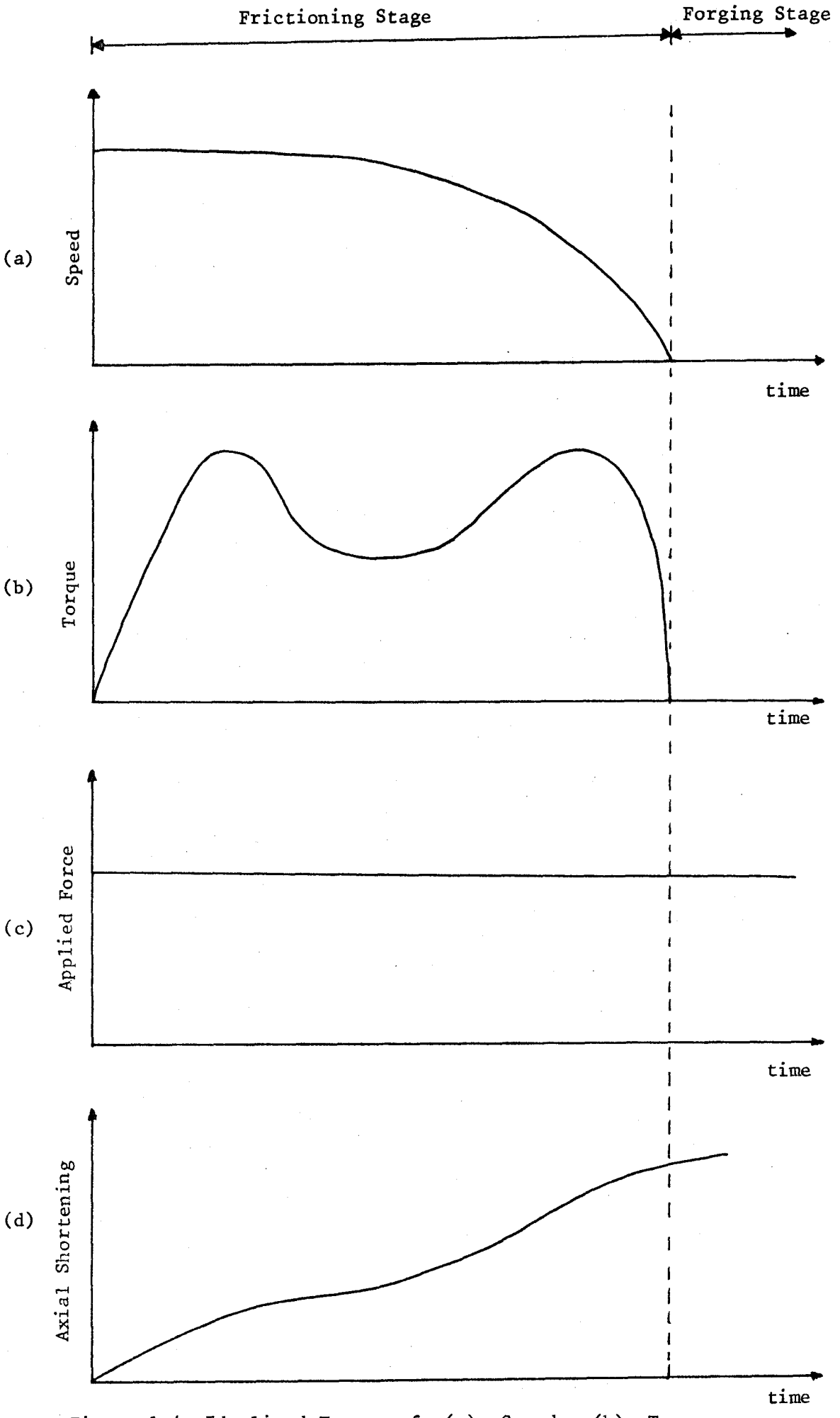

Figure 1.4 Idealised Traces of (a) Speed, (b) Torque, (c) Applied Force and (d) Axial Shortening for the Inertial Process.

The differences mentioned above between the inertia and continuous drive techniques can be seen in the idealised traces of Figures 1.4 and 1.2 respectively. We notice for the case of inertia welding [Figure 1.4] that the initial and terminal peak torques are present but the equilibrium phase is non-existent. We also note that the time taken for the torque to fall to zero, after the terminal peak torque has been reached, is much shorter for inertia welding than for the continuous drive method.

1.2.3 Orbital Welding

Although the two friction welding techniques mentioned above produce sound welds and are by far the most commonly used methods, they are limited to welding components which possess axial symmetry and where angular alignment is not required. This limitation was removed by Searle [9,10] who developed the orbital-welding technique. As suggested by its name, the orbital welding technique is a method of friction welding in which the frictional heat is generated by an orbiting motion between the two rubbing specimens. The difficulty with such a technique is in developing a system to produce the orbital motion. If the moving specimen were simply mounted in an orbiting work holder, which must be heavy in order to have sufficient strength to withstand the applied load, then enormous centrifugal forces would develop and one would need an elaborate and expensive machine. Seeking an alternative method, Searle [10] proposed that both specimens rotate with the same angular speed, about a common axis, in the same sense. Then on displacing the parallel axes of rotation by a small amount e, a simple mathematical analysis (given in Chapter 2) shows that one specimen describes a circular orbit of radius e relative to the other.

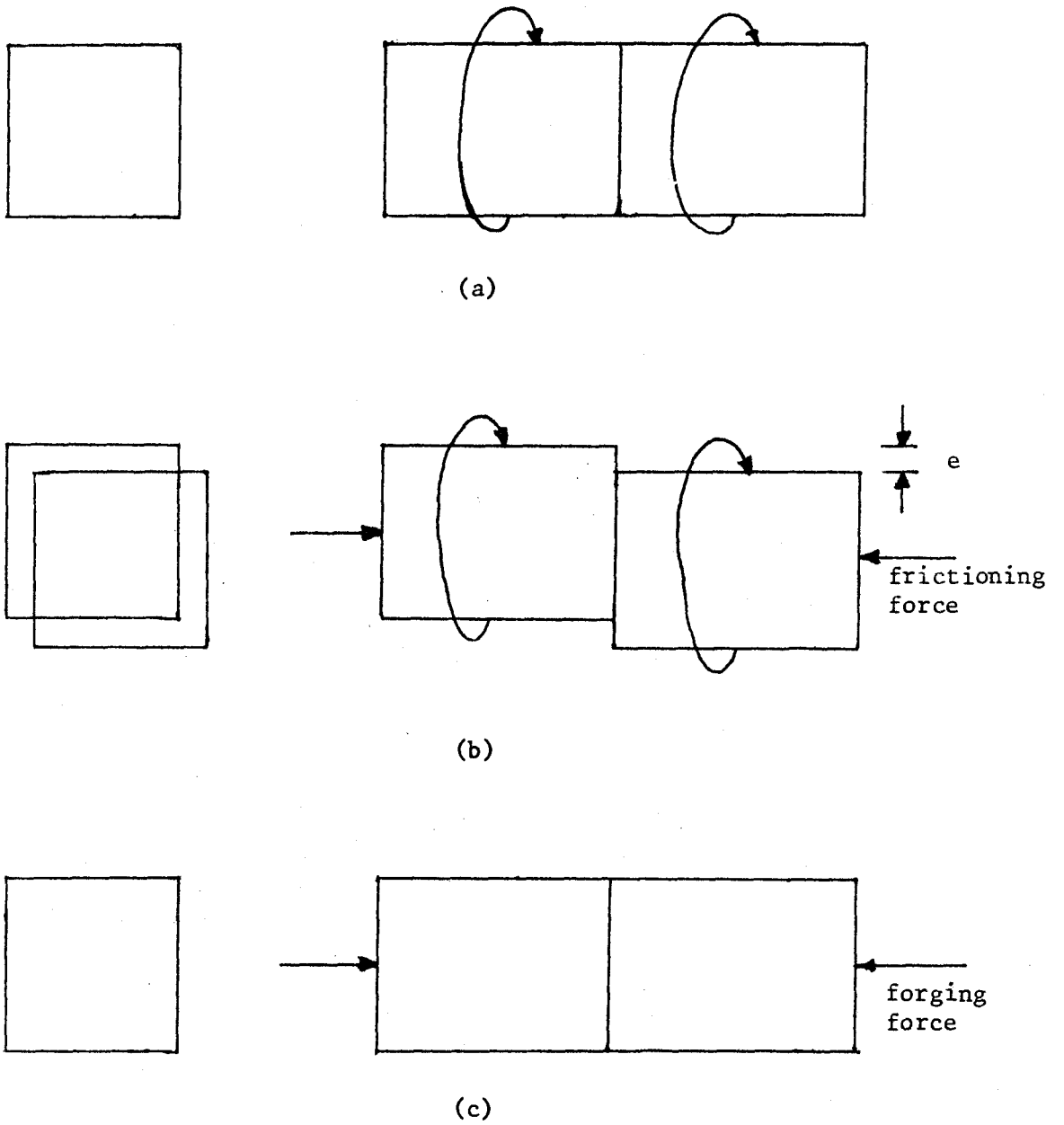

Figure 1.5 The Orbital Process

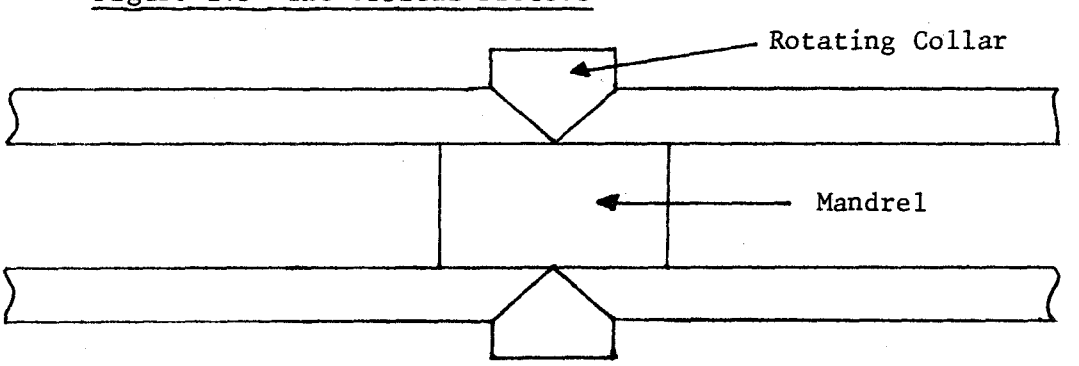

Figure 1.6 Radial Welding Process

This form of motion ensures that at every point of contact, the relative speed between the two specimens is uniform, thus leading to a uniform source of heat generation. The great advantage of using this method is that two similar specimens of arbitrary cross section can be joined and angular alignment is retained. The method is illustrated schematically for the case of square cross-sectional specimens in Figure 1.5.

The specimens are axially aligned in the machine and their angular orientation is set to the position that is desired at the completion of the weld. They are then spun with the same speed, in the same sense about their corresponding axes. [Figure 1.5(a)]. Their axes of rotation are then offset by an amount e, to produce a relative motion between the two specimens with an orbit radius e. [Figure 1.5(b)]. When sufficient heat has been generated, the axes are realigned and a forging force is applied to the still rotating components to forge a weld, as in the continuous drive process [Figure 1.5(c)]. Since the specimens had the correct angular alignment before the process started and were both rotated with the same angular speed throughout, on realignment of the axes the specimens retain the correct angular orientation.

1.2.4 Radial Welding

The one major limitation of the three techniques described so far in this thesis is that at least one of the specimens must be small enough to mount in a machine and rotate with sufficient speed to attain a weld. The welding of very long pipes would therefore be out of the question. However, by holding the two components to be joined stationary and by rotating a third component between them,

thus forming two friction welds, the size of the component to be welded becomes irrelevant. The process is known as radial friction welding [11]. The method is illustrated schematically in Figure 1.6. The parts to be joined are held stationary. Their abbutting ends are chamfered to receive the wedge sectioned ring, which is rotated between them and at the same time compressed radially.

In the bore of the tubes is placed a mandrel which prevents the radial pressure from collapsing the tubes. The mandrel must be made from a material which has a high strength at elevated temperatures and has a low enough thermal conductivity to prevent rapid cooling in the weld area.

The three important features of this method are: (i) it can be used for very large components, (ii) angular alignment can be achieved, (iii) internal upset collars, in tubes, can be avoided. The one limitation of the method is it only applies to circular components.

Although all four methods methods mentioned above have received extensive experimental investigation [2-11] the mathematical models that have been derived are very limited. The aim of this thesis is to improve and extend existing models and to develop new ones, which could be used to assist the engineer to make better welds. We deal mainly in this thesis with phases II and III of the frictioning stage in the continuous drive process although phases I and IV are briefly examined. A simple model of the forging stage has been presented by Rich and Roberts [12], who used plasticity to predict the dispersion of material from the interface and to determine an upper bound for the forging pressure but this stage is not considered in this thesis. In later chapters we briefly examine inertial and orbital welding but radial welding is not investigated.

1.3 The Frictioning Stage

1.3.1 The Continuous Drive Process

The main objective of this thesis as stated above, is to produce mathematical models to describe the frictioning stage of the continuous drive process. As we have already stated, the frictioning stage can be divided into four phases, each of which must be modelled separately. In order to obtain models relevant to each of these phases we must have a basic knowledge of the underlying physics and this is given below.

Phase I.

When the rotating specimen is brought into contact with the stationary one sliding takes place between the two unlubricated surfaces. On initial contact the highest surface asperities will form adhesion junctions and siezure develops [4,7]. At the junctions where the adhesion between the surfaces is stronger than the parent metal, shearing takes place within a short distance either side of the interface, so fragments of metal are transferred from one specimen to the other and vice versa. As this wearing down process continues, the area of real contact gets larger, thus increasing the number of adhesions and siezures. This leads to an increase in the frictional force and hence resisted torque [See Figure 1.2]. As rubbing proceeds, the interfacial temperature goes higher, the rubbing surfaces soften and the area of real contact increase further leading to a greater increase in the frictional force. The temperature continues to rise until it eventually reaches a value (sometimes called the conditioning temperature) at which the transferred metal fragments at the interface become soft and 'plastic'. The time taken to reach the conditioning temperature we call the conditioning time and it marks the end of Phase I.

This initial frictioning process is extremely complicated and it would be very difficult to develop a mathematical model to describe it fully. However, during Phase I, the amount of heat generated represents only about 10% of the total heat generated throughout the entire weld cycle so it is thought adequate to use a simple model to describe this phase. We follow Rykalin [13], Vill [14] and Rich and Roberts [15], whose models are briefly discussed in Chapter 2, and assume that during Phase I heat is generated entirely at the rubbing interface by sliding friction [1]. Models based on this assumption are presented in Chapter 2. The conditioning time and conditioning temperature are calculated from these models and the solutions are used as initial conditions for some of the work presented in Chapter 4.

Phase II.

This is a transition phase during which the layer of transferred fragments at the rubbing interface changes into a layer of plasticised material [4]. The plasticised layer offers less resistance to rubbing and the resisting torque is seen to fall [See Figure 1.2]. As more heat is generated in this plastic layer its thickness and the interfacial temperature both increase. The applied axial load causes the softened material to be squeezed out and the formation of the upset collar begins. As the material softens with increasing temperature the rate of which heat is generated decreases and hence the rate of growth of the plasticised layer is reduced. Eventually, at some later time, the rate of growth of the plasticised layer becomes zero. In this situation the rate at which heat is produced by frictional dissipation is exactly equal to the rate at which heat is lost by forced convection, due to upsetting, plus the second order losses over the lateral surfaces of the specimens. This is the end of Phase II.

Rich and Roberts [15] incorporated Phase II in their model by using a constructed heat input function which decayed with time in a manner characteristic of the phase. However, their model does not describe the mechanical process that produces the heating within the softened layer. In this thesis Phase II is modelled by examining the mechanical deformations that take place in the softened layer.

The chief problem in modelling Phase II, therefore, is in choosing the right constitutive equations to describe the behaviour of the softened material. These equations must represent the relationship between stress and strain rate for the material as accurately as possible but at the same time they must remain tractable. Investigations into high strain rate data using hot torsion and tensile tests have been made [16,17] and, based on this data, relationships between stress and strain rate have been postulated. These relationships are given in Chapter 3. However, they remain difficult to solve even in their simplest forms and since, in this thesis, we are looking for simple models to describe the mechanisms in the softened layer we follow Bahrani et al [18] and use the well known Bingham model [19,20]. The basic equations describing the Bingham substance are presented in Chapter 3.

In Chapter 5 a simple description of Phase II is given where the softened layer is modelled as a Bingham substance. The model is based on that of Bahrani [18] although certain modifications are made since Bharani's model is only validin Phase III. In Chapter 4 more elaborate models of Phase II are given for the special case in which the Bingham number is taken to be zero. The substance then reduces to a viscous fluid [21] (of high viscosity) as considered by Atthey [22], whose model, which is summarised near the beginning of Chapter 4, forms the basis for much of the later work in that Chapter.

Phase III.

During this equilibrium phase, the heat generated by viscous dissipation in the plastic region is equal to the heat lost by forced convection in the upsetting process plus the superficial losses due to radiation and convection over the outside surfaces of the specimens. The temperature, thickness of the plasticised layer, and torque consequently remain constant in this phase and the whole system is in a state of equilibrium. It is reasonable to model this phase using the same constitutive equations as introduced for Phase II, although the governing equations of Phase III are usually easier to solve since they are independent of time. Solutions for Phase III for the viscous fluid and the Bingham material are presented in Chapters 4 and 5 respectively.

Phase IV.

This phase begins when the final brake is applied to the rotating specimen. As the rubbing speed decreases the rate of heat generation falls and the thickness of the plastic region decreases. As a result the torque rises until it reaches its terminal peak torque, after which it falls to zero with the speed of rotation. Again we can use the same constitutive equations as for Phase II and III and a simple solution is derived in Chapter 4.

1.3.2 Inertial Welding

The history of the torque, applied load, angular velocity and rate of axial shortening for a typical inertia weld are shown in Figure 1.4. Wang et al., [8,23] examined this process by assuming that heat is generated entirely at the interface by sliding friction, and making the further assumption that the product of the coefficient of friction and

the applied pressure remains constant throughout the process, thus resulting in a constant torque. The variation of the rubbing speed with time was approximated by a quadratic and they obtained an expression for the interfacial heat input. Using this heat input, the two-dimensional equation of heat conduction was solved, taking into account temperature dependent thermal properties, using finite difference methods, and the temperature distribution in the radial and axial directions obtained. Again this model does not take into account the existence of a softened layer and the volumetric heat generation therein. In order to gain insight into the actual mechanics in the softened layer a simple solution, based on the viscous fluid model, is given in Chapter 4.

1.3.3 Interfacial Melting.

There is some doubt as to whether melting temperatures are ever reached at the interface. Several experimental investigations [4,5,6] suggest melting does not occur but the case where the interface does melt has been considered by several authors [15,23,24].

Rich and Roberts [15] assumed that once the interface had reached melting temperature it would remain at that temperature. On applying this condition of constant melting temperature at the interface and making the assumptions of no axial shortening and constant thermal properties, Rich and Roberts were able to solve the linear one-dimensional equation of heat conduction. They obtained an analytic solution using integral transforms.

Cheng [24] assumed that once a molten layer was formed at the interface, it was squeezed into the 'flash' and that new material was brought to the interface. Thus treating the interface as a moving

molten front, at the melting temperature, he solved the non-linear one-dimensional equation of heat conduction, taking account of variable thermal properties, and obtained a numerical solution using finite differences.

Wang and Nagappan [23] followed Chang's approach in their solution for the inertial welding process but assumed the existence of a molten front moving in both the axial and radial directions and solved the two-dimensional equation of heat conduction using finite difference methods.

In this thesis, melting temperatures are predicted by the solutions for high values of the Brinkman number were they are thought to be due to the inadequate representation of the temperature dependent viscosity. Models involving a molten interface are discussed no further.

1.4 The Upset Collar

During Phases II, III and IV the upset collar is continuously being developed. The formation of this collar is undesirable when welding tubes, since it clearly causes obstructions inside the tubes and for the case of very long tubes cannot be machined away. It is therefore thought useful to model the development of this collar and one such approach, consistent with the viscous fluid model discussed in Chapter 4, is presented in Chapter 6.

CHAPTER 2

THE CONDITIONING PHASE

2.1 The Interfacial Power Inputs

During Phase I of the frictioning stage, heat is generated entirely at the rubbing interface by sliding friction [14,1]. In this situation the general expression for the rate of heat generation per unit area (or the specific power) at a general point may be written [13].

$$q = fpV \ , \qquad (2.1.1)$$

where f, p and V represent the local coefficient of friction, applied pressure and rubbing velocity respectively. The coefficient of friction at a given point will in general depend on the composition of the components being joined, the state and temperature of the rubbing surfaces, the applied pressure and the rubbing speed [1,13, 25, 26]. The pressure and rubbing speed will depend on position. For the conventional friction welding process the rubbing speed is proportional to the radial distance from the axis of rotation r and (2.1.1) then takes the form [25].

$$q = fp\omega r \ , \qquad (2.1.2)$$

where ω is the angular velocity of the rotating component. The total rate of interfacial heat generation can be obtained by integrating (2.1.2) over the entire cross-section, yielding [13,15].

$$Q = 2\pi \int_{r_1}^{r_2} fp\omega r^2 dr \qquad (2.1.3)$$

where r_2 and r_1 are the external and internal radii respectively of the tubes being joined (for solid bars $r_1 = 0$) . Before the integral in equation (2.1.3) can be evaluated the dependence of f and p on r must be specified. The exact nature of this dependence is unknown, however, but several forms which have been introduced in the literature are given below.

(i) The simplest assumption is that the quantity $fp\omega r$ remains uniform uniform over the cross section [13,14,25]. Gelman and Sander [25] suggested this would be so if f were constant and p inversely proportional to r . Unfortunately, the latter is not suitable for solid cross-sections since the pressure would have a singularity at the centre $r = 0$. Vill [14] suggested, after experimental examination of the heated specimens, that this assumption of uniform heat generation over the cross-section is invalid for the first 1.5 - 2 seconds of the weld cycle but may be used thereafter.

(ii) The second, and more commonly used approach [13,25], is to assume that both f and p are uniform leading to a power input that varies linearly along the radius.

(iii) By observing experimentally the relationship between the heat output and speed of rotation Vill [14] suggested that f should take the form

$$f = k/(\omega r)^2 \qquad (2.1.4)$$

where k is a constant of proportionality. This, again, is not suited to solid cross-sections due to the singularity at the centre.

All three above assumptions allow (2.1.3) to be integrated and the total input power obtained.

Voznesenskii [26] postulated that for small times, when there is no appreciable wear of the surfaces, the pressure may be regarded as uniform throughout the cross-section. For later times when the surfaces had 'lapped in' and uniform wear of the surfaces could be assumed, he suggested that p could be taken as inversely proportional to r. Using experimentally obtained values for the power input Voznesenskii then obtained numerical values of f with the aid of the above assumptions and equation (2.1.3).

2.1.1 Power Input for Orbital Welding

Considering the continuous drive process, we derived (2.1.2) from (2.1.1) by noting that $V = \omega r$. However for the orbital process this is not so and the velocity profile for this process is derived here.

During the orbital process both specimens are rotated with the same speed in the same sense, the axes of rotation being displaced a small amount e [See Figure 2.1].

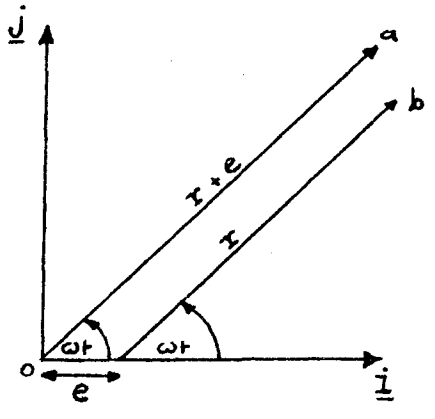

Figure 2.1 Vector Diagram for the Orbital Process

Let a and b be two points on the surfaces A and B respectively that were in contact at time $t = 0$. [Figure 2.1]. The position vectors $\underline{R}_A$ and $\underline{R}_B$ of the point a and b respectively, at time t , with respect to the origin O are given by

$$\underline{R}_A = (r+e)\cos\omega t\underline{i} + (r+e)\sin\omega t\underline{j} \quad , \tag{2.1.4}$$

and

$$\underline{R}_B = (r\cos\omega t+e)\underline{i} + r\sin\omega t\underline{j} \quad . \tag{2.1.5}$$

In the above, ω is the angular velocity and $\underline{i}$ and $\underline{j}$ are unit vectors in the x and y directions.

The position vector of a relative to b , defined by

$$\underline{R}_{AB} = \underline{R}_A - \underline{R}_B \quad ,$$

can be expressed using (2.1.4) and (2.1.5) as

$$\underline{R}_{AB} = (e\cos\omega t-e)\underline{i} + e\sin\omega t\ \underline{j} \tag{2.1.6}$$

Differentiating both sides of this equation with respect to t yields an expression for the relative velocity between a and b , namely

$$\underline{V}_{AB} = -\omega e\sin\omega t\underline{i} + \omega e\cos\omega t\underline{j} \quad . \tag{2.1.7}$$

By inspection of (2.1.6) it is easily deduced that the point a moves in a circle of radius e relative to b with constant angular velocity ω and passes through b once every revolution of the specimens. It is also obvious from (2.1.7) that the relative velocity of a relative to b has constant magnitude ωe . This analysis only applies to two points that were initially on the x axis but a little more algebra reveals that the above can be said about any two points on opposite surfaces. We therefore conclude that the relative

velocity between any two points on opposing surfaces is constant and equal to ωe . Finally if we make the assumption that f and p are uniform over the cross-section then the specific power input at any points of contact would be uniform and given by

$$q = fp\omega e \ . \qquad (2.1.8)$$

2.2 Temperature Profiles

In order to obtain temperature profiles in the specimens being welded, Rykalin et al. [13] and Vill [14] assumed that the rate of heat generation was uniform over the interface. On making the further assumptions that the thermal conductivity $\bar{k}$ and the specific heat capacity $\bar{C}_v$ are constant, the heat emission from the lateral surfaces is negligible, there is no heat exchange in the chucks and considering the tubes to have infinite length, the authors were able to solve analytically the one-dimensional equation of heat conduction subject to the appropriate boundary conditions. As stated earlier, the assumption of uniform heat generation across the interface is invoked for the first 1.5 - 2 seconds but Vill [14] assumed that although this solution is inaccurate at small times, it is appropriate for most of the weld cycle. One of the most striking features of the solution is that the interface temperature is proportional to $\sqrt{t}$ and grows indefinitely. Rykalin et al. [13] suggested that for the special case of short specimens with a small diameter, heated by a small power source this rate of growth would be retarded by heat emission from the lateral surfaces and heat exchange in the chucks. Both the latter effects were excluded in Rykalin's simple model.

Although the assumption of uniform heat generation across the interface is reasonable when $t > 1.5$ seconds, the assumption that q is independent of t is very inaccurate. If the angular velocity remains constant then the rate of heat generation is proportional to the torque and as can be seen from the idealised trace in Figure 1.2, the torque varies greatly with t. Observing this fact Rich and Roberts [15] retained the assumption of uniform power across the interface but approximated the actual power-time form by

$$q = A + Be^{-\lambda t} \quad , \tag{2.2.1}$$

where A,B and λ are constants depending on the particular welding conditions. Taking the specimens to have finite length and making all the other assumptions of Rykalin et al., and Vill, Rich and Roberts were able to solve the equation of linear heat conduction using integral transforms.

It has already been stated that the above models are only valid for $t > 1.5$ seconds. However, the time period 1.5 - 2 seconds usually takes us well into Phase II of the frictioning stage, in which case heat is no longer generated by sliding friction at the interface but by viscous shearing in a softened layer of material close to the interface. During Phase II upsetting takes place and although Rykalin suggests that the rate of growth of the interface temperature could be retarded by inclusion of heat emission from the lateral surfaces and heat exchange in the chucks the dominant cooling agent is forced convection due to the upsetting.

We thus conclude that although these models were presented to represent the majority of the weld cycle, the idea of sliding friction is only really valid during Phase I. Unfortunately, as mentioned in

Vill [14], the interfacial heat generation cannot be assumed to be uniform over the cross-section during this phase. So we present below a slightly amended form of the above models to describe this conditioning phase. Phase II is considered extensively in Chapters 3,4 and 5.

2.3 The Conditioning Time

In this section, we consider the friction welding of thin walled tubes. If we assume that the tube wall thickness is much smaller than the mean radius (i.e. $h \ll \bar{R}$, where h is the wall thickness and $\bar{R}$ is the mean radius) then the variations in f, p and V over the cross-section will be small, hence the power input q may be assumed to be uniformly distributed. From inspection of the idealised torque trace in Figure 1.2 we see that to a good approximation during Phase I, the torque and hence the power increases linearly with time. We thus postulate, for the interfacial heat generation, the relation

$$q = \frac{1}{2} T_{qo} \omega \bar{t} / h \qquad (2.3.1)$$

where ω is the angular velocity and T_{qo} is the slope of the torque curve during Phase I which must be obtained experimentally.
The $\frac{1}{2}$ is introduced since we consider one tube only. Making all the assumptions of Rykalin and Vill, it is therefore necessary to solve the equation of linear heat conduction

$$\frac{\partial^2 T}{\partial \bar{Z}^2} = \frac{1}{D} \frac{\partial T}{\partial \bar{t}} \qquad (2.3.2)$$

subject to the boundary conditions

$$\frac{\partial \bar{T}}{\partial \bar{Z}} = -\frac{1}{2} T_{qo} \frac{\omega \bar{t}}{h} \quad \text{on} \quad \bar{Z} = 0 \tag{2.3.3}$$

$$\bar{T} \to T_{AM} \quad \text{as} \quad \bar{Z} \to \infty \tag{2.3.4}$$

$$\bar{T} = T_{AM} \quad \text{at} \quad \bar{t} = 0 \tag{2.3.5}$$

where $\bar{Z}$ is taken in the axial direction of the tubes and T_{AM} is the ambient temperature.

It is convenient here to introduce the dimensionless variables θ_I, Z and t defined by

$$\theta_I = \frac{T-T_{AM}}{T_{AM}}, \quad Z = \frac{\bar{Z}}{Z_{po}}, \quad t = \bar{t}/t_I \tag{2.3.6}$$

where t_I is a typical value of the conditioning time. The quantity Z_{po} is a typical value for the thickness of the plastic region which develops during Phase II but is introduced here to give compatibility of these solutions with those obtained in a later section. Using (2.3.6), equations (2.3.2) to (2.3.5) become

$$\frac{\partial^2 \theta_I}{\partial Z^2} = \frac{1}{F_O} \frac{\partial \theta_I}{\partial t}, \tag{2.3.7}$$

$$\frac{\partial \theta_I}{\partial Z} = -\chi t \quad \text{on} \quad Z = 0 \tag{2.3.8}$$

$$\theta_I \to 0 \quad \text{as} \quad Z \to \infty \tag{2.3.9}$$

and

$$\theta_I = 0 \quad \text{at} \quad t = 0, \tag{2.3.10}$$

where χ and the Fourier number F_0 are defined by

$$\chi = \frac{T_{qo}\omega Z_{po} t_I}{2T_{AM} h} \quad \text{and} \quad F_0 = \frac{Dt_I}{Z_{po}^2} \tag{2.3.11}$$

Equation (2.3.7) is readily solved subject to the boundary conditions (2.2.8) to (2.3.10) yielding the solution

$$\theta_I = 8\chi\sqrt{F_0}\, t^{3/2}\, i^3 \operatorname{erfc}(Z/2\sqrt{F_0 t}) , \tag{2.3.12}$$

in which $i^3 \operatorname{erfc}(Z\sqrt{F_0 t})$ is defined by [27]

$$6i^3\operatorname{erfc}(x) = \frac{1}{\sqrt{\pi}}(1+x^2)e^{-x^2} - \left[\frac{3}{2} + x^2\right] x \operatorname{erfc}(x) \tag{2.3.15}$$

and $\operatorname{erfc}(x)$ is the complementary error function given by [27]

$$\operatorname{erfc}(x) = \frac{2}{\sqrt{\pi}} \int_x^\infty e^{-y^2} dy \tag{2.3.14}$$

We notice that the interface temperature is now proportional to $t^{3/2}$, as against the variation $t^{\frac{1}{2}}$ predicted by Rykalin and Vill. The above solution is only valid during the conditioning phase and we must now introduce some criterion to determine the end of this phase. Later in this thesis Phase II is modelled in two ways. In Chapter 4 the softened layer is modelled as a viscous fluid and in Chapter 5 as a Bingham substance. We therefore introduce here two criteria for determining the end of Phase I corresponding to the above two models. In each case the existence of a softened layer during Phase II is assumed and as we only consider thin walled tubes we also assume that the interface between the softened material and the solid material is parallel to the weld interface. This assumption is discussed in more

detail later in the thesis.

For the viscous fluid model, the plane dividing the softened and solid regions is assumed to be at the conditioning temperature T_c, the temperature at which the material begins to soften. Clearly there will be no precise value for T_c but t is known to be $O(700^oC)$. For convenience we shall take

$$T_c = 700^oC \ , \tag{2.3.15}$$

when using the viscous fluid model. We assume that the end of the conditioning phase is attained when the interface has temperature T_c and the time taken for this we call the conditioning time t_c. Hence with the aid of (2.3.6) and (2.3.12) we see that t_c is the solution of

$$\frac{T_c - T_{AM}}{T_{AM}} = 4\chi\sqrt{F_o}\, t_c^{3/2}/3\sqrt{\pi} \tag{2.3.16}$$

For a Bingham substance a different definition of t_c is introduced. A detailed description of the Bingham substance is given in Chapter 3, from which it can be deduced that for our simple one-dimensional model the conditioning phase is over when the inequality

$$T_{qo}\bar{t} \geq 2\pi\bar{R}^2 h\sigma_o \tag{2.3.17}$$

is satisfied. The yield stress is assumed to be dependent on temperature and following Baharani et al. [18] we shall postulate the linear relation

$$\sigma_o = \sigma_{AM}\left[1-\varepsilon_I\theta_I\right] \ , \tag{2.3.18}$$

where σ_{AM} is the value of σ_o at ambient temperature and ε_I is the slope which is suitably chosen so that σ_o approximates the data given by Hawkyard et al. [28].

From (2.3.17) and (2.3.18) we deduce

$$T_{qo}\bar{t} = 2\pi\bar{R}^2 h\sigma_{AM}\left[\bar{1}-\varepsilon_I\theta_I(0)\right] \quad . \tag{2.3.19}$$

Substituting (2.3.12) into this equation and regrouping, we obtain

$$\psi t_c = \left[1 - 4\chi\varepsilon_I \sqrt{F_0}\, t_c^{3/2}/3\sqrt{\pi}\right] \tag{2.3.20}$$

where the non-dimensional quantity ψ is defined by

$$\psi = \frac{T_{qo}t_I}{2\pi\bar{R}^2 h\sigma_{AM}} \quad . \tag{2.3.21}$$

It is trivial to show that (2.3.20) has one real positive solution which is therefore the conditioning time.

2.3.1 Results and Discussion

Typical values of the physical quantities are $h = 2 \times 10^{-3}$m, $\bar{R} = 10^{-2}$m, $t_I = 0.55$, $Z_{po} = 10^{-3}$m, $T_{AM} = 293$K, $T_c = 973$K , $\sigma_{AM} = 10^8 Nm^{-2}$, $\varepsilon = 0.3$ and $F_0 = 2.5$. Using the values these conditioning times for both models were calculated using equations (2.3.16) and (2.3.20) and these are plotted against T_{qo} for various values of ω in Figure 2.2. The solid and broken lines denote the viscous and Bingham models respectively. We note in both cases that t_c decreases with increasing values of ω and T_{qo}. This result is intuitively obvious since increasing either of these parameters increases the rate of heat generation.

In Figure 2.3 the interface temperature for the Bingham model, obtained from equation (2.3.12) with $z = 0$, is plotted against T_{qo} for various values of ω . Here we see that the interface temperature increases with increasing ω . This again is due to the increase in heat input. However, we note that increasing the torque leads to a decrease in $\theta_I(0)$. This we expect since increasing T_{qo} leads to the yield condition being satisfied at earlier times.

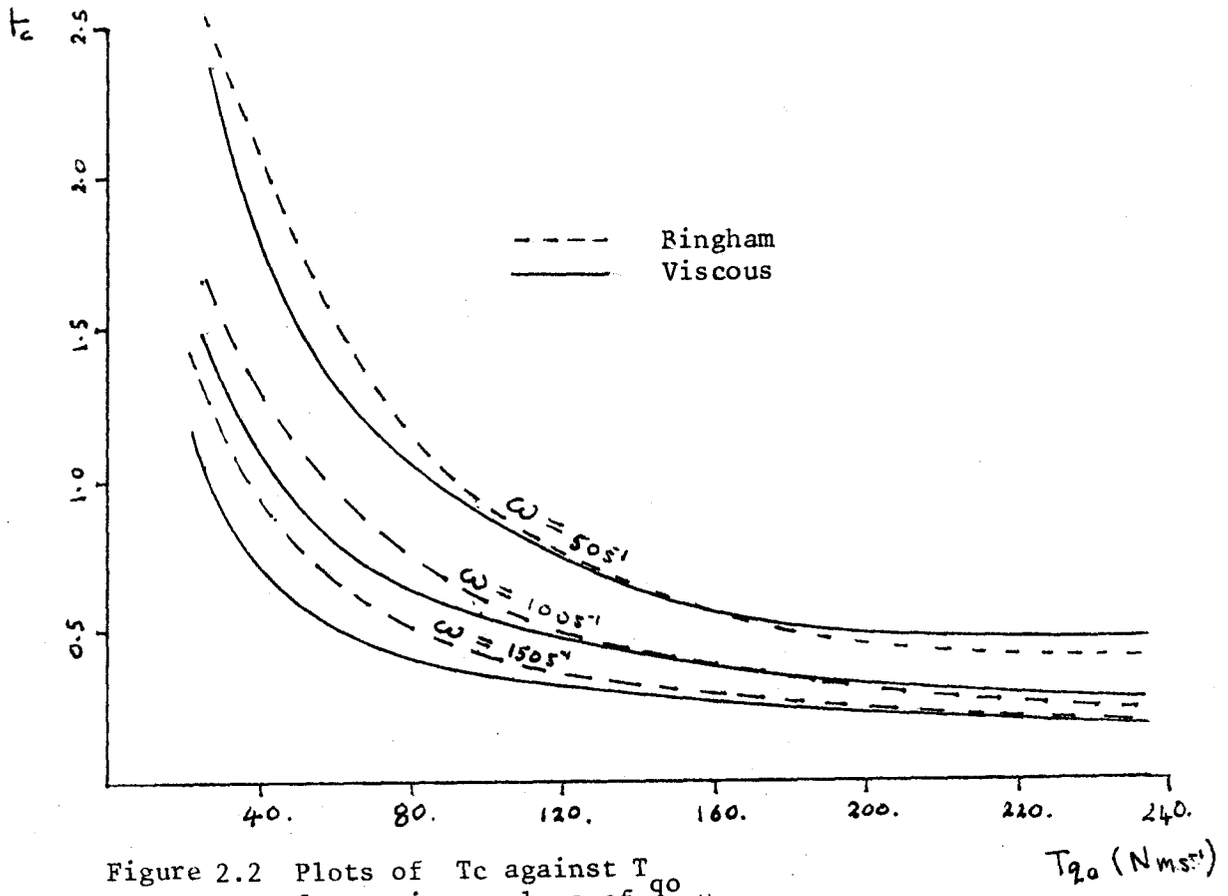

Figure 2.2 Plots of Tc against T_{qo} for various values of ω

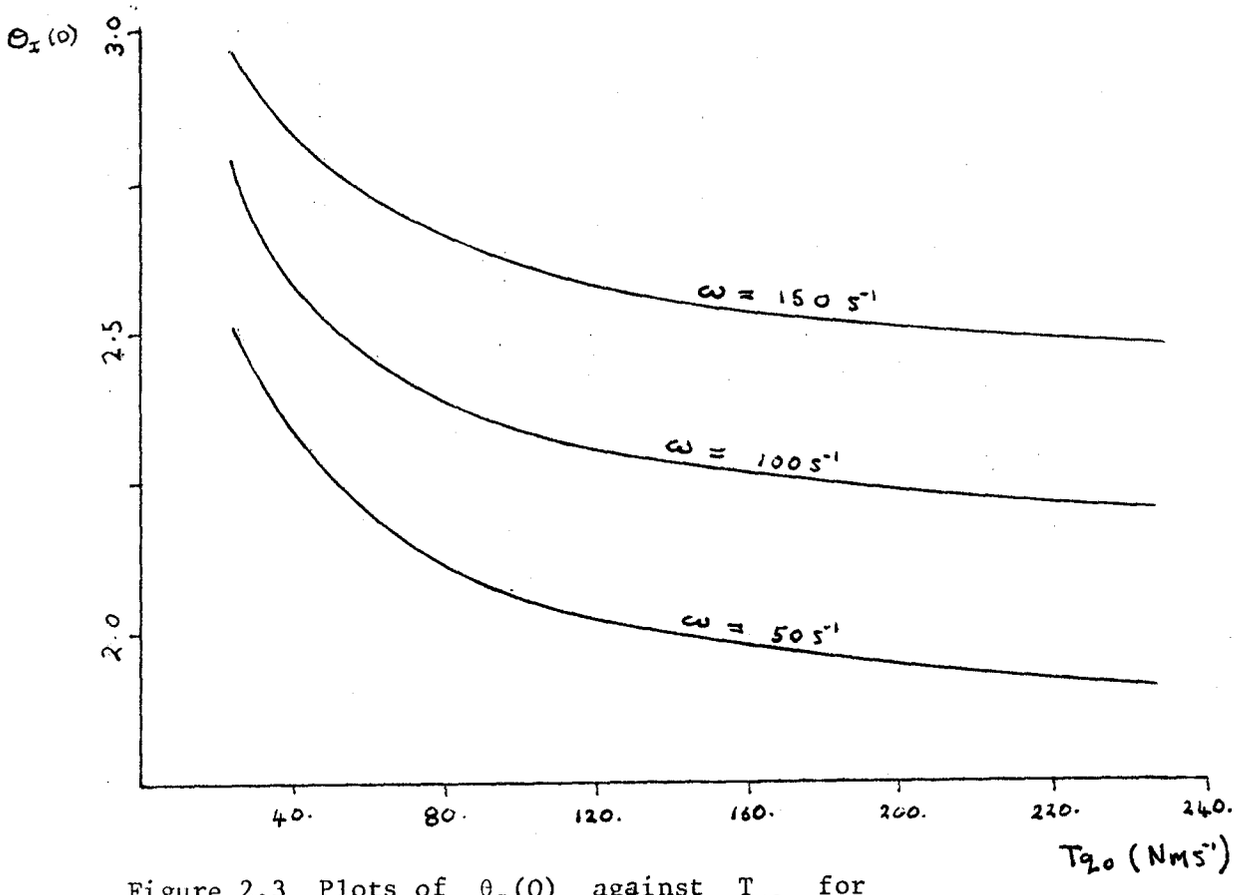

Figure 2.3 Plots of $\theta_I(0)$ against T_{qo} for various values of ω

CHAPTER 3

DERIVATION OF THE GOVERNING EQUATIONS AND THE BOUNDARY CONDITIONS FOR THIN WALLED TUBES. (PHASES II, III.and IV).

3.1 Introduction

During phases II, III and IV a softened layer of material always exists on each side of the interface between the two specimens being welded. The governing equations describing the motion in this layer, we shall assume to be the same for each phase, but the boundary and initial conditions will be different. In this chapter the particular forms of the momentum and energy balance equations appropriate for thin walled tubes are derived, and the forms of the boundary conditions are discussed.

Consider the friction welding of two identical thin walled tubes and in order to simplify the analysis let us assume that the tubes rotate about a common axis with the same angular speed ($\frac{1}{2}\ \omega$ rad $^{-1}$) but in opposite senses. (See Figure 3.1).

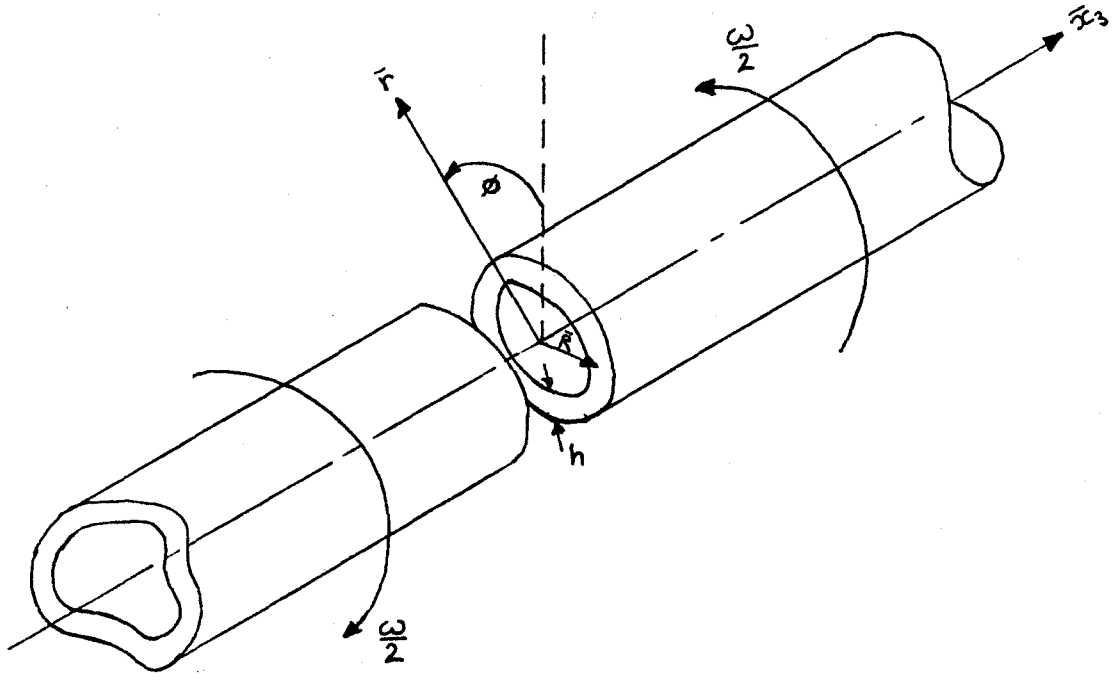

Figure 3.1 Geometry for the Case of Welding Thin Walled Tubes.

Under these assumptions the weld interface becomes a plane of symmetry, and only one tube need be considered. The restriction to thin walled tubes implies that the wall thickness is much smaller than the mean radius of the tube, $\bar{R}$. All the problems considered here are also axisymmetric, that is independent of ϕ, the angular component of the polar coordinate system $(\bar{r}, \phi, x_3)$.

In these situations it is customary to introduce a Cartesian coordinate system $(\bar{x}_1, \bar{x}_2, \bar{x}_3)$ where the $\bar{x}_1$ and $\bar{x}_3$ axes are taken to be in the radial and the axial directions respectively, choosing the plane $\bar{x}_3 = 0$ to be the plane of symmetry between the two specimens (see Fig. 3.2).

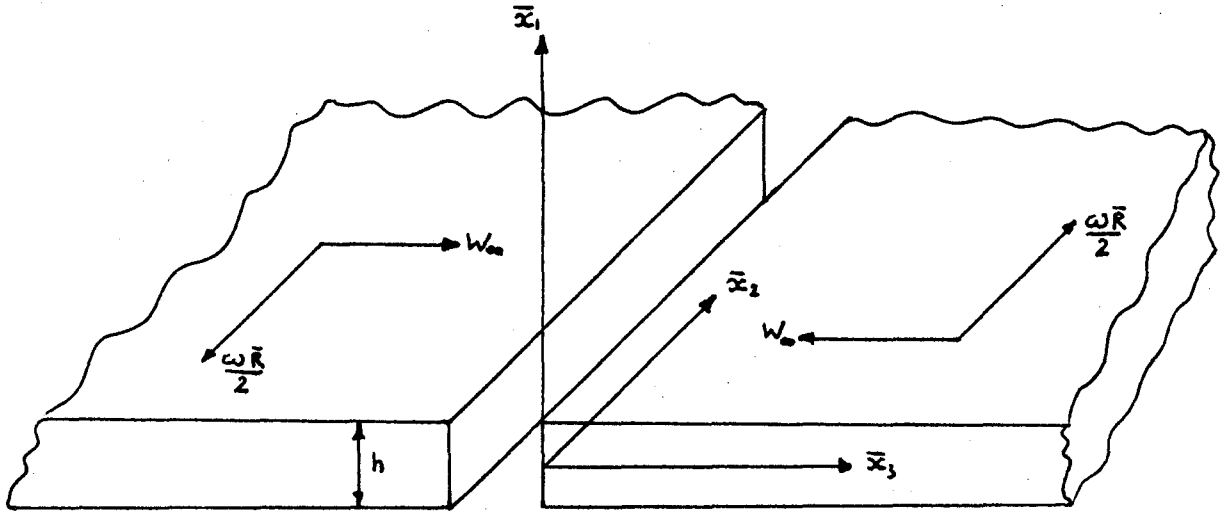

Figure 3.2 Cartesian Coordinate System.

For this two-dimensional version of the axisymmetric problem it is appropriate to assume that all derivatives with respect to $\bar{x}_2$ vanish, i.e. $\partial/\partial\bar{x}_2 \equiv 0$.

3.2 Equations of Motion

With respect to the Cartesian coordinate system introduced above the general form of the equation expressing balance of linear momentum, in the absence of body forces, is given by [21].

$$\frac{D\bar{v}_j}{D\bar{t}} = \frac{1}{\rho}\frac{\partial \sigma_{ij}}{\partial \bar{x}_i} \quad (j = 1, 2, 3) \tag{3.2.1}$$

where the differential operator $D/D\bar{t}$ is defined by

$$\frac{D}{D\bar{t}} = \frac{\partial}{\partial \bar{t}} + \bar{v}_i \frac{\partial}{\partial \bar{x}_i} \tag{3.2.2}$$

The corresponding form for the continuity equation is

$$\frac{\partial \rho}{\partial t} + \frac{\partial}{\partial \bar{x}_i}(\rho \bar{v}_i) = 0 \tag{3.2.3}$$

In equations (3.2.1) and (3.2.3) ρ denotes the density, $\bar{v}_i$ is the velocity component in the $\bar{x}_i$ direction and σ_{ij} is the component, in the $\bar{x}_i$ direction, of the stress exerted on the fluid across an element of surface (internal or external) whose outward drawn normal is in the $\bar{x}_j$ direction, In most simple situations the balance of angular momentum implies that σ_{ij} is symmetric. In the absence of heat sources the energy balance equation takes the form

$$\rho \frac{DE}{Dt} = \Phi - \frac{\partial q_i}{\partial \bar{x}_i} \tag{3.2.4}$$

where E represents the internal energy per unit mass, Φ is the rate of dissipation of mechanical energy per unit volume and q_i is the heat flux per unit area in the $\bar{x}_i$ direction.

3.3 The Constitutive Equations

At this stage it is necessary to introduce some model to describe the softened material near the interface $\bar{z} = 0$. High strain rate data from hot torsion tests and also from tensile and compression tests, on metals have been found to follow the relationship [16, 17]

$$\sigma = \sigma_n \dot{\varepsilon}^n \tag{3.3.1}$$

where σ is the flow stress, $\dot{\varepsilon}$ is the local strain rate and σ_n and n are constant which depend on temperature. However, it has been shown [17] that the data is much better correlated by a relationship containing constants which are independent of the temperature T, viz.

$$\dot{\varepsilon} = A(\sinh\alpha\sigma)^m \exp(-Q/RT) \tag{3.3.2}$$

in which A, α, m and Q are constant for the particular metal and R is the gas constant. Unfortunately it would be difficult to proceed and obtain solutions using the highly nonlinear relationship between stress and strain rate expressed in (3.3.2) and for this reason simpler models are sought. The introduction of a simple model might enable us to obtain some comparatively straightforward solutions to the complex problems under discussion, and hence allow us to gain insight into the mechanisms occurring during friction welding. For the present therefore, following Bahrani et al [18] , the tube is assumed to

comprise a Bingham material. The latter behaves elastically at low stress values when a certain inequality is satisfied but once the inequality is violated the material begins to flow like a viscous fluid, the viscosity of which we shall assume to be dependent on temperature and local strain rate. Chapter 4, the main chapter of this thesis, is concerned with the case where the softened layer is modelled as a viscous fluid which will be seen later to be a special case of the Bingham substance. It will also be shown later that a simplified form of the relationship (3.3.2) can be incorporated into the viscous fluid model provided that the viscosity μ is assumed to take a particular dependence on the temperature and the local strain rate.

Before stating the constitutive equations for the Bingham substance, let us introduce some notation. Let the displacement of a particle from its initial position be denoted by ℓ_i. Then the strain tensor , ℓ_{ij}, is defined by

$$\ell_{ij} = \frac{1}{2}\left[\frac{\partial \ell_i}{\partial \bar{x}_j} + \frac{\partial \ell_j}{\partial \bar{x}_i}\right] , \qquad (3.3.3)$$

whereas the rate of strain tensor, $\dot{\ell}_{ij}$, is represented in terms of the velocity gradients by

$$\dot{\ell}_{ij} = \frac{1}{2}\left[\frac{\partial \bar{v}_i}{\partial \bar{x}_j} + \frac{\partial \bar{v}_j}{\partial \bar{x}_i}\right] . \qquad (3.3.4)$$

Denoting deviatoric tensors by a prime, ', the relationships between σ'_{ij} , ℓ'_{ij} and $\dot{\ell}'_{ij}$ and σ_{ij}, ℓ_{ij} and $\dot{\ell}_{ij}$ respectively can be written

$$\sigma'_{ij} = \sigma_{ij} + \bar{p}\,\delta_{ij} \,, \tag{3.3.5}$$

$$\ell'_{ij} = \ell_{ij} - \frac{1}{3}\,\Delta\,\delta_{ij} \,, \tag{3.3.6}$$

$$\dot{\ell}'_{ij} = \dot{\ell}_{ij} - \frac{1}{3}\,\dot{\ell}_{hh}\,\delta_{ij} \,, \tag{3.3.7}$$

where $\bar{p}$ is the hydrostaticpressure and Δ is the dilatation which are defined by

$$\bar{p} = -\frac{1}{3}\,\sigma_{hh} \tag{3.3.8}$$

and

$$\Delta = \ell_{hh} \,. \tag{3.3.9}$$

The general constitutive equation for a Bingham material can now be written [19, 20]

$$\left.\begin{aligned} \sigma_{ii} &= 3\,K\,\Delta \\ \sigma'_{ij} &= 2\,\bar{\eta}\,\ell'_{ij} \end{aligned}\right\} \text{ if } \frac{1}{2}\,\sigma'_{ij}\,\sigma'_{ij} \leqslant \bar{\sigma}_o^2 \tag{3.3.10}$$

and

$$\sigma'_{ij} = (2\bar{\mu} + \bar{\sigma}_o / \sqrt{\bar{I}})\,\dot{\ell}'_{ij} \text{ if } \frac{1}{2}\,\sigma'_{ij}\,\sigma'_{ij} \geqslant \bar{\sigma}_o^2 \tag{3.3.11}$$

Equation (3.3.10) therefore holds in the elastic region with equation (3.3.11) being valid in the flow region. The constants k, $\bar{\eta}$ and $\bar{\mu}$ denote the bulk modulus, modulus of rigidity and viscosity respectively, $\bar{\sigma}_o$ is called the yield stress, which will in general depend on the temperature, and $\bar{I}$ is the second invariant of the rate of strain tensor defined by

$$\bar{I} = \frac{1}{2}\,\dot{\ell}'_{ij}\,\dot{\ell}'_{ij} \,. \tag{3.3.12}$$

In this work it is assumed that the elastic region may be treated as a rigid body and, from now on, this will be referred to as the solid region. Thus in the solid region the displacements are all taken to be identically zero and equation (3.3.3) then implies that

$$\ell_{ij} = 0 \quad \forall_{i,j} \ . \tag{3.3.13}$$

It follows from equations (3.3.6), (3.3.9) and (3.3.13) that equations (3.3.10) can be disregarded.

Incompressibility of the flowing material is also assumed, and using equations (3.2.3) and (3.3.4) this incompressibility condition can be written

$$\dot{\ell}_{ii} = 0 \ . \tag{3.3.14}$$

With the aid of equations (3.3.5), (3.3.7) and (3.3.14) the constitutive equation (3.3.11) can now be expressed in the form

$$\sigma_{ij} = - \bar{p} \, \delta_{ij} + \left(2\bar{\mu} + \frac{\bar{\sigma}_o}{\sqrt{\bar{I}}} \right) \dot{\ell}_{ij} \ , \tag{3.3.15}$$

provided that $\frac{1}{2} \sigma'_{ij} \, \sigma'_{ij} \geq \bar{\sigma}_o^2$,

where $$\bar{I} = \frac{1}{2} \dot{\ell}_{ij} \dot{\ell}_{ij} \ . \tag{3.3.16}$$

In all subsequent work in this thesis the regime in which flow takes place will be known as the plastic region. Denoting the position of the yield surface (or thickness of the plastic region) by $\bar{z}_p$ we can write

$$\left.\begin{aligned} &\tfrac{1}{2}\,\sigma'_{ij}\,\sigma'_{ij} \geq \bar{\sigma}_o^2 \text{ for } 0 \leq \bar{x}_3 \leq \bar{z}_p \\ \text{and}\quad &\tfrac{1}{2}\,\sigma'_{ij}\,\sigma'_{ij} \leq \bar{\sigma}_o^2 \text{ for } \bar{x}_3 \geq \bar{z}_p \quad . \end{aligned}\right\} \qquad (3.3.17)$$

The function $\bar{z}_p$ thus gives the position of the plastic/solid interface.

It now remains necessary to define forms for the heat flux per unit area, q_i, and the internal energy, E. We shall assume that the heat flux q_i is related to the temperature gradient $\partial T/\partial \bar{x}_i$ by Fourier's law of heat conduction [27] ; viz.

$$q_i = -\bar{k}\frac{\partial T}{\partial \bar{x}_i} \qquad (3.3.18)$$

where $\bar{k}$ is the thermal conductivity. The internal energy may be expressed in terms of differentials as

$$dE = c_v dT - \bar{p}\,d\left(\frac{1}{\rho}\right), \qquad (3.3.19)$$

where c_v represents the specific heat capacity.

3.4 Derivation of the Governing Differential Equations in Non-Dimensional Variables for Thin Walled Tubes

In this section the forms of equations (3.2.1) to (3.2.4) which are appropriate for the friction welding of thin walled tubes, are derived.

3.4.1 Balance of Linear Momentum

It is usually useful when solving a problem to introduce non-dimensional variables. Hence we define x, z, z_p, u, v and w by

$$\left.\begin{aligned} x &= \bar{x}_1/h,\ z = \bar{x}_3/z_{po},\ z_p = \bar{z}_p/z_{po} \\ u &= \bar{v}_1/u_\infty,\ v = 2\bar{v}_2/\omega\bar{R},\ w = \bar{v}_3/w_\infty \end{aligned}\right\} \qquad (3.4.1)$$

where z_{po}, u_∞ and w_∞ are typical values of the thickness of the plastic region, the velocity in the $\bar{x}_1$ (radial) direction and the burnoff velocity respectively. Using the assumption that all derivatives with respect to $\bar{x}_2$ vanish, the component of the strain rate tensor, given by equation (3.3.4), may be written in terms of these new variables as

$$\left.\begin{aligned} \dot{\ell}_{xx} &= \frac{u_\infty}{h}\frac{\partial u}{\partial x},\ \dot{\ell}_{yy} = 0,\ \dot{\ell}_{zz} = \frac{w_\infty}{z_{po}}\frac{\partial w}{\partial z} \\ \dot{\ell}_{xy} &= \frac{\omega\bar{R}}{4h}\frac{\partial v}{\partial x},\ \dot{\ell}_{xz} = \frac{1}{2}\left(\frac{u_\infty}{z_{po}}\frac{\partial u}{\partial z} + \frac{w_\infty}{h}\frac{\partial w}{\partial x}\right),\ \dot{\ell}_{yz} = \frac{\omega\bar{R}}{4z_{po}}\frac{\partial v}{\partial z} \end{aligned}\right\} \qquad (3.4.2)$$

In order to obtain approximate forms of the complicated governing differential equations, realistic values of the constants appearing in our theory need to be inserted. The solutions to our simplified equations will then be relevant to actual welding situations. In practice when welding tubes of a mean radius $\bar{R}$ of O(1cm) and a wall thickness h of O (1mm) the values for ω usually lie within the range (100-200) rads./sec. In these situations, with an applied force, F_A, lying in the range (3-8)KN, the values for the thickness of the plastic region z_{po} and rate of burnoff w_∞ are typically found to be O(1mm) and O(1mms^{-1}) respectively. The quantity u_∞ cannot be found directly from experimental data , but substituting the relevant strain rate component into the equation of incompressibility (3.3.14) yields

$$\frac{u_\infty}{h}\frac{\partial u}{\partial x} + \frac{w_\infty}{z_{po}}\frac{\partial w}{\partial z} = 0. \qquad (3.4.3)$$

In order that both terms of this equation are of the same order of magnitude we require

$$u_\infty = w_\infty \beta, \tag{3.4.4}$$

where the dimensionless parameter β is defined by

$$\beta = h/z_{po} . \tag{3.4.5}$$

From equations (3.3.12) and (3.4.2) the expression for $\overline{I}$ can be written in full as

$$\overline{I} = \frac{1}{2}\left\{\frac{w_\infty^2}{z_{po}^2}\left[\left(\frac{\partial u}{\partial x}\right)^2 + \left(\frac{\partial w}{\partial z}\right)^2\right] + \frac{\omega^2\overline{R}^2}{8z_{po}^2}\left[\left(\frac{\partial v}{\partial z}\right)^2 + \frac{1}{\beta^2}\left(\frac{\partial v}{\partial x}\right)^2\right]\right.$$

$$\left. + \frac{w_\infty^2}{2z_{po}^2}\left[\frac{1}{\beta}\frac{\partial w}{\partial x} + \beta\frac{\partial u}{\partial z}\right]^2\right\} . \tag{3.4.6}$$

Using the data presented in this paragraph, a careful investigation of the magnitude of all terms in equations (3.4.6) reveals that, to a first approximation, $\overline{I}$ is given by

$$\overline{I} \approx \frac{\omega^2\overline{R}^2}{16z_{po}^2}\left[\left(\frac{\partial v}{\partial z}\right)^2 + \frac{1}{\beta^2}\left(\frac{\partial v}{\partial x}\right)^2\right] . \tag{3.4.7}$$

At this stage we introduce the further dimensionless variables μ, σ_o, I, p and t defined by

$$\left.\begin{aligned} &\mu = \overline{\mu}/\mu_o,\ \sigma_o = \overline{\sigma}_o/\sigma_A,\ I = \overline{I}/(\omega^2\overline{R}^2/16z_{po}^2) \\ &t = \overline{t}/t_o,\ p = \overline{p}/p_A \end{aligned}\right\} \tag{3.4.8}$$

where μ_o is a typical value for the viscosity, σ_A is the average value of the yield strength taken over the typical temperature range experienced, t_o is typically the time duration of the particular

welding cycle under consideration and P_A is the pressure applied to the tube through the axial force F_A. It is now possible, using equations (3.3.15), (3.4.2), (3.4.7) and (3.4.8) to write down the component of the stress tensor in terms of the dimensionless variables as follows:

$$\sigma_{xx} = - P_A\, p + \frac{2\mu_o w_\infty}{z_{po}} \left[\mu + \frac{B\sigma_o}{2\sqrt{I}}\right] \frac{\partial u}{\partial x} \quad , \tag{3.4.9}$$

$$\sigma_{yy} = - P_A\, p, \tag{3.4.10}$$

$$\sigma_{zz} = - P_A\, p + \frac{2\mu_o w_\infty}{z_{po}} \left[\mu + \frac{B\sigma_o}{2\sqrt{I}}\right] \frac{\partial w}{\partial z} \tag{3.4.11}$$

$$\sigma_{xy} = \frac{\mu_o \omega \bar{R}}{2h} \left[\mu + \frac{B\sigma_o}{2\sqrt{I}}\right] \frac{\partial v}{\partial x} \quad , \tag{3.4.12}$$

$$\sigma_{xz} = \frac{\mu_o w_\infty}{h} \left[\mu + \frac{B\sigma_o}{2\sqrt{I}}\right] \left[\frac{\partial w}{\partial x} + \beta^2 \frac{\partial u}{\partial z}\right] \quad , \tag{3.4.13}$$

$$\sigma_{yz} = \frac{\mu_o \omega \bar{R}}{2 z_{p_o}} \left[\mu + \frac{B\sigma_o}{2\sqrt{I}}\right] \frac{\partial v}{\partial z} \quad , \tag{3.4.14}$$

Where the Bingham number B is defined by

$$B = \frac{4\sigma_A z_{po}}{\mu_o \omega \bar{R}} \tag{3.4.15}$$

Under normal conditions the temperature in the plastic region during friction welding of mild steel lies between 700°C and 1200°C and over this temperature range the average value of the yield stress σ_A is found from tables [28, 29] to be of $O(10^7\ Nm^{-2})$. The pressure P_A based on the applied force F_A and cross-sectional area of a tube of mean

radius 1cm and wall thickness 1mm is $O(10^8\ Nm^{-2})$. A typical time scale for phase II is O(1s) while for phase IV the time scale is O(0.1s), (see trace in Fig.4.3( ). A value for the viscosity μ_o is not readily available, however, but one will be chosen which leads to a realistic value for the torque. The total force exerted by the fluid, in the azimuthal direction, on an elemental annulus of the surface $\bar{x}_3 = \bar{z}_p(\bar{r},\bar{t})$ is given by

$$\delta F = \left\{\sigma_{\theta z}(\bar{r},\bar{z}_p(\bar{r},\bar{t}))n_z + \sigma_{r\theta}(\bar{r},\bar{z}_p(\bar{r},\bar{t}))n_r\right\}\delta S \qquad (3.4.16)$$

where n_r and n_z are the components of the normal vector to the elemental surface, δS, in the radial and axial directions respectively. In terms of our cylindrical polar system equation (3.4.16) may be expressed.

$$\delta F = 2\pi\bar{r}\left\{\sigma_{\theta z}(\bar{r},\bar{z}_p(\bar{r},\bar{t})) - \sigma_{r\theta}(\bar{r},\bar{z}_p(\bar{r},\bar{t}))\frac{\partial \bar{z}_p}{\partial \bar{r}}\right\}\delta\bar{r} \qquad (3.4.17)$$

The total reacted torque T_q is thus given by

$$T_q = 2\pi\left\{\int_{\bar{R}-\frac{1}{2}h}^{\bar{R}+\frac{1}{2}h}\left\{\sigma_{\theta z}(\bar{r},\bar{z}_p(\bar{r},\bar{t})) - \sigma_{r\theta}(\bar{r},\bar{z}_p(\bar{r},\bar{t}))\frac{\partial \bar{z}_p}{\partial \bar{r}}\right\}\bar{r}^2 d\bar{r}\right. \qquad (3.4.18)$$

From the above it is readily seen that, in terms of our two-dimensional Cartesian coordinate system, the torque can be approximated by

$$T_q \approx 2\pi\bar{R}^2 h\left\{\int_{-\frac{1}{2}}^{\frac{1}{2}}\left\{\sigma_{yz}(x,z_p(x,t)) - \sigma_{xy}(x,z_p(x,t))\frac{\partial z_p}{\partial x}\right\}dx\right\} \qquad (3.4.19)$$

However, for the two-dimensional model it is convenient to work with the torque/unit area, T_q^*, which may be expressed as

$$T_q^* = \bar{R}\int_{-\frac{1}{2}}^{\frac{1}{2}} \sigma_{yz}\left[x, z_p(x,t)\right]dx - \bar{R}\int_{-\frac{1}{2}}^{\frac{1}{2}} \sigma_{xy}\left[x, z_p(x,t)\right]\frac{\partial z_p}{\partial x}\,dx \qquad (3.4.20)$$

With the aid of equations (3.4.12) and (3.4.14) it can be seen, by comparing the orders of magnitude of both sides of equation (3.4.20) that

$$T_q^* = O(\bar{R}^2 \mu_o \omega / z_{po}). \qquad (3.4.21)$$

It is found by experiment that typical values for T_q^* are $O(10^5 Nm^{-1})$, thus we deduce from equation (3.4.21) with the aid of the data given previously in this chapter, that μ_o is $O(10^4 kgm^{-1}s^{-1})$.

On susbstituting equations (3.4.9) to (3.4.14) for the stress components in the plastic region into equation (3.2.1), there results, after the use of the definitions (3.4.1),(3.4.4) and (3.4.5) and some rearrangement, the equations of motion

$$\gamma\frac{\partial u}{\partial t} + u\frac{\partial u}{\partial x} + w\frac{\partial u}{\partial z} = -\frac{C_p}{2\beta^2}\frac{\partial p}{\partial x} +$$

$$\frac{1}{\beta^2 Re}\left\{\frac{\partial}{\partial z}\left[\left\{\mu + \frac{B\sigma_o}{2\sqrt{I}}\right\}\left\{\frac{\partial w}{\partial x} + \frac{1}{\beta^2}\frac{\partial u}{\partial z}\right\}\right] + 2\frac{\partial}{\partial x}\left[\left\{\mu + \frac{B\sigma_o}{2\sqrt{I}}\right\}\frac{\partial u}{\partial x}\right]\right\}, \qquad (3.4.22)$$

$$\gamma\frac{\partial v}{\partial t} + u\frac{\partial v}{\partial x} + w\frac{\partial v}{\partial z} = \frac{1}{Re}\left\{\frac{\partial}{\partial z}\left[\left\{\mu + \frac{B\sigma_o}{2\sqrt{I}}\right\}\frac{\partial v}{\partial z}\right]\right.$$

$$\left. + \frac{1}{\beta^2}\frac{\partial}{\partial x}\left[\left\{\mu + \frac{B\sigma_o}{2\sqrt{I}}\right\}\frac{\partial v}{\partial x}\right]\right., \qquad (3.4.23)$$

and

$$\gamma\frac{\partial w}{\partial t} + u\frac{\partial w}{\partial x} + w\frac{\partial w}{\partial z} = -\frac{C_p}{2}\frac{\partial p}{\partial z} +$$

$$\frac{1}{Re}\left\{2\frac{\partial}{\partial z}\left[\left(\mu + \frac{B\sigma_o}{2\sqrt{I}}\right)\frac{\partial w}{\partial z}\right] + \frac{1}{\beta^2}\frac{\partial}{\partial x}\left[\left(\mu + \frac{B\sigma_o}{2\sqrt{I}}\right)\left(\frac{\partial w}{\partial x} + \beta^2\frac{\partial u}{\partial z}\right)\right]\right\}, \qquad (3.4.24)$$

Where the Reynolds number, Re, based on motion in the axial direction, the pressure coefficient C_p and the dimensionless parameter γ are defined by

$$Re = \frac{\rho w_\infty z_{po}}{\mu_o}, \quad C_p = \frac{p_A}{\frac{1}{2}\rho w_\infty^2}, \quad \gamma = \frac{z_{po}}{w_\infty t_o}. \qquad (3.4.25)$$

Using the data given earlier in this chapter and taking the value for the density ρ to be 7800 Kg m^{-3}, the appropriate value for mild steel, the orders of magnitude of the above parameters are found to be

$$Re = O(10^{-6}), \quad C_p = O(10^{10}), \quad \gamma = O(1). \qquad (3.4.26)$$

From these results it is immediately obvious that the non linear inertial terms on the left hand sides of equations (3.4.22) to (3.4.24) may be neglected. The nature of the remaining equations suggests that the pressure p may be expressed in the form

$$p = p_o + p_1/C_p\ Re \qquad (3.4.27)$$

Substituting equation (3.4.27) into equations (3.4.22) to (3.4.24) (and neglecting the inertial terms) then leads to the set of non-dimensional equations

$$-\frac{C_p}{2}\,Re\,\frac{\partial p_o}{\partial x}-\frac{1}{2}\frac{\partial p_1}{\partial x}+\frac{\partial}{\partial z}\left\{\left(\mu+\frac{B\sigma_o}{2\sqrt{I}}\right)\left(\frac{\partial w}{\partial x}+\beta^2\frac{\partial u}{\partial z}\right)\right\}$$

$$+2\frac{\partial}{\partial x}\left\{\left(\mu+\frac{B\sigma_o}{2\sqrt{I}}\right)\frac{\partial u}{\partial x}\right\}=0, \qquad (3.4.28)$$

$$\frac{\partial}{\partial z}\left\{\left(\mu+\frac{B\sigma_o}{2\sqrt{I}}\right)\frac{\partial v}{\partial z}\right\}+\frac{1}{\beta^2}\frac{\partial}{\partial x}\left\{\left(\mu+\frac{B\sigma_o}{2\sqrt{I}}\right)\frac{\partial v}{\partial x}\right\}=0, \qquad (3.4.29)$$

and $$-\frac{C_p\,Re}{2}\frac{\partial p_o}{\partial z}-\frac{1}{2}\frac{\partial p_1}{\partial z}+2\frac{\partial}{\partial z}\left\{\left(\mu+\frac{B\sigma_o}{2\sqrt{I}}\right)\frac{\partial w}{\partial z}\right\}$$

$$+\frac{1}{\beta^2}\frac{\partial}{\partial x}\left\{\left(\mu+\frac{B\sigma_o}{2\sqrt{I}}\right)\left(\frac{\partial w}{\partial x}+\beta^2\frac{\partial u}{\partial z}\right)\right\}=0. \qquad (3.4.30)$$

Finally, with the aid of the definitions (3.4.4) and (3.4.5) the equation of incompressibility (3.4.3) takes the dimensionless form

$$\frac{\partial u}{\partial x}+\frac{\partial w}{\partial z}=0. \qquad (3.4.31)$$

For our Bingham model equations (3.4.28) to (3.4.30) and (3.4.31) are the forms of the linear momentum and continuity equations respectively which hold in the plastic region in a thin tube, under the conditions typically arising during friction welding. Let us now derive the analogous form of the energy balance equations.

3.4.2 Balance of Energy

In the plastic region the form for Φ, the rate of heat generation by viscous dissipation, is

$$\Phi = \sigma_{ij} \dot{\ell}_{ij} \tag{3.4.32}$$

and with the aid of equations (3.3.14), (3.3.15) and (3.3.16), (3.4.32) can be written

$$\Phi = 2\left[2\bar{\mu} + \frac{\bar{\sigma}_o}{\sqrt{\bar{I}}}\right]\bar{I} \ . \tag{3.4.33}$$

Let us now introduce the dimensionless variables θ, c_v and k defined by

$$\theta = \frac{T-T_{AM}}{T_c-T_{AM}} \ , \ c_v = \bar{c}_v/c_{vo}, \quad k = \bar{k}/k_o \ . \tag{3.4.34}$$

In the above T_{AM} is the ambient temperature, T_c is the conditioning temperature and c_{vo} and k_o are the average values of the specific heat capacity and thermal conductivity taken over the temperature range 700°C - 1200°C, the range typically experienced in the plastic region during the friction welding of mild steel.

With the aid of equations (3.4.7), (3.4.8) and (3.4.15) equation (3.4.33), to a first approximation, takes the form

$$\Phi \approx \mu_o\left[\frac{\omega\bar{R}}{2z_{po}}\right]^2\left[\mu + \frac{B\sigma_o}{2\sqrt{I}}\right]\left[\left[\frac{\partial v}{\partial z}\right]^2 + \frac{1}{\beta^2}\left[\frac{\partial v}{\partial x}\right]^2\right] \tag{3.4.35}$$

for $0 \leqslant z \leqslant z_p(x,t)$.

With the assumption of incompressibility it can be shown with the aid of equation (3.3.19) that equation (3.2.4) may be expressed in the form

$$\rho c_v \frac{DT}{Dt} = \Phi - \frac{\partial q_i}{\partial \bar{x}_i} \qquad (3.4.36)$$

Substituting equations (3.3.18) and (3.4.35) into equation (3.4.36) and using the definitions (3.4.1), (3.4.4), (3.4.5), (3.4.8) and (3.4.33) and rearranging, the energy equation for the plastic region becomes

$$\frac{\partial}{\partial z}\left(k \frac{\partial \theta}{\partial z}\right) + \frac{1}{\beta^2} \frac{\partial}{\partial x}\left(k \frac{\partial \theta}{\partial x}\right) + Br\left(\mu + \frac{B\sigma_o}{2\sqrt{I}}\right)\left(\left(\frac{\partial v}{\partial z}\right)^2 + \frac{1}{\beta^2}\left(\frac{\partial v}{\partial x}\right)^2\right)$$

$$= P_e c_v\left(u\frac{\partial \theta}{\partial x} + w\frac{\partial \theta}{\partial z}\right) + \frac{c_v}{Fo}\frac{\partial \theta}{\partial t}, \quad 0 \leqslant z \leqslant z_p(x,t) \qquad (3.4.37)$$

where the dimensionless quantities Br, the Brinkman number Pe, the Peclet number, and Fo, the Fourier number are defined by

$$Br = \frac{\mu_o \omega^2 \bar{R}^2}{4k_o(T_c - T_{AM})}, \quad Pe = \frac{w_\infty z_{po}}{(k_o/\rho c_v)_o}, \quad Fo = \frac{(k_o/\rho c_{vo})}{t_o} z_{po}^2 .$$

(3.4.38)

Typical values for k_o and c_{vo} are 20(w/mK) and 420(J/kgK) respectively, and it is assumed that $T_c = 700^oC$ and $T_{AM} = 15^oC$. With these values and those introduced earlier it can be shown that under normal friction welding conditions

$$Br = O(1), \quad Pe = O(1), \quad Fo = O(1) \qquad (3.4.39)$$

Equation (3.4.37) is, therefore, the approximate form of the energy equation in the plastic region for the friction welding of thin walled tubes.

In an entirely analagous way one deduces that the corresponding form of the energy equation in the solid region is given by

$$\frac{\partial}{\partial z}\left[k_s \frac{\partial \theta_s}{\partial z}\right] + \frac{1}{\beta^2}\frac{\partial}{\partial x}\left[k_s \frac{\partial \theta_s}{\partial x}\right] = -\,Pe\ {}^{c}v_s\, W_o \frac{\partial \theta_s}{\partial z} + \frac{{}^{c}v_s}{Fo}\frac{\partial \theta_s}{\partial t},$$

$$z \gtrsim z_p(x,t), \qquad (3.4.40)$$

where the subscript 's' is used to denote quantities appropriate to the solid region and the dimensionless variables θ_s, k_s and ${}^{c}v_s$ are defined in a similar manner to θ, k and c_v. The function $w_o(t)$ is the dimensionless burnoff velocity which is assumed to depend only on time t.

3.5 Boundary and Initial Conditions

The boundary and initial conditions which must be applied to the partial differential equations obtained in the previous section are now discussed.

In practice the burnoff velocity W_o see trace Fig. 4.31 is found to be approximately constant over almost the entire welding cycle. Thus the applied force must be balanced by the hydrostatic pressure and the viscous forces acting on the plastic/solid interface $\bar{x}_3 = \bar{z}_p(\bar{r},\bar{t})$. In terms of cylindrical polars this may be expressed

$$2\pi \int_{\bar{R}-\frac{1}{2}h}^{\bar{R}+\frac{1}{2}h} \bar{r}\,\sigma_{rz}\left[\bar{r},\bar{z}_p(\bar{r},\bar{t})\right] \frac{\partial \bar{z}_p}{\partial \bar{r}}\,d\bar{r} - 2\pi \int_{R-\frac{1}{2}h}^{\bar{R}+\frac{1}{2}h} \bar{r}\,\sigma_{zz}\left[\bar{r},\bar{z}_p(\bar{r},\bar{t})\right] d\bar{r} =$$

$$2\pi \bar{R} h P_A, \qquad (3.5.1)$$

Again for our two dimensional model it is more convenient to work in terms of forces/unit area and the above equation may be approximated by

$$\int_{-\frac{1}{2}}^{\frac{1}{2}} \left\{ \left[\frac{\sigma_{xz}}{\beta} (x,\ z_p(x,t)) \right] \frac{\partial z_p}{\partial x} - \sigma_{zz}(x, z_p(x,t)) \right\} dx = P_A \qquad (3.5.2)$$

On substituting equations (3.4.11) and (3.4.13) into equation (3.5.2) there results, after a little rearrangement and with the aid of definition (3.4.1), the equation

$$\int_{-\frac{1}{2}}^{\frac{1}{2}} \left\{ \frac{\mu_o w_\infty}{\beta h} \left(\mu + \frac{B\sigma_o}{2\sqrt{I}} \right) \left(\frac{\partial w}{\partial x} + \beta^2 \frac{\partial u}{\partial z} \right) \Bigg|_{z=z_p(x,t)} \frac{\partial z_p}{\partial x} + P_A\, p \Bigg|_{z=z_p(x,t)} \right.$$

$$\left. - 2 \frac{\mu_o w_\infty}{z_{po}} \left(\mu + \frac{\sigma_o}{2\sqrt{I}} \right) \frac{\partial w}{\partial z} \Bigg|_{z=z_p(x,t)} \right\} dx = P_A \qquad (3.5.3)$$

The conditions on the velocity component are straight forward. Symmetry requirements on the weld interface $\bar{z} = 0$ imply that the velocity components $\bar{v}$ and $\bar{w}$ and the velocity gradient $\partial\bar{u}/\partial\bar{z}$ must vanish. Thus we may write

$$\bar{v}(\bar{x},o,\bar{t}) = 0,\ \bar{w}(\bar{x},o,\bar{t}) = 0,\ \frac{\partial \bar{u}}{\partial \bar{x}} (\bar{x},o,\bar{t}) = 0;\ -\tfrac{1}{2}h \leqslant \bar{x} \leqslant \tfrac{1}{2}h \qquad (3.5.4)$$

At the plastic/solid interface $\bar{z} = \bar{z}_p$ continuity of velocity leads

$$\left.\begin{aligned} \bar{u}(\bar{x},\bar{z}_p,t) &= 0 \\ \bar{v}(\bar{x},\bar{z}_p,t) &= \tfrac{1}{2}\omega\bar{R} \\ \bar{w}(\bar{x},\bar{z}_p,t) &= -W_o(t)\ . \end{aligned}\right\} -\frac{h}{2} \leqslant \bar{x} \leqslant \frac{h}{2} \qquad (3.5.5)$$

The position of the plastic/solid boundary is defined by the Bingham yield criterion,

$$\tfrac{1}{2}\sigma'_{ij}\,\sigma'_{ij} = \bar{\sigma}_o^2 \text{ on } \bar{z} = \bar{z}_p \qquad (3.5.6)$$

Using equations (3.3.5), (3.3.14) and (3.3.15) this condition can be written

$$\left(2\bar{\mu} + \frac{\bar{\sigma}_o}{\sqrt{\bar{I}}}\right)^2 \bar{I} = \bar{\sigma}_o^2 \text{ on } \bar{z} = \bar{z}_p \qquad (3.5.7)$$

Since only thin walled tubes have been considered in this chapter the amount of material extruded from the inner and outer surfaces of the tube will be approximately the same. It seems reasonable therefore to assume that these extruded values will be identical and consequently in our two-dimensional model it is assumed that $\bar{x} = 0$ is a plane of symmetry. The velocity component $\bar{u}$ must therefore satisfy

$$\bar{u}(o,\bar{z},\bar{t}) = 0, \; o \leq \bar{z} \leq \bar{z}_p \; . \qquad (3.5.8)$$

It should be noted that the velocity component and the pressure terms are time dependent but the derivatives with respect to t have been disregarded in the governing equations of motion. The system is thus assumed to be quasi-steady and no initial conditions for it are required.

Let us now consider the thermal boundary conditions. From symmetry there will be no heat flux across the planes $\bar{z} = o$ and $\bar{x} = o$ and hence the conditions

$$\frac{\partial T}{\partial \bar{z}}(\bar{x},o,\bar{t}) = 0, \; \frac{\partial T}{\partial \bar{x}}(o,\bar{z},\bar{t}) = 0, \qquad (3.5.9)$$

must be satisfied. At the plastic/solid interface it is natural to

impose continuity of both the temperature and the component of heat flux normal to the surface, giving the conditions

$$T(\bar{x},\bar{z}_p,\bar{t}) = T_s(\bar{x},\bar{z}_p,\bar{t}) \tag{3.5.10}$$

and

$$k\frac{\partial T}{\partial n}(\bar{x},\bar{z}_p,\bar{t}) = k_s\frac{\partial T_s}{\partial n}(\bar{x},\bar{z}_p,\bar{t}) \ , \tag{3.5.11}$$

where $\frac{\partial}{\partial n}$ denotes differentiation along the normal to the surface $\bar{z} = \bar{z}_p(\bar{x},\bar{t})$. Equation (3.5.11) may be expressed in the alternative form

$$k\left[\frac{\partial T}{\partial \bar{z}} - \frac{\partial \bar{z}_p}{\partial \bar{x}}\frac{\partial T}{\partial \bar{x}}\right] = k_s\left[\frac{\partial T_s}{\partial \bar{z}} - \frac{\partial \bar{z}_p}{\partial \bar{x}}\frac{\partial T_s}{\partial \bar{x}}\right] \text{on } \bar{z} = \bar{z}_p \ . \tag{3.5.12}$$

Over the time scales considered here heat transfer will only be significant in the solid close to the plastic/solid interface. It is reasonable to assume, therefore, that the tube has infinite length and that far away from $\bar{z} = \bar{z}_p$ the temperature maintains its ambient value. Expressed mathematically this condition is

$$T_s(\bar{x},\bar{z},\bar{t}) \to T_{AM} \text{ as } \bar{z} \to \infty \tag{3.5.13}$$

At the outer surfaces of the solid region, $\bar{x} = \pm h/2$, we shall assume that heat is lost by radiation and forced convection. This condition may be expressed mathematically as

$$-k_s\frac{\partial T}{\partial \bar{x}} = -h_c\left[T_s - T_{AM}\right] - \sigma\varepsilon(T_s^4 - T_{AM}^4), \text{ on } \bar{x} = h/2, \tag{3.5.14}$$

where hc is the surface heat transfer coefficient, σ is the Stefan-Boltzman constant and ε is the surface emissivity. The same condition

can be applied to the surface $\bar{x} = -h/2$ but this need not be considered in view of the symmetry condition $(3.5.9)_2$. For the plastic region the outer surfaces are continuously moving with time, and so it is very difficult to specify precise conditions on these surfaces. In order to make the problem tractable we assume that these outer surfaces remain fixed and that heat is lost at the surfaces by forced convection and radiation, as for the solid region, in which case we may write

$$- k \frac{\partial T}{\partial \bar{x}} = - h_c \left[T - T_{AM} \right] - \sigma\varepsilon(T^4 - T_{AM}^4) \text{ on } \bar{x} = h/2 \qquad (3.5.15)$$

Finally it is necessary to specify the initial temperature profiles at the start of phase II. The appropriate values are those occurring at the end of the conditioning phase, so we have in the solid region

$$T_s(\bar{x},\bar{z},o) = T_c(\bar{z}) \ . \qquad (3.5.16)$$

An initial condition for the plastic region is unnecessary since the region is assumed not to exist at $t = 0$.

All the relevant boundary and initial conditions have been given above, but it is helpful to express these in dimensionless form.

On dividing both sides of equation (3.5.3) by the quantity $\frac{1}{2}\rho w_\infty^2 h$ and making use of the definitions (3.4.5) and (3.4.25) we have, after a little rearrangement, the dimensionless equation

$$\int_{-\frac{1}{2}}^{\frac{1}{2}} c_p \, Re \, P \Big|_{z=z_p(x,t)} + \frac{2}{\beta^2} \left[\mu + \frac{B\sigma_o}{2\sqrt{I}} \right] \left[\frac{\partial w}{\partial x} + \beta^2 \frac{\partial u}{\partial z} \right] \Big|_{z=z_p(x,t)} \frac{\partial z_p}{\partial x}$$

$$-4 \left[\mu + \frac{B\sigma_o}{2\sqrt{I}} \right] \frac{\partial w}{\partial z} \Big|_{z=z_p(x,t)} dx = c_p Re \qquad (3.5.17)$$

On substituting equation (3.4.27) into the above the pressures p_o and p_1 must satisfy

$$\int_{-\frac{1}{2}}^{\frac{1}{2}} \Bigg(c_p \, Re \, p_o \Big|_{z=z_p(x,t)} + \left\{ p_1 + \frac{2}{\beta^2} \left(\mu + \frac{\beta \sigma_o}{2\sqrt{I}} \right) \left(\frac{\partial w}{\partial x} + \beta^2 \frac{\partial u}{\partial z} \right) \frac{\partial z_p}{\partial x} \right.$$

$$\left. - 4 \left| \mu + \frac{B\sigma_o}{2\sqrt{I}} \right| \frac{\partial w}{\partial z} \right\} \Big|_{z=z_p(x,t)} \Bigg) dx = c_p \, Re \qquad (3.5.18)$$

With the use of definitions (3.4.5), (3.4.15) and (3.4.25) the boundary conditions on the velocity components (3.5.4), (3.5.5) and (3.5.8) take the forms

$$v(x,o,t) = 0, \; w(x,o,t) = 0, \; \frac{\partial u}{\partial x}(x,o,t) = 0; \; -\tfrac{1}{2} \leqslant x \leqslant \tfrac{1}{2}, \qquad (3.5.19)$$

$$\left.\begin{aligned} u(x,z_p,t) &= 0, \\ v(x,z_p,t) &= 1, \\ w(x,z_p,t) &= -w_o(t), \end{aligned}\right\} \quad -\tfrac{1}{2} \leqslant x \leqslant \tfrac{1}{2} \qquad (3.5.20)$$

where $w_o(t)$ is defined by $w_o(t) = W_o(t)/w_\infty$ (3.5.21)

and the Bingham yield criterion (3.5.7) becomes

$$\left(\mu + \frac{B\sigma_o}{2\sqrt{I}} \right)^2 I = \frac{B^2 \sigma_o^2}{4} \quad \text{on } z = z_p \qquad (3.5.22)$$

The corresponding thermal boundary conditions (3.5.9), (3.5.10), (3.5.12), (3.5.13), (3.5.14) and (3.5.15), with the aid of definitions (3.4.1) and (3.4.33), can be written

$$\frac{\partial \theta}{\partial z}(x,o,t) = 0, \; \frac{\partial \theta}{\partial x}(o,z,t) = 0, \qquad (3.5.23)$$

$$\theta(x,z_p,t) = \theta_s(x,z_p,t) \; , \qquad (3.5.24)$$

$$k\left[\frac{\partial\theta}{\partial z} - \frac{\partial z_p}{\partial x}\frac{\partial\theta}{\partial x}\right] = k_s\left[\frac{\partial\theta_s}{\partial z} - \frac{\partial z_p}{\partial x}\frac{\partial\theta_s}{\partial x}\right] \quad \text{on } z = z_p, \tag{3.5.25}$$

$$\theta_s(x,z,t) \to 0 \text{ as } z \to \infty \tag{3.5.26}$$

$$-\frac{\partial\theta}{\partial x} = -Bi\theta - H_R\{(\theta(T_c/T_{AM}-1)+1)^4-1\} \text{ on } x = \tfrac{1}{2}. \tag{3.5.27}$$

and

$$-\frac{\partial\theta_s}{\partial x} = -Bi\theta_s - H_R\{(\theta_s(T_c/T_{AM}-1)+1)^4-1\} \text{ on } x = \tfrac{1}{2}, \tag{3.5.28}$$

where Bi is the Biot number [30] defined by

$$Bi = \frac{h_c\, h}{k}\ , \tag{3.5.29}$$

and the dimensionless parameter H_R is given by

$$H_R = \frac{\sigma\varepsilon h\, T_{AM}^3}{k(T_c/T_{AM}-1)}\ . \tag{3.5.30}$$

The dimensionless form of the initial condition (3.3.16) is

$$\theta_s(x,z,o) = \theta_c(z)\ . \tag{3.5.31}$$

Having derived the governing equations and boundary conditions a number of solutions are obtained in the following two chapters after introducing various simplifying assumptions.

CHAPTER 4

VISCOUS FLUID MODELS

4.1 Introduction

In Chapter 3 the softened layer of material, the so-called plastic region, was modelled as a Bingham substance, and it was remarked that with this assumption the equations become tractable. They remain difficult to solve, however, and initially it is found helpful to introduce the further postulate that B, the Bingham number, is zero. Recalling equations (3.4.28) to (3.4.31) it is clear that with the latter assumption the softened material is represented by a viscous fluid, and it is then appropriate to assume that this fluid has a large viscosity which will in general be a non-linear function of the temperature θ and the strain rates $\partial v/\partial z$ and $\partial v/\partial x$. i.e.

$$\mu = \mu(\theta, \partial v/\partial z, \partial v/\partial x) \qquad (4.1.1)$$

Some solutions for the viscous fluid model are given in this chapter, whereas investigation of the more complicated equations for the Bingham substance is delayed until Chapter 5.

4.2 Governing Equations and Boundary and Initial Conditions

The general equations for a thin tube when the plastic region is modelled by a viscous fluid, found from the equations of motion (3.4.28), (3.4.29) and (3.4.30) and the energy equations (3.4.37) and

and (3.4.40) by putting B = 0 are

$$\frac{C_p Re}{2}\frac{\partial p_o}{\partial x} + \frac{1}{2}\frac{\partial p_1}{\partial x} = \frac{\partial}{\partial z}\left(\mu\left(\frac{\partial w}{\partial x} + \beta^2\frac{\partial u}{\partial z}\right)\right) + 2\frac{\partial}{\partial x}\left(\mu\frac{\partial u}{\partial x}\right) \quad , \tag{4.2.1}$$

$$\frac{\partial}{\partial z}\left(\mu\frac{\partial v}{\partial z}\right) + \frac{1}{\beta^2}\frac{\partial}{\partial x}\left(\mu\frac{\partial v}{\partial x}\right) = 0 \ , \tag{4.2.2}$$

$$\frac{C_p Re}{2}\frac{\partial p_o}{\partial z} + \frac{1}{2}\frac{\partial p_1}{\partial z} = 2\frac{\partial}{\partial z}\left(\mu\frac{\partial w}{\partial z}\right) + \frac{1}{\beta^2}\frac{\partial}{\partial x}\left(\mu\left(\frac{\partial w}{\partial x} + \beta^2\frac{\partial u}{\partial z}\right)\right) \ , \tag{4.2.3}$$

$$\frac{\partial}{\partial z}\left(k\frac{\partial\theta}{\partial z}\right) + \frac{1}{\beta^2}\frac{\partial}{\partial x}\left(k\frac{\partial\theta}{\partial x}\right) + Br\mu\left(\left(\frac{\partial v}{\partial z}\right)^2 + \frac{1}{\beta^2}\left(\frac{\partial v}{\partial x}\right)^2\right) =$$

$$c_v Pe\left(u\frac{\partial\theta}{\partial x} + w\frac{\partial\theta}{\partial z}\right) + \frac{c_v}{Fo}\frac{\partial\theta}{\partial t} \quad , \quad 0 \leqslant z \leqslant z_p \tag{4.2.4}$$

and

$$\frac{\partial}{\partial z}\left(k_s\frac{\partial\theta_s}{\partial z}\right) + \frac{1}{\beta^2}\frac{\partial}{\partial x}\left(k_s\frac{\partial\theta_s}{\partial x}\right) = -Pe\ W_o\ c_{v_s}\frac{\partial\theta_s}{\partial z} + \frac{c_{v_s}}{F_o}\frac{\partial\theta_s}{\partial t}, \quad z \geqslant z_p. \tag{4.2.5}$$

This system of equations remains complicated, however, and further simplification are necessary if analytical solutions are to be obtained.

When friction welding thin walled tubes the rubbing velocity v varies only slightly in the radial direction across the interface and metallurgical examination of a diametric cross-section, of a welded specimen reveals that the isotherms are then almost perpendicular to the

z-axis. The above observation suggests that the temperature profiles θ and θ_s and hence z_p, since we later define z_p to be an isotherm, may, to a first approximation, be assumed to be independent of x. This assumption on z_p implies, with reference to conditions $(3.5.19)_2$ and $(3.5.20)_3$, that the velocity component w is independent of x on both $z = 0$ and $z = z_p$. It thus seems reasonable to assume that w is independent of x throughout the range $-\frac{1}{2} \leqslant x \leqslant \frac{1}{2}$. Hence for the whole of this chapter we postulate

$$z_p = z_p(t),\ v = v(z,t),\ w = w(z,t),\ \theta = \theta(z,t),\ \theta_s = \theta_s(z,t) \qquad (4.2.6)$$

and it is this key assumption which allows us to proceed.further and obtain analytic solutions appropriate to the friction welding of thin tubes. On splitting equations (4.2.1) to (4.2.3) into two subsystems, one O(Re Cp) and the other O(1), and making use of the postulate (4.2.6), one obtains

$$O(Cp\ Re) \quad \frac{\partial p_o}{\partial x} = 0 \ , \qquad (4.2.7)$$

$$\frac{\partial p_o}{\partial z} = 0 \ , \qquad (4.2.8)$$

$$O(1) \quad \frac{1}{2}\frac{\partial p_1}{\partial x} = \beta^2 \frac{\partial}{\partial z}\left(\mu \frac{\partial u}{\partial z}\right) + 2\frac{\partial}{\partial x}\left(\mu \frac{\partial u}{\partial x}\right) \ , \qquad (4.2.9)$$

$$\frac{\partial}{\partial z}\left(\mu \frac{\partial v}{\partial z}\right) = 0 \ , \qquad (4.2.10)$$

$$\frac{1}{2}\frac{\partial p_1}{\partial z} = 2\frac{\partial}{\partial z}\left(\mu \frac{\partial w}{\partial z}\right) + \frac{\partial}{\partial x}\left(\mu \frac{\partial u}{\partial z}\right) \ . \qquad (4.2.11)$$

It is easily seen through (4.1.1) and $(4.2.6)_{2,4}$ that μ may now be taken to be independent of x and expressed in the form

$$\mu = \mu(\mathcal{Q}, \partial v/\partial z) \ . \tag{4.2.12}$$

The equation of incompressibility (3.4.30) remains in the form

$$\frac{\partial u}{\partial x} + \frac{\partial w}{\partial z} = 0, \tag{4.2.13}$$

but is repeated here for convenience.

On splitting the condition (3.5.18) into two subsystems, one $O(Cp\ Re)$ and the other $O(1)$, and putting $B = 0$, the conditions on the pressure component, in view of assumption (4.2.6) reduce to

$$O(Cp\ Re) \qquad \int_{-\frac{1}{2}}^{\frac{1}{2}} p_o(x,z_p,t)\ dx = 1, \tag{4.2.14}$$

and

$$O(1) \qquad \int_{-\frac{1}{2}}^{\frac{1}{2}} p_1(x,z_p,t) - 4\mu \frac{\partial w}{\partial z}\bigg|_{z=z_p} dx = 0 \tag{4.2.15}$$

The boundary conditions on the velocity components u, v and w are unaltered by assumption (4.2.6), consequently we can write

$$\frac{\partial u}{\partial z}(x,o,t) = 0,\ -\tfrac{1}{2} \leqslant x \leqslant \tfrac{1}{2};\ v(o,t) = 0,\ w(o,t) = 0, \tag{4.2.16}$$

$$u(x,z_p,t) = 0,\ -\tfrac{1}{2} \leqslant x \leqslant \tfrac{1}{2};\ v(z_p,t) = 1,\ w(z_p,t) = -w_o(t), \tag{4.2.17}$$

$$u(o,z,t) = 0,\ 0 \leqslant z \leqslant z_p(t) \ . \tag{4.2.18}$$

For the viscous fluid model the Bingham yield criterion (3.5.22) is no longer appropriate and z_p, the position of the 'yield surface' , must

be determined by an alternative condition. The obvious choice is to assume that the temperature on the plastic/solid interface remains fixed at the conditioning temperature and therefore recalling definition (3.4.34), we assume that z_p is the isotherm $\theta = 1$. Using condition (3.5.24) and the postulate (4.2.6), the quantity z_p is therefore defined by

$$\theta(z_p,t) = \theta_s(z_p,t) = 1 \tag{4.2.19}$$

In view of assumption $(4.2.6)_{4,5}$ the heat flow has been restricted to the one-dimensional flow in the direction of the z-axis and so the conditions governing the loss of heat by convection and radiation over the 'curved' surfaces of the tubes, (3.5.27) and (3.5.28) can no longer be employed. However, for this case of uni-directional heat flow the heat loss through the outer surface may be modelled by a volumetric heat loss which can be incorporated into the problem by introducing a heat sink H into the energy equations (4.2.4) and (4.2.5). The latter can then be shown, with the aid of $(4.2.6)_{4,5}$, to take the forms

$$\frac{\partial}{\partial z}\left(k\frac{\partial\theta}{\partial z}\right) + Br\mu\left(\frac{\partial v}{\partial z}\right)^2 - 2H_L(\theta) =$$

$$c_v pew\frac{\partial\theta}{\partial z} + \frac{c_v}{Fo}\frac{\partial\theta}{\partial t}\ , \quad 0 \leqslant z \leqslant z_p, \tag{4.2.20}$$

and

$$\frac{\partial}{\partial z}\left(k_s\frac{\partial\theta_s}{\partial z}\right) - 2H_L(\theta_s) = -Pew_o c_v\frac{\partial\theta_s}{\partial z} + \frac{ev_s}{Fo}\frac{\partial\theta_s}{\partial t}\ , \quad z \geqslant z_p \tag{4.2.21}$$

where H_L is given by (see chapter 3)

$$H_L(u) = B_i u + H_R\{(u(T_c/T_{AM} - 1) + 1)^4 - 1\} \tag{4.2.22}$$

Conditions (3.5.23), (3.5.24) and (3.5.26) remain unchanged, but are now rewritten for convenience:-

$$\frac{\partial \theta}{\partial z}(o,t) = 0 \qquad (4.2.23)$$

$$\theta(z_p,t) = \theta_s(z_p,t) = 1, \qquad (4.2.24)$$

$$\theta_s(z,t) \to 0 \text{ as } z \to \infty \qquad (4.2.25)$$

condition $(3.5.23)_2$ being satisfied identically for all x for this one dimensional model. However, under the postulate $(4.2.6)_{1,4}$ condition (3.5.25) reduces to

$$k \frac{\partial \theta}{\partial z}(z_p,t) = k_s \frac{\partial \theta_s}{\partial z}(z_p,t) , \qquad (4.2.26)$$

and rewriting the initial condition (3.5.31) we have

$$\theta_s(z,o) = \theta_c(z) . \qquad (4.2.27).$$

In the following sections the partial differential equations (4.2.7) to (4.2.13), (4.2.20) and (4.2.21) are solved subject to the boundary conditions (4.2.14) to (4.2.18) and (4.2.23) to (4.2.25) and the initial condition (4.2.27), under a number of simplifying assumptions.

4.3 Velocity and Pressure Profiles - No Burnoff

A key assumption made by Atthey [22] whose model is discussed in some detail in the following section, was that no axial shortening (or burnoff) takes place. In all friction welds some material is

extruded from the plastic region and in practice, therefore, axial shortening of the specimens must occur. However, the assumption of no burnoff considerably simplifies the equations and in order to obtain a simple analytical solution which has some of the qualitative features of a more general solution Atthey's approach seems reasonable. For the present, therefore, we follow Atthey and assume

$$w \equiv 0, \tag{4.3.1}$$

in which case the Peclet number, Pe is also zero.

Remembering, in view of (4.1.1), $(4.2.6)_2$ and $(4.2.6)_4$, that μ may be assumed to be independent of x the equations of motion for the plastic region (4.2.7) to (4.2.11) reduce, with the aid of (4.3.1) to

$$O(CpRe)\ \frac{\partial p_o}{\partial x} = 0, \tag{4.3.2}$$

$$\frac{\partial p_o}{\partial z} = 0, \tag{4.3.3}$$

$$O(1)\ \frac{\partial p_1}{\partial x} = 2\beta^2 \frac{\partial}{\partial z}\left(\mu \frac{\partial u}{\partial z}\right) + 4\mu \frac{\partial^2 u}{\partial x^2}\ , \tag{4.3.4}$$

$$\frac{\partial}{\partial z}\left(\mu \frac{\partial v}{\partial z}\right) = 0\ , \tag{4.3.5}$$

and

$$\frac{\partial p_1}{\partial z} = 2\mu \frac{\partial^2 u}{\partial x \partial z}\ , \tag{4.3.6}$$

whilst the condition of incompressibility (4.2.13) becomes

$$\frac{\partial u}{\partial x} = 0. \tag{4.3.7}$$

The boundary conditions (4.2.14) to (4.2.18) are unchanged under assumption (4.3.1) but clearly conditions $(4.2.16)_3$ and $(4.2.17)_3$

are no longer necessary.

The partial differential equations (4.3.2) to (4.3.7) are integrated below to give the pressure and velocity profiles in the plastic region.

It is obvious from equations (4.3.2) and (4.3.3) that the dimensionless pressure p_o is a function of t only, that is

$$p_o = p_o(t) \tag{4.3.8}$$

and substitution of the above into the boundary condition (4.2.14) then yields the solution

$$p_o = 1. \tag{4.3.9}$$

The hydrostatic pressure, therefore, is approximately constant throughout the plastic region.

Integrating the equation of incompressibility (4.3.7) with respect to x we deduce that the velocity component u takes the form

$$u = u(z,t), \tag{4.3.10}$$

and making use of the boundary condition (4.2.18) it follows that

$$u \equiv 0. \tag{4.3.11}$$

On substituting this zero value for u into the equations (4.3.4) and (4.3.6) it is clear that the quantity p_1 is also a function of time only, and to satisfy the condition (4.2.15) it is necessary that

$$p_1 \equiv 0. \tag{4.3.12}$$

Now turning our attention to the velocity component $v(z,t)$ we obtain, after integrating equation (4.3.5) with respect to z, the equation

$$\mu \frac{\partial v}{\partial z} = \tau(t), \tag{4.3.13}$$

Where $\tau(t)$ is the dimensionless shear stress. A further integration of this equation with respect to z and the use of the boundary condition $(4.2.16)_2$ yields

$$v = \tau \int_0^z \frac{dz}{\mu} \tag{4.3.14}$$

In order that condition $(4.2.17)_2$ is satisfied it then follows that the shear stress τ and the thickness of the plastic region z_p are related through

$$1 = \tau \int_0^{z_p} \frac{dz}{\mu} \tag{4.3.15}$$

The integrals in equations (4.3.14) and (4.3.15) cannot be evaluated until the viscosity μ is known in terms of z and t. In general μ will be specified as a function of θ and $\partial v/\partial z$ which in turn depend on z and t. It will in these situations, therefore, be necessary to solve equations (4.3.14) and (4.3.15) simultaneously with the energy equations (4.2.20) and (4.2.21).

In the following two sections the velocity profiles derived above are used to obtain some simple solutions appropriate to phase II of the weld cycle.

4.4 Summary of Atthey's Solution - No Burnoff

The only published work adopting the viscous fluid model is due to Atthey [22]. His equations can be derived from those stated in section 4.2 under a number of simplifying assumptions, and since the solution is important for later developments in this thesis a summary of his paper is now given.

In Atthey's model the heat loss terms H_L in equations (4.2.20) and (4.2.21) are neglected. This is a reasonable assumption since it can be shown, with the aid of data given in Krieth and Black [30] that the Biot number Bi and the radiation coefficient H_R are $O(0.01)$.

In general the specific heat capacities c_v and c_{vs} and the thermal conductivities k and k_s are found to be non-linear functions of the temperature θ. Temperatures in the plastic region range from 700^oC to 1200^oC when welding mild steel and over such a large range it seems that the temperature dependence of the above mentioned quantities could be important. However, in order to simplify the equations Atthey assumed that c_v, c_{v_s}, k and k_s are all constant and recalling definition (3.4.34) , one can without loss of generality, take $c_v = c_{v_s} = k = k_s = 1$.

Atthey also assumed, as has been discussed in section 4.3 that no axial shortening takes place. The cooling effect due to forced convection is therefore absent and consequently the temperatures derived from his simplified model will be over estimates.

Finally Atthey neglected the conditioning phase assuming that all points in the tube, $z > 0$, are initally at ambient temperature, apart from the interface, $z = 0$, which was assumed to be initially at conditioning temperature.

4.4.1. The equations of energy balance and boundary conditions.

Introducing the above assumptions into the equations of energy balance (4.2.20) and (4.2.21) the latter reduce to

$$\frac{\partial^2 \theta}{\partial z^2} + Br\mu\left(\frac{\partial v}{\partial z}\right)^2 = \frac{1}{F_o}\frac{\partial \theta}{\partial t} \quad , \quad 0 \leq z \leq z_p \qquad (4.4.1)$$

and

$$\frac{\partial^2 \theta_s}{\partial z^2} = \frac{1}{F_o}\frac{\partial \theta_s}{\partial t} \quad , \qquad z \geq z_p \quad . \qquad (4.4.2)$$

Equation (4.4.2) is the usual one-dimensional unsteady heat conduction equation, whereas (4.4.1) contains an extra internal heat generation term arising from viscous shearing within the plastic region.

The assumptions introduced at the beginning of section 4.4 slightly modify the thermal initial condition and some of the thermal boundary conditions stated in section 4.2. Since the thermal conductivities k and k_s are both taken to be unity, equation (4.2.26) is replaced by

$$\frac{\partial \theta}{\partial z}(z_p, t) = \frac{\partial \theta_s}{\partial z}(z_p, t), \qquad (4.4.3)$$

Whereas neglecting the conditioning phase implies that the initial condition (4.2.27) reduces to

$$\theta_s(z,0) = 0. \qquad (4.4.4)$$

The remaining conditions (4.2.23), (4.2.24) and (4.2.25) are unchanged.

4.4.2 Similarity Transformation

As we remarked earlier in this chapter the viscosity is in general a non-linear function of temperature θ and strain rate $\partial v/\partial z$, and over the ranges of temperature and strain rate that are present during a normal friction welding cycle, one would expect the variation in viscosity to be important as is seen in Section 4.12. However, in order to obtain a simple analytical solution Atthey made the further assumption that the viscosity μ is constant and recalling definition (3.4.8), we can therefore take, without loss of generality.

$$\mu = 1. \tag{4.4.5}$$

On substituting (4.4.5) into equations (4.3.14) and (4.3.15), the integrations are readily performed leading to

$$v = \tau(t)z, \tag{4.4.6}$$

and

$$\tau = 1/z_p, \tag{4.4.7}$$

and with the aid of these equations the energy equation for the plastic region (4.4.1) can be expressed

$$\frac{\partial^2\theta}{\partial z^2} + \frac{Br}{z_p^2} = \frac{1}{F_o}\frac{\partial\theta}{\partial t}, \quad 0 \leq z \leq z_p. \tag{4.4.8}$$

The forms of the energy equations (4.4.2) and (4.4.8) suggest the existence of a similarity solution where the similarity variable η is defined by

$$\eta = \frac{z}{z_p} \quad , \tag{4.4.9}$$

provided that z_p grows with time according to

$$z_p = 2\,\alpha\sqrt{F_o\,t} \quad , \tag{4.4.10}$$

α being a constant of proportionality.

Substituting equations (4.4.9) and (4.4.10) into equation (4.4.8) leads to the ordinary differential equation

$$\frac{d^2\theta}{d\eta^2} + 2\alpha^2\eta\,\frac{d\theta}{d\eta} + Br = 0, \quad 0 \leq \eta \leq 1 \tag{4.4.11}$$

and applying a similar procedure to equation (4.4.2) for the solid region yields

$$\frac{d^2\theta_s}{d\eta^2} + 2\alpha^2\eta\frac{d\theta}{d\eta} = 0, \qquad \eta \geq 1 \tag{4.4.12}$$

In terms of η the boundary and initial conditions (4.2.23), (4.2.24), (4.2.25), (4.4.3) and (4.4.4) can be written

$$\frac{d\theta}{d\eta}(o) = 0, \tag{4.4.13}$$

$$\theta(1) = \theta_s(1) = 1, \tag{4.4.14}$$

$$\frac{d\theta}{d\eta}(1) = \frac{d\theta_s}{d\eta}(1), \tag{4.4.15}$$

$$\theta_s(\eta) \to 0 \text{ as } \eta \to \infty \ . \tag{4.4.16}$$

It should be noted that the two conditions (4.2.26) and (4.4.4) are replaced by the single condition (4.4.16) as is customary in this type of solution.

4.4.3 Temperature profiles.

On multiplying equation (4.4.11) by $e^{\alpha^2\eta^2}$ it may be readily integrated twice with respect to η yielding upon application of the boundary condition (4.4.13) and $(4.4.14)_1$, the solution

$$\theta = 1 + \frac{Br}{\alpha^2} \int_{\alpha\eta}^{\alpha} D(u)\, du, \quad 0 \leq \eta \leq 1 . \tag{4.4.17}$$

In the above D(u) is Dawson's integral, [31], which is defined by

$$D(u) = e^{-u^2} \int_0^u e^{v^2}\, dv \tag{4.4.18}$$

It should be noted that equation (22) in Attheys paper [22] is incorrect due to a sign mistake in the second exponential term and the corrected expression is given by (4.4.17).

Integrating equation (4.4.12) in a similar manner to (4.4.11) and applying the boundary conditions $(4.4.14)_2$ and (4.4.16) gives the solution

$$\theta_s = \mathrm{erfc}(\alpha\eta)/\mathrm{erfc}(\alpha), \qquad \eta \geq 1 \tag{4.4.19}$$

in which erfc(x) is the complementary error function [27] defined by

$$\mathrm{erfc}(u) = \frac{2}{\sqrt{\pi}} \int_u^{\infty} e^{-t^2} dt. \tag{4.4.20}$$

Finally substituting equations (4.4.17) and (4.4.19) into condition (4.4.15) leads to the following algebraic equation in α.

$$\frac{2\alpha^2 e^{-\alpha^2}}{Br\sqrt{\pi}} - \operatorname{erfc}(\alpha)\, D(\alpha) = 0 \qquad (4.4.21)$$

There is no analytical solution to the above equation and a numerical solution must be sought. The Newton-Raphson iterative procedure is found to be a suitable method for solving (4.4.21) since the derivative with respect to α can easily be obtained. As with all iterative procedures it is necessary to find an approximate starting value. On expanding (4.4.21) for small Br we obtain the approximation

$$\alpha \approx \frac{\sqrt{\pi}}{2} Br\left(1 - Br + O(Br^2)\right) , \qquad (4.4.22)$$

which may be used to obtain starting values for α when Br is small. It is also felt useful to give the expansion of (4.4.21) for large values of Br, not only to obtain starting values for α when Br is large, but as a check on the accuracy of the approximate solution which is developed in a later section.

Referring to the definition of Dawsons integral (4.4.18) it is seen that $D(\alpha)$ may be expressed in the form

$$D(\alpha) = \frac{e^{-\alpha^2}}{2} \int_{-\alpha}^{\alpha} e^{v^2}\, dv \qquad (4.4.23)$$

Expressing the above in the form

$$D(\alpha) = \frac{e^{-\alpha^2}}{4} \int_{-\alpha}^{\alpha} 2ve^{v^2} \frac{dv}{v} , \qquad (4.4.24)$$

and integrating by parts results in the expression

$$D(\alpha) = \frac{1}{2\alpha} + \frac{e^{-\alpha^2}}{4}\int_{-\alpha}^{\alpha}\frac{e^{v^2}}{v^2}\,dv \qquad (4.4.25)$$

This procedure may be repeated indefinitely, however, for our purposes the first two terms are sufficient and we have

$$D(\alpha) = \frac{1}{2\alpha} + \frac{1}{4\alpha^3} + \frac{3e^{-\alpha^2}}{8}\int_{-\alpha}^{\alpha}\frac{e^{v^2}}{v^4}\,dv. \qquad (4.4.26)$$

The expansion for enfc(α) for large α is found in Carslaw and in Jaeger[27] and given by

$$\operatorname{erfc}(\alpha) = \frac{e^{-\alpha^2}}{2}\left\{\frac{1}{\alpha} - \frac{1}{2\alpha^3} + \frac{3}{4\alpha^5} + O\left(\frac{1}{\alpha^7}\right)\right\} \qquad (4.4.27)$$

Now on substituting equation (4.4.26) and (4.4.27) into (4.4.21) and truncating the expression after the first two terms, the approximate solution for α is found to be

$$\alpha = \left(\frac{\sqrt{\pi}}{8}\right)^{\frac{1}{4}} Br^{\frac{1}{4}} + O\left(Br^{\frac{-1}{4}}\right) \qquad (4.4.28)$$

Using expansions (4.4.22) and (4.4.28) to obtain starting values, the values of α are computed for various values of Br and the results are presented in table 4.1.

Br	α
0.1	0.081
0.2	0.149
0.3	0.207
0.4	0.259
0.5	0.305
0.6	0.346
0.7	0.383
0.8	0.418
0.9	0.449
1.0	0.478
2.0	0.690
4.0	0.927
6.0	1.073
8.0	1.179
10.0	1.263

Table 4.1.

Having obtained values of α, the temperature profiles θ and θ_s, the position of the plastic/solid interface $z_p(t)$ and the dimensionless shear stress $\tau(t)$ are obtained for various values of the Brinkman number, Br , using equations (4.4.17), (4.4.19), (4.4.10) and (4.4.7) respectively. These results are presented and discussed in section 4.6.

4.5 Variable Viscosity - No Burnoff

Although in the last section it was assumed that the viscosity remained constant it has already been stated that for the one-dimensional models under consideration the viscosity μ will, in general, be a non-linear function of the temperature T and the strain rate $\partial v/\partial z$. A form for the dependence of μ on T and $\partial v/\partial z$ is now postulated.

Referring to equation (3.3.2) the relationship appropriate to our one-dimensional model is

$$\frac{\partial v}{\partial z} = A(\sinh\alpha\sigma_{yz})^m \exp(-Q/RT), \tag{4.5.1}$$

which may be rearranged to yield

$$\sinh(\alpha\sigma_{yz}) = \left(\frac{1}{A}\right)^{\frac{1}{m}} \left(\frac{\partial v}{\partial z}\right)^{\frac{1}{m}} \exp\left(\frac{Q}{mRT}\right) . \tag{4.5.2}$$

The form of equation (4.5.2) is much too complicated to use in obtaining simple analytic solution. We therefore postulate here that the left hand side of this equation be replaced by a linear term, that is

$$\sigma_{yz} = H\left(\frac{\partial v}{\partial z}\right)^{\frac{1}{m}} \exp\left(\frac{Q}{mRT}\right) , \tag{4.5.3}$$

where H is a constant. Equation (4.5.3) is a good approximation to (4.5.2) for small values of σ_{yz} but it becomes less reliable as σ_{yz} increases. However even for large σ_{yz} it retains the qualitative effects of varying T and $\partial v/\partial z$.

We shall now compare equation (4.5.3) with the appropriate relationship between σ_{yz} and $\partial v/\partial z$ for the viscous fluid model.

Putting B = 0 in equation (3.4.14) we obtain

$$\sigma_{yz} = \tau_{\infty}\, \mu \frac{\partial v}{\partial z} \quad , \tag{4.5.4}$$

where τ_{∞} is defined by

$$\tau_{\infty} = \frac{\mu_o \omega \bar{R}}{2 z_{po}} \tag{4.5.5}$$

It is easily seen that if we put

$$H = \tau_{\infty} \tag{4.5.6}$$

and assume that μ takes the form

$$\mu = \left(\frac{\partial v}{\partial z}\right)^{\frac{1}{m}-1} \exp\left\{\frac{Q}{mR\left(\theta(T_c - T_{AM}) + T_{AM}\right)}\right\}, \tag{4.5.7}$$

where T has been replaced by θ using (3.4.34), then equation (4.5.3) may be replaced by (4.5.4).

Although we now have an expression for the viscosity, which results in a relationship between the stress and strain rate tensors bearing the qualitative features of expression (3.3.2), it still remains difficult to handle. Therefore in this section a simple extension to Atthey's solution is sought to demonstrate the effect of the viscosity decaying with increasing temperature. To this end it is proposed to take μ to be independent of $\partial v/\partial z$ but to be inversely proportion to θ, and recalling definition (3.4.8) we can write

$$\mu = 1/\theta \qquad (4.5.8)$$

Although (4.5.7) predicts a much faster decay of μ with increasing θ than (4.5.8), the latter allows us to obtain a simple similarity solution which illustrates qualitatively the effect of viscosity decreasing as the temperature increases. A solution incorporating the full effect of equation (4.5.7) is delayed until Section 4.12.

4.5.1 Governing Equations

Substituting equation (4.5.8) into equation (4.3.14), the velocity component v becomes

$$v = \tau(t) \int_0^z \theta dz, \qquad (4.5.9)$$

and the corresponding relationship between τ and z_p (4.3.15) is

$$1 = \tau(t) \int_0^{z_p(t)} \theta dz. \qquad (4.5.10)$$

On substituting equations (4.5.8) and (4.5.9) into (4.4.1), the energy equation for the plastic region may be written

$$\frac{\partial^2 \theta}{\partial z^2} + Br\ \tau^2 \theta = \frac{1}{F_o} \frac{\partial \theta}{\partial t}, \qquad 0 \leq z \leq z_p. \qquad (4.5.11)$$

The energy equation for the solid region remains as equation (4.4.2) and the latter and equation (4.5.11) must now be solved subject

to the boundary conditions (4.2.23) (4.2.24), (4.2.25) and (4.4.3), and the initial conditions (4.4.4).

4.5.2 Similarity Transformation.

Again the forms of equations (4.4.2), (4.5.10) and (4.5.11) suggest the existence of a similarity solution, where the similarity variable is defined by equation (4.4.9). It is also necessary that z_p and τ depend on t through

$$z_p = 2\alpha_v \sqrt{F_o\, t}\ , \tag{4.5.12}$$

and

$$\tau = \beta_v/2\ \sqrt{Fo\ t}\ , \tag{4.5.13}$$

where α_v and β_v are constants of proportionality. Substituting equations (4.4.9), (4.5.12) and (4.5.13) into equations (4.5.11) yields the ordinary differential equation

$$\frac{d^2\theta}{d\eta^2} + 2\alpha_v^2\eta\frac{d\theta}{d\eta} + Br\,\beta_v^2\,\alpha_v^2\,\theta = 0, \qquad 0 \leq \eta \leq 1 \tag{4.5.14}$$

and the corresponding equation for the solid region is given by (4.4.12) with α replaced by α_v.

On substituting equations (4.4.9), (4.5.12) and (4.5.13) into equation (4.5.10) we obtain

$$1 = \beta_v\ \alpha_v \int_o^1 \theta(\eta)\ d\eta\ , \tag{4.5.15}$$

a relationship between α_v and β_v.

The two ordinary differential equations (4.4.12) and (4.5.14) must now be solved subject to conditions (4.4.13) to (4.4.16).

4.5.3 Temperature Profiles.

Clearly the temperature profile for the solid region θ_s will take the same form as (4.4.19) and, rewritten for convenience, it is

$$\theta_s = \operatorname{erfc}(\alpha_v \eta)/\operatorname{erfc}(\alpha_v), \qquad \eta \geq 1. \tag{4.5.16}$$

There does not seem to be an analytical closed form solution to equation (4.5.14), however, so a series solution is sought in the form

$$\theta = Co \sum_{n=o}^{\infty} A_n \eta^n, \qquad 0 \leq \eta \leq 1 \tag{4.5.17}$$

The presence of the coefficient Co allows us to take

$$A_o \equiv 1. \tag{4.5.18}$$

On substituting equation (4.5.17) for θ into equation (4.5.14) there results

$$Co \sum_{n=o}^{\infty} A_n \left(n(n-1)\eta^{n-2} + 2\alpha_v^2 n\eta^n + Br\beta_v^2\alpha_v^2\eta^n\right) = 0, \tag{4.5.19}$$

and by equating to zero the coefficients of η^n ($n = 0, 1, 2, \ldots$) we deduce that the A_n's are related by the difference equation

$$A_{n+2} = -\alpha_v^2 \frac{(2n + Br\beta_v^2)A_n}{(n+1)(n+2)}, \qquad n \geq 0. \tag{4.5.20}$$

Applying the boundary condition (4.4.13) to equation (4.5.17) gives the additional result

$$A_1 \equiv 0. \tag{4.5.21}$$

It is evident from equations (4.5.20) and (4.5.21) that

$$A_{2n+1} = 0, \qquad n \geq 0, \tag{4.5.22}$$

and

$$A_{2n+2} = -\alpha_v^2 \frac{(4n + Br\beta_v^2)}{2(2n+1)(n+1)} A_{2n}, \qquad n \geq 0 . \tag{4.5.23}$$

In view of equations (4.5.22) and (4.5.23) it is clear that equation (4.5.17) may now be expressed as

$$\theta = Co \sum_{n=0}^{\infty} A_{2n} \eta^{2n} , \qquad 0 \leq \eta \leq 1 , \tag{4.5.24}$$

where the A_{2n}'s are determined completely in terns of β_v, for all $n \geq 0$, by equations (4.5.18) and (4.5.23). Substituting the series (4.5.24) into conditions (4.4.14), and (4.5.15) yields the pair of equations

$$Co \sum_{n=0}^{\infty} A_{2n} = 1, \tag{4.5.25}$$

and

$$Co\beta_v\alpha_v \sum_{n=0}^{\infty} \frac{A_{2n}}{2n+1} = 1. \tag{4.5.26}$$

The constant Co is readily eliminated from the above two equations to give the following equation in α_v and β_v

$$\sum_{n=0} A_{2n} \left(1 - \alpha_v\beta_v/(2n+1)\right) = 0. \tag{4.5.27}$$

Finally substituting equations (4.5.16) and (4.5.24) into condition (4.4.15) leads to

$$Co \sum_{n=0}^{\infty} n A_{2n} = \frac{-\alpha_v e^{-\alpha_v}}{\sqrt{\pi}\ erfc(\alpha_v)} . \tag{4.5.28}$$

Using equation (4.5.25) to eliminate Co from the above, gives, after a little rearrangement,

$$\sum_{n=0}^{\infty} A_{2n} \left[n + \frac{\alpha_v e^{-\alpha_v^2}}{\sqrt{\pi}\ \mathrm{erfc}(\alpha_v)} \right] = 0, \qquad (4.5.29)$$

a second equation in α_v and β_v. Equations (4.5.27) and (4.5.29) must now be solved simultaneously.

There appears to be no analytic solution, however, and a numerical procedure must be adopted.

Equations (4.5.27) and (4.5.29) are readily solved using Powell's method of least squares [32] . This method is, again, an iterative procedure and approximate starting values are required. On expanding (4.5.27) and (4.5.29) for small values of Br, the approximate forms

$$\alpha_v = \frac{\sqrt{\pi}}{2} Br \left(1 - (\sqrt{\pi} + \frac{1}{3}) Br + O(Br^2)\right) , \qquad (4.5.30)$$

and

$$\beta_v = \frac{2}{\sqrt{\pi} Br} + 2 + O(Br) \qquad (4.5.31)$$

are obtained. Using these approximations, as starting values, the values of α_v and β_v were computed, using Powell's method, for small values of Br. For larger values of Br the values α_{v_n} and β_{v_n} were computed, using as starting values the values of $\alpha_{v_{n-1}}$ and $\beta_{v_{n-1}}$ from the previous computation. The summations were truncated after the first 15 terms and accuracy to 4 decimal places was obtained for all values of Br that were used. The results obtained are presented in table 4.2.

Br	α_v	β_v
0.1	0.078	12.352
0.2	0.141	6.660
0.3	0.193	4.739
0.4	0.238	3.760
0.5	0.276	3.164
0.6	0.310	2.759
0.7	0.340	2.465
0.8	0.367	2.240
0.9	0.392	2.062
1.0	0.415	1.918
2.0	0.572	1.220
4.0	0.734	0.804
6.0	0.828	0.638
8.0	0.893	0.544
10.0	0.942	0.481

Table 4.2

Having obtained values of α_v and β_v it is easy to compute Co using equation (4.5.25) and again, for all the values of Br used it proves sufficient to truncate the series after the first 15 terms.

The temperature profiles θ and θ_s, the thickness of the plastic region z_p and the dimensionless shear stress τ are then obtained using equations (4.5.24), (4.5.16), (4.5.12) and (4.5.13) respectively. These results are presented, and compared with those from the previous section, in section 4.6.

4.6 Results and Discussion of Sections 4.4 and 4.5

In this section various results are presented and the essential features and limitations of both models of sections 4.4 and 4.5 are discussed and compared.

Values of the constant α for various values of the Brinkman number Br, the only control parameter in these models which have been presented in table 4.1 are substituted into equation (4.4.10) and the plots of z_p against time are subsequently computed. Values of the dimensionless shear stress τ are then found using (4.4.7). Likewise using the values of α_v and β_v given in table 4.2 the plots of z_p and τ against time for the variable viscosity model are obtained using equations (4.5.12) and (4.5.13) respectively. These results are shown in Figures 4.1 and 4.2. The curves in Figure 4.1 illustrate the growth of the thickness of the plastic region with time for both models, the solid line represents the constant viscosity model whereas the dotted line represents the variable viscosity case. It is readily seen from these curves that increasing the value of Br, that is increasing the rate of heat generation, gives an increase in the rate of growth of the plastic region. It is also borne out that allowing the viscosity to fall with increasing temperature gives a reduction in the rate of growth of z_p for a given value of Br. As Br decreases the difference between the two models decreases and in the limit as $Br \to 0$ the values of z_p from the two models become assymptotically identical as could have been envisaged by inspection of equations (4.4.22) and (4.5.30).

The curves in Figure 4.2 illustrate the decay of the shear stress with time. It is seen that an increase in the Brinkman number results in a decrease in τ and that for a given value of Br the shear stress τ is lower for the variable viscosity model than for the constant viscosity one.

Comparison of these curves with the phase II section of the torque trace (see Figure 4.3b) reveals that for smaller times there is some qualitative agreement. However, for larger times Figures 4.1 and 4.2 show that z_p grows indefinitely, τ approaches zero and no steady state is reached. This is a consequence of neglecting the effect of upset. Without upset there is no cooling of the plastic region by forced convection, hence as time in increases the heat generated within the plastic region is only lost by conduction down the tube and the plastic/solid boundary is driven along indefinitely.

The temperature profiles for Atthey's model are computed for various values of Br, with the aid of the values of α in table 4.1, using equations (4.4.17) and (4.4.19) for the plastic and solid regions respectively. Using the values of α_v and β_v in table 4.2 the temperature profiles in the plastic region, for the variable viscosity model, are computed using equations (4.5.24) and (4.5.25); again truncating the series after 15 terms is found to be adequate. For the solid region equation (4.4.19) is used with α replaced by α_v. The temperature profiles for both models plotted against the variable η, which is defined by (4.4.9), for various values of Br are plotted in Figure 4.3. It is seen that increasing Br increases the interface temperature and that the variable viscosity model predicts the lower temperatures. These temperatures are over estimates since the forced convection cooling terms are absent. It is important to note that the interface temperatures predicted by both models are independent of time. This results from neglecting axial shortening; the correction made by including this is presented in sections 4.8 and 4.9. Although these temperature profiles are initially inaccurate it is seen in Sections 4.12 and 4.13 that for slightly later times the accuracy is much improved.

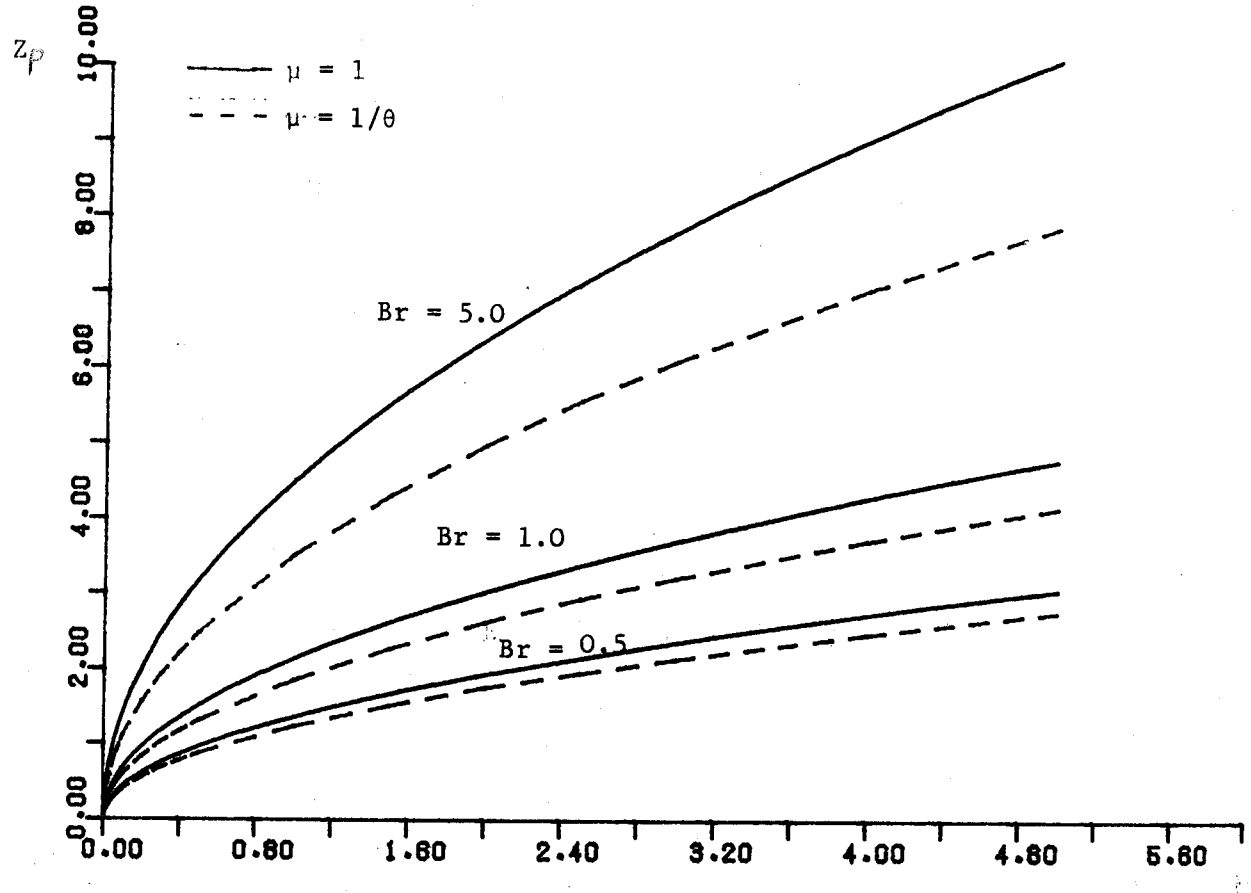

Figure 4.1 Graphs of Z_p against t.

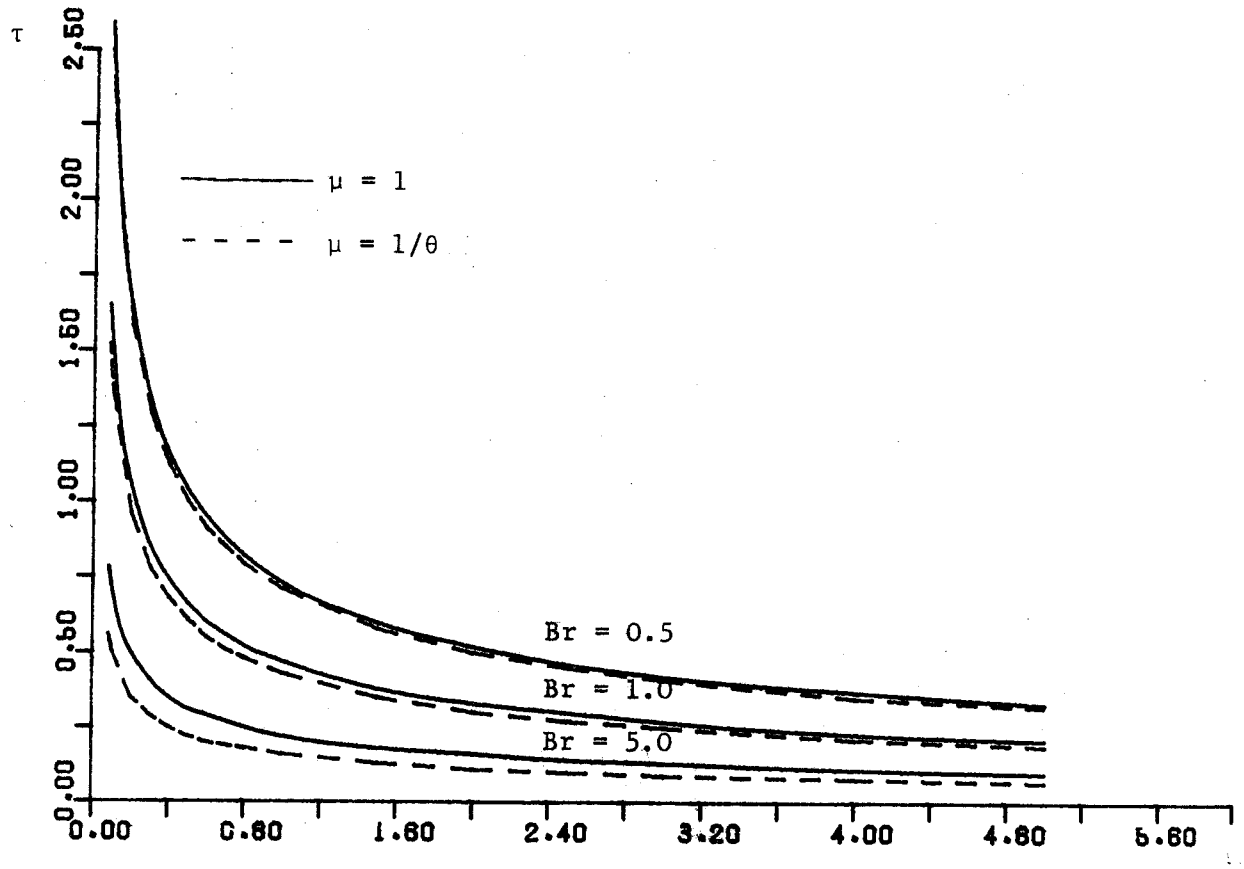

Figure 4.2 Graphs of τ against t

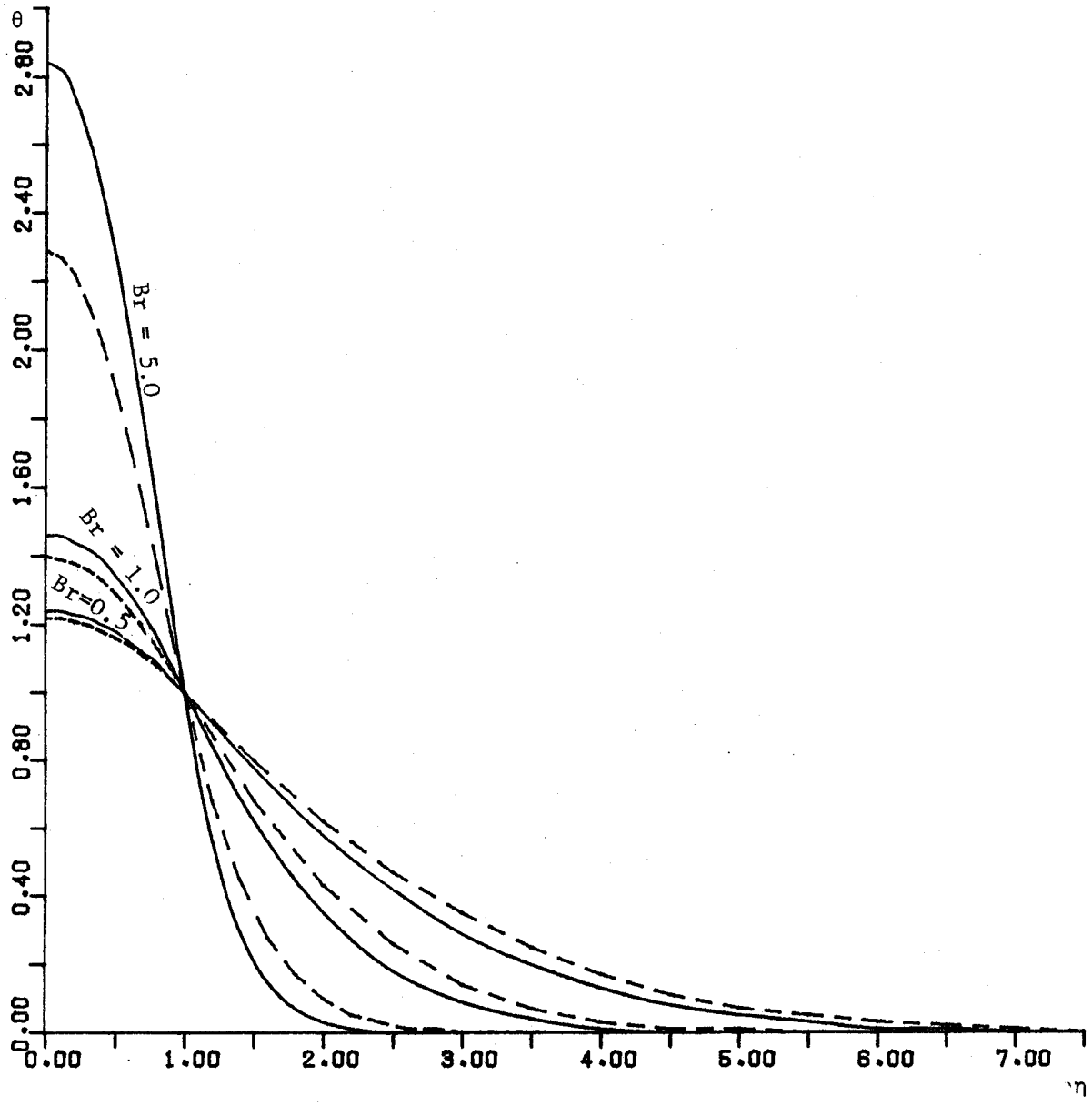

Figure 4.3 Graphs of θ against η

Figure 4.4 indicates the variation of the interface temperature with Br for both models. It has already been stated that allowing the viscosity to fall with increasing temperature results in lower temperatures for a given Br. However, it is seen from Figure 4.4. that for both models a critical value of Br exists where melting would occur at the interface. The melting temperature θ_m being obtained from definition (3.4.34) based on the numerical values for mild steel.

$$Tc = 700^{o}C,\ T_A = 15^{o}C,\ T_M = 1510^{o}C \qquad (4.6.1)$$

With the values of μ_o and k_o given in chapter 3 it is seen from definition (3.4.38) and Figure 4.4 that with our model melting can occur well within the working range of ω. However experimental examination of the friction

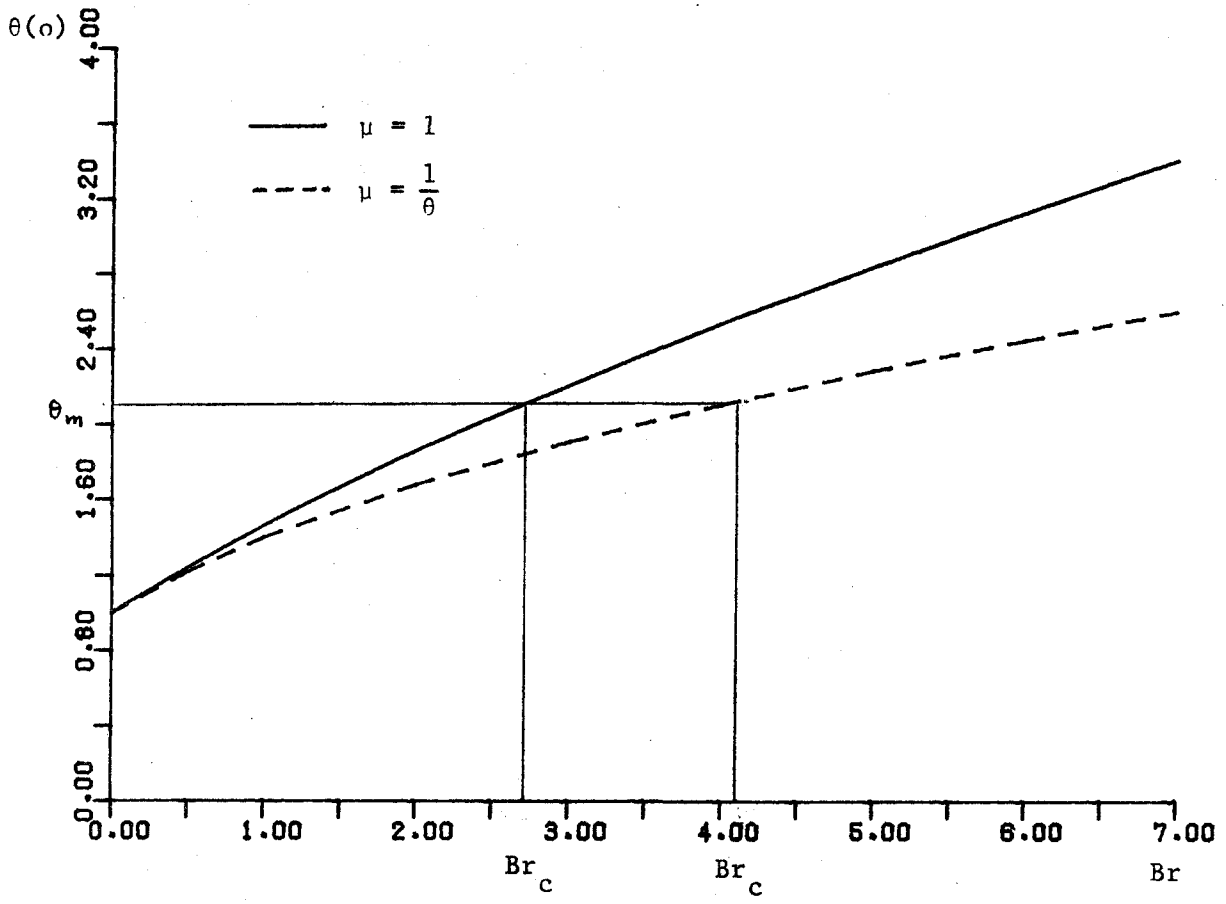

Figure 4.4 Graphs of interface temperature against Br.

welding of mild steel (3,4) indicate that melting does not occur. These statements are consistent with the view that the temperatures predicted from our model are over estimates, the main two reasons being the neglect of burnoff and the over simplified viscosity model. There is thus a need for more elaborate models and these are presented later in this chapter.

4.7 Velocity and Pressure Profiles - Including Burnoff

When burnoff is included the velocity components and the pressure in the plastic region are the solutions of equations (4.2.7) to (4.2.11) and (4.2.13) which satisfy the boundary conditions (4.2.14) to (4.2.18). In this section assumption (4.2.12), that the viscosity is a function of temperature θ and the strain rate $\partial v/\partial z$ but is independent of x, is again introduced.

From equations (4.2.7), (4.2.8) and (4.2.10) it is evident that the pressure component Po and the velocity component v are independent of the axial velocity component w. Thus the solutions for these quantities when burnoff is present are identical to those in the absence of burnoff and, consequently recalling equations (4.3.9), (4.3.14) and (4.3.15), we deduce that for the problems considered in this section

$$P_o \equiv 1, \tag{4.7.1}$$

$$v = \tau(t)\int_o^z \frac{dz}{\mu} , \tag{4.7.2}$$

and

$$1 = \tau(t)\int_o^z p\frac{dz}{\mu} . \tag{4.7.3}$$

In view of assumption (4.2.6), the equation of incompressibility (4.2.13) is readily integrated with respect to x to yield

$$u = -x\frac{\partial w}{\partial z} + f(z,t), \tag{4.7.4}$$

in which f is an arbitrary function of z and t. The boundary condition (4.2.18) then implies that the function f must be identically zero, so we have

$$u = -\dot{x}\frac{\partial w}{\partial z} . \tag{4.7.5}$$

This equation for u is now substituted into the two equations of motion (4.2.9) and (4.2.11) and, remembering that μ is independent of x, the equations become

$$\frac{1}{2}\frac{\partial p_1}{\partial x} = -\beta^2 x \frac{\partial}{\partial z}\left(\mu\frac{\partial^2 w}{\partial z^2}\right) \tag{4.7.6}$$

and

$$\frac{1}{2}\frac{\partial p_1}{\partial z} = 2\frac{\partial}{\partial z}\left(\mu\frac{\partial w}{\partial z}\right) - \mu\frac{\partial^2 w}{\partial z^2} . \tag{4.7.7}$$

These equations can easily be solved. Integration of equation (4.7.6) with respect to x leads to the expression

$$p_1 = -\beta^2 x^2 \frac{\partial}{\partial z}\left(\mu\frac{\partial^2 w}{\partial z^2}\right) + g(z,t), \tag{4.7.8}$$

where g is an arbitrary function of z and t. On differentiating both sides of equation (4.7.8) with respect to z and using equation (4.7.7) to eliminate $\partial p_1/\partial z$ we obtain the identity

$$4\frac{\partial}{\partial z}\left(\mu\frac{\partial w}{\partial z}\right) - 2\mu\frac{\partial^2 w}{\partial z^2} \equiv -\beta^2 x^2 \frac{\partial^2}{\partial z^2}\left(\mu\frac{\partial^2 w}{\partial z^2}\right) + \frac{\partial g}{\partial z} . \tag{4.7.9}$$

Since the above holds for all x in $(\frac{1}{2}, -\frac{1}{2})$ the functions μ, w and g, which are all independent of x, must necessarily satisfy

$$\frac{\partial_2}{\partial z^2}\left(\mu\frac{\partial^2 w}{\partial z^2}\right) = 0 \tag{4.7.10}$$

and

$$4\frac{\partial}{\partial z}\left(\mu\frac{\partial w}{\partial z}\right) - 2\mu\frac{\partial^2 w}{\partial z^2} = \frac{\partial g}{\partial z} \quad . \tag{4.7.11}$$

Repeated integration of equation (4.7.10) with respect to z then gives

$$w = \int_o^z\int_o^1 \frac{\left(C_o(t)k + C_1(t)\right)}{\mu}\, dk\, dl + C_2(t)z + C_3(t), \tag{4.7.12}$$

where C_0, C_1, C_2 and C_3 are arbitrary functions of t only.

The velocity component u may now be obtained by substituting the above into equation (4.7.5) giving

$$u = -x\left(\int_o^z \frac{\left(C_o k + C_1\right)}{\mu}\, dk + C_2\right) \tag{4.7.13}$$

The functions C_1, C_2 and C_3 are easily determined by using expressions (4.7.12) and (4.7.13) in the boundary conditions $(4.2.16)_{1,3}$ and $(4.2.17)_1$, and the resulting expressions for w and u are

$$w = C_o\int_o^z\int_{z_p}^1 \frac{k}{\mu}\, dk\, dl, \tag{4.7.14}$$

and

$$u = -x\, C_o\int_{z_p}^z \frac{k}{\mu}\, dk. \tag{4.7.15}$$

The unknown function $C_o(t)$ is found, using $(4.2.17)_3$ and (4.7.14), to be

$$C_o = -w_o(t) \Big/ \int_o^{z_p} \int_{z_p}^{1} \frac{k}{\mu} \, dk \, dl \tag{4.7.16}$$

From experimental evidence (see Figure 4.31) it is observed that the upset rate is virtually constant over the entire welding cycle provided that the applied force is kept constant. As a result we shall assume that w_o is constant and, recalling definition (3.5.21), we take, without loss of generality,

$$w_o = 1 \, . \tag{4.7.17}$$

Then from equations (4.7.16) and (4.7.17) we deduce that the final form for C_o is

$$C_o = -1 \Big/ \int_o^{z_p} \int_{z_p}^{1} \frac{k}{\mu} \, dk \, dl. \tag{4.7.18}$$

Having determined the velocity components u, v and w we turn our attention to the pressure p_1. On integrating equation (4.7.11) with respect to z we have

$$g = 4\mu \frac{\partial w}{\partial z} - 2 \int \mu \frac{\partial^2 w}{\partial z^2} \, dz + e(t) \tag{4.7.19}$$

where e is an arbitrary function of time introduced through the integration. Substituting equation (4.7.14) for w into the above then yields

$$g = C_o \left\{ 4\mu \int \frac{k}{\mu} \, dk - z^2 \right\} + e(t). \tag{4.7.20}$$

Finally using equations (4.7.14) and (4.7.20) in equation (4.7.8) leads to

$$p_1 = 4\, C_o \mu \int_{z_p}^{z} \frac{k}{\mu}\, dk - C_o(\beta^2 x^2 + z^2) + e. \qquad (4.7.21)$$

The unknown function e is determined by substituting equations (4.7.14) and (4.7.21) into condition (4.2.15) and the resulting expression for p_1 may be written

$$p_1 = 4C_o\mu \int_{z_p}^{z} \frac{k}{\mu}\, dk + C_o \left[(z_p^2 - z^2) + \beta^2 \left\{ \frac{1}{12} - x^2 \right\} \right], \qquad (4.7.22)$$

where we recall that C_o is given by (4.7.18).

Thus including burnoff but retaining the other assumptions of Atthey, we have deduced that within the plastic region the pressure component p_0 and p_1 are given by (4.7.1) and (4.7.22) respectively, and the velocity components u, v and w by (4.7.15), (4.7.2) and (4.7.14) respectively. However, the integrals which appear in most of these expressions cannot be evaluated until μ is known as a function of z and t. Since μ will in general be specified as a function of θ and $\partial v/\partial z$ it will be necessary, as for the case of no burnoff, to solve the above equations simultaneously with the energy equations (4.2.20) and (4.2.21).

4.8 Inclusion of Burnoff - Heat Balance Integral Solution -

In this section Atthey's simple model, described in section 4.4 is extended to incorporate the effect of burnoff. The structure of the governing equations for this more complicated model does not allow a similarity or other analytical solution to be found, thus an approximate or numerical solution must be sought. An approximate solution is obtained in this section using the well known heat balance integral method [33],

which in fact forms the basis of much of the work in this chapter and is discussed in detail here.

All the assumptions introduced by Atthey and discussed in Section 4.4 are retained in this section, except that the velocity component w and hence the Peclet number Pe are no longer taken to be zero. The present section therefore generalises section 4.4 in the same way that section (4.7) extended section 4.3. With the inclusion of burnoff the energy equations (4.4.1) and(4.4.2) are amended to incorporate the forced convection terms and these are presented in Section 4.8.2. However, the thermal boundary and initial conditions remain unchanged and are given by (4.2.23), (4.2.24), (4.2.25) , (4.4.3) and (4.4.4).

4.8.1 Discussion of the Method.

The major complication present in the above mentioned system of partial differential equations and boundary conditions is due to the non-linearity in conditions (4.2.24) and (4.4.3). The nonlinearity of these conditions arises because the latter are to be applied on a moving boundary whose position is a priori unknown. Goodman [33] encountered similar difficulties when seeking solutions to heat conduction problems involving a change of phase. (Sometimes called Stefan problems).

Heat transfer problems involving a phase change, and hence a moving boundary, are non-linear and, except in special cases, must be solved either by integrating the energy equation numerically or by using approximate techniques. Seeking analytical solutions to these mathematically complicated problems Goodman resorted to approximate integral techniques similar to the Polhausen type solutions used in boundary layer theory. In his paper Goodman [33] introduced the heat balance integral method by considering a simple heat conduction problem with linear boundary conditions to which an exact solution has been given [27]. The problem considered was one of heat transfer in a semi-infinite slab, $z>0$, initially at uniform temperature $-\theta_o$, with a prescribed heat flux H(t) on the face

$z = 0$. This problem may be stated mathematically as

$$\frac{\partial^2 \theta}{\partial z^2} = \frac{1}{F_o} \frac{\partial \theta}{\partial t}, \qquad z > 0, \; t > 0 \tag{4.8.1}$$

with boundary conditions

$$\theta = -\theta_o \text{ at } t = 0, \; z > 0 \tag{4.8.2}$$

and

$$\frac{\partial \theta}{\partial z} = -H(t) \text{ on } z = 0, \; t > 0. \tag{4.8.3}$$

This problem has been solved exactly in Carslaw and Jaeger [27].

In order to proceed with his approximate technique Goodman introduced the thickness of the thermal layer $\delta(t)$, analagous to the boundary layer thickness in boundary layer theory. The position of $\delta(t)$, for the problem considered, is defined by assuming that, for all practical purposes, the material in the domain $z > \delta(t)$ is at equilibrium temperature $-\theta_o$ and hence there is no heat flux across $z = \delta$. These conditions can be expressed in the form

$$\theta(\delta, t) = -\theta_o \tag{4.8.4}$$

and

$$\frac{\partial \theta}{\partial z}(\delta, t) = 0 \tag{4.8.5}$$

The so-called heat balance integral is obtained by integrating both sides of equations (4.8.1) with respect to z between the limits $z = 0$ and $z = \delta(t)$, yielding

$$\frac{1}{Fo} \frac{d}{dt} \left[\int_o^\delta \theta dz + \theta_o \delta \right] = \left[\frac{\partial \theta}{\partial z}(\delta, t) - \frac{\partial \theta}{\partial z}(o, t) \right], \; t > 0. \tag{4.8.6}$$

Equation (4.8.1) is therefore satisfied only 'on average' and this averaged equation, the heat balance integral, is analagous to the momentum integral equation in boundary layer theory. We now proceed in a manner similar to Polhausen [34] in boundary layer theory, and assume a polynomial approximation to the temperature profile θ. For the problem considered by Goodman a profile in z of the form

$$\theta = a(t) + b(t)z + c(t)z^2, \tag{4.8.7}$$

was assumed when the coefficient a, b and c are functions of t only. The values of a, b and c are found by substituting equation (4.8.7) into conditions (4.8.3), (4.8.4) and (4.8.5) and the resulting expression for θ is

$$\theta = -\theta_o + \frac{H}{2\delta}(\delta - z)^2 \tag{4.8.8}$$

Substituting equations (4.8.3), (4.8.5) and (4.8.8) into (4.8.6) finally yields the ordinary differential equation

$$\frac{1}{6}\frac{d}{dt}\left[\delta^2 H\right] = FoH, \tag{4.8.9}$$

whose solution satisfying $\delta(o) = 0$ is

$$\delta = \sqrt{6Fo}\left[\frac{1}{H}\int_o^t H(t_1)dt_1\right]^{\frac{1}{2}} . \tag{4.8.10}$$

In the particular case when H is constant δ is given by

$$\delta = \sqrt{6Fot} \quad , \tag{4.8.11}$$

and the surface temperature obtained by putting $z = 0$ in (4.8.8) and making use of (4.8.11) is

$$\theta = -\theta_o + \sqrt{\frac{3}{2}}\ H\sqrt{Fot} \quad , \tag{4.8.12}$$

The exact solution to the problem, given in Carslaw and Jaeger [27] is

$$\theta = -\theta_o + \sqrt{\frac{4}{\pi}}\ H\sqrt{Fot} \ . \tag{4.8.13}$$

Comparing equations (4.8.12) and (4.8.13) reveals that the approximate solution differs from the exact solutions only by a numerical factor and the error is about 9%. This error can in fact, be reduced to about 2% using a cubic representation for θ [33]

The above gives a brief outline of the simple, yet effective, heat balance integral method which is used extensively in the present and the following chapters.

4.8.2 The Energy Equations and Boundary Conditions.

With all the assumptions made by Atthey in section 4.4, except that W and hence Pe are now taken to be non-zero, the energy equations (4.4.1) and (4.4.2) are amended to incorporate the forced convection terms, and it is easily deduced from equations (4.2.20) and (4.2.21) that the appropriate forms are

$$\frac{\partial^2 \theta}{\partial z^2} + Br\mu\left(\frac{\partial v}{\partial z}\right)^2 = Pe\ w\frac{\partial \theta}{\partial z} + \frac{1}{Fo}\frac{\partial \theta}{\partial t} \ , \quad 0 \leq z \leq z_p \tag{4.8.14}$$

and

$$\frac{\partial^2 \theta_s}{\partial z^2} = -Pe\ w_o\frac{\partial \theta_s}{\partial z} + \frac{1}{Fo}\frac{\partial \theta_s}{\partial t} \ , \quad z \geq z_p . \tag{4.8.15}$$

The thermal boundary and initial conditions are, as we have already stated,

identical to those used in section (4.4) and are given by (4.2.23), (4.2.24), (4.2.25), (4.4.3) and (4.4.4).

4.8.3 The Assumption of Constant Viscosity and its Implications

In this subsection we again make the simplest assumptions about the viscosity μ, that it is constant, and as previously we can then without loss of generality choose it to be unity (See (4.4.5)). It follows that the velocity component v is given by (4.4.6) and that relationship (4.4.7) holds.

Substituting (4.4.5) into equations (4.7.14), (4.7.15) and (4.7.22) we deduce that the velocity components w and u and the pressure component p_1 are given by

$$w = \frac{C_o z}{6} (z^2 - 3z_p^2) , \tag{4.8.16}$$

$$u = \frac{C_o x}{2} (z_p^2 - z^2) , \tag{4.8.17}$$

and

$$p_1 = C_o \left[(z^2 - z_p^2) + \beta^2 \left[\frac{1}{12} - x^2 \right] \right]. \tag{4.8.18}$$

Using assumption (4.4.5) in equation (4.7.18) the reduced form for C_o is found to be

$$C_o = 3/z_p^3 . \tag{4.8.19}$$

It follows immediately from equations (4.8.16) to (4.8.19) that the final forms of the velocity component w and u and the pressure component p_1 are given by

$$w = \frac{1}{2} \left(\frac{z}{z_p} \right) \left[\left(\frac{z}{z_p} \right)^2 - 3 \right] , \tag{4.8.20}$$

$$u = \frac{3x}{2z_p} \left[1 - \left(\frac{z}{z_p} \right)^2 \right] , \tag{4.8.21}$$

and $$p_1 = \frac{3}{z_p^2}\left[(z^2 - z_p^2) + \beta^2\left(\frac{1}{12} - x^2\right)\right] , \qquad (4.8.22)$$

On substituting equations (4.4.6) and (4.8.20) for the velocity component v and w respectively, into equation (4.8.14) and expressing the shear stress τ in terms of z_p using (4.4.7) the energy equations for the plastic region becomes

$$\frac{\partial^2\theta}{\partial z^2} + \frac{Br}{z_p^2} = \frac{Pe}{2}\left(\frac{z}{z_p}\right)\left[\left(\frac{z}{z_p}\right)^2 - 3\right]\frac{\partial\theta}{\partial z} + \frac{1}{Fo}\frac{\partial\theta}{\partial t} , \quad 0 \leq z \leq z_p \qquad (4.8.23)$$

With the aid of assumption (4.7.17), the energy equation for the solid region, equation (4.8.15) can be written

$$\frac{\partial^2\theta_s}{\partial z^2} = -Pe\frac{\partial\theta_s}{\partial z} + \frac{1}{Fo}\frac{\partial\theta_s}{\partial t} , \quad z \geq z_p . \qquad (4.8.24)$$

The partial differential equations (4.8.23) and (4.8.24) must now be solved subject to the conditions (4.2.23), (4.2.24), (4.2.25), (4.4.3) and (4.4.4). There is no obvious analytical solution to this system but an approximate solution can be attained using the heat balance integral method and this solution is presented in the following subsection.

4.8.4 Heat Balance Integral Solution.

In order to obtain a heat balance integral solution it is convenient to introduce into equations (4.8.23) and (4.8.24) the new variable η which has been defined by equation (4.4.9) but the latter is restated here for convenience

$$\eta = \frac{z}{z_p(t)} . \qquad (4.8.25)$$

Then the transformed forms of the energy equations are

$$\frac{\partial^2 \theta}{\partial \eta^2} + Br = \frac{Pez_p}{2} \eta(\eta^2 - 3) \frac{\partial \theta}{\partial \eta} + \frac{z_p^2}{Fo} \frac{\partial \theta}{\partial t} - \frac{z_p}{Fo} \frac{dz_p}{dt} \eta \frac{\partial \theta}{\partial \eta} , \tag{4.8.26}$$

for the plastic region, $o \leq \eta \leq 1$, and

$$\frac{\partial^2 \theta_s}{\partial \eta^2} = -Pe\, z_p \frac{\partial \theta_s}{\partial \eta} + \frac{z_p^2}{Fo} \frac{\partial \theta_s}{\partial t} - \frac{z_p}{Fo} \frac{dz_p}{dt} \eta \frac{\partial \theta_s}{\partial \eta} , \tag{4.8.27}$$

for the solid region, $\eta \geq 1$.

In terms of η the conditions (4.2.23), (4.2.24), (4.2.25), (4.4.3) and (4.4.4) transform to

$$\frac{\partial \theta}{\partial \eta}(o,t) = 0, \tag{4.8.28}$$

$$\theta(1,t) = \theta_s(1,t) = 1, \tag{4.8.29}$$

$$\frac{\partial \theta}{\partial \eta}(1,t) = \frac{\partial \theta_s}{\partial \eta}(I,t) \tag{4.8.30}$$

and

$$\theta_s(\eta,t) \to 0 \text{ as } \eta \to \infty . \tag{4.8.31}$$

The initial condition (4.4.4) is included in the transformed condition (4.8.31) since it is assumed that initially the plastic region has zero thickness, that is

$$z_p(o) = 0 \tag{4.8.32}$$

We shall now seek an heat balance integral solution to the above problem, by associating with the plastic region, the position of the thermal layer $z = \delta(t)$, of Section 4.8, to the position of the plastic/solid interface $z = z_p(t)$. With this definition and in view of equation (4.8.25), the heat balance integral for the plastic region is obtained by integrating both sides of equation (4.8.26) with respect to η between the limits $\eta = 0$ and $\eta = 1$, yielding

$$\frac{\partial \theta}{\partial \eta}(1,t) - \frac{\partial \theta}{\partial \eta}(o,t) + Br = \frac{Pe\ z_p}{2}\int_o^1 \eta(\eta^2-3)\frac{\partial \theta}{\partial \eta}\,d\eta$$

$$+ \frac{z_p^2}{Fo}\frac{d}{dt}\int_o^1 \theta d\eta - \frac{z_p}{Fo}\frac{dz_p}{dt}\int_o^1 \eta \frac{\partial \theta}{\partial \eta}\,d\eta. \qquad (4.8.33)$$

In this plastic region a simple quadratic temperature profile of the form

$$\theta = a_o(t) + a_1(t)\eta + a_2(t)\eta^2 \quad , \qquad (4.8.34)$$

is assumed, where a_o, a_1, and a_2 are functions of time only. In order to satisfy the boundary conditions (4.8.28) and (4.8.29), it is necessary that $a_1 = 0$ and $a_0 = 1-a_2$. The temperature profile is then given by

$$\theta = 1 + (\eta^2 - 1)a_2(t), \qquad (4.8.35)$$

where a_2 remains undetermined. Substituting equation (4.8.35) for θ into the heat balance integral (4.8.33) and performing the necessary integrations yields, after some algebra, the ordinary differential equation connecting a_2 and z_p.

$$2a_2 + Br = -\frac{2}{3}\frac{z_p^2}{Fo}\frac{da_2}{dt} - \frac{2}{3}\frac{z_p}{Fo}a_2\frac{dz_p}{dt} - \frac{4}{5}Pe\ z_p\ a_2. \qquad (4.8.36)$$

In the solid region we assume the existence of a thermal layer $z = \delta(t) > z_p(t)$, such that all the material in the domain $z > \delta(t)$ will be at ambient temperature thus implying that the heat flux across $z = \delta(t)$ may be taken to be zero. These conditions may be expressed

$$\theta_s(\delta,t) = 0, \qquad (4.8.37)$$

$$\frac{\partial \theta_s}{\partial z}(\delta,t) = 0 \tag{4.8.38}$$

and in terms of the variable η become

$$\theta_s(s,t) = 0, \tag{4.8.39}$$

$$\frac{\partial \theta_s}{\partial \eta}(s,t) = 0, \tag{4.8.40}$$

where $s(t)$ is defined by

$$s = \delta(t)/z_p(t). \tag{4.8.41}$$

The heat balance integral for the solid region is then obtained by integrating both sides of equation (4.8.27) with respect to η between the limits $\eta = 1$ and $\eta = s(t)$. The resulting equation is

$$\frac{\partial \theta_s}{\partial \eta}(s,t) - \frac{\partial \theta_s}{\partial \eta}(1,t) = -Pe\, z_p \left[\theta_s(s,t) - \theta_s(1,t)\right] + \frac{z_p^2}{Fo}\left[\frac{d}{dt}\int_1^s \theta_s(\eta,t)d\eta - \frac{ds}{dt}\theta_s(s,t)\right] - \frac{z_p}{Fo}\frac{dz_p}{dt}\int_1^s \eta\frac{\partial \theta_s}{\partial \eta}\, d\eta \tag{4.8.42}$$

We now assume a temperature profile for the solid region of the form

$$\theta_s = b_o(t) + b_1(t)\eta + b_2(t)\eta^2 , \quad 1 \leq \eta \leq s(t) \tag{4.8.43}$$

and $$\theta_s = 0, \qquad \eta \geq s(t) \tag{4.8.44}$$

which automatically satisfies condition (4.8.31). On substituting (4.8.43) for θ_s into the conditions $(4.8.29)_2$, (4.8.39) and (4.8.40) the functions b_o, b_1 and b_2 are obtained in terms of s and the resulting expression for θ_s is

$$\theta_s = (s - \eta)^2/(s - 1)^2 , \quad 1 \leq \eta \leq s \tag{4.8.45}$$

Finally, making use of condition (4.8.30) the quantity s may be expressed in terms of $a_2(t)$ in the form

$$s = 1 - 1/a_2 \tag{4.8.46}$$

and (4.8.45) reduces to

$$\theta_s = a_2^2(1 - 1/a_2 - \eta)^2 , \qquad 1 \leq \eta \leq s. \tag{4.8.47}$$

Substitution of this expression for θ_s into the heat balance integral (4.8.42) and the subsequent calculation of the integrals again leads to an ordinary differential equation for z_p and a_2, namely

$$- 2a_2 = Pe\ z_p - \frac{z_p^2}{3Fo} \frac{d}{dt}\left(\frac{1}{a_2}\right) + \frac{z_p}{Fo}\left(1 - \frac{1}{3a_2}\right)\frac{dz_p}{dt} \tag{4.8.48}$$

The two ordinary differential equations (4.8.36) and (4.8.49) form a coupled system for the two unknown functions z_p and a_2. In order to solve these equations it is necessary to know the initial conditions on z_p and a_2. The initial condition for z_p is given by (4.8.32). To obtain the initial condition for a_2 we consider the total thermal energy of the plastic region, E_p, which is defined by

$$\bar{E}_p(\bar{z}_p) = \int_0^{\bar{z}_p} \rho\, \bar{C}_v T \; d\bar{z} . \tag{4.8.49}$$

Recalling definitions (3.4.1) and $(3.4.34)_{1,2}$ the above equation may be written in the dimensionless form

$$E_p(z_p) = \int_0^{z_p} C_v\left(\frac{T_{AM}}{T_c} + \theta(1 - T_{AM}/T_c)\right) dz \tag{4.8.50}$$

where the dimensionless thermal energy E_p is defined by

$$E_p = \overline{E}_p / \rho\, C_{vo}\, T_c\, z_{po} \qquad (4.8.51)$$

With the assumption that C_v is constant, and taken to be unity, and introducing the variable η, through the definition (4.8.25) equation (4.8.50) becomes

$$E_p(z_p) = z_p \int_0^{T_{AM}/T_c} \theta(1 - T_{AM}/T_c)\, d\eta \,. \qquad (4.8.52)$$

When equation (4.8.35) is substituted into the above and the integral calculated, there results

$$E_p(z_p) = z_p \frac{T_{AM}}{T_c} + z_p(1 - T_{AM}/T_c)(1 - 2/3\ a_2) \,. \qquad (4.8.53)$$

Since E(o) must be zero we deduce, with the aid of condition (4.8.32), that

$$\lim_{t \to 0} a_2\, z_p = 0 \qquad (4.8.54)$$

We now have the necessary conditions, namely (4.8.32) and (4.8.54), to solve the equations (4.8.36) and (4.8.48). In general there appears to be no analytical solution to these equations so a numerical solution must be sought. However, for the special case when no upset takes place, that is when Pe = 0, an analytical solution can be obtained and it is thought useful to give this solution here so that, by comparison with the solution given in section 4.4, an assessment of the accuracy of the heat balance integral method can be made.

4.8.5 Solution with Zero Pe - no burnoff -

When burnoff is ignored and the Peclet number Pe is taken to be zero in equations (4.8.36) and (4.8.48) the latter reduce to

$$2a_2 + Br = -\frac{2}{3}\frac{z_p^2}{Fo}\frac{da_2}{dt} - \frac{2}{3}\frac{z_p}{Fo}\, a_2\, \frac{dz_p}{dt}, \qquad (4.8.55)$$

and

$$2a_2 = \frac{z_p^2}{3Fo}\frac{d}{dt}\left(\frac{1}{a_2}\right) + \frac{z_p}{Fo}\left(\frac{1}{3a_2} - 1\right)\frac{dz_p}{dt} \qquad (4.8.56)$$

respectively. Multiplying equation (4.8.55) by the integrating factor a_2 and integrating it with respect to t yields, on the application of the initial condition (4.8.32), the expression for z_p in terms of a_2

$$z_p = \left[-\frac{3F_o}{a_2^2}\int_o^t a_2(2a_2 + Br)dt\right]^{\frac{1}{2}} . \qquad (4.8.57)$$

Similarly multiplying (4.8.56) by $(1-3a_2)^2/a_2^2$ and integrating it with respect to t, yields some algebra

$$z_p = \left[\frac{12\,Fo\,a_2^2}{(1-3a_2)^2}\int_0^t \frac{(1-3a_2)}{}\,dt\right]^{\frac{1}{2}} . \qquad (4.8.58)$$

The right hand sides of equations (4.8.57) and (4.8.58) can be equated to yield the single integral equation.

$$-\int_o^t a_2(2a_2 + Br)dt = \frac{4a_2^4}{(1-3a_2)^2}\int_o^t (1-3a_2)\,dt \qquad (4.8.59)$$

It is easily verified that the solutions

$$a_2 = a_{20} \qquad (4.8.60)$$

and

$$z_p = 2z_1\sqrt{Fot} \quad , \qquad (4.8.61)$$

where

$$z_1 = \left[-\frac{3(2a_{20} + Br)}{4\,a_{20}}\right]^{\frac{1}{2}} \qquad (4.8.62)$$

and a_{20} is a constant, satisfy equations (4.8.57), (4.8.59) and the initial conditions (4.8.32) and (4.8.54), identically, provided that a_{20} is a solution of the cubic equation

$$a_{20}^3 - \frac{3}{2} a_{20}^2 + \left(\frac{1}{2} - \frac{3}{4} Br\right) a_{20} + \frac{1}{4} Br = 0. \qquad (4.8.63)$$

It is easily deduced fromequation (4.8.62) that in order for z_p to be real for all positive values of the Brinkman number, a_{20} must satisfy the inequalities

$$-\frac{1}{2} Br < a_{20} < 0. \qquad (4.8.64)$$

We shall now show that the above cubic equation (4.8.63) has only one negative real root for all positive values of Br. Suppose that all roots are real. From the general theory of cubics it is thus known that the product of the three roots for this particular case, is negative and equal to $-\frac{1}{4} Br$. We then deduce that the equation has either three negative roots or one negative root and two positive ones. But also from equation (4.8.63) we note that the sum of the roots is positive and equal to $\frac{3}{2}$ from which it follows that, provided all three roots are real, equation (4.8.63) has one negative root and two positive ones. The only remaining possibility is that (4.8.63) has two complex roots, a + ib and a - ib,and one real root, c, say. Then the product of the roots satisfies

$$c(a^2 + b^2) = -\frac{1}{4} Br \qquad (4.8.65)$$

from which we conclude that $c < 0$. Thus equation (4.8.63) has exactly one negative real root. However, we still need to show that this negative root satisfies the inequality

$$a_{20} > -\frac{1}{2} Br, \qquad (4.8.66)$$

for all + ve values of the Brinkman number. A close inspection of the behaviour of (4.8.63) for small values of Br reveals that the negative roots takes the asymptotic form

$$a_{20} = -\frac{1}{2}\,Br + \frac{1}{4}\,Br^2 + O\left(Br^3\right) , \qquad (4.8.67)$$

which clearly satisfies (4.8.66). For large values of Br the corresponding asymptotic form is

$$a_{20} = -\frac{\sqrt{3}}{2}\sqrt{Br} + \frac{7}{12} - \frac{11\sqrt{3}}{16}\left(\frac{1}{\sqrt{Br}}\right) + O\left(\frac{1}{Br}\right) , \qquad (4.8.68)$$

which again for large values of Br, that is $Br > \sqrt{3}$, satisfies (4.8.66). Using (4.8.67) and (4.8.68) to obtain starting values, the values of a_{20} are computed, using the Newton-Raphson iterative procedure, over a wide range of Brinkman numbers and the results are presented in table (4.3). The plot of these results in Figure 4.5 shows that (4.8.66) is satisfied for all positive values of Br. Also presented in table 4.3 are the values of the quantities z_1 and s obtained using equations (4.8.62) and (4.8.46) and the relevant values of a_{20} and Br. The values of z_1 can be compared with the values of α in table 4.1 and some assessment of the accuracy of this approximate method made. In particular substituting equation (4.8.67) into (4.8.62) and expanding for small Br yields

$$z_1 = \frac{\sqrt{3}}{2}\,Br\,\left(1 - \frac{3}{4}\,Br + O(Br^2)\right) \qquad (4.8.69)$$

Comparison of the leading term of the above equation with the leading term in equation (4.4.22) reveals that, for small values of Br, the error is about 3%. Similarly substituting, (4.8.68) into (4.8.62) and expanding for large Br yields

$$z_1 = \left(\frac{\sqrt{3}}{2}\right)^{\frac{1}{2}} Br^{\frac{1}{4}} \left[1 - \frac{11}{12\sqrt{3}} \left(\frac{1}{\sqrt{Br}}\right) + O\left(\frac{1}{Br}\right)\right] \qquad (4.8.70)$$

Comparison of the leading term in this equation with the leading term of (4.4.28) shows that the error here is about 30% for very large Br. However for values of Br less than 10, which is well within the physical ranges, the error is less than 10%.

A20

Br	a_{20}	z_1	s
0.1	-0.050	0.080	21.086
0.2	-0.098	0.150	11.149
0.3	-0.146	0.211	7.863
0.4	-0.191	0.264	6.232
0.5	-0.235	0.312	5.259
0.6	-0.277	0.354	4.612
0.7	-0.317	0.393	4.152
0.8	-0.356	0.429	3.807
0.8	-0.393	0.462	3.538
1.0	-0.430	0.482	3.323
2.0	-0.744	0.727	2.343
4.0	-1.220	0.979	1.819
6.0	-1.596	1.148	1.627
8.0	-1.916	1.277	1.522
10.00	-2.200	1.382	1.455

Table 4.3

The temperature profiles θ and θ_s, the thickness of the plastic region z_p and the dimensionless shear stress τ are now readily computed using equations (4.8.35), (4.8.45), (4.8.61) and (4.4.7) respectively.

The results are presented and discussed in section 4.10 and comparison is made with Attheys solution to give an overall assessment of the accuracy of the method.

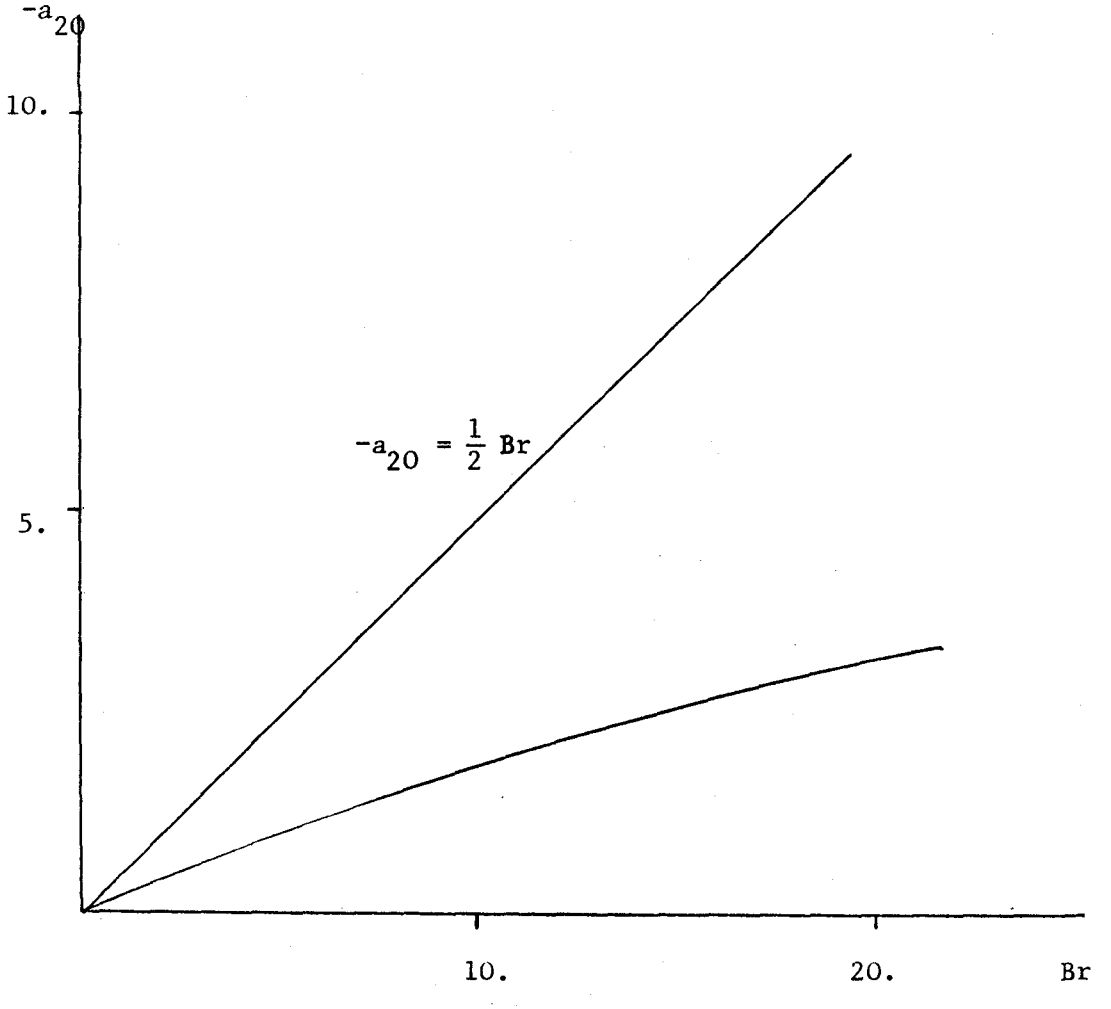

Figure 4.5 Plot of $-a_{20}$ against Br.

4.8.6. Solution with non-zero Pe.

As we have already stated when the convection terms are retained in equations (4.8.36) and (4.8.48) no analytical solution can be obtained and a numerical solution must be sought. For this pair of simple ordinary differential equations the Runge-Kutta [35] forward step

method is felt to be suitable and this is the method used here. However, there is a singularity in the rate of growth of the plastic region, $d z_p / dt$, at time $t = 0$, thus the numerical procedure must be started after a small time has elapsed when the system has become more stable and the rate of growth of z_p is finite. Let us therefore obtain a series solution to the equations (4.8.36) and (4.8.48) which is valid for small times. This solution will then provide the starting values for the full numerical solution.

The form of the equations (4.8.36) and (4.8.48) suggest that the leading terms in our series will be those given by equations (4.8.60) and (4.8.61) derived for the case with $Pe = 0$. We could start the numerical procedure from these terms alone however, it is felt useful to also derive the second terms to compare them with the corresponding terms of a series solution to the exact equations, which is derived in section (4.9), again for an assessment of the accuracy of the method.

For small time let us assume that z_p and a_2 may be expanded in the forms

$$z_p = 2 z_1 \sqrt{Fo}\ t^{\frac{1}{2}} + 2 z_2 \sqrt{Fo}\ Pet^m + \ldots, \qquad (4.8.71)$$

and

$$a_2 = a_{20} + a_{21} Pet^n + \ldots, \qquad (4.8.72)$$

where n and m are arbitrary real numbers which satisfy the conditions

$$n > 0, \quad m > \tfrac{1}{2} \quad . \qquad (4.8.73)$$

Equations (4.8.71) and (4.8.72) then necessarily satisfy the conditions (4.8.32) and (4.8.54).

Substituting equations (4.8.71) and (4.8.72) into the differential equations (4.8.36) and (4.8.48) results in the pair of identities

$$2a_{20} + 2a_{21}\,Pet^{n} + \ldots + Br = -\frac{8}{3}\,(z_1^{2}t + 2z_1z_2\,Pet^{\frac{1}{2}+m} + \ldots)(na_{21}Pet^{n-1}+\ldots)$$

$$-\frac{4}{3}\,(z_1t^{\frac{1}{2}} + z_2Pet^{m} + \ldots)(z_1t^{-\frac{1}{2}} + 2m\,z_2Pet^{m-1} + \ldots)(a_{20} + a_{21}Pet^{n} + \ldots)$$

$$-\frac{8}{5}\,Pe\,(z_1\sqrt{Fo}\,t^{\frac{1}{2}} + z_2\sqrt{Fo}\,Pet^{m} + \ldots)(a_{20} + a_{21}Pet^{n} + \ldots), \qquad (4.8.74)$$

and

$$-2(a_{20} + a_{21}Pet^{n} + \ldots) \equiv 2Pe\,\sqrt{Fo}(z_1t^{\frac{1}{2}} + z_2Pet^{m} + \ldots) +$$

$$\frac{4}{3a_{20}^{2}}\,(z_1^{2}t + 2z_1z_2Pet^{\frac{1}{2}+m} + \ldots)(1 - 2a_{21}Pet^{n}/a_{20} + \ldots)(na_{21}Pet^{n-1} + \ldots) +$$

$$\frac{4}{3a_{20}}\,(z_1t^{\frac{1}{2}} + z_2Pet^{m} + \ldots)(\tfrac{1}{2}z_1t^{-\frac{1}{2}} + mz_2Pet^{m-1} + \ldots)(3a_{20} - 1 + 3a_{21}Pet^{n}+\ldots)$$

$$(1 - a_{21}Pet^{n}/a_{20} + \ldots)$$

$$(4.8.75)$$

On multiplying out the first few terms of the above identities and grouping terms together we obtain

$$2a_{20} + Br + \frac{4}{3}\,z_1^{2}\,a_{20} \equiv -\left\{\frac{4}{3}\,z_1^{2}(2n+1) + 2\right\}\,a_{21}Pet^{n}$$

$$-\frac{4}{3}\,z_1z_2Pea_{20}\,(1 + 2m)\,t^{m-\frac{1}{2}} - \frac{8}{5}\,Pez_1\,Fo\,a_{20}\,t^{\frac{1}{2}} + \ldots \qquad (4.8.76)$$

and

$$-2a_{20} - \frac{2z_1^2}{3a_{20}}(3a_{20} - 1) = 2a_{21}\,Pe\left[1 + \frac{z_1^2}{3a_{20}^2}(2n+1)\right]t^n$$

$$+ \frac{2z_1z_2}{3a_{20}}Pe(3a_{20} - 1)(2m + 1)t^{m-\frac{1}{2}} + 2Pe\,z_1\sqrt{Fo}\,t^{\frac{1}{2}} + \ldots. \qquad (4.8.77)$$

Equating to zero the coefficients of unity yields the pair of equations

$$2a_{20}\left[1 + \frac{2}{3}z_1^2\right] = -Br \qquad (4.8.78)$$

and

$$3a_{20}^2 = -z_1^2(3a_{20} - 1) \quad , \qquad (4.8.79)$$

the solutions of which are given, of course, by (4.8.62) and the negative root of (4.8.63).

After a close inspection of (4.8.76) and (4.8.77) one deduces that a solution to a_{21} and z_2 can only be obtained if

$$n = m - \tfrac{1}{2} = \tfrac{1}{2}. \qquad (4.8.80)$$

Then equating to zero the coefficients of $t^{\frac{1}{2}}$ yields the equations

$$\left[\frac{4}{3}z_1^2 + 1\right]a_{21} + 2z_1z_2a_{20} + \frac{4}{5}z_1a_{20}\sqrt{Fo} = 0 \qquad (4.8.81)$$

and

$$a_{21}\left[\frac{2z_1^2}{3a_{20}^2} + 1\right] + \frac{z_1z_2}{a_{20}}(3a_{20} - 1) + z_1\sqrt{Fo} = 0 \qquad (4.8.82)$$

The pair of linear simultaneous equations is readily solved to yield the solutions

$$a_{21} = \frac{\frac{6}{5}\sqrt{Fo}\, z_1\, a_{20}(2 - a_{20})}{4z_1^{\,2}(3a_{20} - 2) + 3a_{20}(3 - 2a_{20}) - 3} \qquad (4.8.83)$$

$$z_2 = -\frac{\left(12\sqrt{Fo}\, z_1\, a_{20} + 5a_{21}(3 + 4z_1^{\,2})\right)}{30\, z_1\, a_{20}} \qquad (4.8.84)$$

The values of a_{21} and z_2 obtained using the above pair of equations, with the aid of the results given in table 4.3 are presented in table 4.4 for various values of Br. The accuracy of these quantities is assessed in a later section.

Br	a_{21}	z_2
0.1	0.006	-0.106
0.2	0.020	-0.196
0.3	0.036	-0.268
0.4	0.052	-0.326
0.5	0.067	-0.373
0.6	0.081	-0.411
0.7	0.094	-0.442
0.8	0.105	-0.468
0.9	0.115	-0.489
1.0	0.124	-0.508
2.0	0.181	-0.609
4.0	0.231	-0.674
6.0	0.258	-0.700
8.0	0.277	-0.715
10.0	0.292	-0.724

Table 4.4

The values of z_1 and a_{20} presented in table 4.3 and the values of z_2 and a_{21} presented in table 4.4 are now substituted into equations

(4.8.71) and (4.8.72), with $m = \frac{1}{2}$ and $n = 1$. With a value for t chosen initially close to zero starting values of a_2 and z_p are then obtained. Using these starting values and a suitable step length Δt values of z_p and a_2 against time are computed using the Runge-Kutta simple forward step method. Having obtained these results the values of s are computed using equation (4.8.46) and subsequently the temperature profiles and the shear stress τ are evaluated using equations (4.8.35)(4.8.47) and (4.4.7) respectively. These results are presented in section 4.10.

4.9 Inclusion of Burnoff-series Solution for Small Time -.

In this section we again consider the situation in which burnoff is allowed ($Pe \neq 0$) and develop series solutions for the temperature profile and thickness of the plastic region which are valid for small times. These series solutions are used to assess the accuracy of the solution of section 4.8 and to illustrate the effect that inclusion of burnoff has on the solution of section 4.4. The governing equations, in the variable η, defined by (4.8.25), are (4.8.26) and (4.8.27) and the appropriate boundary conditions are (4.8.28) to (4.8.31). As we have already stated there is no obvious analytical solution to this system of non-linear partial differential equations. However the complication of the non-linearity is removed by expressing θ, θ_s and z_p as series in powers of $t^{\frac{1}{2}}$, so we write

$$\theta(\eta,t) = \theta_0(\eta) + \sqrt{t}\, Pe\, \theta_1(\eta) + O(t), \qquad (4.9.1)$$

$$\theta_s(\eta,t) = \theta_{s0}(\eta) + \sqrt{t}\, Pe\, \theta_{s1}(\eta) + O(t), \qquad (4.9.2)$$

and

$$z_p(t) = 2z_1 \sqrt{Fo}\sqrt{t} + 2z_2\, Pe \sqrt{Fo}\, t + O(t^{\frac{3}{2}}) \qquad (4.9.3)$$

On substituting the series (4.9.1) to (4.9.3) into the energy equations (4.8.26) and(4.8.27) we obtain the identities

$$\frac{d^2\theta_o}{d\eta^2} + \sqrt{t}\,Pe\frac{d^2\theta_1}{d\eta^2} + \ldots + Br \equiv$$

$$Pe\,\sqrt{Fo}\,(z_1\sqrt{t} + z_2 Pe\,t + \ldots)\eta(\eta^2-3)\left(\frac{d\theta_o}{d\eta} + \sqrt{t}\,Pe\,\frac{d\theta_1}{d\eta} + \ldots\right)$$

$$+ 4\left(z_1^2 t + 2z_1z_2\,Pe\,t^{\frac{3}{2}} \ldots\right)\left(\frac{Pe\theta_1}{2\sqrt{t}} + \ldots\right)$$

$$- 2\left(z_1^2 + 3z_1z_2\,Pe\,\sqrt{t} + \ldots\right)\eta\left(\frac{d\theta_o}{d\eta} + \sqrt{t}\,Pe\,\frac{d\theta_1}{d\eta} + \ldots\right) \qquad (4.9.4)$$

and

$$\frac{d^2\theta_{SO}}{d\eta^2} + \sqrt{t}\,Pe\,\frac{d^2\theta_{S1}}{d\eta^2} + \ldots \equiv$$

$$- 2\,Pe\,\sqrt{Fo}\left(z_1\sqrt{t} + z_2\,Pe\,t + \ldots\right)\left(\frac{d\theta_{SO}}{d\eta} + \sqrt{t}\,Pe\,\frac{d\theta_{S1}}{d\eta} + \ldots\right)$$

$$+ 4\left(z_1^2\,t + 2z_1z_2\,Pe\,t^{\frac{3}{2}} + \ldots\right)\left(\frac{Pe\theta_{S1}}{2\sqrt{t}} + \ldots\right)$$

$$- 2\left(z_1^2 + 3z_1z_2\,Pe\,\sqrt{t} + \ldots\right)\eta\left(\frac{d\theta_{SO}}{d\eta} + \sqrt{t}\,Pe\,\frac{d\theta_{S1}}{d\eta} + \ldots\right) \qquad (4.9.5)$$

respectively.

The appropriate boundary conditions, obtained by substituting the series (4.9.1) and(4.9.2) into conditions (4.8.28) to (4.8.31) are found to be

$$\frac{d\theta_o}{d\eta}(0) = \frac{d\theta_1}{d\eta}(0) = \ldots = 0 \qquad (4.9.6)$$

$$\left.\begin{aligned} \theta_0(1) &= \theta_{s0}(1) = 1 \\ \theta_1(1) &= \theta_{s1}(1) = \ldots = 0 \end{aligned}\right\} \qquad (4.9.7)$$

$$\frac{d\theta_0}{d\eta}(1) = \frac{d\theta_{s0}}{d\eta}(1) \ , \ \frac{d\theta_1}{d\eta}(1) = \frac{d\theta_{s1}}{d\eta}(1) \ , \ldots , \qquad (4.9.8)$$

$$\theta_{s0}(\eta) \to 0, \ \theta_{s1}(\eta) \to 0, \ldots , \quad \text{as} \quad \eta \to \infty \qquad (4.9.9)$$

On multiplying out the brackets of the identitites (4.9.4) and (4.9.5) and, in the resulting expressions, equating the coefficient of like terms in t (in ascending powers), the above system is reduced to a set of subsystems of linear ordinary different equations. The solutions of the first two of the subsystems are given below.

4.9.1 First Order Subsystem

The terms independent of t in the identities (4.9.4) and (4.9.5) lead to the pair of equations

$$\frac{d^2\theta_0}{d\eta^2} + 2Z_1^2\eta \frac{d\theta_0}{d\eta} + B_r = 0 \ , \ 0 \leq \eta \leq 1 \qquad (4.9.10)$$

and

$$\frac{d^2\theta_{s0}}{d\eta^2} + 2Z_1^2\eta \frac{d_{\theta s0}}{d\eta} = 0, \ \eta > 1 \ . \qquad (4.9.11)$$

These equations subject to the appropriate boundary conditions, namely

$$\frac{d\theta_0}{d\eta}(0) = 0 \ , \qquad (4.9.12)$$

$$\theta_0(1) = \theta_{s0}(1) = 1 \qquad (4.9.13)$$

$$\frac{d\theta_0}{d\eta}(1) = \frac{d\theta_{s0}}{d\eta}(1) \qquad (4.9.14)$$

and

$$\theta_{s0}(\eta) \to 0 \quad \text{as} \quad \eta \to \infty \quad , \tag{4.9.15}$$

form the first order subsystem. It is immediately obvious that the above system is independent of the Peclet number pe and, in fact, if z_1 is replaced by α they are identical to the system used in Atthey's solution in Section 4.4. Hence recalling equations (4.4.17), (4.4.19) and (4.4.21) the solution of equations (4.9.10) and (4.9.11) which satisfies the conditions (4.9.12) to (4.9.15) is

$$\theta_0 = 1 + \frac{B_r}{Z_1^2} \int_{Z_1\eta}^{Z_1} D(u)du \quad , \tag{4.9.16}$$

$$\theta_{s0} = \operatorname{erfc}(Z_1\eta)/\operatorname{erfc}(Z_1) \quad , \tag{4.9.17}$$

where z_1 is the solution of the transcendental equation

$$\frac{2Z_1^2}{B_r\sqrt{\pi}} e^{-Z_1^2} = \operatorname{erfc}(Z_1)D(Z_1) \quad . \tag{4.9.18}$$

Dawsons integral $D(u)$ and the complementary error function $\operatorname{erfc}(u)$ have been defined by equations (4.4.18) and (4.4.20) respectively.

4.9.2 Second Order Subsystems.

Equating the coefficient of $\sqrt{t}$ in the above identities (4.9.4) and (4.9.5) yields

$$\frac{d^2\theta_1}{d\eta^2} + 2Z_1^2\eta \frac{d\theta_1}{d\eta} - 2Z_1^2\theta_1 = Z_1\left[\sqrt{F_o}\,\eta^2 - 3(2Z_2+\sqrt{F_o})\right]\eta \frac{d\theta_0}{d\eta} \quad , \quad 0 \leq \eta \leq 1 \tag{4.9.19}$$

and

$$\frac{d^2\theta_{s1}}{d\eta^2} + 2Z_1^2\eta \frac{d\theta_{s1}}{d\eta} - 2Z_1^2\theta_{s1} = -2Z_1\left[\sqrt{F_0} + 3Z_2\eta\right] \frac{d\theta_{s0}}{d\eta} , \quad \eta \geq 1 \quad (4.9.20)$$

The appropriate boundary conditions from the set (4.9.6) to (4.9.9) are

$$\frac{d\theta_1}{d\eta}(0) = 0 , \quad (4.9.21)$$

$$\theta_1(1) = \theta_{s1}(1) = 0 , \quad (4.9.22)$$

$$\frac{d\theta_1}{d\eta}(1) = \frac{d\theta_{s1}}{d\eta}(1) \quad (4.9.23)$$

and

$$\theta_{s1}(\eta) \to 0 \quad \text{as} \quad \eta \to \infty . \quad (4.9.24)$$

On substituting the expressions for θ_o and θ_{so} given by equations (4.9.16) and (4.9.17) respectively into equations (4.9.11) and (4.9.20) the latter reduces to

$$\frac{d^2\theta_1}{d\eta^2} + 2Z_1^2\eta \frac{d\theta_1}{d\eta} - 2Z_1^2\theta_1 = B_r\left[3(2Z_2+\sqrt{F_0})-\sqrt{F_0}\,\eta^2\right]\eta D(Z_1\eta) , \quad 0 \leq \eta \leq 1 , \quad (4.9.25)$$

and

$$\frac{d^2\theta_{s1}}{d\eta^2} + 2Z_1^2\eta \frac{d\theta_{s1}}{d\eta} - 2Z_1^2\theta_{s1} = \frac{4Z_1^2}{\sqrt{\pi}}\left[\sqrt{F_0} + 3Z_2\eta\right] e^{-Z_1^2\eta^2} / \operatorname{erfc}(Z_1), \quad \eta \geq 1 \quad (4.9.26)$$

respectively.

As for all linear second order, ordinary differential equations the solutions to (4.9.25) and (4.9.26) may be split into the sum of two terms, the complementary function and the particular integral. Thus we may write

$$\theta_1 = \theta_{1c} + \theta_{1p} \tag{4.9.27}$$

and

$$\theta_{s1} = \theta_{s1c} + \theta_{s1p} \tag{4.9.28}$$

where, in a natural way the subscripts 'c' and 'p' denote the complementary function and the particular integral respectively.

The complementary functions are easily found to be

$$\theta_{1c} = A_1\eta + A_2\left[Z_1\eta\ \mathrm{erfc}(Z_1\eta) - 1/\sqrt{\pi}\ e^{-Z_1^2\eta^2}\right], 0 \leq \eta \leq 1 \tag{4.9.29}$$

and

$$\theta_{s1c} = A_{s1}\eta + A_{s2}\left[Z_1\eta\ \mathrm{erfc}(Z_1\eta) - 1/\sqrt{\pi}\ e^{-Z_1^2\eta^2}\right], \eta \geq 1 \tag{4.9.30}$$

where the constant A, A_{s1}, A_2 and A_{s2} are unknown at this stage.

Having obtained the complementary functions, the particular integrals of equations (4.9.25) and (4.9.26) could now be obtained in a systematic manner using the method of variation of parameters [36] . The right hand sides of the equations are not simple, however, and it is found easier to obtain the particular integrals directly.

The nature of the right hand side of equation (4.9.25) suggests that we look for a particular integral in the form

$$\theta_1 = \phi(\eta) + \chi(\eta)D(Z_1\eta)\ ,\ 0 \leq \eta \leq 1 \tag{4.9.31}$$

where ϕ and χ are abitrary functions of η. Substituting equation (4.9.31) into equation (4.9.25) yields

$$\frac{d^2\phi}{d\eta^2} + 2Z_1^2\eta\frac{d\phi}{d\eta} - 2Z_1^2\phi + 2Z_1\frac{d\chi}{d\eta} +$$

$$\left[\frac{d^2\chi}{d\eta^2} - 2Z_1^2\eta\frac{d\chi}{d\eta} - 4Z_1^2\chi\right]D(Z_1\eta) =$$

$$B_r\left[3(2Z_2 + \sqrt{F_0}) - \sqrt{F_0}\,\eta^2\right]\eta D(Z_1\eta) \ , \tag{4.9.32}$$

and this equation is satisfied provided that ϕ and χ are solutions of the pair of equations

$$\frac{d^2\phi}{d\eta^2} + 2Z_1^2\eta\frac{d\phi}{d\eta} - 2Z_1^2\phi = -2Z_1\frac{d\chi}{d\eta} \tag{4.9.33}$$

and

$$\frac{d^2\chi}{d\eta^2} - 2Z_1^2\eta\frac{d\chi}{d\eta} - 4Z_1^2\chi = B_r\left[3(2Z_2 + \sqrt{F_0}) - \sqrt{F_0}\,\eta^2\right]\eta \ . \tag{4.9.34}$$

To solve the above, we first find a function $\chi(\eta)$ which satisfies equation (4.9.34) and then proceed to solve (4.9.33) for ϕ. The nature of the right hand side of equation (4.9.34) suggests that we seek a solution for χ in the form

$$\chi = a_1\eta + a_2\eta^3 \tag{4.9.35}$$

and after substituting into equation (4.9.34) it follows immediately that

$$a_1 = \frac{B_r}{10Z_1^2}\left[\frac{\sqrt{F_0}}{Z_1^2} - 5(2Z_2 + \sqrt{F_0})\right] \ , \ a_2 = \frac{B_r\sqrt{F_0}}{10Z_1^2} \tag{4.9.36}$$

With the use of equations (4.9.35) and (4.9.36), equation (4.9.33) becomes

$$\frac{d^2\phi}{d\eta^2} + 2Z_1^2\eta\frac{d\phi}{d\eta} - 2Z_1^2\phi = -\frac{3B_r\sqrt{F_0}\,\eta^2}{5Z_1} - \frac{B_r}{5Z_1}\left[\frac{\sqrt{F_0}}{Z_1^2} - 5(2Z_2 + \sqrt{F_0})\right], \tag{4.9.37}$$

and it is now easy to show that a solution of this equation has the form

$$\phi = b_1 + b_2\eta^2 \tag{4.9.38}$$

provided that b_1 and b_2 are given by

$$b_1 = -\frac{B_r}{10Z_1^3}\left[\frac{2\sqrt{F_0}}{Z_1^2} + 5(2Z_2 + \sqrt{F_0})\right], \quad b_2 = \frac{-3B_r\sqrt{F_0}}{10Z_1^3} \tag{4.9.39}$$

It follows from equations (4.9.31), (4.9.35), (4.9.36), (4.9.38) and (4.9.39) that the particular integral of equation (4.9.25) is

$$\theta_{1p} = -\frac{B_r}{10Z_1^3}\left\{\left[\frac{2\sqrt{F_0}}{Z_1^2} + 5(2Z_2 + \sqrt{F_0})\right] + 3\sqrt{F_0}\,\eta^2\right\}$$

$$+\frac{B_r}{10Z_1^2}\left\{\left[\frac{\sqrt{F_0}}{Z_1^2} - 5(2Z_2 + \sqrt{F_0})\right] + \sqrt{F_0}\,\eta^2\right\}\eta D(Z_1), \quad 0 \leq \eta \leq 1 \tag{4.9.40}$$

Inspection of equation (4.9.26) suggests that we look for a particular integral in the form

$$\theta_{s1} = \left[a_{s1} + a_{s2}\eta\right]e^{-Z_1^2\eta^2} \tag{4.9.41}$$

where a_{s1} and a_{s2} are both constants. Substitution of this expression into equation (4.9.20) leads to the solution

$$\theta_{slp} = -\frac{1}{\sqrt{\pi}}\left[\sqrt{F_0} + 2Z_2\eta\right]e^{-Z_1^2\eta^2}/\mathrm{erfc}(Z_1) \quad \eta \geq 1 . \qquad (4.9.42)$$

Having now obtained the complementary functions and particular integrals to equations (4.9.25) and (4.9.26) we can write down, with the aid of equations (4.9.27) and (4.9.28), the complete solutions in the forms

$$\theta_1 = A_1\eta + A_2\left[Z_1\eta\ \mathrm{erfc}(Z_1\eta) - 1/\sqrt{\pi}\ e^{-Z_1^2\eta^2}\right] -$$

$$\frac{B_r}{10Z_1^3}\left\{\left[\frac{2\sqrt{F_0}}{Z_1^2} + 5(2Z_2 + \sqrt{F_0})\right] + 3\sqrt{F_0}\ \eta^2\right\} +$$

$$\frac{B_r}{10Z_1^2}\left\{\left[\frac{\sqrt{F_0}}{Z_1^2} - 5(2Z_2 + \sqrt{F_0})\right] + \sqrt{F_0}\ \eta^2\right\}\eta D(Z_1\eta), \quad 0 \leq \eta \leq 1 \qquad (4.9.43)$$

and

$$\theta_{s1} = A_{s1}\eta + A_{s2}\left[Z_1\eta\ \mathrm{erfc}(Z_1\eta) - 1/\sqrt{\pi}\ e^{-Z_1^2\eta^2}\right]$$

$$- 1/\sqrt{\pi}\left[\sqrt{F_0} + 2Z_2\eta\right]e^{-Z_1^2\eta^2}/\mathrm{erfc}(Z_1) , \quad \eta \geq 1 . \qquad (4.9.44)$$

The unknown constants A_1, A_{s1}, A_2 and A_{s2} are obtained through application of the boundary conditions (4.9.21) to (4.9.24). Firstly we differentiate equations (4.9.43) and (4.9.44) with respect to η to obtain the dimensionless heat fluxes.

$$\frac{d\theta_1}{d\eta} = A_1 + A_2 Z_1 \operatorname{erfc}(Z_1\eta) - \frac{3B_r\sqrt{F_0}\,\eta}{5Z_1^3} +$$

$$\frac{B_r}{10Z_1}\left\{\left[\frac{\sqrt{F_0}}{Z_1^2} - 5(2Z_2 + \sqrt{F_0})\right]\eta + \sqrt{F_0}\,\eta^3\right\}\left\{1 - 2Z_1\eta D(Z_1\eta)\right\} +$$

$$\frac{B_r}{10Z_1^2}\left\{\left[\frac{\sqrt{F_0}}{Z_1^2} - 5(2Z_2 + \sqrt{F_0})\right] + 3\sqrt{F_0}\,\eta^2\right\}D(Z_1\eta) \quad , \quad 0 \leq \eta \leq 1 \qquad (4.9.45)$$

and

$$\frac{d\theta_{s1}}{d\eta} = A_{s1} + A_{s2} Z_1 \operatorname{erfc}(Z_1\eta) +$$

$$\frac{2Z_1 e^{-Z_1^2\eta^2}}{\sqrt{\pi}\,\operatorname{erfc}(Z_1)}\left[\sqrt{F_0}\,Z_1\eta + \frac{Z_2}{Z_1}\left(2Z_1^2\eta^2 - 1\right)\right], \quad \eta \geq 1 \ , \qquad (4.9.46)$$

and applying the boundary condition (4.9.21) then gives

$$A_1 = -Z_1 A_2 \qquad (4.9.47)$$

Using this relation in equation (4.9.43) and applying the boundary condition $(4.9.22)_1$ we deduce, after some algebra that

$$A_1 = M_1 Z_2 + M_2 \qquad (4.9.48)$$

where M_1 and M_2 are given by

$$M_1 = \frac{B_r\left[1 + Z_1 D(Z_1)\right]}{Z_1^2(Z_1 - k_2)} \qquad (4.9.49)$$

and

$$M_2 = \frac{B_r\sqrt{F_0}\left\{\left[2 - Z_1 D(Z_1)\right] + 4Z_1^2\left[2 + Z_1 D(Z_1)\right]\right\}}{10Z_1^4(Z_1 - k_2)} \qquad (4.9.50)$$

The quantity k_2 is defined by

$$k_2 = z_1 \operatorname{erfc}(z_1) - 1/\sqrt{\pi}\, e^{-z_1^2} \ . \qquad (4.9.51)$$

It follows from (4.9.44) and condition (4.9.24) that A_{s1} is identically zero, and then condition$(4.9.22)_2$, is satisfied only if

$$A_{s2} = M_3 Z_2 + M_4 \ , \tag{4.9.52}$$

$$\left.\begin{aligned} M_3 &= 2k_3/k_2 \ , \\ M_4 &= \sqrt{F_0}\,k_3/k_2 \ , \end{aligned}\right\} \tag{4.9.53}$$

where k_3 is defined by

$$k_3 = e^{-Z_1^2}/\sqrt{\pi}\ \mathrm{erfc}(Z_1) \ . \tag{4.9.54}$$

With the aid of equations (4.9.45), (4.9.46) and (4.9.47), the boundary condition (4.9.23) leads to the equation

$$A_1\ \mathrm{erf}(Z_1) - \frac{3B_r\sqrt{F_0}}{5Z_1^3} + \frac{B_r}{10Z_1^2}\left[\frac{\sqrt{F_0}}{Z_1^2}\,(1-2Z_1^2) - 10Z_2\right]D(Z_1)$$

$$+ \frac{B_r}{10Z_1}\left[\frac{\sqrt{F_0}}{Z_1^2}\,(1-4Z_1^2) - 10Z_2\right]\left[1 - 2Z_1 D(Z_1)\right] =$$

$$A_{s2}Z_1\ \mathrm{erfc}(Z_1) + 2Z_1k_3\left[\sqrt{F_0}\ Z_1 + \frac{Z_2}{Z_1}\,(2Z_1^2-1)\right] \tag{4.9.55}$$

Finally, substituting equations (4.9.48) and (4.9.52) for A_1 and A_{s2} respectively into the above relationship, results in a

linear algebraic equation with solution

$$Z_2 = \left\{ M_4 Z_1 \operatorname{erfc}(Z_1) - M_2 \operatorname{erf}(Z_1) + 2\sqrt{F_0}\, Z_1^2 k_3 + \frac{B_r F_0}{10 Z_1^4}\left[(2Z_1^2-1)D(Z_1) + 6Z_1 \right.\right.$$

$$\left.\left. + Z_1(4Z_1^2-1)\left(1-2Z_1 D(Z_1)\right)\right]\right\} \Bigg/ \left\{ M_1 \operatorname{erf}(Z_1) - M_3 Z_1 \operatorname{erfc}(Z_1) - 2(2Z_1^2-1)k_3 \right.$$

$$\left. - \frac{B_r}{Z_1^2}\left[D(Z_1) + Z_1\left(1 - 2Z_1 D(Z_1)\right)\right]\right\} \qquad (4.9.56)$$

In principle, it is now possible to go on and obtain higher order terms. However, this would be an extremely tedious and algebraically complicated task and for this reason it was decided to terminate the series after the first two terms. The truncated series solution will be accurate at small times but will become a poorer approximation to the exact solution as time is increased. However it is thought to be a useful solution since it illustrates the effect that the inclusion of Burnoff has on Atthey's solution and also serves to assess the accuracy of the approximate solution developed in section (4.8).

Values of Z_1 are presented in Table 4.1. Since Z_1 is numerically equal to α. With these values of Z_1, Z_2 is easily calculated using equation (4.9.56) for various values of Br and Pe and these values are presented in Table 4.5. A comparison of these values of Z_2 with the values for Z_2 obtained by the heat balance method and presented in Table 4.4, indicates that for small values of Br the error is about 25% but as Br increases, the difference decreases and it is seen that for Br = 10, the error is less than 2%.

Br	Z_2
0.1	-0.144
0.2	-0.243
0.3	-0.316
0.4	-0.370
0.5	-0.477
0.6	-0.448
0.7	-0.477
0.8	-0.500
0.9	-0.520
1 0	-0.537
2.0	-0.631
4.0	-0.692
6.0	-0.716
10.0	-0.738

Table 4.5

Using the values of Z_1 and Z_2 calculated from the exact equations, the temperature profiles θ_1 and θ_{s1} are computed from equations (4.9.43) and (4.9.44) with the aid of (4.9.48) to (4.9.53). Using these temperature profiles and the ones given by (4.9.16) and (4.9.17) the temperature profiles θ and θ_s valid for small times are calculated with the aid of (4.9.1) and (4.9.2) and presented in Section 4.10.

4.10 Results and Discussion of Sections 4.8 and 4.9

In this section, the results of Sections 4.8 and 4.9 are presented and discussed.

In Figure 4.6 the results for Z_p, obtained using the values of Z_1 and a_{20} presented in Table 4.3 and equation (4.8.61), for the case of zero Pe, and the Runge-Kutta process for the case of non-zero Pe, are plotted against t for various values of Pe and Br. Comparison of the curves in Figure 4.6(a) with those for the corresponding exact solutions presented in Figure 4.1 reveals that the difference is very small for low values of Br but becomes greater as Br increases. However the greatest error is less than 5% for Br in the range $0 - 5.0$.

The effect of axial shortening is incorporated in Figures 4.6(b), (c) and (d). It is seen from these Figures that on increasing Pe the thickness of the plastic region decreases. The reason for this is that for larger Pe more heat is lost by forced convections resulting in less heat being available to drive along the plastic/solid interface. It is important to note that as Pe increases, equilibrium is approached more rapidly for a given value of Br. Also increasing Br delays the approach of equilibrium. A qualitative illustration of the effect of both Pe and Br on the time taken to reach equilibrium is given in Section 4.11, in which the steady state values of Z_p and the steady state temperature profiles are also determined.

The curves in Figure 4.7 indicates the decay of the shear stress τ with time. Comparison of the curves in Figure 4.7(a) with the corresponding curves obtained from the exact solution presented in Figure 4.2, again reveals that for small Br the difference between the two solutions is very small but increases with increasing Br.

It is seen from Figures 4.7(b), (c) and (d) that the qualitative agreement between these curves and the torque trace shown in Figure 4.31 is much improved by the inclusion of upset. All quantitative comparisons with experimental data are delayed until Section 4.17.

The temperature profiles computed from equations (4.8.35) and (4.8.47) with the aid of the values of a_2 obtained from the Runge-Kutta process are presented in Figures 4.8(a) to(d)for the times $t = 0.1$ and $t = 1$. Also presented in Figure 4.8 are the temperature profiles obtained in Section 4.9 which are valid for small t only. In Figure 4.8(a) and (b) the solid line represents the heat balance integral solution and the dotted line represents the series solution value for small times. Comparison of these two sets of curves again reveals that the difference between the two solutions is very small. By comparing Figure 4.8(a) with Figure 4.8(b) and Figure 4.8(c) with Figure 4.8(d) the effect of upset is borne out. It is seen that the inclusion of upset gives an overall reduction in temperature. This is a result of cooling due to forced convection. In Figure 4.9 a plot of the interface temperature, $\theta(0)$, against t is given. It is seen that in all cases the interface temperature initially assumes the value predicted by the case $Pe = 0$ and decays to the equilibrium value. The equilibrium value of $\theta(0)$ is found to be independent of Pe but the rate of decay of this quantity increases with increasing Pe. It should also be noted that $\theta(0)$ increases with increasing Br.

In practice, one would expect the interface temperature to rise continually until the equilibrium temperature is attained. The

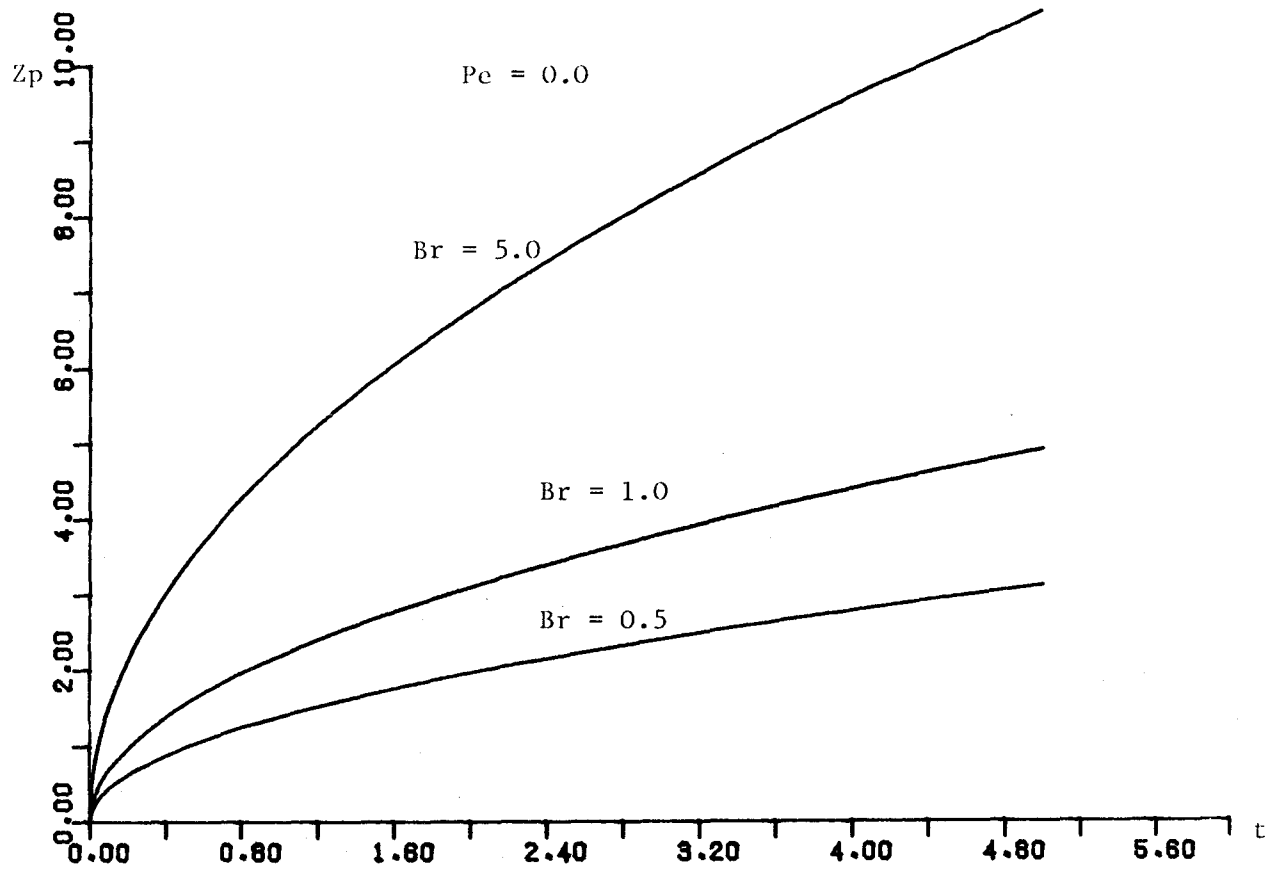

(a)

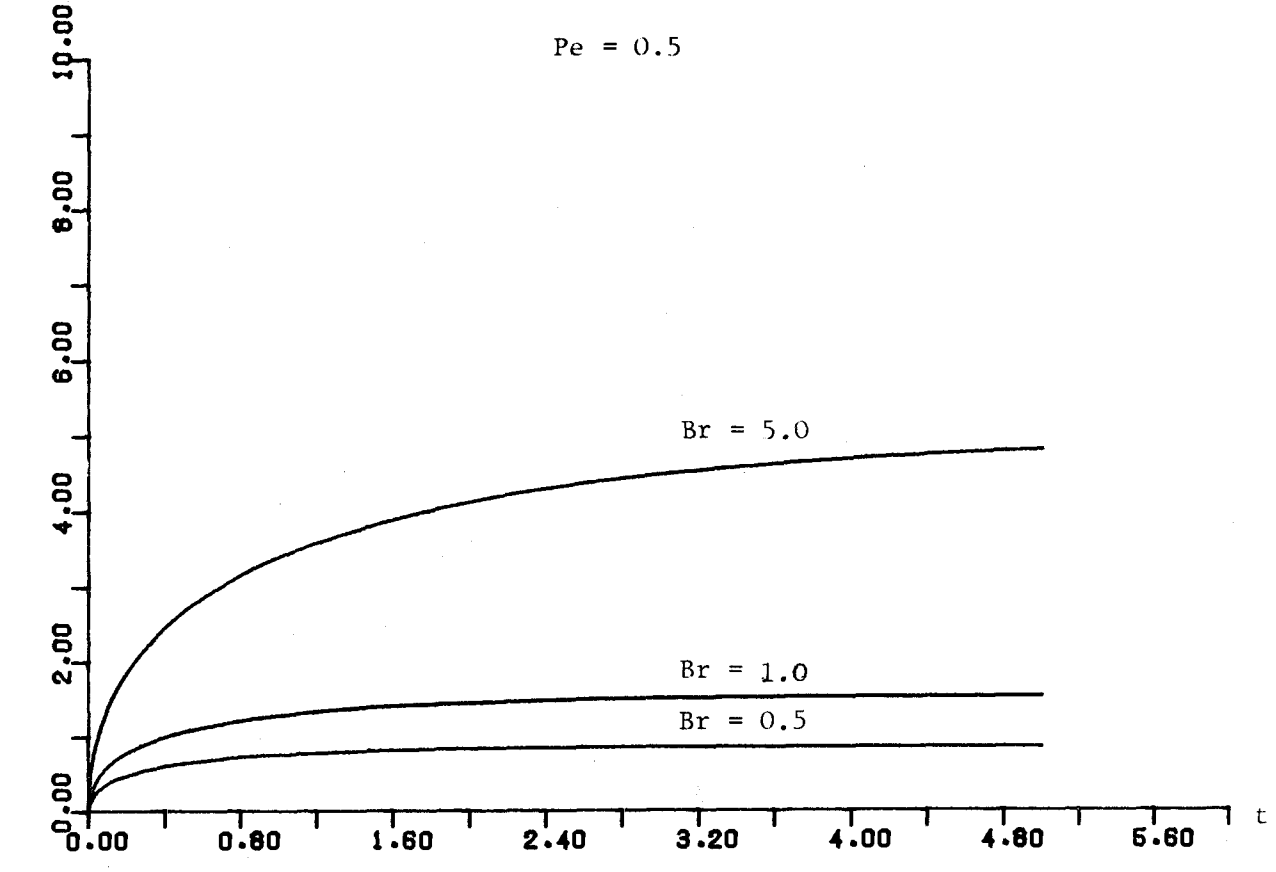

Figure 4.6 Graphs of Zp against t for the case $\mu = 1$

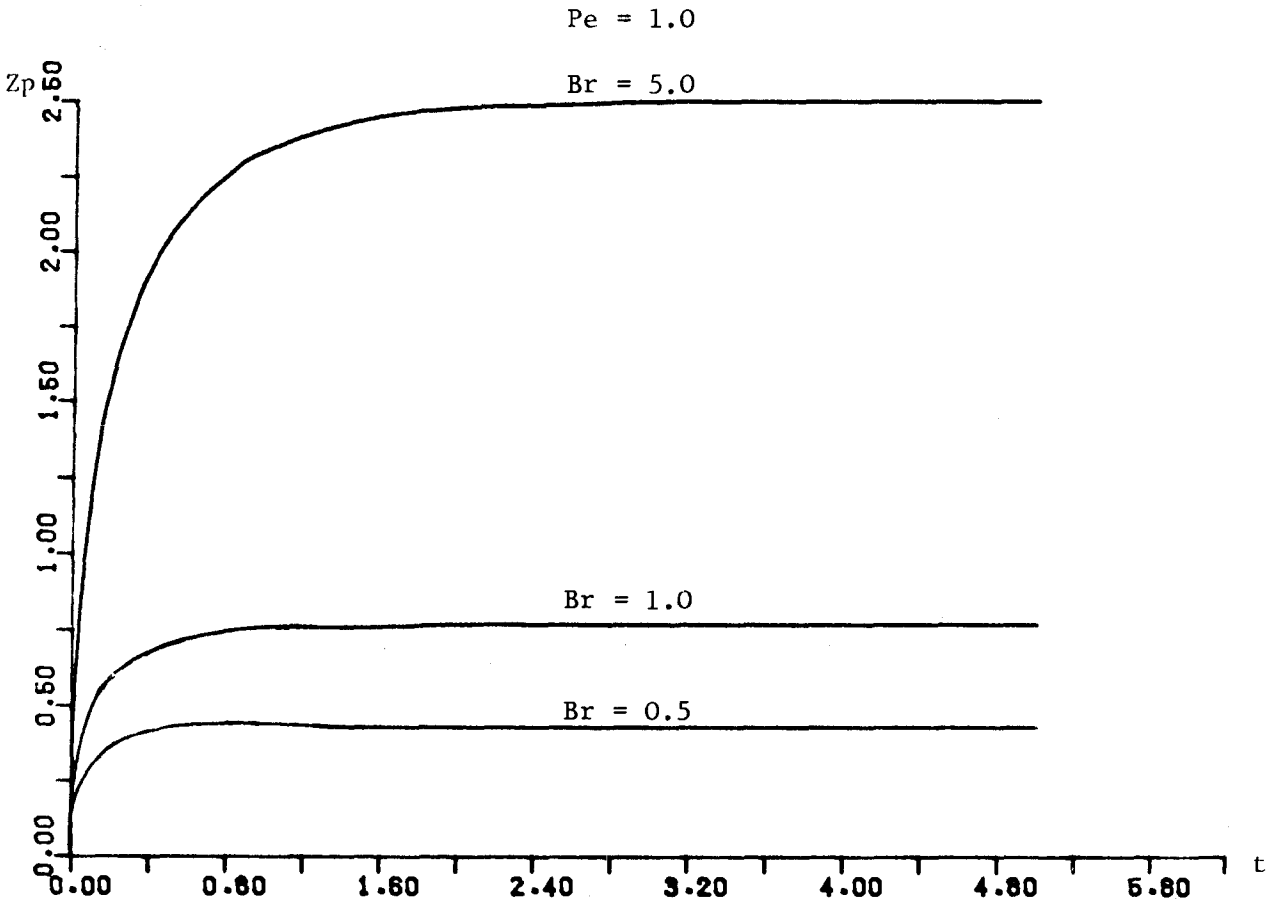

(c)

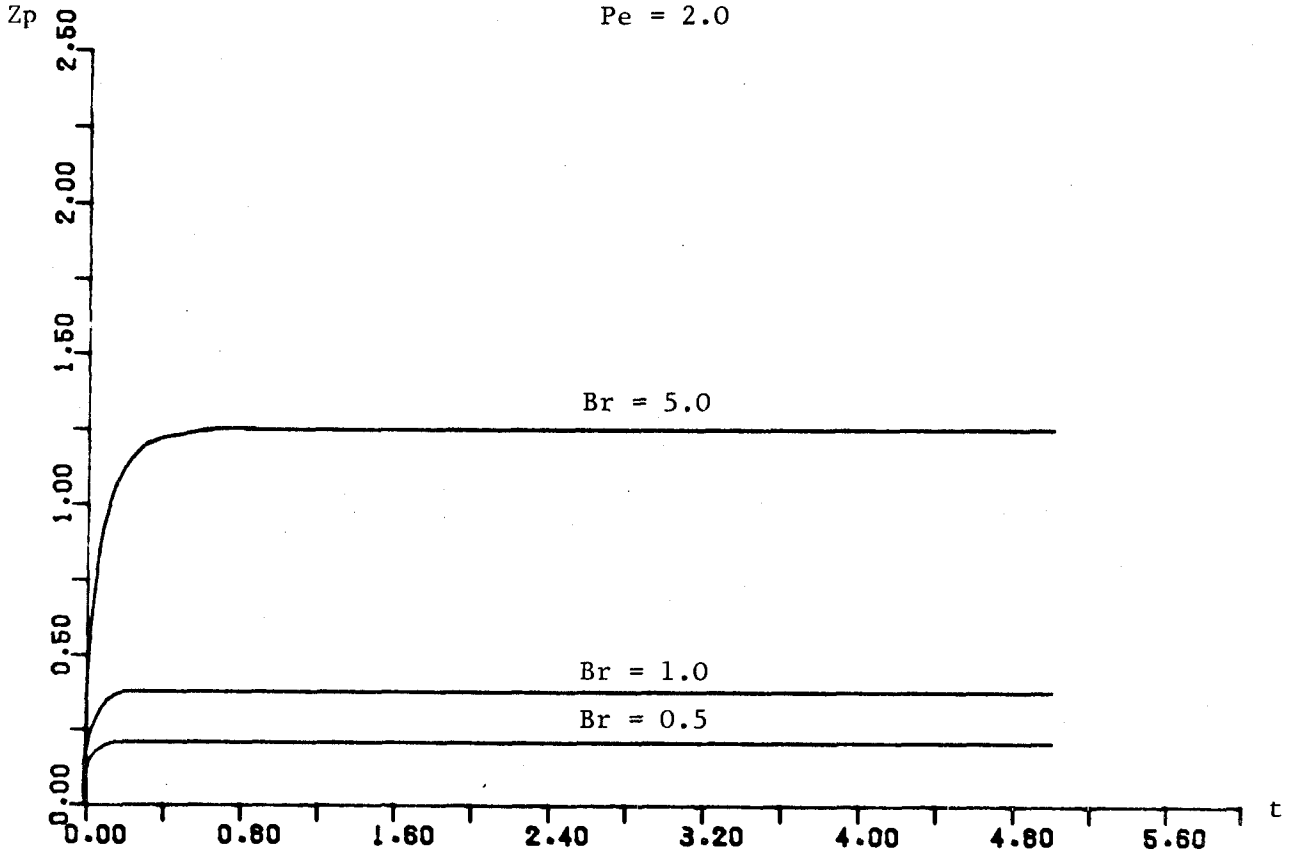

Figure 4.6 Plots of Zp against t for the case $\mu = 1$

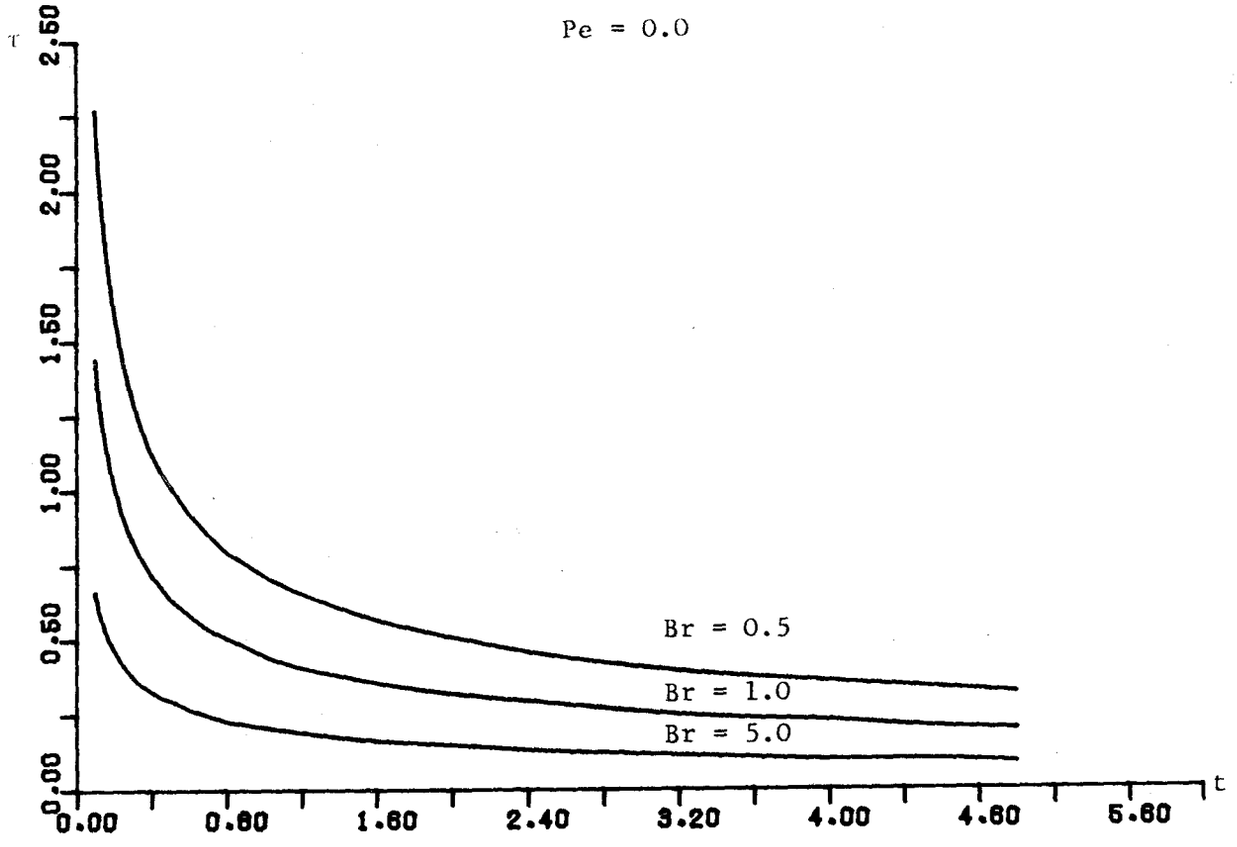

(a)

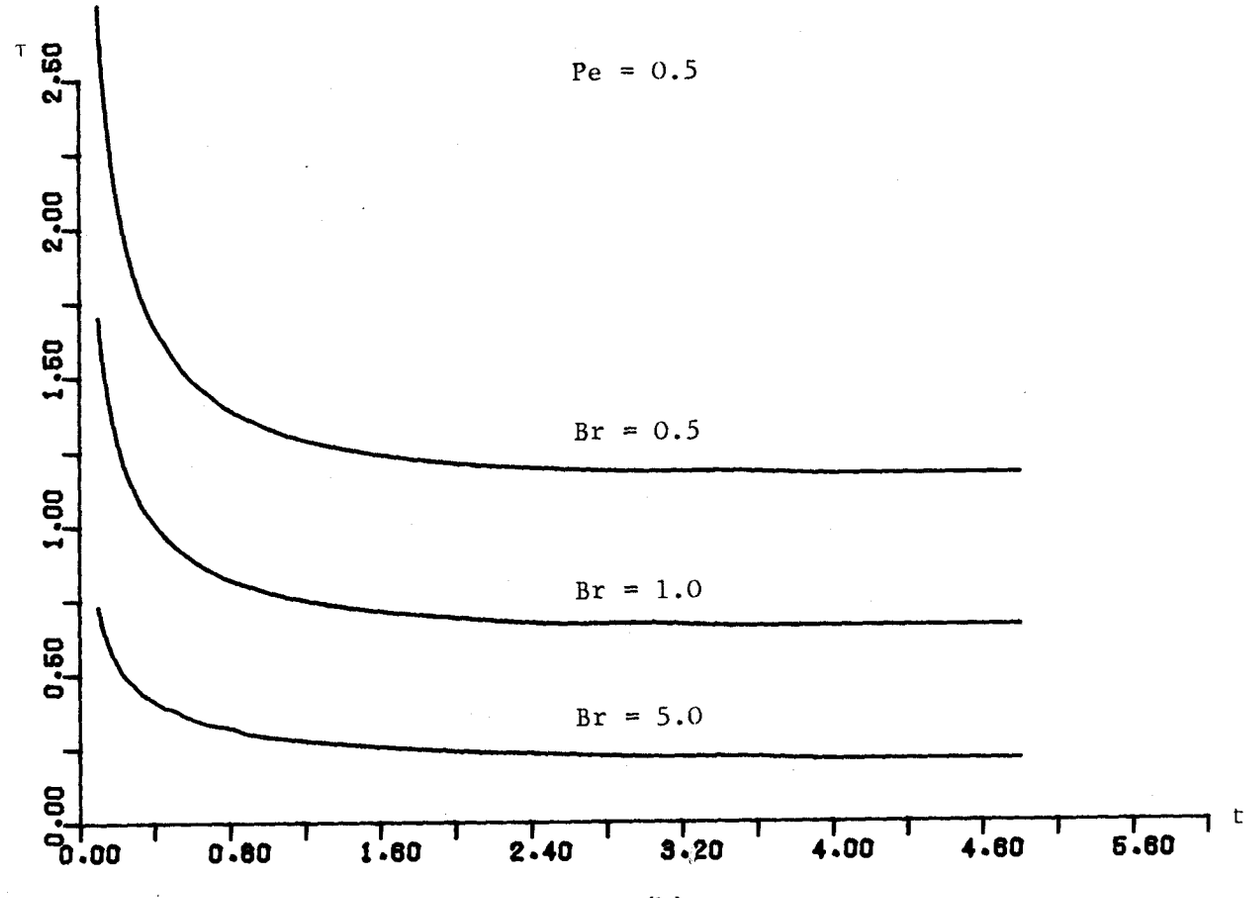

(b)

Figure 4.7 Graphs of τ against t for the case $\mu = 1$

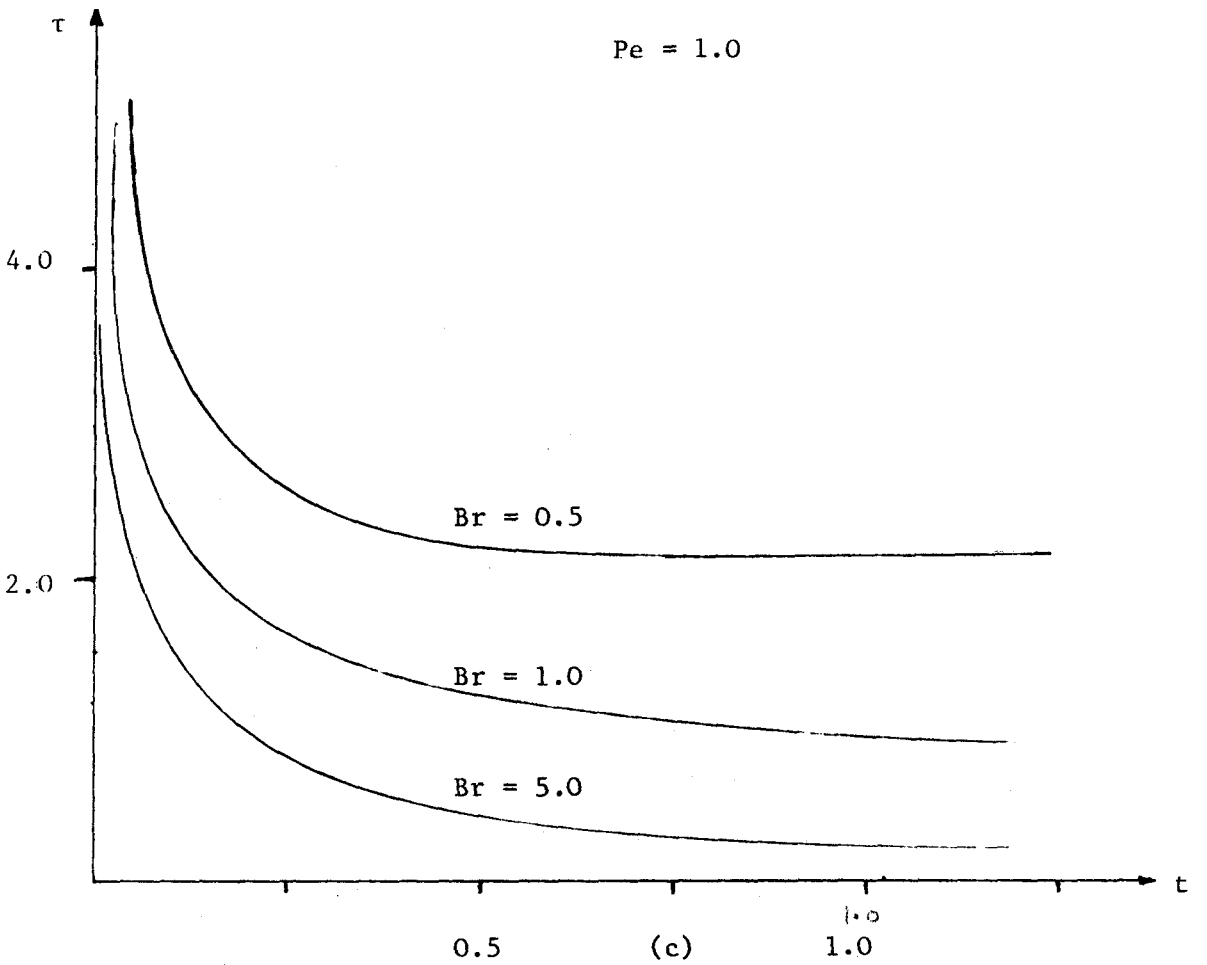

(c)

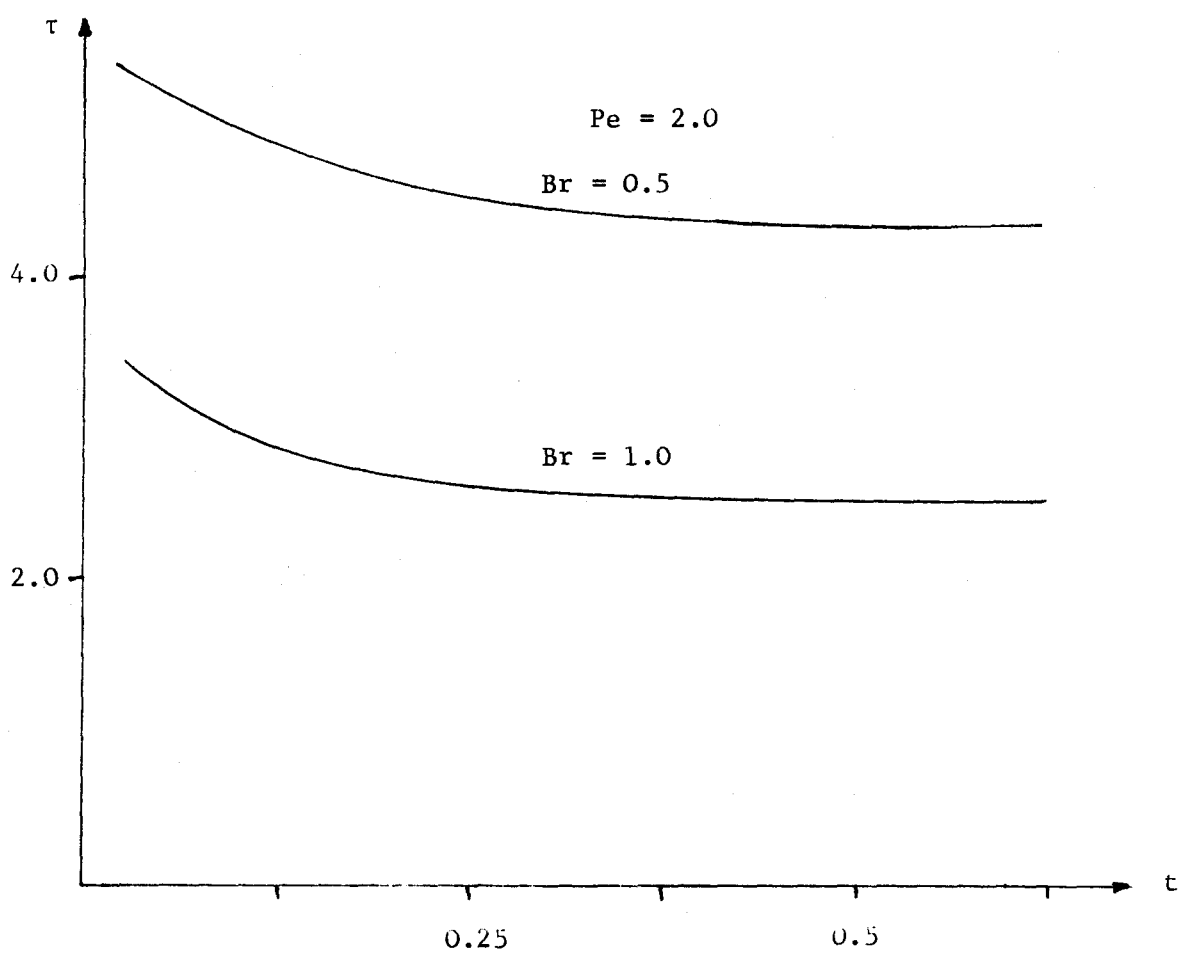

(d)

Figure 4.7 Graphs of τ against t for the case $\mu = 1$

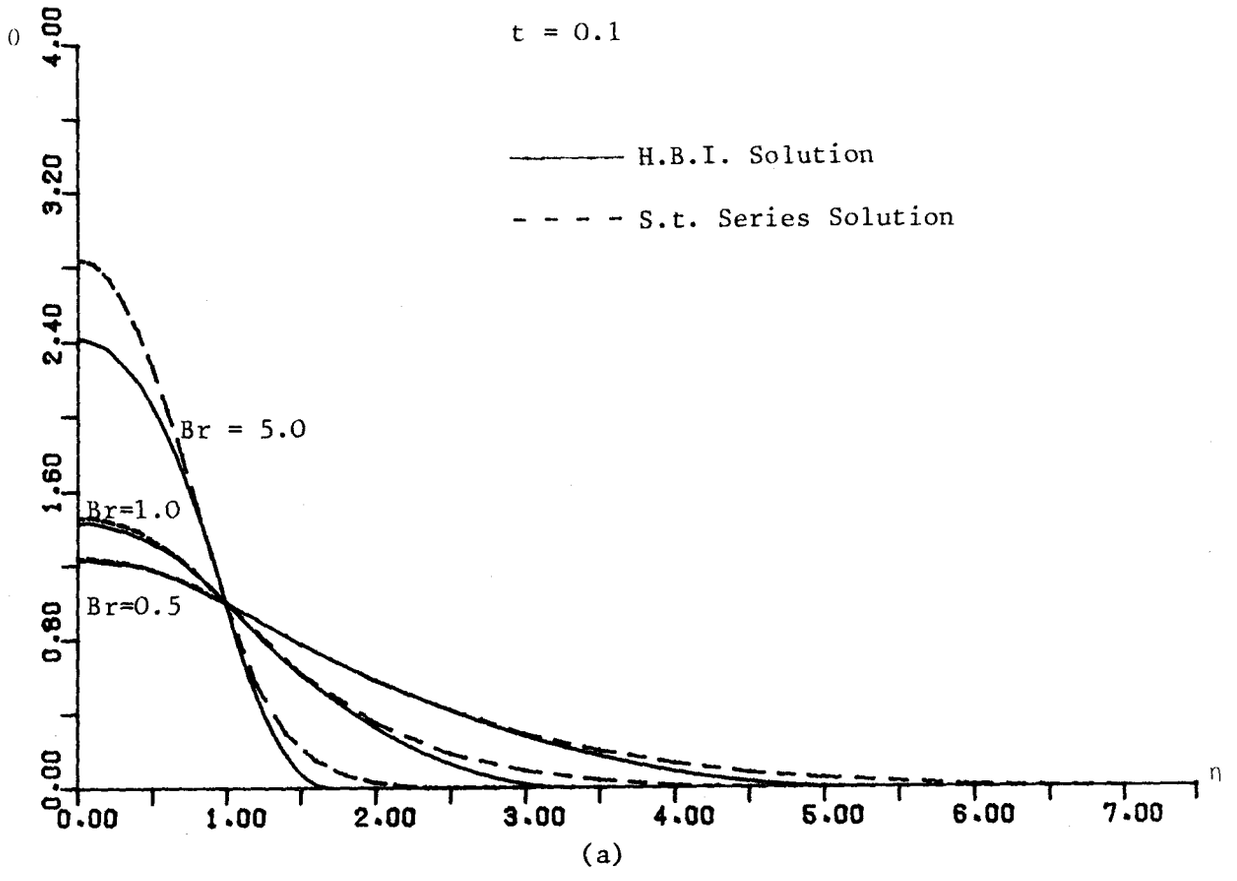

(a)

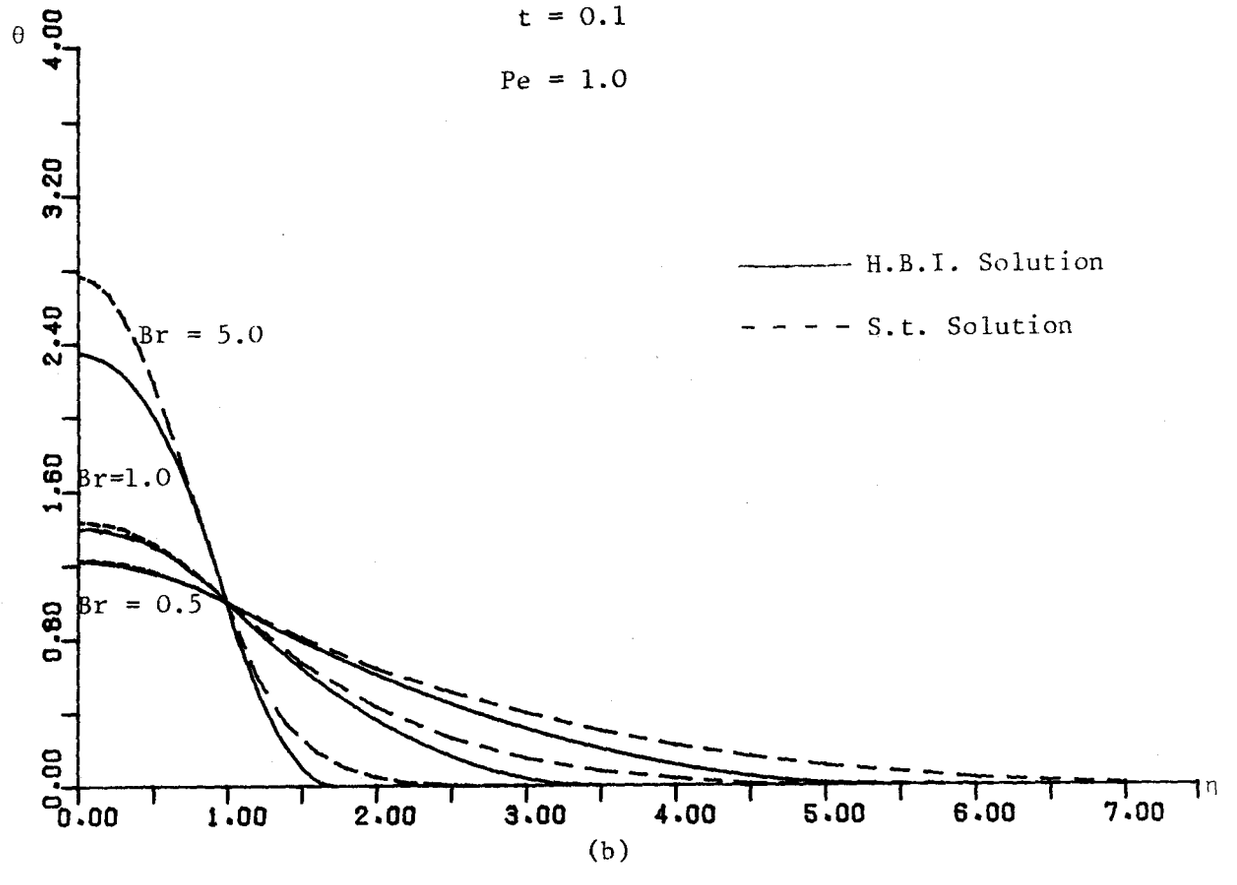

(b)

Figure 4.8 Graphs of θ against η for the case $\mu = 1$

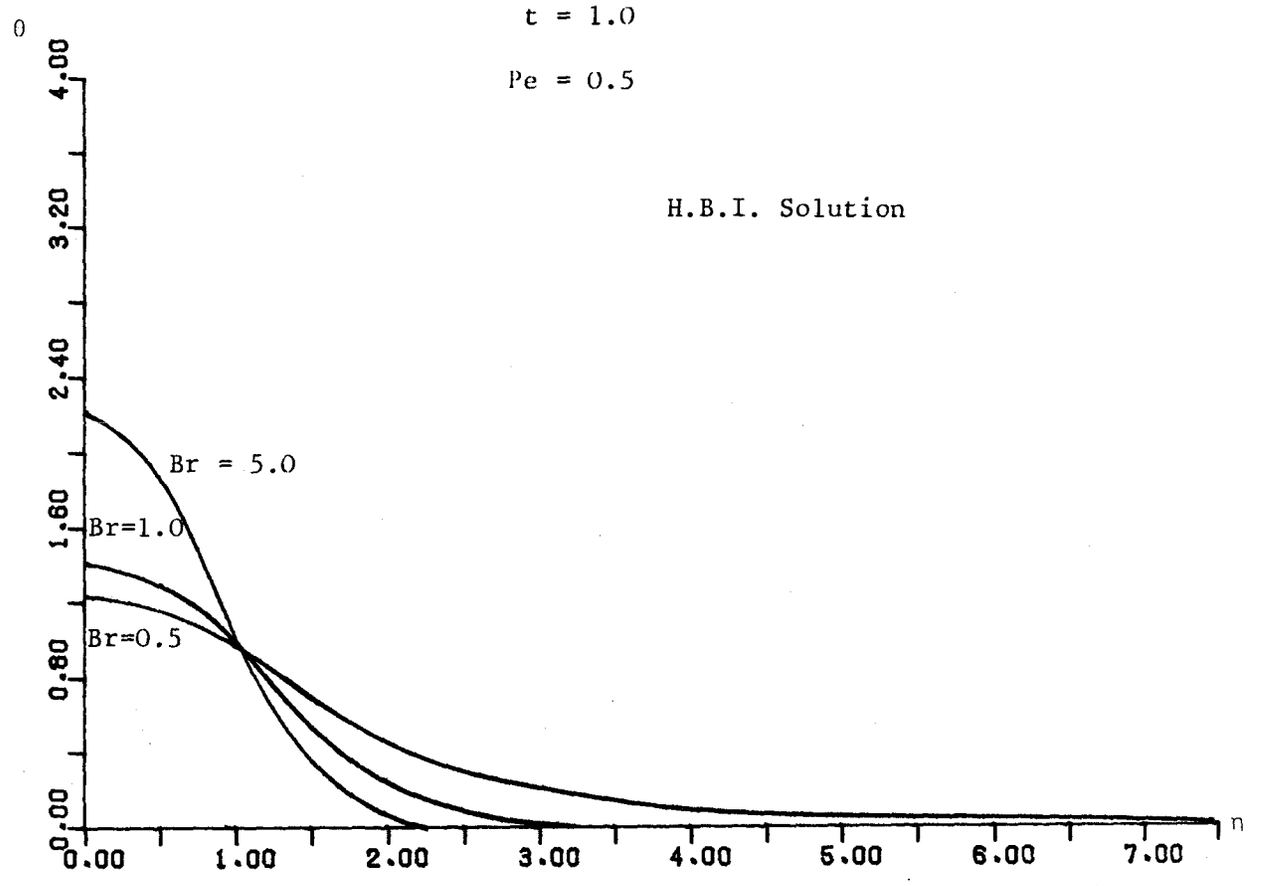

(c)

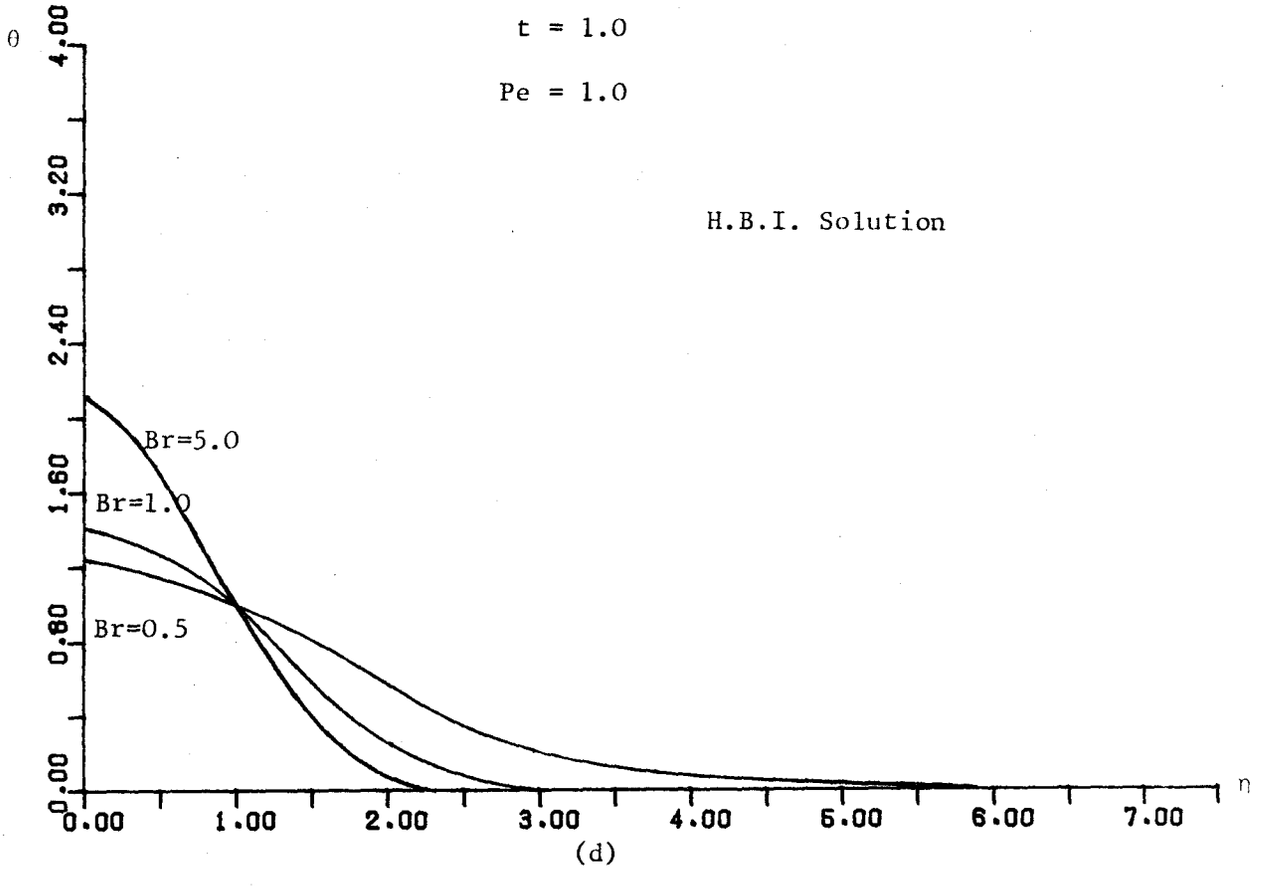

(d)

Figure 4.8 Graphs of θ against η for the case $\mu = 1$.

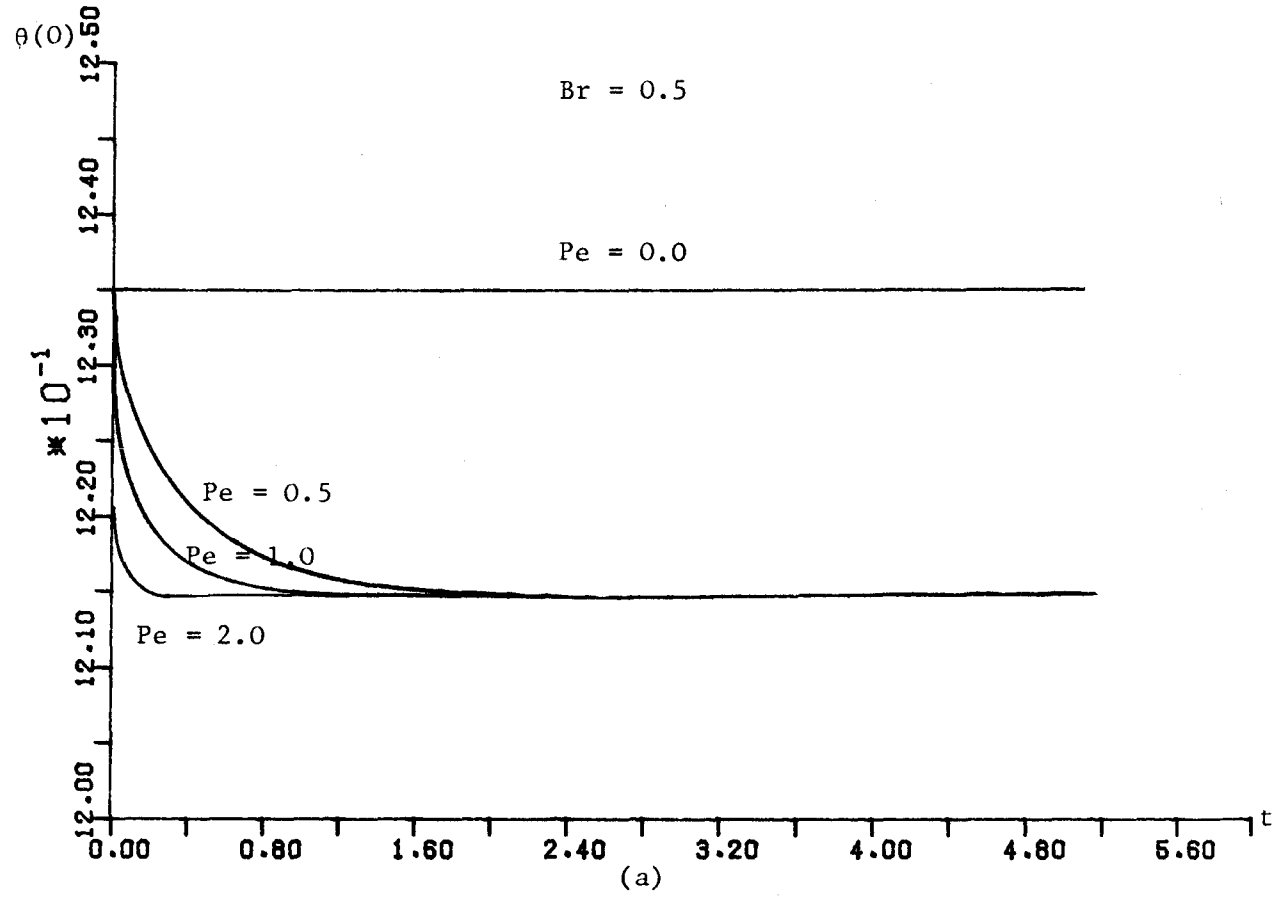

(a)

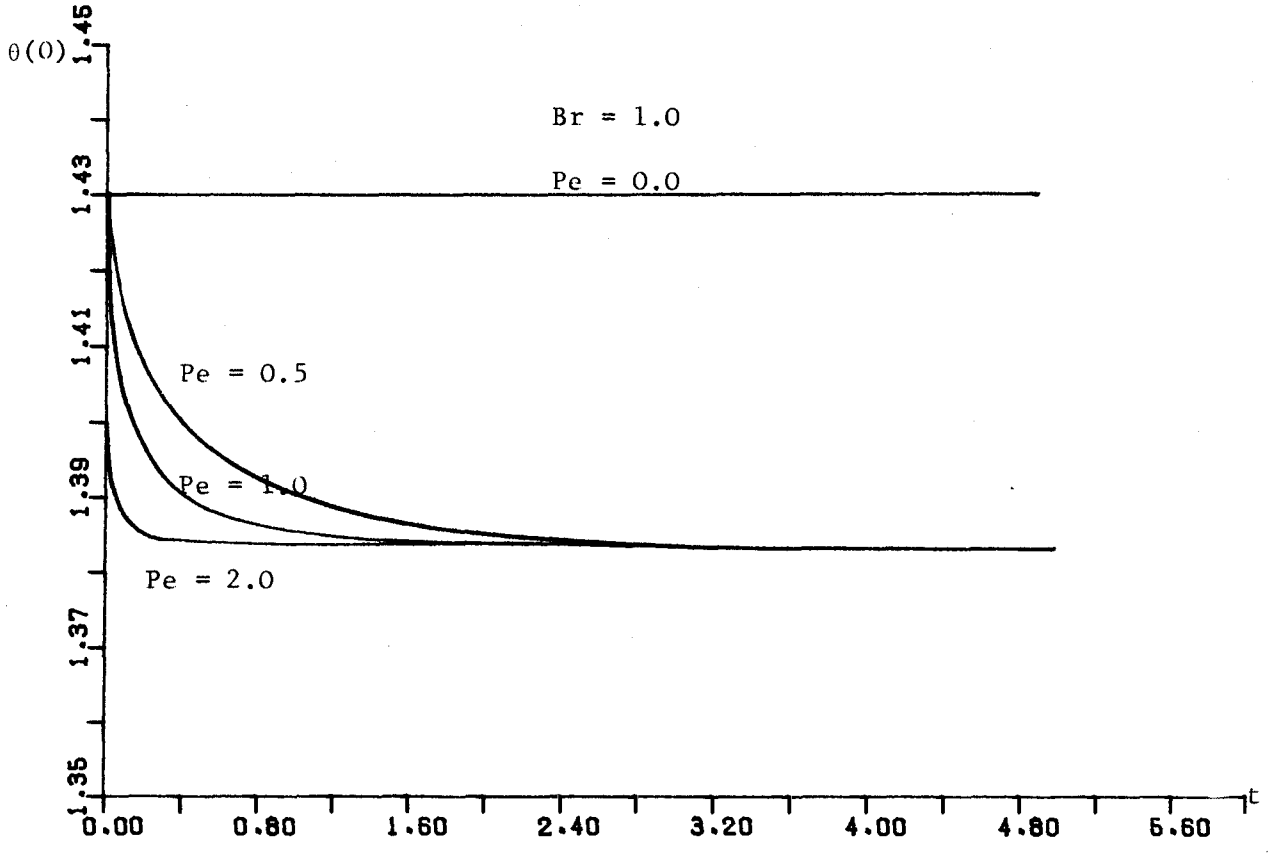

(b)

Figure 4.9 Graphs of Interface Temperature $\theta(0)$ against t for the case $\mu = 1$.

error in the models presented in Section 4.8 and 4.9 is due to the inadequate representation of the viscosity and the neglect of the conditioning phase. More elaborate models of the viscosity are given in Section 4.12. It is shown in this section that although the temperature profiles presented here are initially inaccurate, the accuracy increases rapidly with time.

4.11 Inclusion of Burnoff - Asymptotic Behaviour of Solution Obtained Using Heat Balance Integral Method.

The heat balance integral method of Section 4.8, which describes phase II of the welding cycle, approaches the equilibrium phase asymptotically. Thus the model predicts that the duration of phase II is infinite. It is clear, however, that for all practical purposes, we can take the end of phase II as being when the thickness of the plastic layer reaches some prescribed percentage of its limiting value (e.g. 95% or 99%). In this section, therefore an asymptotic solution valid for large values of time is developed, and using this solution and the above criterion, we can estimate the duration of phase II.

Let us assume here that the solutions to the ordinary differential equations (4.8.36) and (4.8.48) for Z_p and a_2 may be expressed

$$Z_p = Z_{p\infty} + Z_T(t) \qquad (4.11.1)$$

and

$$a_2 = a_{2\infty} + a_T(t) \quad , \qquad (4.11.2)$$

where $Z_{p\infty}$ and $a_{2\infty}$ are the constant equilibrium values and Z_T and a_T are the remaining time dependent terms which are assumed to be small compared with their steady state counterparts. Thus it is assumed that for large t

$$Z_T \ll Z_{p\infty} \ , \quad a_T \ll a_{2\infty} \ , \tag{4.11.3}$$

On substituting equations (4.11.1) and (4.11.2) into equations (4.8.36) and (4.8.48) we obtain

$$2a_{2\infty} + B_r + 2a_T = -\frac{2Z_{p\infty}^2}{3F_0}(1+2Z_T/Z_{p\infty}+Z_T^2/Z_{p\infty}^2)\frac{da_T}{dt}$$

$$-\frac{2a_{2\infty}Z_{p\infty}}{3F_0}(1+Z_T/Z_{p\infty})(1+a_T/a_{2\infty})\frac{dZ_T}{dt}-\frac{4P}{5}Z_{p\infty}a_{2\infty}(1+Z_T/Z_{p\infty})(1+a_T/a_{2\infty}) \tag{4.11.4}$$

and

$$-2a_{2\infty} - 2a_T = Pe\,(Z_{p\infty}+Z_T) +$$

$$\frac{Z_{p\infty}^2}{3F_0a_{2\infty}^2}(1+2Z_T/Z_{p\infty}+Z_T^2/Z_{p\infty}^2)(1-2a_T/a_{2\infty}+\ldots)\frac{da_T}{dt}+$$

$$\frac{(Z_{p\infty}+Z_T)}{3F_0a_{2\infty}}(3a_{2\infty}-1+3a_T)(1-a_T/a_{2\infty})\frac{dZ_T}{dt} \tag{4.11.5}$$

4.11.1 Steady State Solutions

Clearly in the above equations we can equate the steady state

terms giving us the two relationships

$$2a_{2\infty} + Br = -\frac{4Pe}{5} Z_{p\infty} a_{2\infty} \tag{4.11.6}$$

and

$$-2a_{2\infty} = Pe\, Z_{p\infty} \tag{4.11.7}$$

Eliminating $a_{2\infty}$ between equations (4.11.6) and (4.11.7) results in the quadratic

$$2Pe^2 Z_{p\infty}^2 + 5PeZ_{p\infty} - 5Br = 0 \tag{4.11.8}$$

which is readily solved, yielding

$$Z_{p\infty} = \frac{5}{4Pe}\left[\sqrt{1 + \frac{8Br}{5}} - 1\right] . \tag{4.11.9}$$

In the above equation, the positive square root is taken since Z_p must always be positive. The constant $a_{2\infty}$ is obtained from equation (4.11.7) and expressed in the form

$$a_{2\infty} = -\frac{PeZ_{p\infty}}{2} . \tag{4.11.10}$$

Equations (4.11.9) and (4.11.10) give the steady state solutions for $Z_{p\infty}$ and $a_{2\infty}$ respectively and the corresponding steady state temperature profiles can now be obtained using these results and equations (4.8.35), (4.8.47) and (4.8.46). Numerical results for various values of Br and Pe are presented in Section 4.14. It is also useful to give the asymptotic solutions of Z_p for small and large Br for comparison with the exact solution. Expanding

(4.11.9) for small Br we have

$$Z_{p\infty} \sim \frac{Br}{Pe}\left[1 - \frac{2Br}{5} + O(Br^2)\right] \qquad (4.11.11)$$

whereas for large Br we have

$$Z_{p\infty} \sim \frac{\sqrt{5}}{Pe\sqrt{2}}\left[\sqrt{Br} - \frac{\sqrt{5}}{2\sqrt{2}} + \frac{5}{16\sqrt{Br}} + O(Br^{-3/2})\right] \qquad (4.11.12)$$

Also with the aid of equations (4.8.35), (4.8.47), (4.11.10) and (4.11.11) the asymptotic expressions for θ_∞ and $\theta_{s\infty}$, valid for small Br can be shown to be

$$\theta_\infty = 1 + \frac{1}{2}Br(1-\eta^2) - \frac{1}{5}Br^2(1-\eta^2) + \ldots \qquad (4.11.13)$$

and

$$\theta_{s\infty} = 1 + Br(1-\eta) + \ldots, \quad |1-\eta| << 1 \ . \qquad (4.11.14)$$

Expressions (4.11.11) to (4.11.14) are later compared with their counterparts from the exact solution which is derived in Section 4.14.

4.11.2 Solutions of a_T and Z_T.

The remaining time dependent parts of equations (4.11.4) and (4.11.5) may be expressed, after a little rearrangement, in the forms

$$\frac{da_T}{dt} + \frac{a_{2\infty}}{Z_{p\infty}}\frac{dZ_T}{dt} + g_1 a_T + g_2 Z_T + O(Z_T a_T) = 0 \qquad (4.11.15)$$

$$\frac{da_T}{dt} + \frac{a_{2\infty}}{Z_{p\infty}}(3a_{2_\infty} - 1)\frac{dZ_T}{dt} + g_3 a_T + g_4 Z_T + O(Z_T a_T) = 0 \qquad (4.11.16)$$

where terms $O(Z_T a_T)$ have been neglected. The constants g_1, g_2, g_3 and g_4 are defined by

$$\left.\begin{aligned} g_1 &= \frac{3F_0}{Z_{p\infty}^2}\left[1 + \frac{2PeZ_{p\infty}}{5}\right], \quad g_2 = \frac{6F_0 Pea_{2\infty}}{5Z_{p\infty}^2} \\ g_3 &= \frac{6F_0 a_{2\infty}^2}{Z_{p\infty}^2}, \quad g_4 = \frac{3F_0 Pea_{2\infty}^2}{Z_{p\infty}^2} \end{aligned}\right\} \qquad (4.11.17)$$

The nature of the above pair of linear ordinary differential equations suggests that we seek solutions of the form

$$a_T = \lambda_1 e^{nt}, \quad Z_T = \lambda_2 e^{nt}, \qquad (4.11.18)$$

where λ_1 and λ_2 are constant. On substituting (4.11.18) into (4.11.15) and (4.11.16), we deduce that the latter are satisfied identically, provided that λ_1 and λ_2 are solutions of the linear simultaneous equations

$$(n+g_1)\lambda_1 + \left[\frac{a_{2\infty}}{Z_{p\infty}} n + g_2\right]\lambda_2 = 0 \qquad (4.11.19)$$

$$(n+g_3)\lambda_1 + \left[\frac{a_{2\infty}}{Z_{p\infty}} (3a_{2\infty}-1)\, n + g_4\right]\lambda_2 = 0 \qquad (4.11.20)$$

This pair of equations has a non-trivial solution only if n satisfies the determinental condition

$$\begin{bmatrix} (n+g_1) & \left(\frac{a_{2\infty}}{Z_{p\infty}} n + g_2\right) \\ n+g_3 & \left(\frac{a_{2\infty}}{Z_{p\infty}} (3a_{2\infty}-1)n + g_4\right) \end{bmatrix} = 0 \qquad (4.11.21)$$

Multiplying out this determinant results in a quadratic the solutions of which are

$$n_1 = (N_2 - N_1)/N_3 \quad , \tag{4.11.22}$$

$$n_2 = -(N_2 + N_1)/N_3 \quad , \tag{4.11.23}$$

where N_1 and N_2 are defined by

$$\left.\begin{aligned} N_1 &= \left\{a_{2\infty}\left[g_1(3a_{2\infty}-1) - g_3\right] + Z_{p\infty}(g_4-g_2)\right\} \\ N_2 &= \left[N_1^2 - 4a_{2\infty}Z_{p\infty}(3a_{2\infty}-2)(g_1g_4-g_2g_3)\right]^{\frac{1}{2}} \quad , \\ \text{and} \\ N_3 &= 2a_{2\infty}(3a_{2\infty} - 2) \quad . \end{aligned}\right\} \tag{4.11.24}$$

The solutions for λ_1 and λ_2 then take the form

$$\lambda_1 = L(n_j)\lambda_2 \quad , \; j = 1 \text{ and } 2 \tag{4.11.25}$$

where the function $L(n)$ is defined by

$$L(n) = -\left[\frac{a_{2\infty}}{Z_{p\infty}}\, n + g_2\right] \Big/ (n+g_1) \tag{4.11.26}$$

The general solutions for Z_T and a_T may now be expressed in

the forms

$$a_T = L(n_1)\lambda_2 e^{n_1 t} + L(n_2)\mu_2 e^{n_2 t} \qquad (4.11.27)$$

and

$$Z_T = \lambda_2 e^{n_1 t} + \mu_2 e^{n_2 t} \quad , \qquad (4.11.28)$$

where μ_2 is a second constant.

Using the computed values of $a_{2\infty}$ and $Z_{p\infty}$, the values of n_1 and n_2 are calculated from equations (4.11.22) and (4.11.23) with the aid of (4.11.24) and (4.11.17). The values of n_1 and n_2 are found to be negative for all values of Br and Pe considered and, as can be seen from Table 4.6, satisfy $|n_1| < |n_2|$. In view of this, we shall assume that for large time, the expression for Z_T, (4.11.27) can be approximated by

$$Z_T = \lambda_2 e^{n_1 t} \quad . \qquad (4.11.29)$$

4.11.3 Estimation of Time Taken to Reach Equilibrium

Using equations (4.11.1) and (4.11.29), the expression for Zp valid for large times becomes

$$Z_p = Z_{p\infty} + \lambda_2 e^{n_1 t} \qquad (4.11.30)$$

It is proposed in this section to assume that equilibrium is reached when Z_p has attained 95% of its asymptotic steady state value $Z_{p\infty}$. The time taken to reach equilibrium, t_e is thus the solution of

$$0.95\ Z_{p\infty} = Z_{p\infty} + \lambda_2 e^{n_1 t_e} \qquad (4.11.31)$$

	Pe = 0.1		Pe = 0.3	
Br	nl	n_2	n_1	n_2
0.1	-0.066	-9.261	--0.592	-83.349
0.2	-0.059	-2.759	-0.534	-24.827
0.3	-0.054	-1.426	-0.490	-12.833
0.4	-0.051	-0.816	-0.455	- 8.247
0.5	-0.047	-0.661	-0.427	- 5.948
0.6	-0.045	-0.512	-0.403	- 4.604
0.7	-0.045	-0 415	-0.383	- 3.737
0.8	-0.041	-0.349	-0.365	- 3.137
0.9	-0.039	-0.300	-0.350	- 2.700
1.0	-0.037	-0.263	-0.336	- 2.370
2.0	-0.028	-0.121	-0.252	- 1.087
4.0	-0.020	-0.063	-0.182	- 0.563
6.0	-0.017	-0.045	-0.149	- 0.402
8.0	-0.014	-0.036	-0.129	- 0.321
10.0	-0.013	-0.030	-0.115	- 0.271

	Pe = 0.5		Pe = 1.0	
Br	nl	n_2	n_1	n_2
0.1	-0.645	-231.524	-6.580-	-926.095
0.2	-1.483	-68.965	-5.933	-275.859
0.3	-1.361	-35.646	-5.445	-142.585
0.4	-1.265	-22.908	-5.058	-91.632
0.5	-1.186	-16.522	-4.742	-66.089
0.6	-1.120	-12.790	-4.478	-51.158
0.7	-1.063	-10.380	-4.252	-41.522
0.8	-1.014	-8.714	-4.057	-34.856
0.9	-0.933	-6.583	-3.733	-30.005
1.0	-0.933	-6.583	-3.733	-26 333
2.0	-0.699	-3.020	-2.796	-12.079
4.0	-0.506	-1.565	-2.023	-6.261
6.0	-0.414	-1.116	-1.657	-4.462

Table 4.6

The unknown λ_2 should be determined by employing some suitable boundary condition. However, we have no such condition and in order to proceed we shall assume that $\lambda_2 = -Z_{p\infty}$. Equation (4.11.31) can then be reduced to

$$0.05 = e^{n_1 t_e} , \qquad (4.11.32)$$

the solution of which is

$$t_e = -\frac{1}{n_1} \ln 20 . \qquad (4.11.33)$$

Although the accuracy of this solution is unknown, equation (4.11.33) gives a qualitative illustration of the effect of Pe and Br on t_e and the results computed from this equation with the aid of the values in Table 4.6 are presented in Figure 4.10.

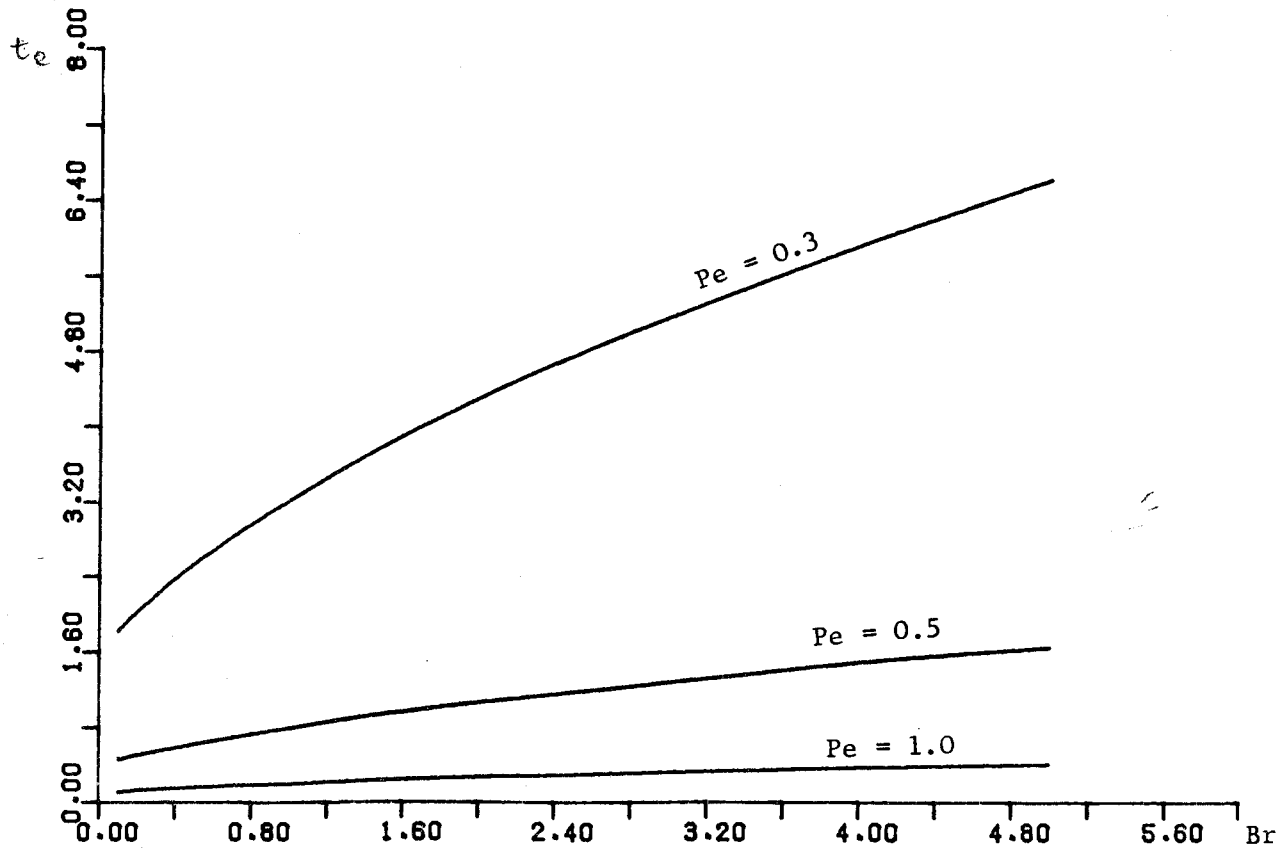

Figure 4.10

Plots of t_e against Br

4.12 Inclusion of Burnoff - Heat Balance Integral Solution, - Variable Viscosity.

In this section we extend the solution obtained in section 4.8 to include the effect of a temperature dependent viscosity. Under the present assumptions, the velocity component v and w are given by (4.7.2) and (4.7.14) respectively, and the appropriate forms of the energy equations are (4.8.14) and (4.8.15) which must be solved subject to the conditions (4.2.23), (4.2.24), (4.2.25), (4.4.3) and (4.4.4).

On substituting equations (4.7.2) and (4.7.14) into equation (4.8.14), and using (4.7.3) to express the shear stress τ in terms of the thickness of the plastic region Z_p, the energy equation for the plastic region becomes

$$\frac{\partial^2\theta}{\partial Z^2} + Br \Big/ \mu\left[\int_a^{Z_p} \frac{dz}{\mu}\right]^2 = Pe\, C_o\left(\int_0^Z \int_{Z_p}^{\ell} \frac{k}{\mu}\, dk d\ell\right)\frac{\partial\theta}{\partial Z}$$

$$+ \frac{1}{F_o}\frac{\partial\theta}{\partial t}, \quad 0 \leq Z \leq Z_p, \qquad (4.12.1)$$

where C_o is defined by (4.7.16). Again introducing assumption (4.7.17) the energy equation for the solid region (4.8.24) remains unchanged. Transforming to the variable η defined by (4.8.25) the energy equations for the plastic and solid regions (4.12.1) and (4.8.24) respectively, become

$$\frac{\partial^2\theta}{\partial\eta^2} + Br \Big/ \mu\left[\int_0^1 \frac{d\eta}{\mu}\right]^2 = Pe\, C_o Z_p^4\left(\int_0^\eta \int_1^{\ell'} \frac{k'}{\mu}\, dk' d\ell'\right)\frac{\partial\theta}{\partial\eta}$$

$$+ \frac{Z_p^2}{F_o}\frac{\partial\theta}{\partial t} - \frac{Z_p}{F_o}\frac{dZ_{p\eta}}{dt}\frac{\partial\theta}{\partial\eta}, \quad 0 \leq \eta \leq 1 \qquad (4.12.2)$$

and

$$\frac{\partial^2\theta_s}{\partial\eta^2} = -\mathrm{Pe}Z_p\frac{\partial\theta_s}{\partial\eta} + \frac{Z_p^2}{F_0}\frac{\partial\theta_s}{\partial t} - \frac{Z_p}{F_0}\frac{dZ_p}{dt}\eta\frac{\partial\theta_s}{\partial\eta}\ ,\ \eta \geq 1\ . \qquad (4.12.3)$$

where k' and ℓ' are defined by

$$k' = k/Z_p \quad \text{and} \quad \ell' = \ell/Z_p \qquad (4.12.4)$$

From (4.7.18) the expression for C_0 transforms, with the aid of assumption(4.7.17), to

$$C_0 = -1/Z_p^3 \int_0^1 \int_1^{\ell'} \frac{k'}{\mu}\, dk'd\ell' \qquad (4.12.5)$$

The transformed boundary conditions are given by (4.8.28) to (4.8.31) respectively. In this section the above system of partial differential equations is solved for the two cases where μ is given by equations (4.5.8) and (4.5.7).

4.12.1 Solution with $\mu = 1/\theta$.

In this subsection we assume as in Section 4.5 that the viscosity μ is inversely proportional to the temperature θ, in which case it is conveniently expressed in the form

$$\mu = 1/\theta\ . \qquad (4.12.6)$$

On substituting equation (4.12.6) into (4.12.2), (4.12.5) and (4.7.3) we have

$$\frac{\partial_2\theta}{\partial\eta^2} + \mathrm{Br}\theta\Big/\left[\int_0^1 \theta d\eta\right]^2 = \mathrm{Pe}C_oZ_p^4\left(\int_0^{\eta}\int_1^{\ell'} \theta(k',t)k'dk'd\ell'\right)\frac{\partial\theta}{\partial\eta} + \frac{Z_p^2}{F_0}\frac{\partial\theta}{\partial t} - \frac{Z_p}{F_0}\frac{dZ_p}{dt}\eta\frac{\partial\theta}{\partial\eta}\ ,\ 0 \leq \eta \leq 1 \qquad (4.12.7)$$

with C_0 and the shear stress τ given by

$$C_0 = -1/Z_p^3 \int_0^1 \int_1^{\ell'} \theta k' dk' d\ell' \qquad (4.12.8)$$

and

$$\tau = 1/Z_p \int_0^1 \theta dk' \qquad (4.12.9)$$

After integrating both sides of equation (4.12.7) with respect to η between the limits $\eta = 0$ and $\eta = 1$ the appropriate heat balance integral can be expressed in the form

$$\frac{\partial\theta}{\partial\eta}\Bigg|_{\eta=0}^{\eta=1} + Br/\left[\int_0^1 \theta d\eta\right] = PeC_0Z_p^4 \int_0^1 \int_0^{\eta} \int_1^{\ell'} \theta(k',t)k'dk'd\ell' \frac{\partial\theta}{\partial\eta} d\eta$$

$$+ \frac{Z_p^2}{F_0}\frac{d}{dt}\int_0^1 \theta d\eta - \frac{Z_p}{F_0}\frac{dZ_p}{dt}\int_0^1 \eta \frac{\partial\theta}{\partial\eta} d\eta \; . \qquad (4.12.10)$$

As for the case of constant viscosity, a quadratic temperature profile is assumed and the appropriate expression which satisfies the boundary conditions (4.8.28) and (4.8.29) is given by (4.8.35). Substituting this expression into equations (4.12.8), (4.12.9) and the heat balance integral equation (4.12.10) and performing the necessary integrations yields

$$C_0 = -3/Z_p^3(2/5\ a_2 - 1) \; , \qquad (4.12.11)$$

and

$$\tau = 1/Z_p\left[1 - 2/3\ a_2\right] \qquad (4.12.12)$$

and

$$2a_2 + Br/[1-2a_2/3] = -\frac{2}{3}\frac{Z_p^2}{F_0}\frac{da_2}{dt} - \frac{2}{3}\frac{Z_p}{F_0}a_2\frac{dZ_p}{dt} + \frac{4Pe\,Z_p a_2}{(2a_2-5)}(1-3a_2/7) \tag{4.12.13}$$

respectively. For the solid region the appropriate heat balance integral equation is given by (4.8.48) since the energy equation for the solid region is independent of viscosity.

The initial conditions to be used with the pair of ordinary differential equations (4.12.13) and (4.8.48) are given by (4.8.32) and (4.8.54). Since there is no analytic solution to this initial value problem, a numerical solution must be sought, as in Section 4.8. Again we use the Runge-Kutta forward step method and a series solution for small times provides the starting values for the numerical solutions. Equation (4.12.13) is similar to (4.8.36) thus it is logical to seek a small time series solution in the form

$$Z = 2Z_1\sqrt{F_0 t} + 2Z_2\sqrt{F_0}\,t + \ldots \tag{4.12.14}$$

$$a_2 = a_{20} + a_{21}\,Pe\sqrt{t} + \ldots \tag{4.12.15}$$

These series automatically satisfy the intial conditions (4.8.32) and (4.8.54) and on substituting them into equations (4.8.48) and (4.12.13) there results the identities

$$-2(a_{20}+a_{21}Pet^{\frac{1}{2}}+\ldots) \equiv 2Pe\sqrt{F_0}(Z_1t^{\frac{1}{2}}+Z_2Pet+\ldots)+$$

$$\frac{4}{3a_{20}^2}(Z_1^2t+2Z_1Z_2Pet^{3/2}+\ldots)(1-2a_{21}Pet^{\frac{1}{2}}/a_{20}+\ldots)(\tfrac{1}{2}a_{21}Pet^{-\frac{1}{2}}+\ldots)+$$

$$\frac{4}{3a_{20}}(Z_1t^{\frac{1}{2}}+Z_2Pet+\ldots)(\tfrac{1}{2}Z_1t^{-\frac{1}{2}}+Z_2Pe+\ldots)(3a_{20}-1+3a_{21}Pet^{\frac{1}{2}}+\ldots)(1-a_{21}Pet^{\frac{1}{2}}/a_{20}+\ldots) \tag{4.12.16}$$

and

$$2a_{20} + 2a_{21}Pe\,t^{\frac{1}{2}}+\ldots+ \frac{Br}{1-2a_{20}/3}\left[1 + 2a_{21}Pe\sqrt{t}/(3-2a_{20})+\ldots\right] \equiv$$

$$-\frac{4}{3}(Z_1 t^{\frac{1}{2}}+Z_2 Pe\,t+\ldots)(Z_1 t^{-\frac{1}{2}}+2Z_2 Pe+\ldots)(a_{20}+a_{21}Pe\,t^{\frac{1}{2}}+\ldots)$$

$$-\frac{8}{3}(Z_1^2 t+2Z_1 Z_2 Pe\ t^{\frac{3}{2}}+\ldots)(\tfrac{1}{2}a_{21}Pe\,t^{-\frac{1}{2}}+\ldots) +$$

$$\frac{8Pe\sqrt{F_0}}{(2a_{20}-5)}(Z_1 t^{\frac{1}{2}}+Z_2 Pe\,t+\ldots)(a_{20}+a_{21}Pe\ \sqrt{t}+\ldots)(1-3a_{20}/7+\ldots)(1-\ldots) \tag{4.12.17}$$

Equating the constant terms in each of the above identities yields the two algebraic equations

$$-a_{20} = \frac{Z_1^2}{3a_{20}}(3a_{20}-1) \tag{4.12.18}$$

and

$$2a_{20} + Br/(1-2a_{20}/3) = -\frac{4}{3}Z_1^2 a_{20}\ . \tag{4.12.19}$$

This pair of equations is identical to the pair (4.8.78) and (4.8.79) apart from the change $Br \to Br/(1-2a_{20}/3)$. Using equation (4.12.18) to eliminate Z_1 from (4.12.19) results in the qaurtic

$$8a_{20}^4 - 24a_{20}^3 + 22a_{20}^2 + (9Br-6)a_{20} - 3Br = 0 \tag{4.12.20}$$

For small values of Br the roots of this equation take the forms

$$\left.\begin{aligned} &a_{201} = -\frac{1}{2}Br+\ldots, a_{202} = \frac{1}{2} - \frac{3}{4}Br+\ldots\ , \\ &a_{203} = 1 + 3Br+\ldots \quad \text{and} \quad a_{204} = \frac{3}{2} - \frac{7}{4}Br+\ldots\ . \end{aligned}\right\} \tag{4.12.21}$$

We could now equate the terms in $t^{\frac{1}{2}}$ in the identities (4.12.16) and (4.12.17) as in Section 4.8 and obtain a pair of equations connecting Z_2 and a_{21}. However, the terms are not really necessary and it is decided to use the lower terms only, Z_1 and a_{20}, in our small time series to obtain starting values.

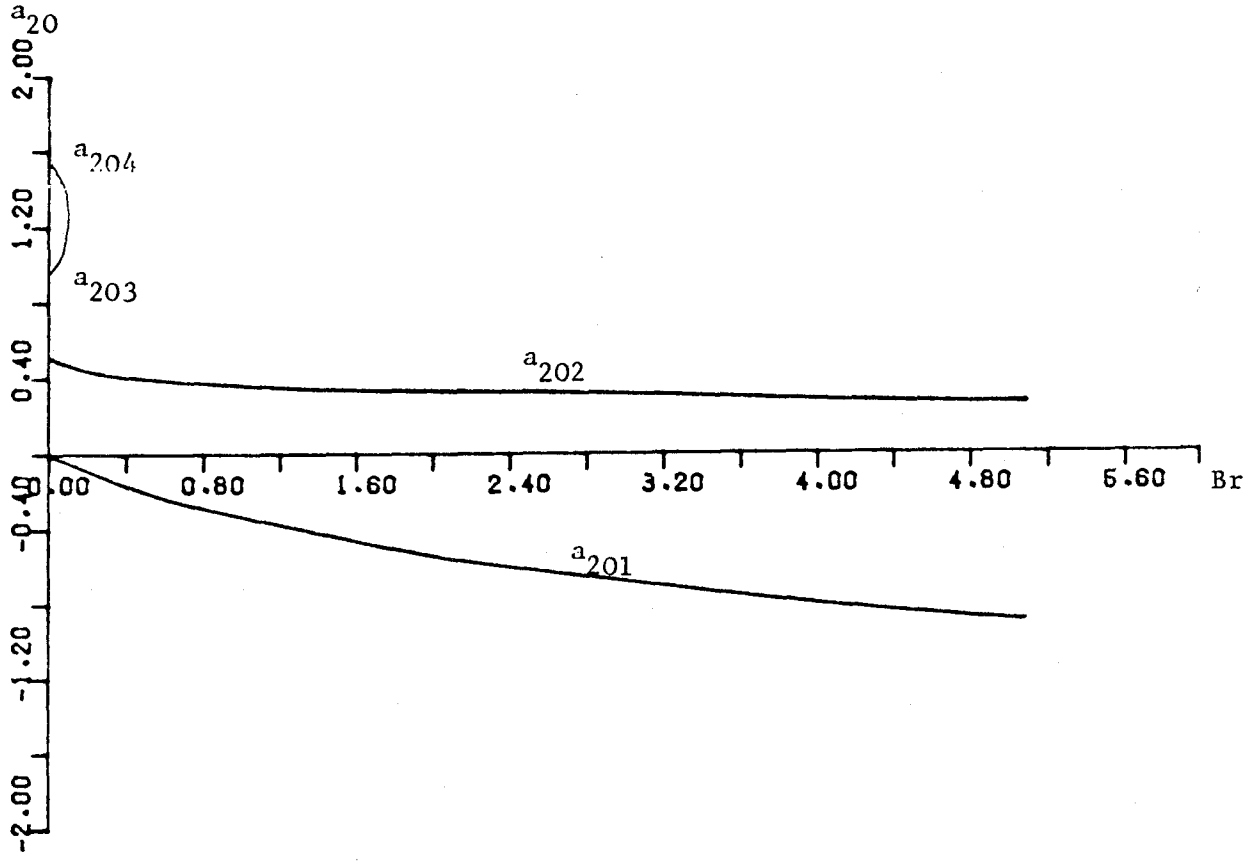

Figure 4.11 Roots of Equation (4.12.20)

Using the expressions in (4.12.21) as starting values, the roots of (4.12.20) have been computed for a wide range of Br, using Newtons method, and the results are plotted in Figure 4.11.

Rearranging equation (4.12.18) we see that

$$Z_1 = \sqrt{\frac{3a_{20}^2}{(1-3a_{20})}}, \qquad (4.12.22)$$

from which we deduce that if Z_1 is to be real, then $a_{20} < \frac{1}{3}$.

In view of this, it is evident from Figure 4.11 that the negative root of (4.12.20), a_{201}, is the only physically realistic solution for a_{20}. Results for this negative root and the corresponding values of Z_1 given by equation (4.12.22) are displayed in Table 4.7.

Br	a_{20}	Z_1
0.1	-0.048	0.078
0.2	-0.093	0.142
0.3	-0.134	0.196
0.4	-0.173	0.243
0.5	-0.203	0.283
0.6	-0.242	0.319
0.7	-0.274	0.351
0.8	-0.303	0.380
0.9	-0.332	0.407
1.0	-0.359	0.431
2.0	-0.579	0.606
4.0	-0.882	0.800
6.0	-1.104	0.121
8.0	-1.283	1.010
10.0	-1.437	1.080

Table 4.7

Considering the particular case of zero axial shortening, that is $Pe = 0$, it is easy to show that equations (4.8.48) and (4.12.13) are satisfied exactly by the expressions

$$Z_p = 2\sqrt{F_0}\, Z_1 \sqrt{t} \qquad (4.12.23)$$

and

$$a_2 = a_{20} \qquad (4.12.24)$$

provided that a_{20} is given by the negative solution of (4.12.20) and Z_1 by (4.12.22). It is possible therefore to make a further assessment of the accuracy of the approximate method by comparing the values of Z_1 in Table 4.7 with the values of α_v in Table 2. In particular expanding the expression for a_{201}, $(4.12.21)_1$, to higher orders in Br and substituting the resulting expression into (4.12.22), the expression for Z_1 for small Br becomes

$$Z_1 = \frac{\sqrt{3}}{2}Br\left[1 - \frac{13}{12}Br + O(Br^2)\right] \qquad (4.12.25)$$

Comparing the lowest order term in this equation with the corresponding term in equation (4.5.30), again reveals that the error is about 3% for small Br. Also comparison of $(4.12.21)_1$ and (4.12.25) with (4.8.67) and (4.8.69) respectively reveals that for small values of Br the effect of the variable viscosity model, (4.12. 6), is negligible.

The corresponding large Br asymptotic solutions for a_{20} and Z_p are

$$a_{20} = -\left(\frac{9}{8}\right)^{1/3} Br^{1/3} + \frac{8}{9} + \ldots \qquad (4.12.26)$$

and

$$Z_1 = \left(\frac{9}{8}\right)^{1/6} Br^{1/6} - \frac{1}{54}\left(\frac{9}{8}\right)^{-1/6} Br^{-1/6} + \ldots \qquad (4.12.27)$$

Comparison of these expressions with their counterparts for constant viscosity (4.8.68) and (4.8.70) shows that, for large Br, the effect of allowing viscosity to vary according to (4.12.6) becomes more significant and it is apparent that the constant viscosity model predicts the larger values of Z_1.

Using the values of Z_1 and a_{20} given in Table 4.7 and the series (4.12.14) and (4.12.15) to obtain starting values, the equations (4.8.48) and (4.12.13) were solved using the Runge-Kutta method and these results are presented at the end of this section.

It is also useful to derive the steady state values, $Z_{p\infty}$ and $a_{2\infty}$. The steady state representations of equations (4.12.13) and (4.8.48) are

$$2a_{2\infty} + Br/\left[1-2a_{2\infty}/3\right] = 4Pe Z_{p\infty} a_{2\infty} \frac{(1-3a_{2\infty}/7)}{(2a_{2\infty}-5)} \qquad (4.12.28)$$

and

$$-2a_{2\infty} = PeZ_{p\infty} \ , \qquad (4.12.29)$$

respectively. Eliminating $a_{2\infty}$ between these two equations results in the quartic

$$3(PeZ_{p\infty})^4+30(PeZ_{p\infty})^3+98(PeZ_{p\infty})^2+21(5-Br)PeZ_{p\infty} - 105Br = 0 \qquad (4.12.29)$$

It can be shown that there is only one positive real root to the above. This positive root can be obtained numerically using Newton's method and results are presented in Section 4.14. However the asymptotic solutions to (4.12.29), for small and large Br are readily obtained and these are given here for comparison with their counterparts from the constant viscosity model (4.11.11) and (4.11.12). For small B_r we have

$$Z_{p\infty} \sim \frac{Br}{Pe}\left[1-11Br/15+O\ (Br^3)\right] \ , \qquad (4.12.30)$$

whereas for large Br the corresponding expression is

$$Z_{p\infty} \sim \frac{B_r^{\frac{1}{3}}}{P_e}\left[7^{1/3} -5Br^{-1/3}/3+O(Br^{-2/3})\right] \qquad (4.12.31)$$

Comparison of equation (4.12.30) with (4.11.11) reveals that the difference between both models for small Br is negligible. However comparison of (4.12.31) with (4.11.12) again shows that for large Br the value of $Z_{p\infty}$ predicted by the variable viscosity model is considerably smaller than that predicted by the constant viscosity one.

4.12.2 Solution with $\mu = (\partial V/\partial Z)^{1/n-1}\exp\{Q/nR\left[\theta(T_c-T_{AM})\pm T_{AM}\right]\}$.

In this section we use the viscosity model discussed in Section 4.5 and given by equation (4.5.7), which is rewritten here for convenience

$$\mu = \left(\frac{\partial V}{\partial Z}\right)^{1/n-1} \exp\left\{\frac{Q}{nR\left[\theta(T_c - T_{AM}) + T_{AM}\right]}\right\} \qquad (4.12.32)$$

Substituting this expression into equation (4.3.13) and rearranging yields

$$\frac{\partial V}{\partial Z} = \tau^n \exp\left\{\frac{-Q}{R\left[\theta(T_c - T_{AM}) + T_{AM}\right]}\right\} \qquad (4.12.33)$$

Integrating this expression with respect to Z we have

$$V = \tau^n \int_0^Z \exp\left\{\frac{-Q}{R\left[\theta(T_c - T_{AM}) + T_{AM}\right]}\right\} dz \,, \qquad (4.12.34)$$

which satisfies boundary conditions $(4.2.16)_2$. In order that condition $(4.2.17)_2$ is satisfied, the thickness of the plastic region Z_p and the shear stress τ must be related by

$$1 = \tau^n \int_0^{Z_p} \exp\left\{\frac{-Q}{R\left[\theta(T_c - T_{AM}) + T_{AM}\right]}\right\} dz \qquad (4.12.35)$$

On substituting equation (4.12.33) into (4.12.32) we see that the viscosity μ may be expressed in the form

$$\mu = \tau^{1-n} \exp\left\{\frac{Q}{R\left[\theta(T_c - T_{AM}) + T_{AM}\right]}\right\} \qquad (4.12.36)$$

Using the latter expression, the energy equation for the plastic region (4.12.2) can be written as

$$\frac{\partial^2\theta}{\partial\eta^2} + Br\tau^{1-n} \Big/ \exp\left[\lambda(\theta)\right] \left[\int_0^1 \exp -\lambda(\theta) d\eta\right]^2 =$$

$$\frac{PeC_0 Z_p^4}{\tau^{1-n}} \left[\int_0^\eta \int_1^{\ell'} k' \exp\left[-\lambda(\theta)\right] dk' d\ell'\right] \frac{\partial\theta}{\partial\eta} +$$

$$\frac{Z_p^2}{F_0} \frac{\partial\theta}{\partial t} - \frac{Z_p}{F_0} \frac{dZ_p}{dt} \eta \frac{\partial\theta}{\partial\eta} \,, \quad 0 \leq \eta \leq 1 \,, \qquad (4.12.37)$$

and the function $C_0(t)$ given by (4.12.5) becomes

$$C_0 = -\tau^{1-n}/Z_p^3 \int_0^1 \int_1^{\ell'} k' \exp[-\lambda(\theta)]\, dk'\, d\ell' \,, \qquad (4.12.38)$$

where the function $\lambda(\theta)$ is defined by

$$\lambda = \frac{Q}{R[\theta(T_c - T_{AM}) + T_{AM}]} \qquad (4.12.39)$$

Integrating both sides of equation (4.12.37) with respect to η between the limits $\eta = 0$ and $\eta = 1$ yields the heat balance integral for the plastic region, namely

$$\frac{\partial\theta}{\partial\eta}(1,t) - \frac{\partial\theta}{\partial\eta}(0,t) + Br\tau^{1-n}/\int_0^1 \exp[-\lambda(\theta)]\, d\eta =$$

$$\frac{PeC_0 Z_p^4}{\tau^{1-n}} \int_0^1 \int_0^{\eta} \int_1^{\ell'} k' \exp[-\lambda(\theta)]\, dk'\, d\ell' \frac{\partial\theta}{\partial\eta}\, d\eta +$$

$$\frac{Z_p^2}{F_0}\frac{d}{dt}\int_0^1 \theta\, d\eta - \frac{Z_p}{F_0}\frac{dZ_p}{dt}\int_0^1 \eta \frac{\partial\theta}{\partial\eta}\, d\eta \,. \qquad (4.12.40)$$

Substituting equation (4.12.38) into this equation and using (4.12.35) to eliminate τ leads to the equations

$$\frac{\partial\theta}{\partial\eta}(1,t) - \frac{\partial\theta}{\partial\eta}(0,t) + Br\, Z_p^{1-1/n}/\left[\int_0^1 \exp[-\lambda(\theta)]\, d\eta\right]^{\frac{1}{n}} =$$

$$-PeZ_p \int_0^1 \int_0^{\eta} \int_1^{\ell'} k' \exp[-\lambda(\theta)]\, dk'\, d\ell' \frac{\partial\theta}{\partial\eta}\, d\eta \Big/ \int_0^1 \int_1^{\ell'} k' \exp[-\lambda(\theta)]\, dk'\, d\ell' +$$

$$\frac{Z_p^2}{F_0}\frac{dt}{dt}\int_0^1 \theta\, d\eta - \frac{Z_p}{F_0}\frac{dZ_p}{dt}\int_0^1 \eta \frac{\partial\theta}{\partial\eta}\, d\eta \,. \qquad (4.12.41)$$

Finally substituting the quadratic profile for θ given by (4.8.35) into this equation leads to the ordinary differential equation connecting a_2 and Z_p

$$2a_2 + \frac{BrZ_p^{1-1/n}}{H_1^{1/n}[a_2(t)]} = -\frac{2}{3}\frac{Z_p^2}{F_0}\frac{da_2}{dt} - \frac{2}{3}\frac{Z_p}{F_0}a_2\frac{dZ_p}{dt} - PeZ_pH_2[a_2(t)] \quad . \qquad (4.12.42)$$

where the functions H_1 and H_2 are defined by

$$H_1 = \int_0^1 \exp\left\{-\lambda\left[1+a_2(\eta^2-1)\right]\right\}d\eta \qquad (4.12.43)$$

and

$$H_2 = \frac{2a_2\int_0^1\int_0^\eta\int_1^{\ell'} k'\exp\left\{-\lambda\left[1+a_2(k'^2-1)\right]\right\}dk'd\ell'\eta d\eta}{\int_0^1\int_1^{\ell'} k'\exp\left\{-\lambda\left[1+a_2(k'^2-1)\right]\right\}dk'd\ell'} \qquad (4.12.44)$$

The heat balance integral for the solid region is again unchanged and we are thus required to solve the pair of ordinary differential equations (4.12.42) and (4.8.48) subject to the initial conditions (4.8.32) and (4.8.54). The most interesting features of this model is thought to be the dependence of μ on the strain rate, $\partial V/\partial Z$, and since we have already examined the effect of decreasing viscosity with increasing temperature we decided to illustrate the solution for the special case where $Q = 0$ for which the equations are simplified considerably. Putting $Q = 0$ in equation (4.12.42) the latter reduces to

$$2a_2 + BrZ_p^{1-1/n} = -\frac{4}{5} PeZ_p a_2 - \frac{2}{3}\frac{Z_p^2}{F_0}\frac{da_2}{dt} - \frac{2}{3}\frac{Z_p}{F_0} a_2 \frac{dZ_p}{dt} \qquad (4.12.45)$$

This equation must now be solved together with (4.8.48) subject to the conditions (4.8.32) and (4.8.54). Again a small time series solution is necessary to obtain starting values to the numerical procedure. Only the lowest order terms in the series are required so we seek solutions in the form

$$Z_p = Z_1 t^{\alpha} + \ldots \qquad (4.12.46)$$

and

$$a_2 = a_{20} t^{\beta} + \ldots \qquad (4.12.47)$$

Substituting (4.12.46) and (4.12.47) into (4.12.45) and (4.8.48) yields

$$2a_{20}t^{\beta} + \ldots + BrZ_1^{1-1/n} t^{\alpha(1-1/n)} + \ldots \equiv -\frac{2Z_1^2}{3F_0} a_{20}\beta t^{2\alpha+\beta-1}$$

$$-\frac{2}{3F_0} Z_1^2 a_{20}\alpha t^{2\alpha+\beta-1} - \frac{4Pe}{5} Z_1 a_{20} t^{\alpha+\beta} + \ldots \qquad (4.12.48)$$

and

$$-2a_{20}t^{\beta} + \ldots \equiv \frac{Z_1^2\beta}{3F_0 a_{20}} t^{2\alpha-\beta-1} + \ldots + \frac{Z_1^2\alpha}{F_0} t^{2\alpha-1}\left(1 - \frac{t^{-\beta}}{3a_{20}}\right) + PeZ_1 t^{\alpha} + \ldots$$

(4.12.49)

After a careful inspection of (4.12.49) one deduces that α and β must satisfy the equation

$$2\alpha - \beta - 1 = \beta \ , \qquad (4.12.50)$$

and then from (4.12.48) that

$$\beta = \alpha\left(1 - \frac{1}{n}\right) \qquad (4.12.51)$$

On solving (4.12.50) and (4.12.51) we have

$$\alpha = n/2 \quad \text{and} \quad \beta = (n-1)/2 \ , \tag{4.12.52}$$

and equating to zero, the coefficients of t^{β} in the identities (4.12.48) and (4.12.49) yields the pair of equations

$$2a_{20} + BrZ_1^{1-1/n} = 0 \tag{4.12.53}$$

and

$$2a_{20} = Z_1^2/6F_0 a_{20} \tag{4.12.54}$$

Using (4.12.54) to express a_{20} in terms of Z_1 we have

$$a_{20} = \pm \ Z_1/\sqrt{12F_0} \tag{4.12.55}$$

It is now seen from (4.12.53) that a real solution to Z_1 exists only if the negative sign is taken in (4.12.55), we then obtain

$$Z_1 = (3F_0)^{n/2} Br^n \quad \text{and} \quad a_{20} = -\frac{1}{2}(3F_0)^{(n-1)/2} Br^n \tag{4.12.56}$$

We could now proceed and obtain higher order terms using the series

$$Z_p = Z_1 t^{\alpha}(1+p_1 t^{\frac{1}{2}}+p_2 t+\ldots) + Z_2 t^{2\alpha}(1+r_1 t^{\frac{1}{2}}+r_2 t+\ldots)+\ldots \tag{4.12.57}$$

and

$$a_2 = a_{20} t^{\beta}(1+q_1 t^{\frac{1}{2}}+q_2 t+\ldots) + a_{21} t^{2\beta}(1+S_1 t^{\frac{1}{2}}+S_2 t+\ldots)+\ldots, \tag{4.12.58}$$

however this would be extremely tedious and it is again decided to obtain starting values to the numerical procedure using the lowest order terms only.

Using (4.12.46) and (4.12.47) with a suitably small value of t, to obtain starting values, (4.12.45) and (4.8.48) were solved using the Runge-Kutta method. In order to do these calculations it was necessary

to choose a value for n. It is suggested in [17] that $n \simeq 5.0$. However this choice of n leads to lengthy computing times and, since we are mainly interested in the qualitative features of the model, n was taken to be 1.5. This choice considerably shortens the computing time, but preserves the main qualitative features of the model. The results are presented in Section 4.12.3. Again it is of interest to examine the steady state solutions, the steady state forms of (4.12.45) and (4.8.48) being

$$2a_{2\infty} + BrZ_{p\infty}^{1-1/n} = -\frac{4}{5} PeZ_{p\infty}a_{2\infty} \tag{4.12.59}$$

and

$$-2a_{2\infty} = PeZ_{p\infty} \quad , \tag{4.12.60}$$

respectively. Eliminating $a_{2\infty}$ from this pair of equations leads, after some rearrangement, to the relation

$$\frac{Br}{PeZ_{p\infty}^{1/n}} - \frac{2PeZ_{p\infty}}{5} = 1 \tag{4.12.61}$$

This equation, again, must be solved numerically and results determined by the Newton-Raphson method are presented in Section 4.14. The asymptotic solutions for small and large Br are given for comparison with (4.11.11) and (4.11.12)

For small Br we have

$$Z_{p\infty} \sim \left(\frac{Br}{Pe}\right)^n \left[1 - \frac{2nPe}{5}\left(\frac{Br}{Pe}\right)^n + \ldots\right] \tag{4.12.62}$$

and the corresponding expression for large Br is

$$Z_{p\infty} \sim \left(\frac{5}{2P_e^2}\right)^{n/n+1} Br^{n/n+1} - \frac{5n}{2Pe(n+1)} + O(B_r^{-n/n+1}) \quad (4.12.63)$$

Since $n > 1$ comparison of (4.12.62) with (4.11.11) reveals that smaller values of $Z_{p\infty}$ are predicted by this model than by the constant viscosity one, for small Br. However for large Br comparison of (4.12.63) with (4.11.12) reveals that the converse is true.

4.12.3 Results and Discussion

The results obtained in the previous two subsections are presented and discussed here. The plots of Z_p and τ against t for various values of Br, for the case $Pe = 0$, are shown in Figures 4.12 and 4.13 respectively. The solid lines represent the case $\mu = 1/\theta$ and the dotted ones represent $\mu = (\partial V/\partial Z)^{1/n-1}$. Comparison of the solid lines in Figures 4.12 and 4.13 with the corresponding dotted lines in Figures 4.1 and 4.2 respectively reveals, again, that the error in the heat balance integral method is less than 5% over the range of B_r given. It is also to be noted from Figures 4.12 and 4.13 that the differences on the values for Z_p predicted by the models $\mu = 1/\theta$ and $\mu = (\partial V/\partial Z)^{1/n-1}$ is quite significant whereas the difference in the shear stress τ is very small.

Figures 4.14(a) and (b) and Figures 4.15(a) and (b) illustrate the effect of upset on the models. It is again seen that higher burnoff rates (higher values for Pe) result in smaller values for Zp and higher values of τ, and equilibrium is reached earlier.

In Figure 4.16(a) and (b) and 4.17(a) and (b) the interface temperatures, $\theta(0,t)$ for the cases $\mu = 1/\theta$ and $\mu = (\partial V/\partial Z)^{1/n-1}$ respectively are plotted against time. The curves in Figures 4.16(a) and (b)

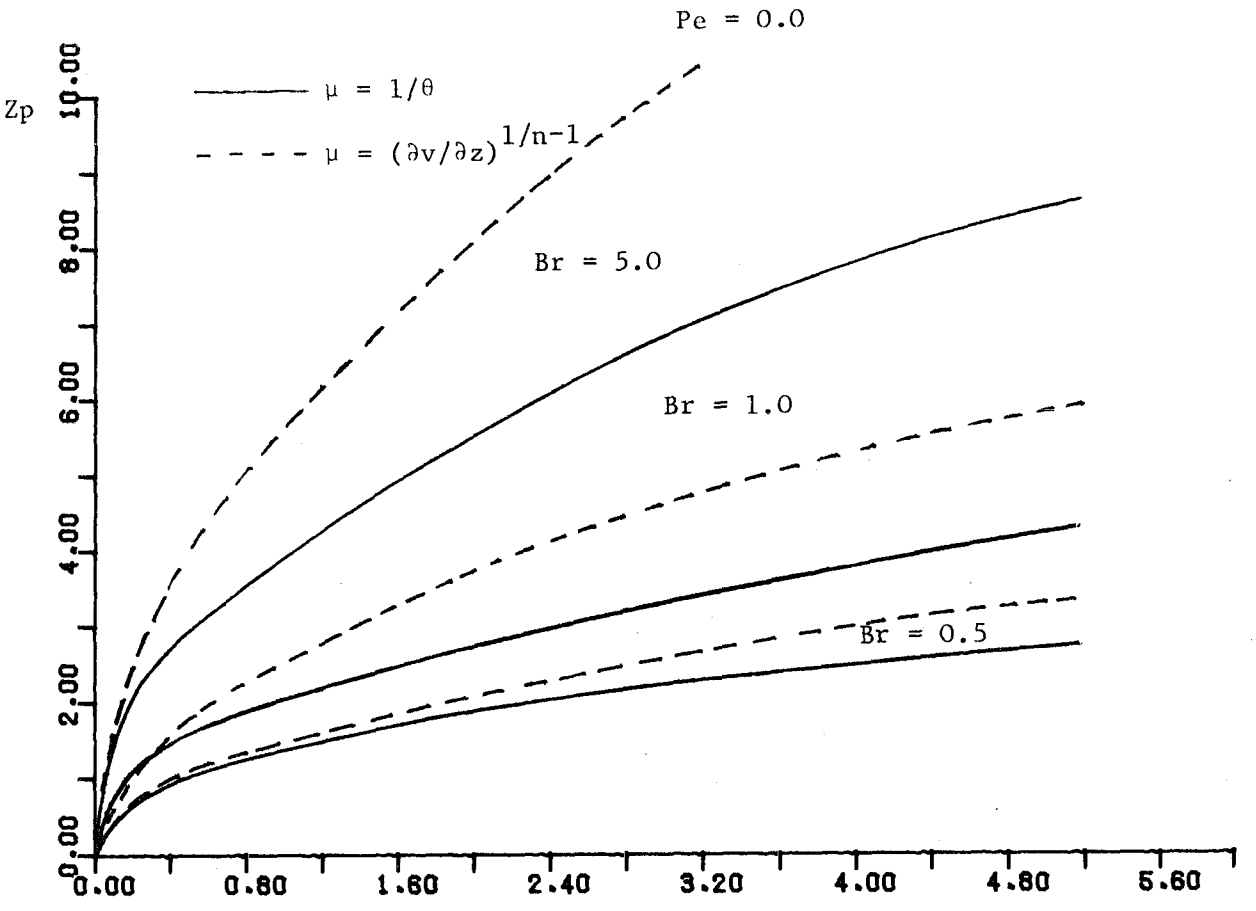

Figure 4.12 Graphs of Zp against t for the cases $\mu = 1/\theta$ and $\mu = (\partial v/\partial z)^{1/n-1}$

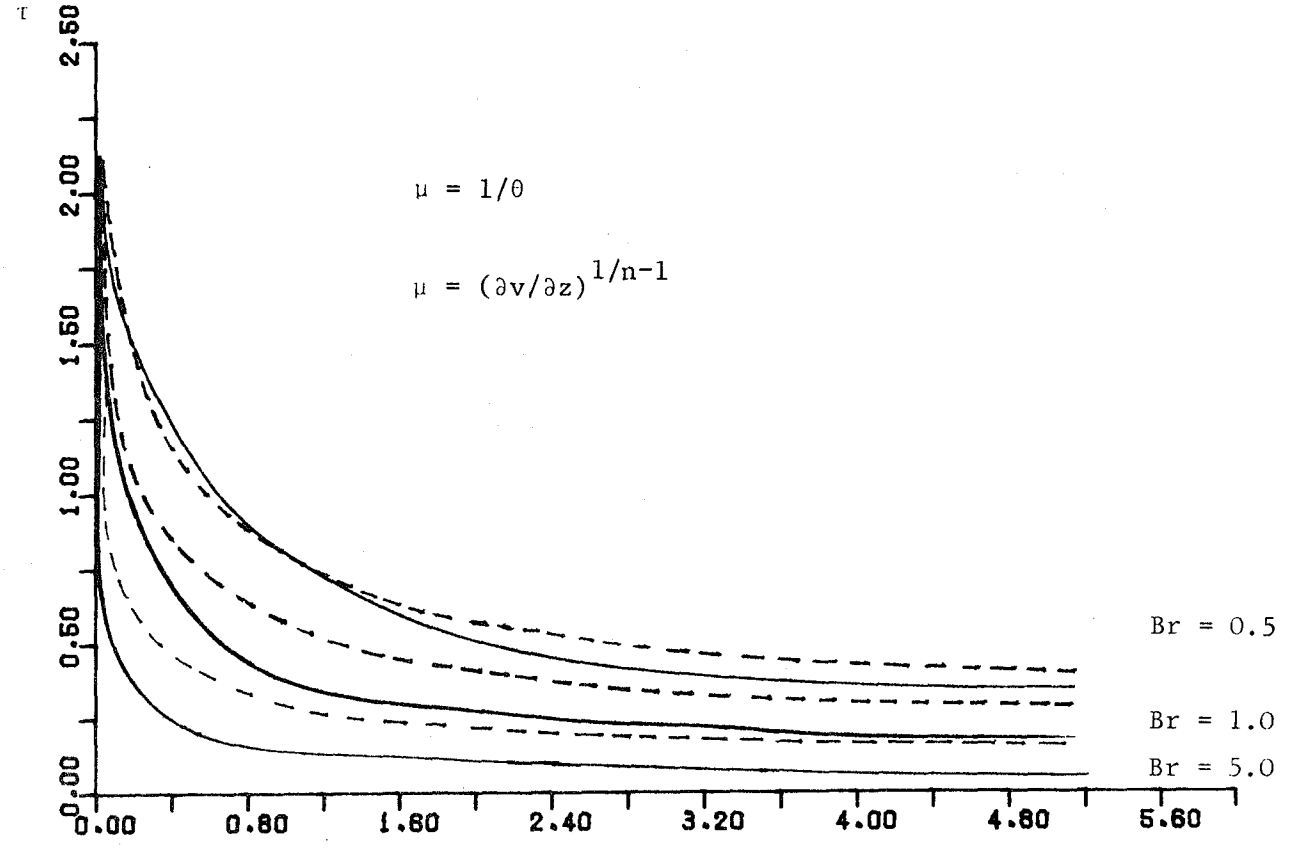

Figure 4.13 Graphs of τ against t for the cases $\mu = 1/\theta$ and $\mu = (\partial v/\partial z)^{1/n-1}$

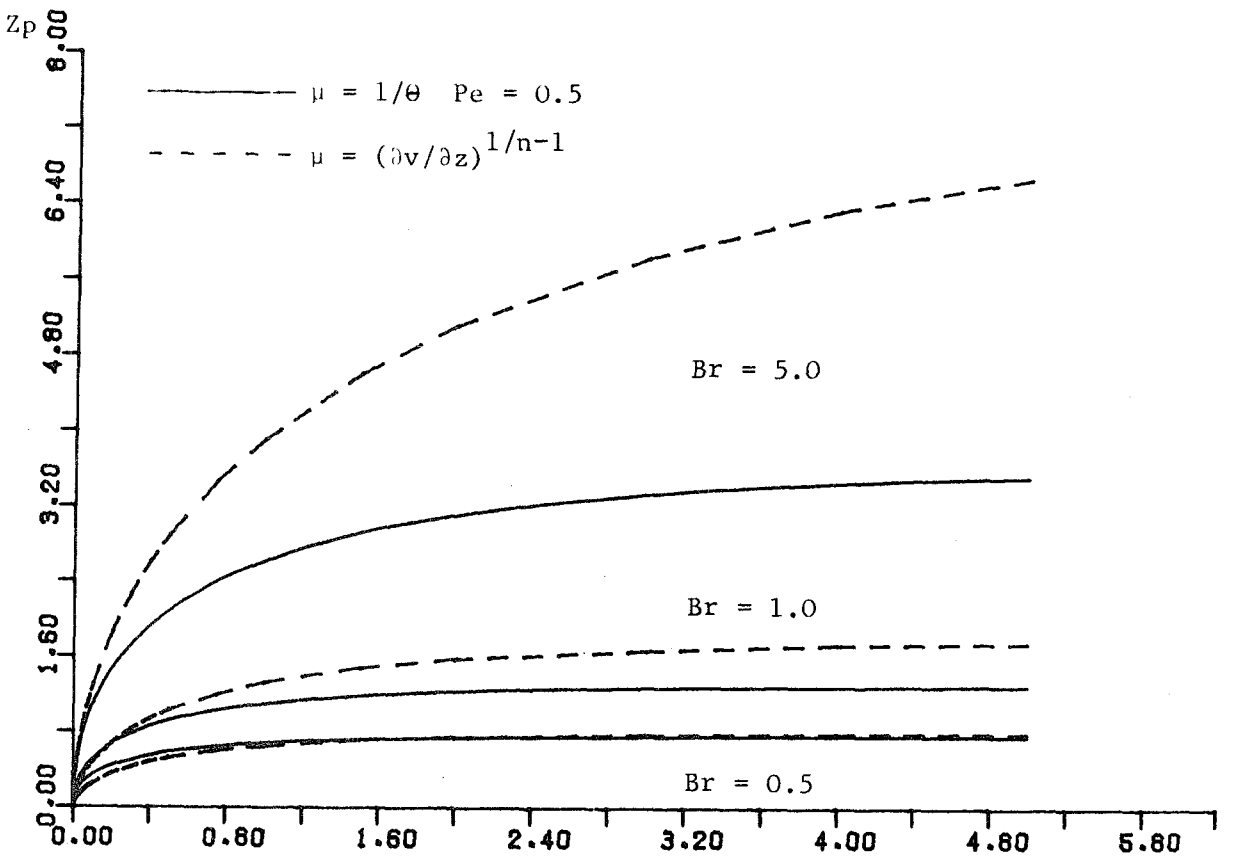

(a)

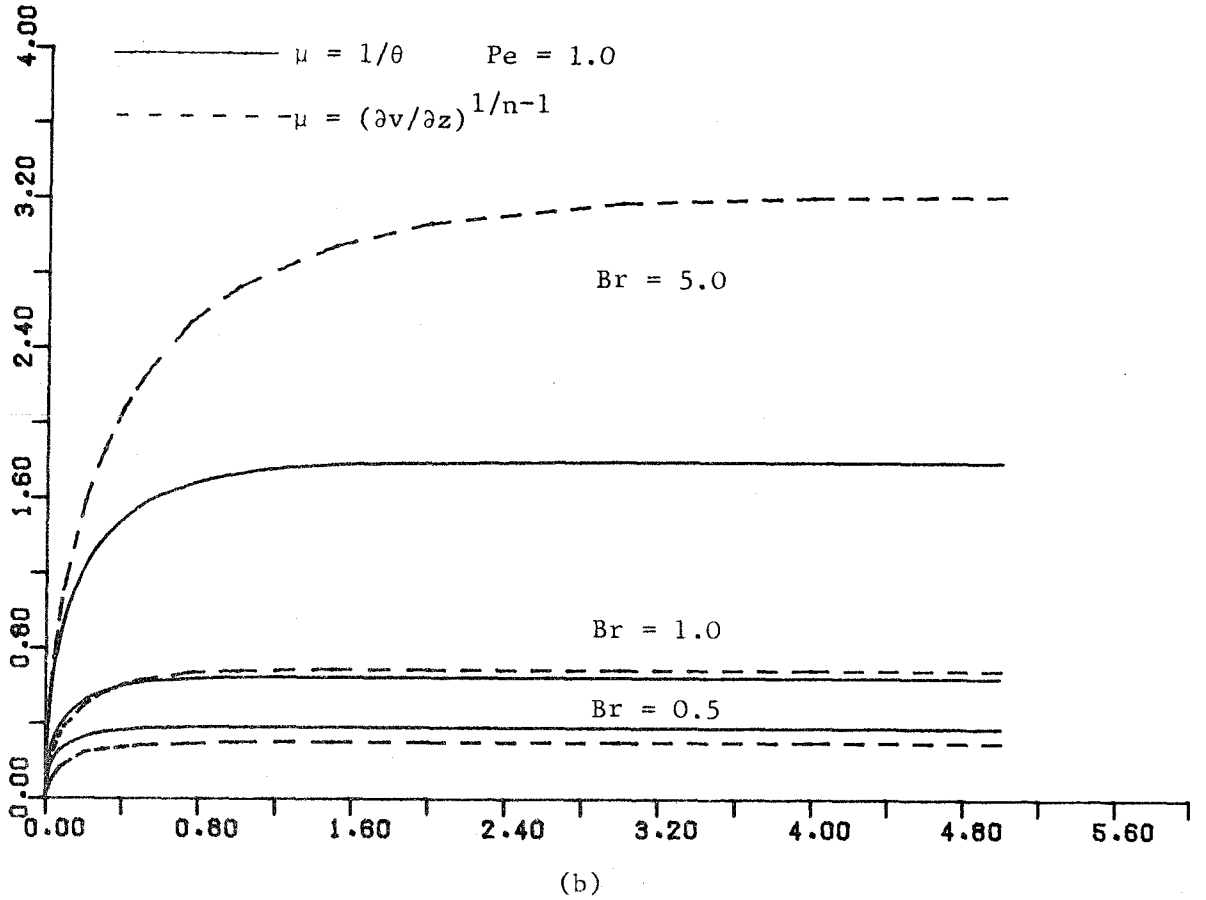

(b)

Figure 4.14 Graphs of Zp against t for the cases $\mu = 1/\theta$ $\mu = (\partial v/\partial z)^{1/n-1}$

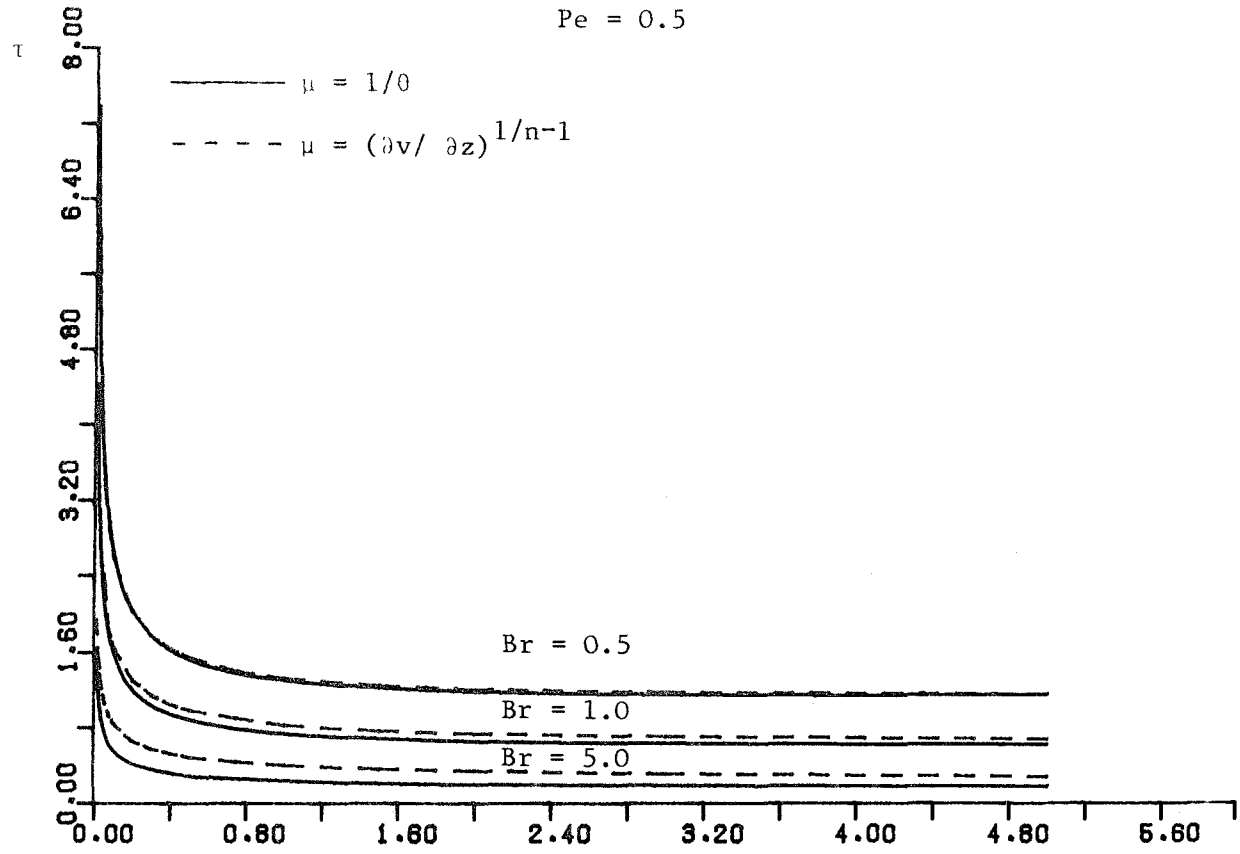

(a)

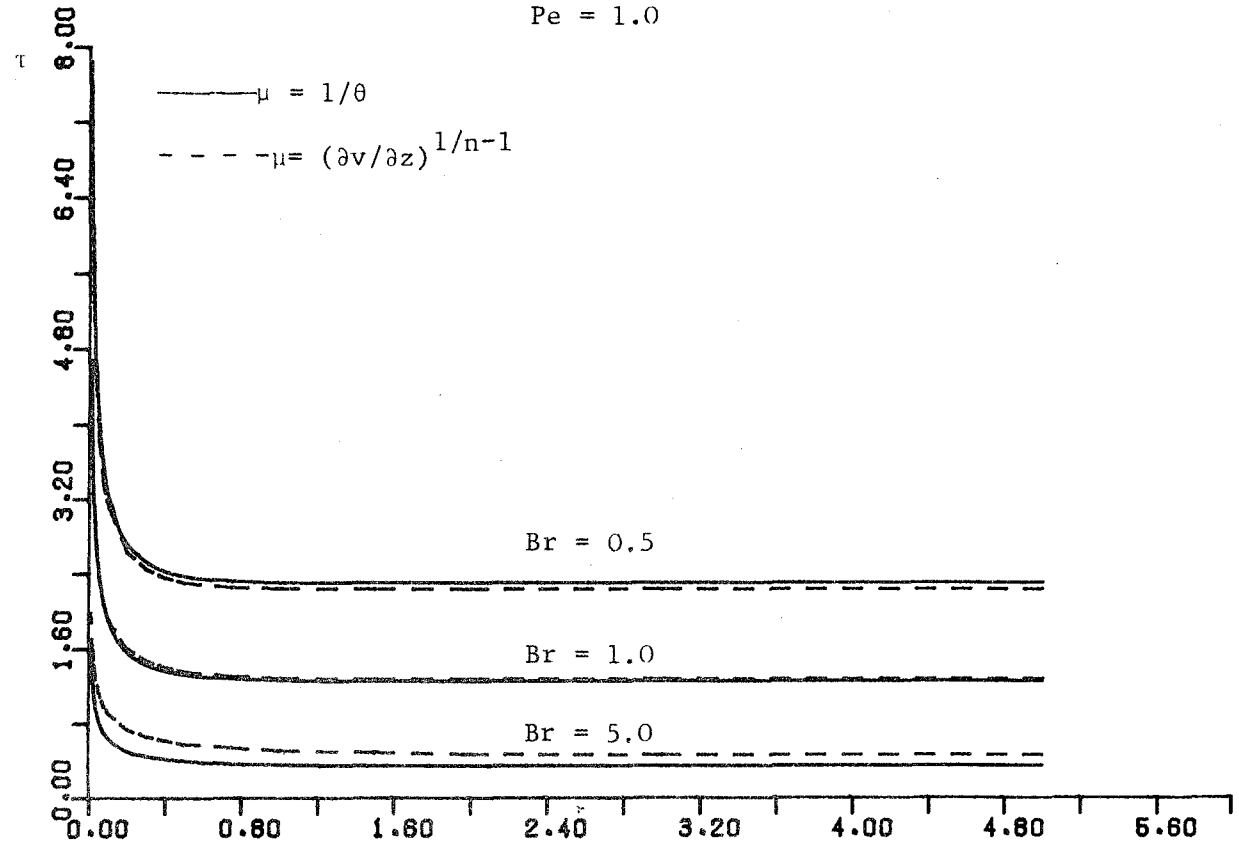

(b)

Figure 4.15 Graphs of τ against t for the cases $\mu = 1/\theta$ and $\mu = (\partial v/\partial z)^{1/n-1}$

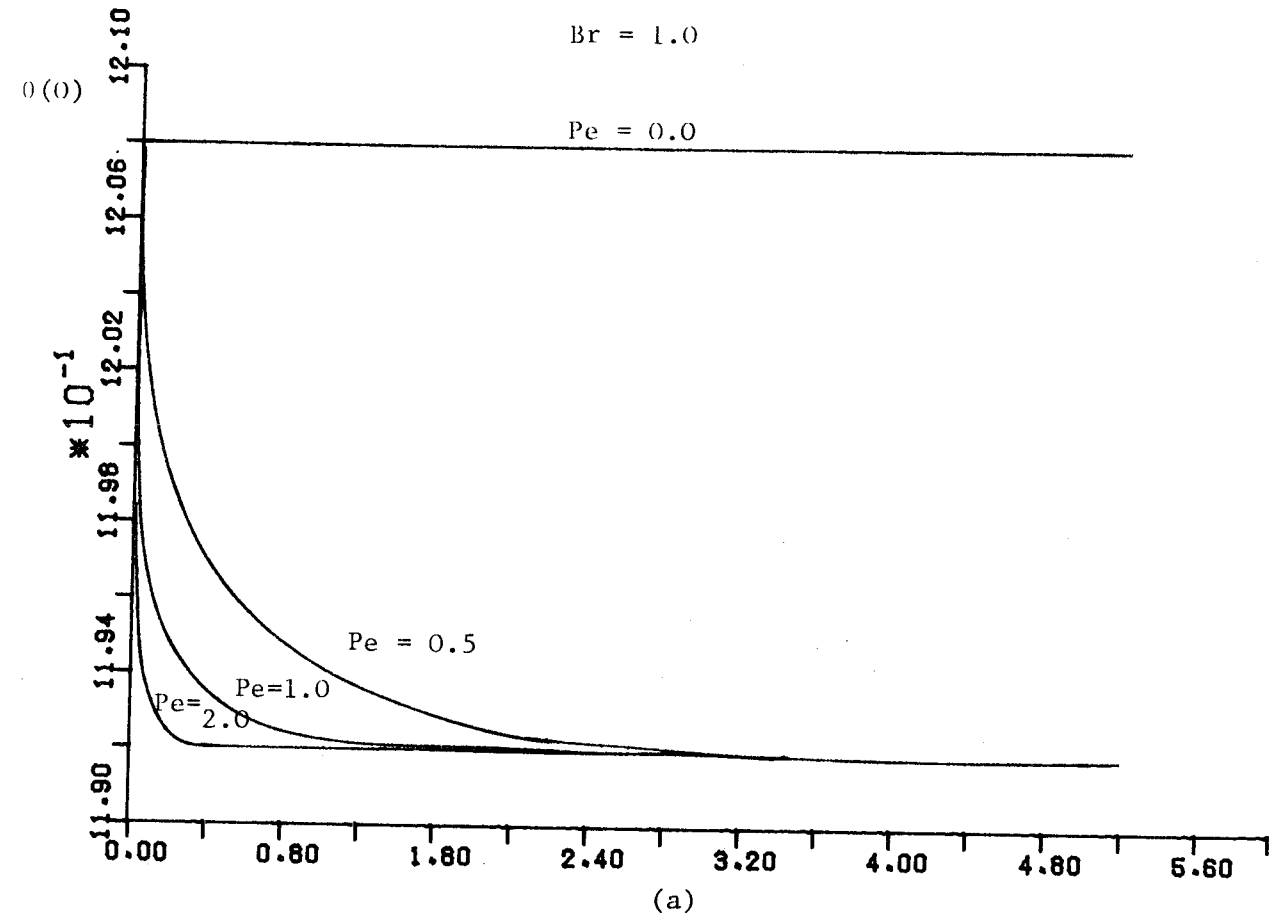

(a)

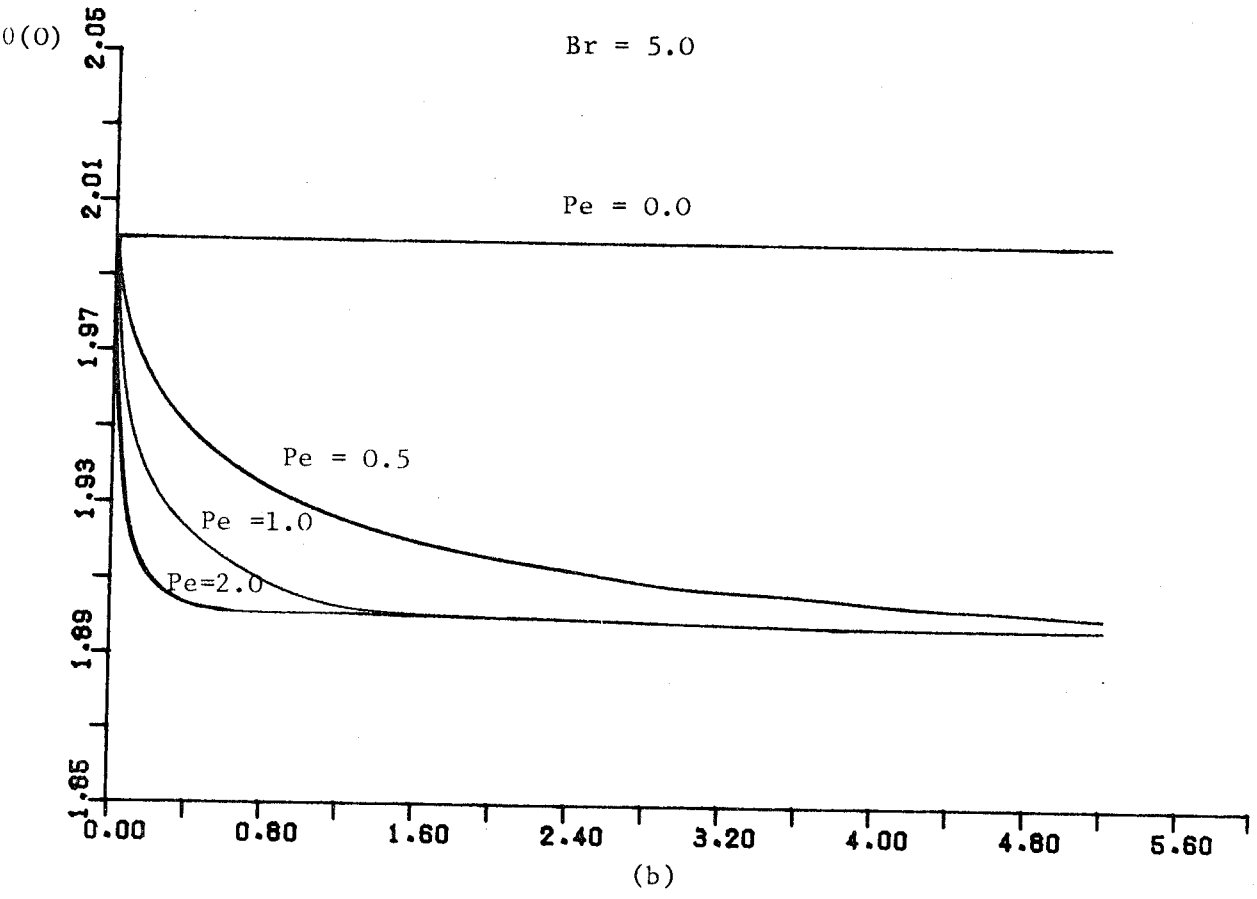

(b)

Figure 4.16 Graphs of interface temperature against t for the case $\mu = 1/0$

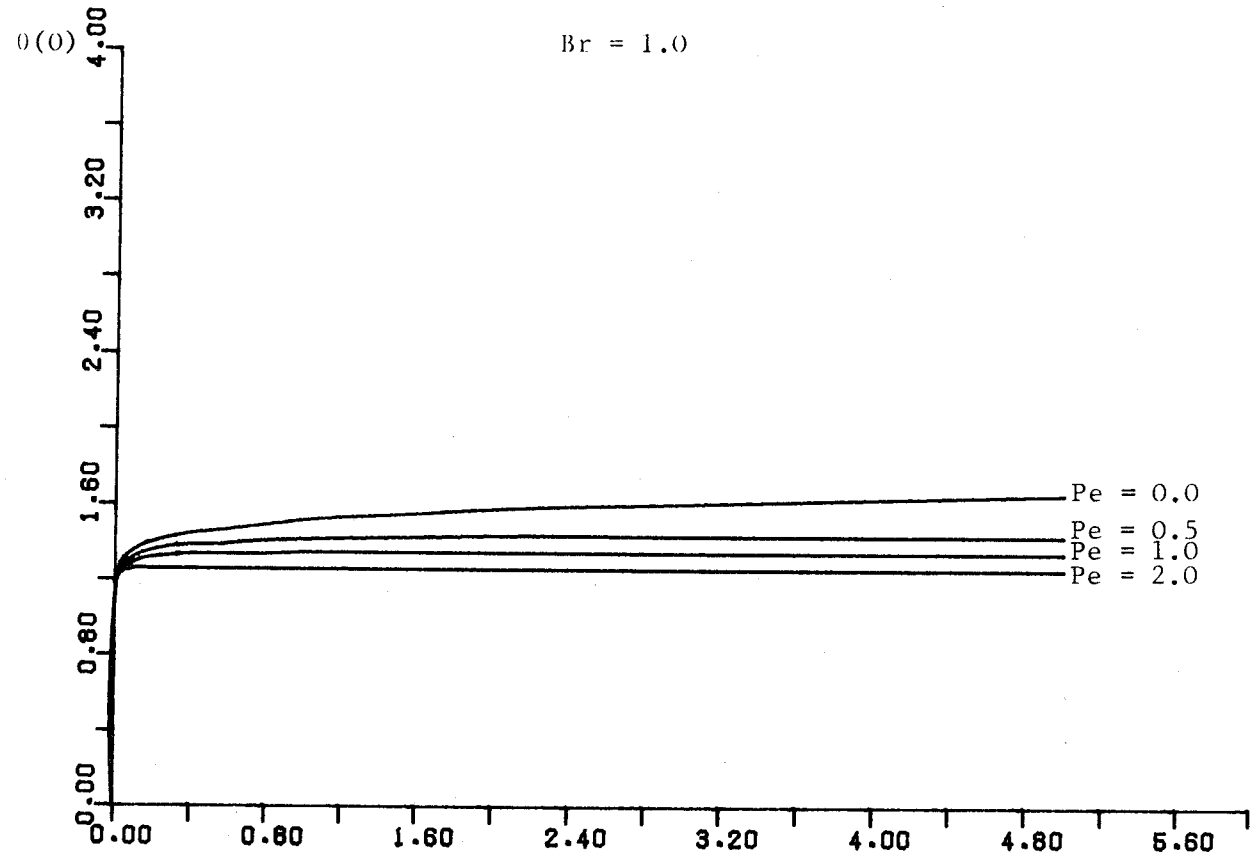

(a)

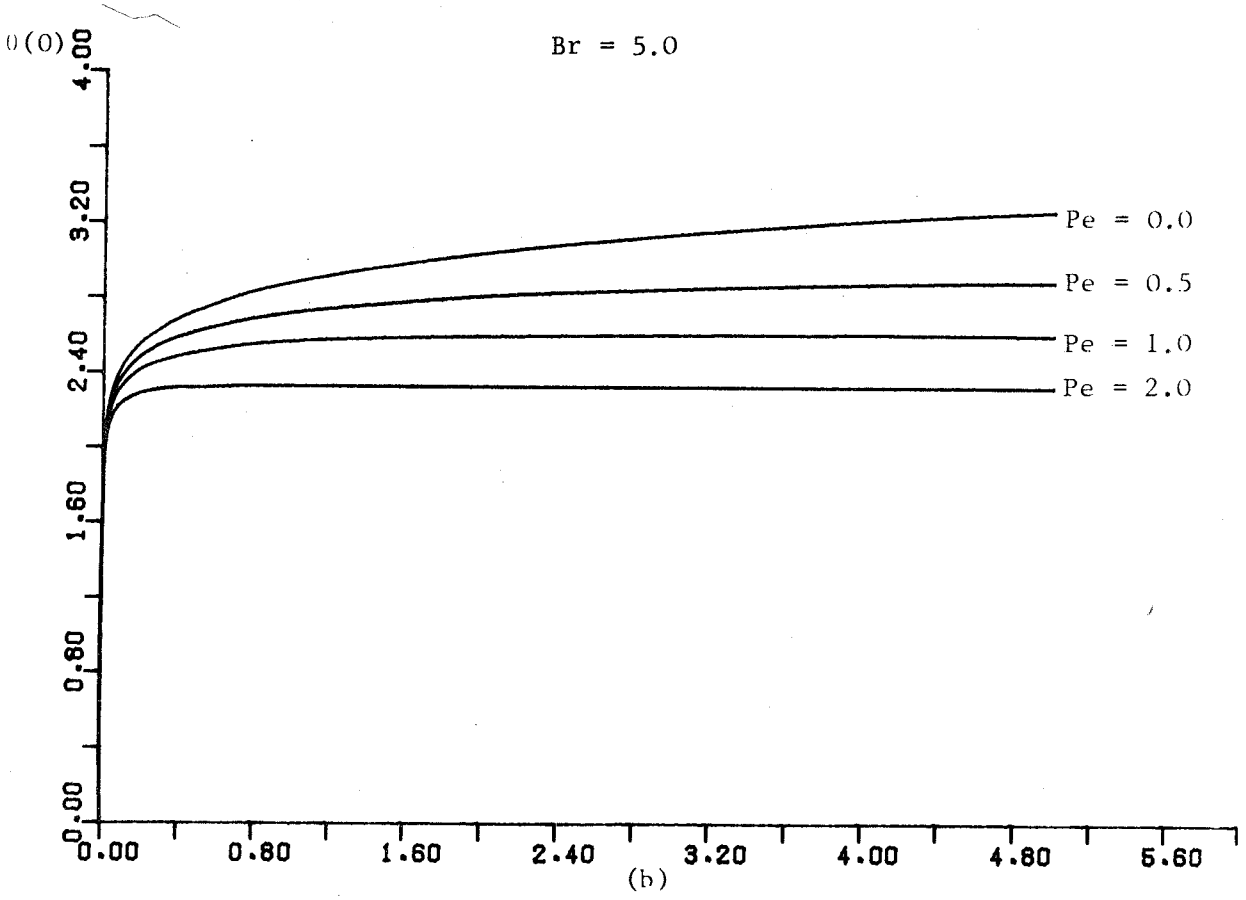

(b)

Figure 4.17 Graphs of interface temperature against t for the case $\mu = (\partial v/\partial z)^{1/n-1}$

are similar to those in Figures 4.9(a), (b) and (c). For the case non-zero Pe the interface temperature initially assumes the value predicted by zero Pe and then decays to its equilibrium value; the rate of decay increasing with Pe . As we have mentioned before we would expect a continuous rise towards equilibrium and no overshoot, thus the models with $\mu = 1$ and $\mu = 1/\theta$ are initially in error. However inspection of Figures 4.17(a) and (b) reveals that in the case where $\mu = (\partial V/\partial Z)^{1/n-1}$ the interface temperatures intially assumes the conditioning temperature, regardless of the value of Pe , and rapidly rises towards steady state and never exceeds it. This is a direct result of the form chosen for the viscosity. The initial singularity in the strain rate, $\partial V/\partial Z$, produces a zero initial value for the viscosity, which in turn leads to zero heat generation. The strain rate then falls rapidly leading to a rapid increase in heat generation and the interface temperature attains about 80% of its equilibrium value in the first 0.001 seconds. However, for times greater than this value it is noted, using Figures 4.9, 4.16 and 4.17, that the temperatures in $\theta(0,t)$ predicted by all these models, $\mu = 1$, $\mu = 1/\theta$ and $\mu = (\partial V/\partial Z)^{1/n-1}$, vary only slightly with t .

4.13 Effect of conditioning phase

In all the solutions obtained up to now in this chapter, the conditioning phase has been ignored. It has been assumed, in all cases, that the interface, $Z = 0$, is initially at the conditioning temperature but that elsewhere, $Z > 0$, the material is at ambient temperature. In this section, the conditioning phase is included and the solution obtained by the heat balance integral method in Section 4.8 is extended to take account of the changed initial condition.

Retaining all the assumptions of Section (4.8) except the initial condition (4.4.4), the energy equations for the plastic and solid regions are given by (4.8.23) and (4.8.24) respectively. The boundary and initial conditions to be used here are given by (4.2.23), (4.2.24), (4.2.25), (4.4.3) and (4.2.27).

To obtain a heat balance integral solution to the system described above it is convenient to introduce the dimensionless temperature variable ϕ_s, in the solid region, defined by

$$\phi_s(Z,t) = \theta_s(Z,t) - \theta_c(Z) \quad , \quad Z > Z_p \tag{4.13.1}$$

where θ_c is the temperature profile present at the end of the conditioning phase. With this definition (4.8.24) becomes

$$\frac{\partial^2 \phi_s}{\partial Z^2} + \frac{d^2 \theta_c}{dZ^2} = Pe \left[\frac{\partial \phi_s}{\partial Z} + \frac{d\theta_c}{dZ} \right] + \frac{1}{F_o} \frac{\partial \phi_s}{dZ} \quad , \quad Z \geq Z_p \tag{4.13.2}$$

and the boundary conditions (4.2.24), (4.2.25) and (4.4.3) become

$$\theta\ (Z_p,t) = \phi_s(Z_p,t) + \theta_c(Z_p) = 1 \quad , \tag{4.13.3}$$

$$\phi_s(Z,t) \to 0 \quad \text{as} \quad Z \to \infty \tag{4.13.4}$$

and

$$\frac{\partial \theta}{\partial Z}\ (Z_p,t) = \frac{\partial \phi_s}{\partial Z}\ (Z_p,t) + \theta_c'(Z_p) \quad , \tag{4.13.5}$$

where the $(')$ denotes differentiation with respect to Z, with condition (4.2.23) remaining unchanged. Finally the amended form of the initial condition (4.2.27) is

$$\phi_s(Z,0) = 0 \quad . \tag{4.13.5}$$

Introducing the variable η, defined by (4.8.25), into equation (4.13.2) yields

$$\frac{\partial^2\phi_s}{\partial\eta^2} + \frac{d^2\theta_c}{d\eta^2}(Z_p\eta) = -PeZ_p\left[\frac{\partial\phi_s}{\partial\eta} + \frac{d\theta_c}{d\eta}(Z_p\eta)\right] +$$

$$+ \frac{Z_p^2}{F_0}\frac{\partial\phi_s}{\partial t} - \frac{Z_p}{F_0}\frac{dZ_p}{dt}\eta\frac{\partial\phi_s}{\partial\eta} \quad , \quad \eta \geq 1 \qquad (4.13.7)$$

and the boundary conditions (4.13.3) to (4.13.5) transform to

$$\theta(1,t) = \phi_s(1,t) + \theta_c(Z_p) = 1 \ , \qquad (4.13.8)$$

$$\phi_s(\eta,t) \to 0 \quad \text{as} \quad \eta \to \infty \qquad (4.13.9)$$

and

$$\frac{\partial\theta}{\partial\eta}(1,t) = \frac{\partial\phi_s}{\partial\eta}(1,t) + Z_p\theta_c'(Z_p) \qquad (4.13.10)$$

Again the initial condition (4.13.6) is incorporated into (4.13.9) since it is assumed that $Z_p(0) = 0$.

The energy equation for the plastic region, in terms of η, is given by (4.8.26) and the boundary condition on $\eta = 0$ by (4.8.28).

The above system is now solved by the heat balance integral method. For the plastic region the temperature profile may again be expressed by (4.8.35) and after applying the integral method the averaged energy equation for the plastic region is given by (4.8.36). For the solid region we again assume the existence of a thermal layer $1 \leq \eta \leq S(t)$ and use the conditions (4.8.39) and (4.8.40) on $\eta = S$. Thus assuming a quadratic temperature profile in the form

$$\phi_s = b_0 + b_1\eta + b_2\eta^2 \ , \ 1 \leq \eta \leq S \ , \qquad (4.13.11)$$

where b_0, b_1 and b_2 are functions of t only, and using the conditions $(4.13.8)_2$, (4.13.10), (4.8.39) and (4.8.40) we deduce that

$$\phi_s = \left[1-\theta_c(Z_p)\right]\left[\frac{(S-\eta)}{(S-1)}\right]^2 , \qquad (4.13.12)$$

where S is given by

$$S = 1 - \frac{2\left[1-\theta_c(Z_p)\right]}{2a_2-Z_p\theta'_c(Z_p)} \qquad (4.13.13)$$

and use has been made of the assumption that

$$\theta_c(S) = 0 \quad \text{and} \quad \theta'_c(S) = 0 \qquad (4.13.14)$$

The temperature ϕ_s is assumed to be zero for $\eta > S$, thus condition (4.13.9) is satisfied automatically.

The heat balance integral is obtained by integrating equation (4.13.7) with respect to η between the limits $\eta = 1$ and $\eta = S$ yielding

$$\frac{\partial\phi_s}{\partial\eta}(S,t) - \frac{\partial\phi_s}{\partial\eta}(1,t) + Z_p\theta'_c(S) - Z_p\theta'_c(Z_p) =$$

$$- PeZ_p\left[\phi_s(S,t)-\phi_s(1,t) + \theta_c(S) - \theta_c(Z_p)\right] +$$

$$\frac{Z_p^2}{F_0}\left[\frac{d}{dt}\int_1^S \phi_s d\eta - \frac{dS}{dt}\phi_s(S,t)\right] - \frac{Z_p}{F_0}\frac{dZ_p}{dt}\int_1^S \eta\frac{\partial\phi_s}{\partial\eta}d\eta \qquad (4.13.15)$$

Finally substituting equation (4.13.12) into (4.13.15) and making use of (4.13.13) and (4.13.14) leads to, after some algebra:

$$-2a_2 = PeZ_p - \frac{2Z_p^2}{3F_0}\left\{\frac{[\theta_c'(Z_p)+Z_p\theta_c''(Z_p)][1-\theta_c(Z_p)]^2}{[2a_2-Z_p\theta_c'(Z_p)]^2} - \right.$$

$$\left.\frac{2[1-\theta_c(Z_p)]\theta_c'(Z_p)}{2a_2-Z_p\theta_c'(Z_p)}\right\}\frac{dZ_p}{dt} + \frac{4Z_p^2[1-\theta_c(Z_p)]^2}{3F_0|2a_2-Z_p\theta_c'(Z_p)|^2}\frac{da_2}{dt}$$

$$+ \frac{[1-\theta_c(Z_p)]Z_p}{F_0}\left[1 - \frac{2[1-\theta_c(Z_p)]}{3[2a_2-Z_p\theta_c'(Z_p)]}\right]\frac{dZ_p}{dt} \qquad (4.13.16)$$

The intial condition on Z_p is given by (4.8.32) and it is easily shown by considering the total thermal energy of the plastic region that the initial condition (4.8.54) remains valid. Again there is no analytic solution to the pair of equations (4.8.36) and (4.13.16) which are to be solved subject to conditions (4.8.32) and (4.8.54) and a numerical solution must be sought. Using the Runge-Kutta method we again require a small time series solution to avoid the complications due to the singularity at $t = 0$ and to provide starting values for the numerical procedure.

Using the simple model for the conditioning phase given in Chapter 2 the initial temperature distribution, $\theta_c(Z)$,

$$\theta_c(Z) = 6\sqrt{\pi}\, i^3\, \mathrm{erfc}(\Delta z) \qquad (4.13.17)$$

where the constant Δ is equal to $1/2\sqrt{Fot_c}$. Expanding the right hand side of (4.13.17) for small z we obtain

$$\theta_c(Z) = 1 - \frac{3\sqrt{\pi}}{2}\Delta Z + 3\Delta^2 Z^2 + O(\Delta^3 Z^3) \qquad (4.13.18)$$

Successive differentiation of this expression with respect to Z yields

$$\theta_c' = -\frac{3\sqrt{\pi}\,\Delta}{2} + \sigma\Delta^2 Z + O(\Delta^2 Z^2) \tag{4.13.19}$$

and

$$\theta_c'' = \sigma\Delta^2 + O(\Delta Z) \tag{4.13.20}$$

Since for small times the thickness of the plastic region, Z_p, may be assumed small, equations (4.13.18), (4.13.19) and (4.13.20) can be substituted into (4.13.16), yielding

$$-2a_2 = P_e Z_p - \frac{2Z_p^2}{3F_0}\left\{\frac{\left[-3\sqrt{\pi}\,\Delta/2+O(\Delta^2 Z_p)\right]\left[3\sqrt{\pi}\,\Delta Z_p/2+O(\Delta^2 Z_p^2)\right]^2}{\left[2a_2+3\sqrt{\pi}\,\Delta Z_p/2+O(\Delta^2 Z_p^2)\right]^2}\right.$$

$$\left. + \frac{\left[3\sqrt{\pi}\,\Delta Z_p/2+O(\Delta^2 Z_p^2)\right]\left[3\sqrt{\pi}\,\Delta+O(\Delta^2 Z_p^2)\right]}{\left[2a_2+3\sqrt{\pi}\,\Delta Z_p/2+O(\Delta^2 Z_p^2)\right]}\right\}\frac{dZ_p}{dt} + \frac{\left[9\pi\Delta^2 Z_p^4+O(\Delta^3 Z_p^5)\right]}{3F_0\left[2a_2+3\sqrt{\pi}\,\Delta Z_p/2+O(\Delta^2 Z_p^2)\right]^2}\frac{da_2}{dt}$$

$$+ \frac{\left[3\sqrt{\pi}\,\Delta Z_p^2+O(\Delta^2 Z_p^3)\right]}{2F_0}\left[1 - \frac{\sqrt{\pi}\,\Delta Z_p+O(\Delta^2 Z_p^2)}{\left[2a_2+3\sqrt{\pi}\,\Delta Z_p/2+O(\Delta^2 Z_p^2)\right]}\right]\frac{dZ_p}{dt} \tag{4.13.21}$$

A close inspection of equations (4.8.36) and (4.13.21), analagous to the discussion of equations (4.8.36) and (4.8.48) in Section 4.8, reveals that the series expressions for Z_p and a_2 at small time take the forms

$$Z_p = Z_1 t^{2/5} + Z_2 t^{3/5} + \ldots \tag{4.13.22}$$

and

$$a_2 = a_{21} t^{1/5} + a_{22} t^{2/5} + \ldots \tag{4.13.23}$$

which satisfy the initial conditions (4.8.32) and (4.8.54).

On substituting these series into (4.8.36) and (4.13.21) there results the pair of identities

$$2a_{21}t^{1/5}+\ldots+B_r = -\frac{2Z_1^2a_{21}}{15F_0}(1+2Z_2t^{1/5}/Z_1+\ldots)(1+2a_{22}t^{1/5}/a_{21}+\ldots)$$

$$-\frac{2Z_1^2a_{21}}{15F_0}(1+Z_2t^{1/5}/Z_1+\ldots)(2+3Z_2t^{1/5}/Z_1+\ldots)(1+a_{22}t^{1/5}/a_{21}+\ldots)$$

$$-\frac{4}{5}P_ea_{21}Z_1t^{3/5}(1+Z_2t^{1/5}/Z_1+\ldots)(1+a_{22}t^{1/5}/a_{21}+\ldots) \qquad (4.13.24)$$

and

$$-2a_{21}t^{1/5}-2a_{22}t^{2/5}-\ldots = Pe(Z_1t^{2/5}+\ldots) -$$

$$\left[\frac{Z_1^3}{5F_0}t^{1/5}+\ldots\right]\left[\frac{-9\pi^{3/2}\Delta^3Z_1t^{4/5}}{8a_{21}^2t^{2/5}+\ldots}+\frac{3\pi\Delta^2Z_1t^{2/5}}{a_{21}t^{1/5}+\ldots}\right]$$

$$+\frac{3\pi\Delta^2Z_1^4t^{8/5}+\ldots}{4F_0a_{21}^2t^{2/5}+\ldots}\left[\frac{a_{21}}{5}t^{-4/5}+\ldots\right]+$$

$$\frac{3\sqrt{\pi}\,\Delta Z_1^3t^{1/5}}{5F_0}\left[1-\frac{\sqrt{\pi}\Delta Z_1t^{2/5}}{2a_{21}t^{1/5}+\ldots}\right] \qquad (4.13.25)$$

Equating the coefficient of the time independent terms in (4.13.24) and the coefficient of $t^{1/5}$ in (4.13.25) results in the pair of equations

$$B_r = - \frac{2Z_1^2 a_{21}}{5F_0} \tag{4.13.26}$$

and

$$-2a_{21} = \frac{3\sqrt{\pi}\ \Delta Z_1^3}{5F_0} \tag{4.13.27}$$

This pair of equations is now readily solved to yield the solutions

$$Z_1 = \sqrt[5]{\frac{25B_r F_0^2}{3\sqrt{\pi}\ \Delta}} \tag{4.13.28}$$

and

$$a_{21} = - \frac{3\sqrt{\pi}\ \Delta Z_1^3}{10F_0} \tag{4.13.29}$$

It is now possible to truncate the series (4.13.22) and (4.13.23) after the first term, and by using (4.13.28) and (4.13.29) and a suitably small value for t, the numerical solution can be started.

Numerical values of Z_1 and a_{21} were computed for various values of B_r and using these values the full solutions were calculated using the Runge-Kutta method. At the same time the dimensionless shear stress τ and the thickness of the thermal layer in the solid region S were computed using equations (4.7.3) and (4.13.13). These results are presented in the following subsection.

4.13.1 Results and Discussion

Using results obtained by the Runge-Kutta process, the plots of Z_p and τ against t for various values of Br, for the case $Pe = 0$, are shown in Figures 4.18 and 4.19 respectively. By comparing these curves with the corresponding ones, for the case $\theta_s(Z,0) = 0$,

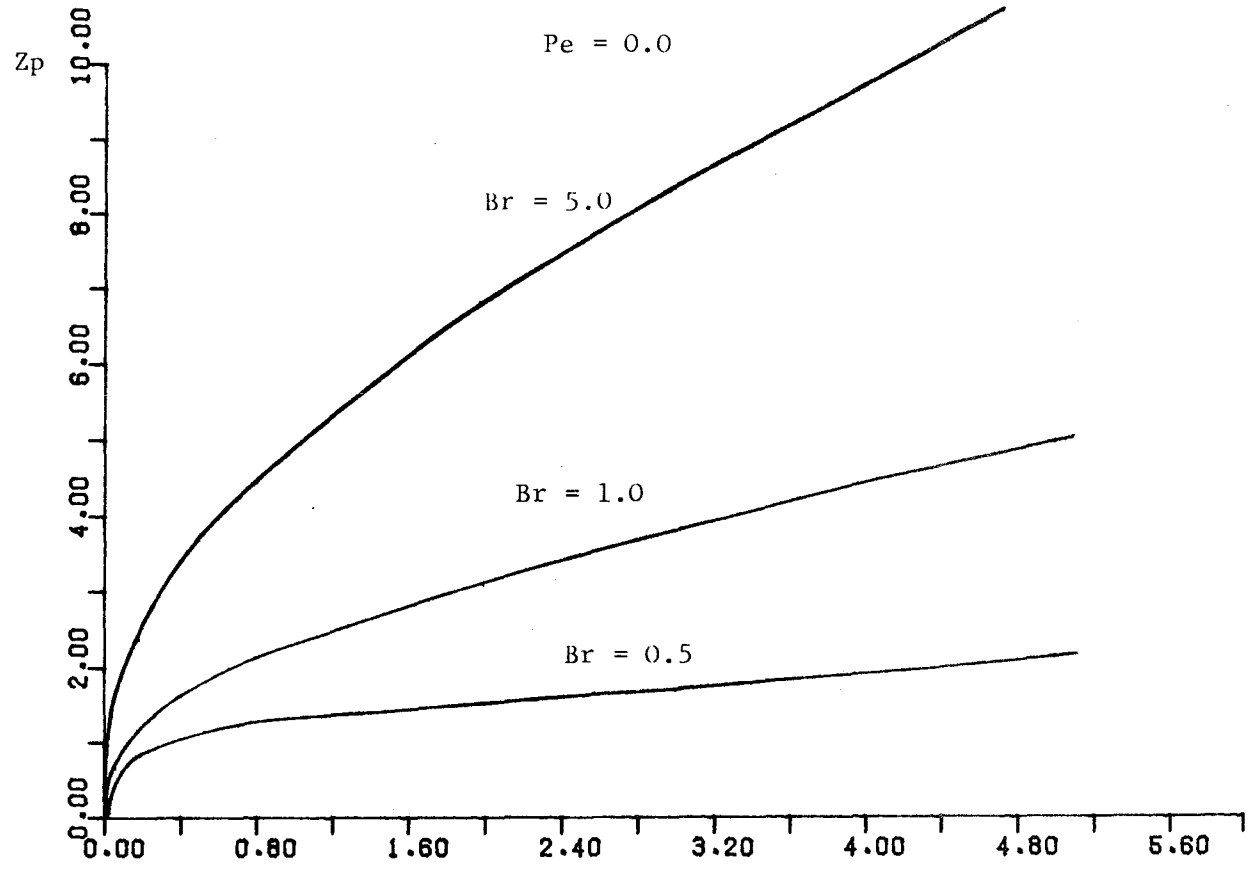

Figure 4.18 Graphs of Zp against t for the case $\theta_s(z,0) = \theta_c(z)$

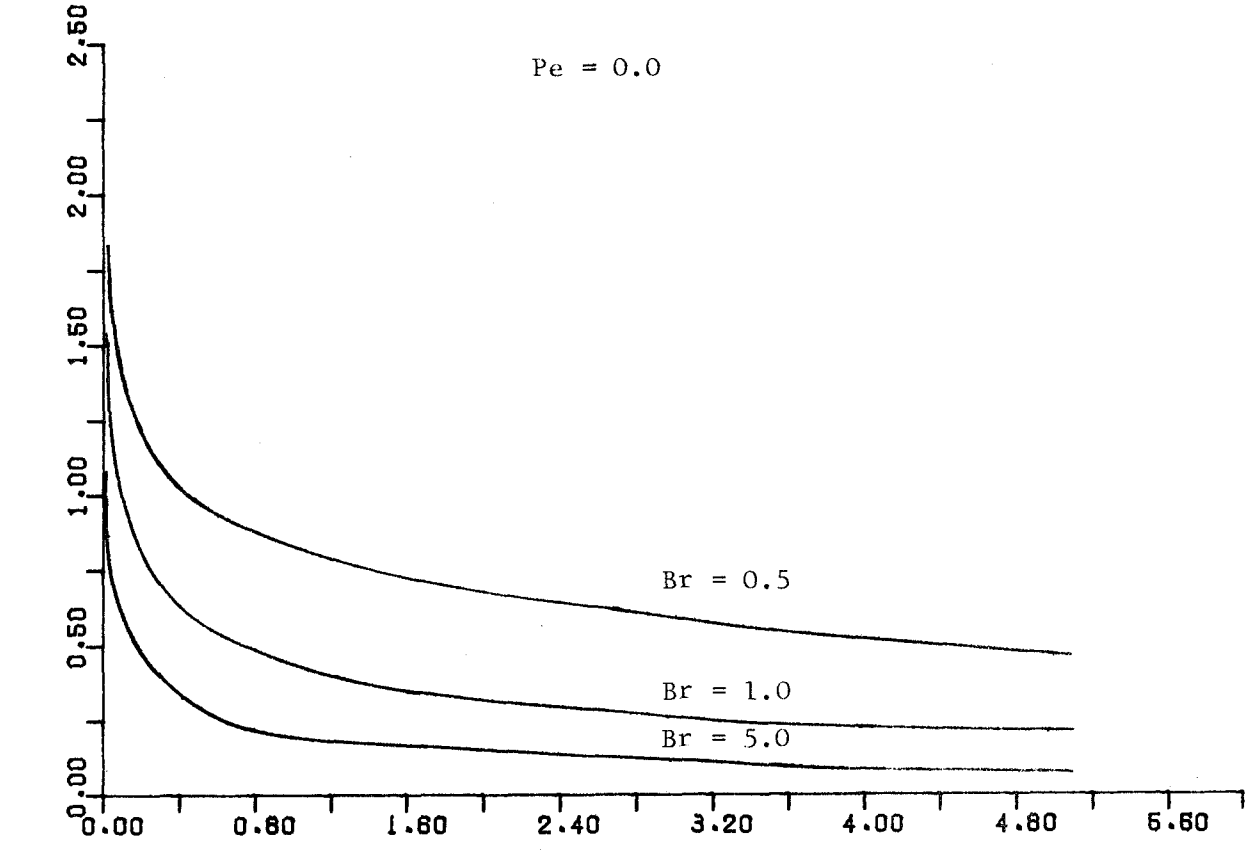

Figure 4.19 Graphs of τ against t for the case $\theta_s(z, 0) = \theta_c(z)$

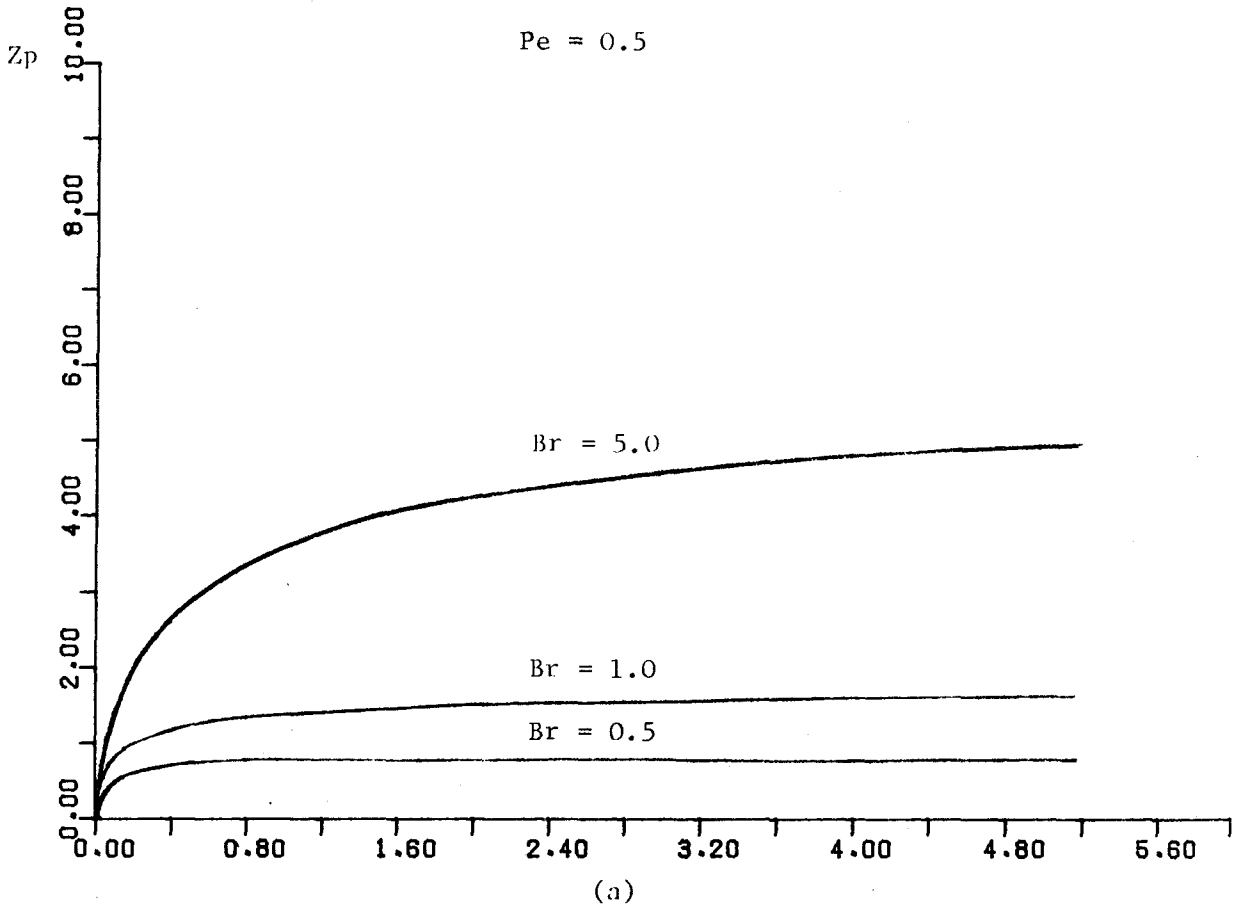

(a)

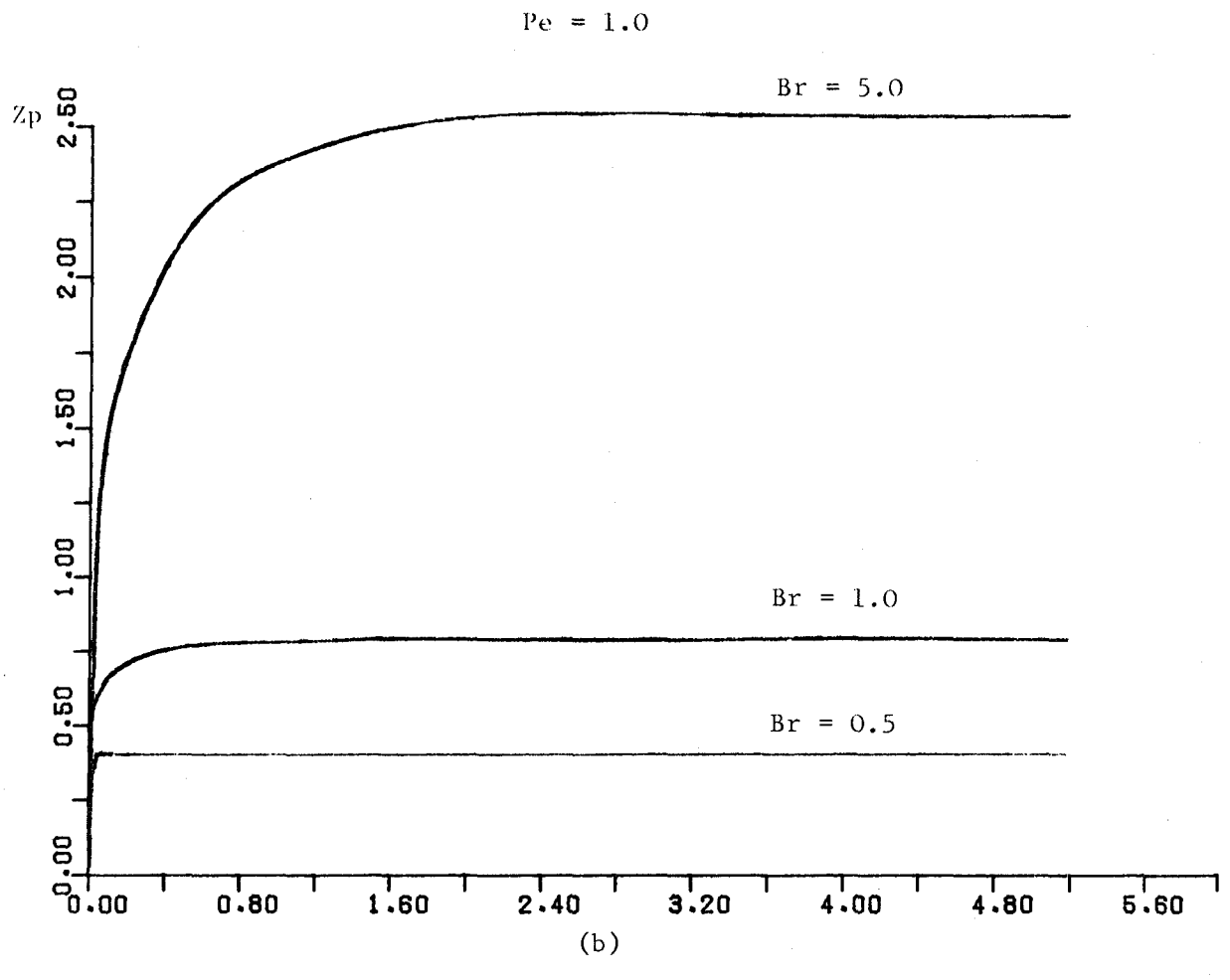

(b)

Figure 4.20 Graphs of zp against t for the case $\theta_s(z,0) = \theta_c(z)$

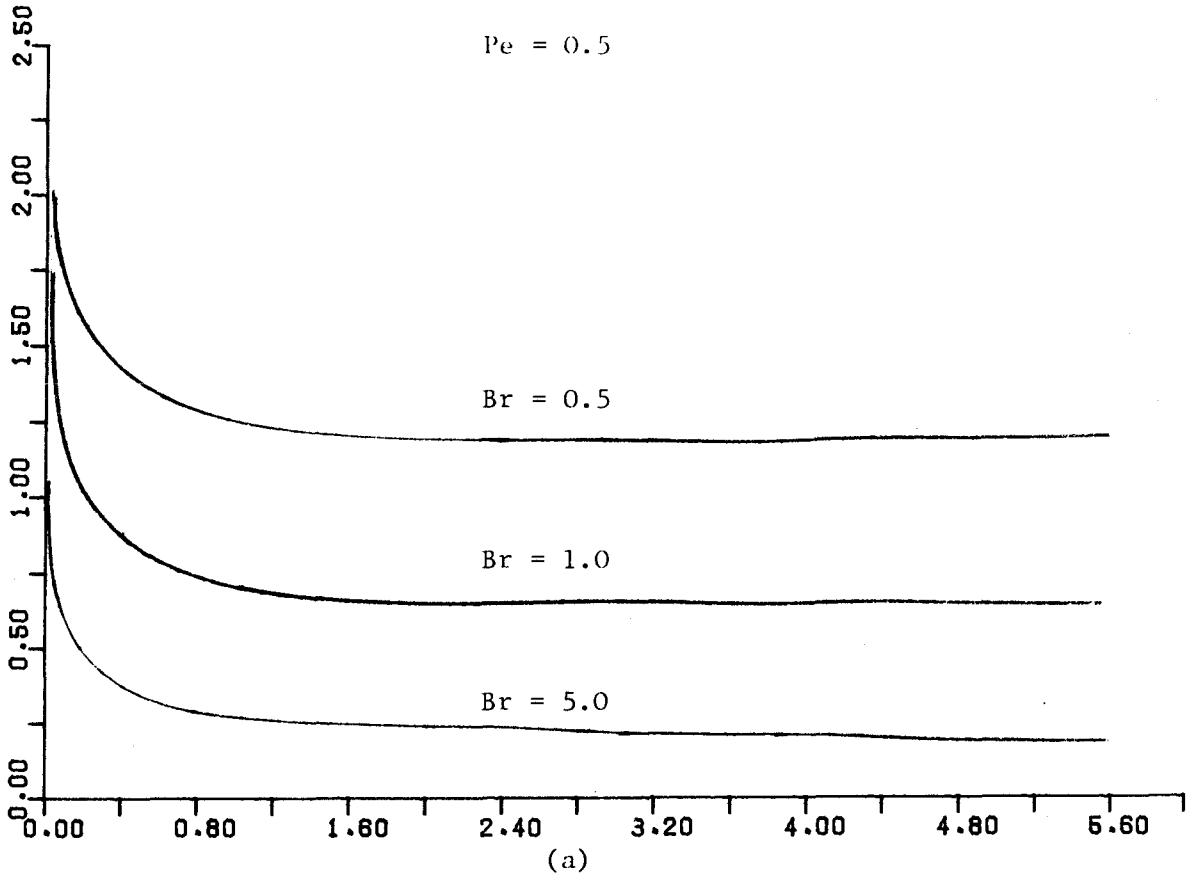

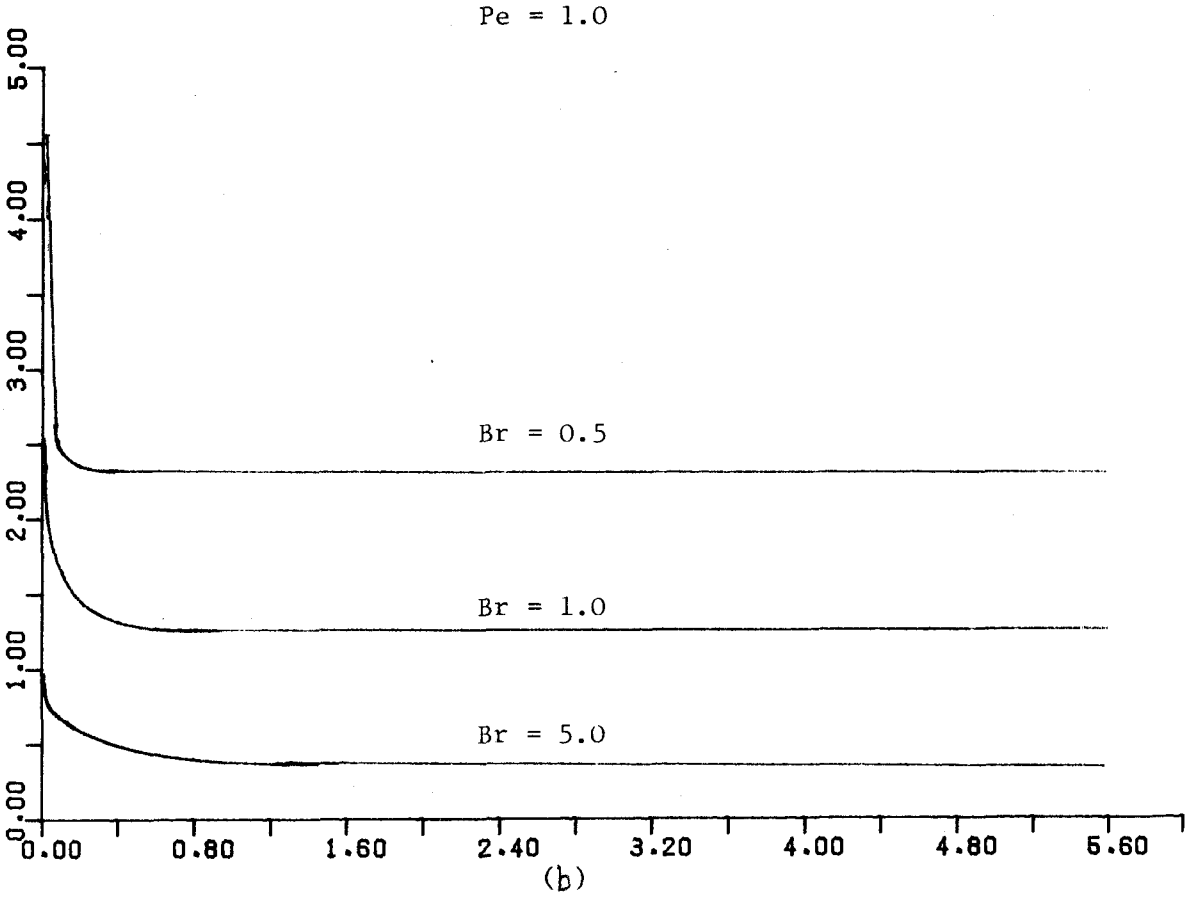

Figure 4.21 Graphs of τ against t for the case $\theta_s(z, 0) = \theta_c(z)$.

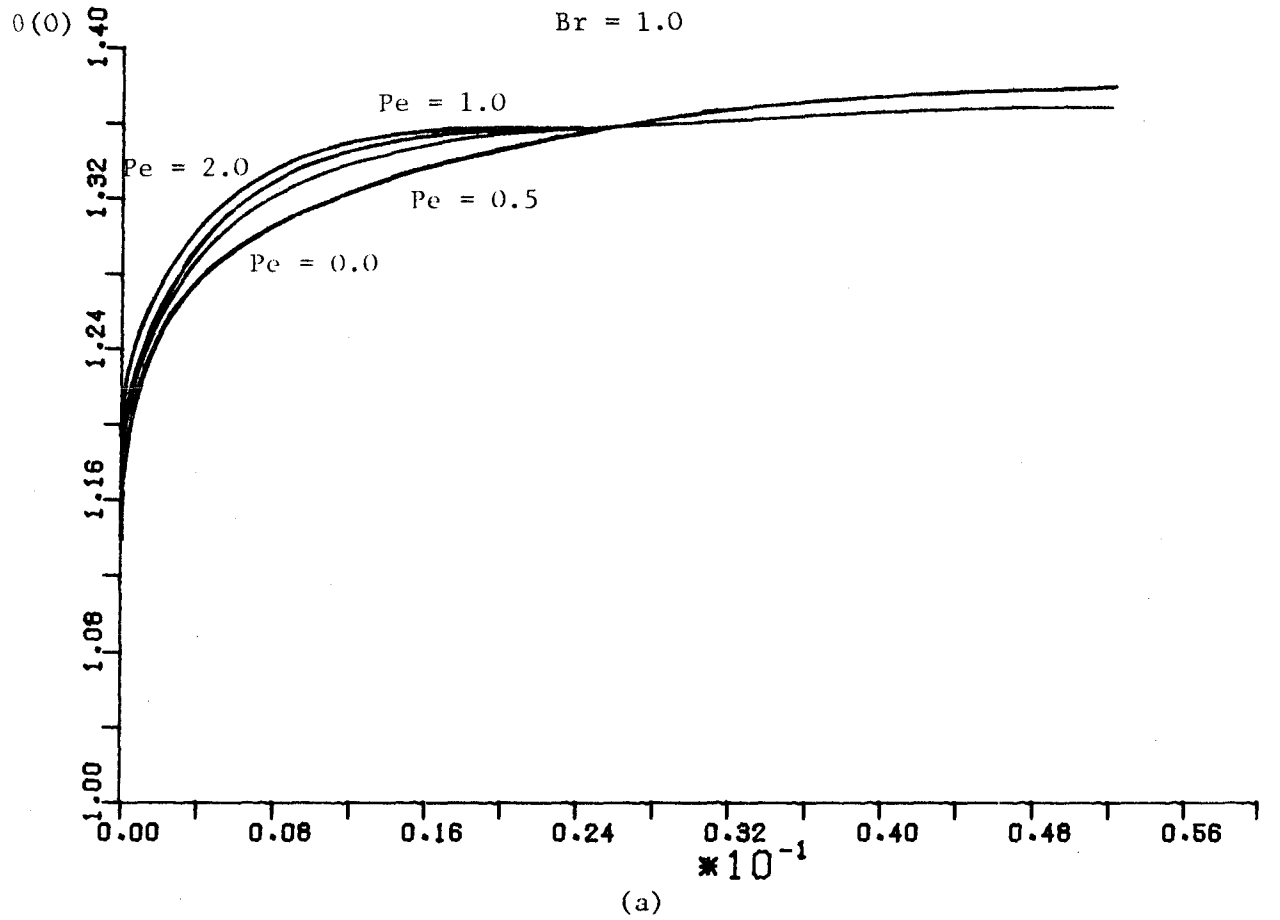

(a)

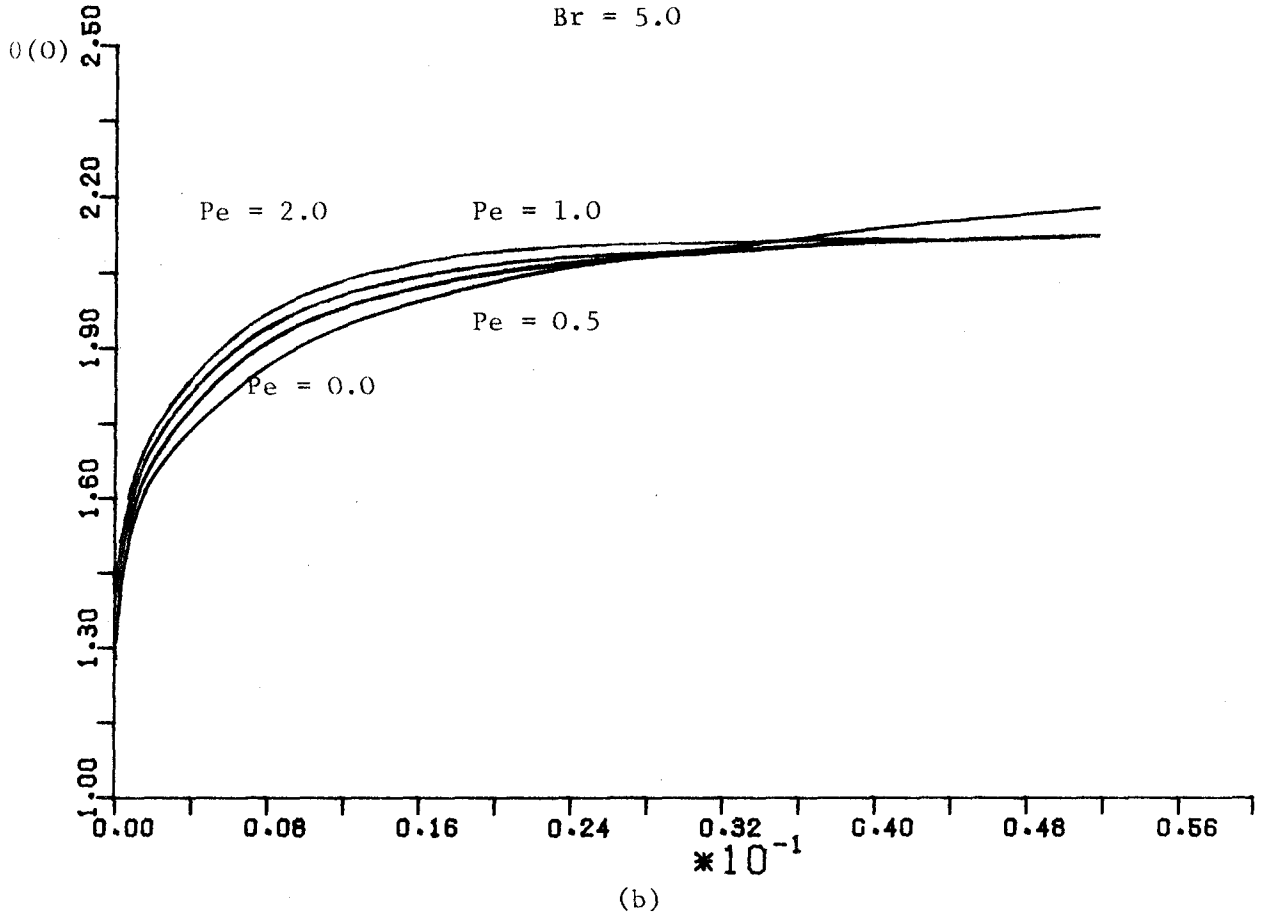

(b)

Figure 4.22 Plots of Interface Temperature against t for the case

$\theta_s(z, 0) = \theta_c(z)$

in Figures 4.6 and 4.7 reveals again that differences are small. In fact for the case $\theta_s(Z,0) = 0$. Z_p behaves like $t^{\frac{1}{2}}$, for small t , whereas when $\theta_s(Z,0) = \theta_c(Z)$ Z_p is asymptotic to $t^{2/5}$. For large t the same steady state solution is approached by both models and thus it is deduced that neglecting the conditioning phase does not affect the solution for large times and that the quantities Z_p and τ are not greatly affected for small time. However comparing the curves in Figure 4.22 with those in Figure 4.9 reveals that the behaviour of the interface temperatures differ vastly between the two models although the same steady state values are approached. It is seen that when the conditioning phase is included, the interface temperature initially assumes the conditioning temperature , $\theta = 1$, and rises rapidly towards the steady state whereas when the phase is neglected, the interface temperature initially assumes the value corresponding to $Pe = 0$ and decays towards the steady state value (see Figure 4.9). We thus deduce that neglecting the conditioning phase leads to large errors initially in the temperature profiles but that the errors reduce rapidly with increasing time.

4.14 The Equilibrium Phase

Up to now all the models considered in this Chapter have been relevant to the phase II stage of the welding cycle. It has been noted that providing upset is included in these models then a steady state solution is approached. A steady state exists in practice and the period of time over which the steady state conditions endure is called the equilibrium phase or phase III. (See Figure 1.2). In this section an exact solution is developed for the equilibrium phase of the model described in Section 4.8, that is upset is included but constant viscosity is assumed.

With all the assumptions of Sections 4.8 the energy equations (4.8.23) and (4.8.24), for steady state, reduce to

$$\frac{d^2\theta_\infty}{dZ^2} + \frac{Br}{Z_{p\infty}^2} = \frac{Pe}{2}\left(\frac{Z}{Z_{p\infty}}\right)\left[\left(\frac{Z}{Z_{p\infty}}\right)^2 - 3\right]\frac{d\theta_\infty}{dZ} \qquad (4.14.1)$$

and

$$\frac{d^2\theta_{s\infty}}{dZ^2} = -Pe\,\frac{d\theta_{s\infty}}{dZ} \qquad (4.14.2)$$

where the subscript (∞) denotes steady state. The boundary conditions (4.2.23), (4.2.24), (4.2.25) and (4.4.3) become

$$\frac{d\theta_\infty}{dZ}(0) = 0 \quad , \qquad (4.14.3)$$

$$\theta_\infty(Z_{p\infty}) = \theta_{s\infty}(Z_{p\infty}) = 1 \quad , \qquad (4.14.4)$$

$$\theta_{s\infty}(Z) \to \infty \quad \text{as} \quad Z \to \infty \qquad (4.14.5)$$

and

$$\frac{\partial\theta_\infty}{\partial Z}(Z_{p\infty}) = \frac{d\theta_{s\infty}}{dZ}(Z_{p\infty}) \qquad (4.14.6)$$

It is convenient at this stage to introduce the new variable defined by

$$\zeta = Z/Z_{p\infty} \quad . \qquad (4.14.7)$$

In terms of ζ the above equations become

$$\frac{d^2\theta_\infty}{d\zeta^2} + Br = \frac{PeZ_{p\infty}}{2}\,\zeta(\zeta^2-3)\,\frac{d\theta_\infty}{d\zeta} \qquad (4.14.8)$$

and

$$\frac{d^2\theta_{s\infty}}{d\zeta^2} = -PeZ_{p\infty}\,\frac{d\theta_{s\infty}}{d\zeta} \quad , \qquad (4.14.9)$$

which must be solved subject to

$$\frac{d\theta_\infty}{d\zeta}(0) = 0 \qquad (4.14.10)$$

$$\theta_\infty(1) = \theta_{s\infty}(1) = 1 \qquad (4.14.11)$$

$$\theta_{s\infty}(\zeta) \to 0 \quad \text{as} \quad \zeta \to \infty \qquad (4.14.12)$$

and

$$\frac{d\theta_\infty}{d\zeta}(1) = \frac{d\theta_{s\infty}}{d\zeta}(1) \qquad (4.14.13)$$

An analytic solution to this system is derived here. On multiplying equation (4.14.8) by the integrating factor $\exp\left|-R(\zeta)\right|$, where

$$R(\zeta) = PeZ_{p\infty}\zeta^2(\zeta^2-6)/8 \qquad (4.14.14)$$

the equation can be expressed

$$\frac{d}{d\zeta}\left[\exp\left[-R(\zeta)\right]\frac{d\theta_\infty}{d\zeta}\right] = -\,Br\,\exp\left[-R(\zeta)\right] . \qquad (4.14.15)$$

On integrating this equation with respect to ζ we have

$$\exp\left[-R(\zeta)\right]\frac{d\theta_\infty}{d\zeta} = A - Br\int_0^\zeta \exp\left[-R(\zeta)\right]d\zeta \quad , \qquad (4.14.16)$$

and applying the boundary condition (4.14.10) it follows that the constant of integration, A, is identically zero. A further integration of equation (4.14.16) and the application of the boundary condition $(4.14.11)_1$ yields

$$\theta_\infty = 1 - Br \int_1^\zeta \exp\left[R(u)\right] \int_0^u \exp\left[-R(v)\right] dvdu \qquad (4.14.17)$$

The solution to equation (4.14.9) which satisfies the boundary conditions (4.14.12) and $(4.14.11)_2$ is easily seen to be

$$\theta_{s\infty} = \exp\left[-PeZ_{p\infty}(\zeta-1)\right] \quad . \qquad (4.14.18)$$

Finally on the application of the remaining boundary condition (4.14.13) there results a transcendental equation in $Z_{p\infty}$, namely

$$Br \exp\left[R(1)\right] \int_0^1 \exp\left[-R(\zeta)\right] d\zeta = PeZ_{p\infty} \; . \qquad (4.14.19)$$

This equation was solved numerically using the Newton-Raphson iterative procedure and in Figure 4.23 numerical values of $Z_{p\infty}$ for various values of Pe are plotted against Br. Values of $Z_{p\infty}$ obtained by the heat balance method and given by equation (4.11.9) are also given for comparison.

We also present here the asymptotic solutions to equation (4.14.19) for both small and large Br for comparison with their counterparts for the heat balance integral given by equations (4.11.11) and (4.11.12).

For the case $Br \ll 1$ it is appropriate to seek a series solution in the form

$$Z_{p\infty} = Brg_1 + Br^2 g_2 + \ldots \qquad (4.14.20)$$

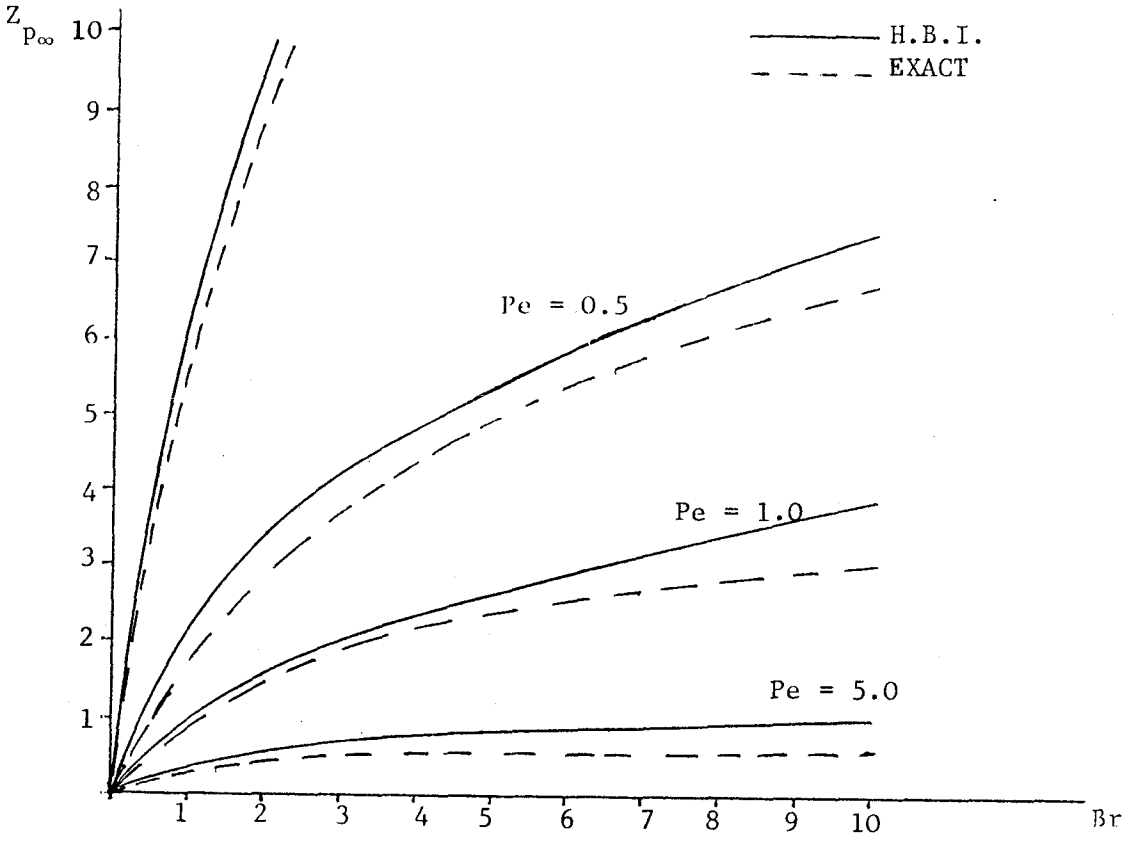

Figure 4.23 Plots of $Z_{p\infty}$ against Br for the case $\mu = 1$ from the heat balance integral solution and the exact solution.

Substituting this series into equation (4.14.19) and expanding for small Br leads to the identity

$$Br\left[1 - 5/8\ BrPeg_1 + O(Br^2)\right]\left\{\int_0^1 \left[1 - Br\,Peg_1 u^2(u^2-6)/8 + O(Br^2)\right]du\right\}$$

$$\equiv BrPeg_1 + Br^2 Peg_2 + O(Br^3)\ , \qquad (4.14.21)$$

which, after performing the integrations and rearranging, becomes

$$Br - \frac{2}{5}Br^2 Peg_1 + O(Br^2) \equiv Br\ Peg_1 + Br^2 Peg_2 + O(Br^3)\ , \qquad (4.14.22)$$

Equating the coefficient of like terms in this identity gives g_1 and g_2 and hence, with the aid of equation (4.14.20), we can write

$$Z_{p_\infty} = \frac{Br}{Pe} - \frac{2Br^2}{5Pe} + O(Br^3)\ . \qquad (4.14.23)$$

Furthermore, on substituting this expression into equations (4.14.17) and (4.14.18) we have the asymptotic solution for small B_r of the temperature profiles θ_∞ and $\theta_{s\infty}$ respectively.

$$\theta_\infty = 1 + \frac{1}{2} B_r(1-\zeta^2) + \frac{Br^2}{120}\left[15(\zeta^4-1) - 2(\zeta^6-1)\right] + O(Br^3) \tag{4.14.24}$$

and

$$\theta_{s\infty} = 1 + Br(1-\zeta) + \frac{Br^2}{10}\left[5(1-\zeta)^2 - 4(1-\zeta)\right] + O(Br^3), \quad [1-\zeta] << 1 . \tag{4.14.25}$$

It is seen by comparison of equations (4.14.23), (4.14.24) and (4.14.25) with (4.11.11), (4.11.13) and (4.11.14) respectively that the first two terms in each series are identical which indicates that the approximate solution is in very good agreement with the exact solution for small Br .

In order to obtain an asymptotic solution for large Br we note that

$$\int_0^1 \exp\left[-R(\zeta)\right] d\zeta \equiv \frac{1}{2}\int_{-1}^{1} \frac{PeZ_{p\infty}}{2}(3-\zeta^2)\zeta \exp\left[-R(\zeta)\right] \left(\frac{2}{PeZ_{p\infty}(3-\zeta^2)\zeta}\right) d\zeta \tag{4.14.26}$$

The right hand side of this identity is now readily integrated by part yielding, with the aid of definition (4.4.14),

$$\int_0^1 \exp\left[-R(\zeta)\right] d\zeta \equiv \frac{1}{PeZ_{p\infty}} e^{5PeZ_{p\infty}/8} + \frac{3}{PeZ_{p\infty}}\int_{-1}^{1} \frac{(1-\zeta^2)}{(3\zeta-\zeta^3)^2} \exp\left[-R(\zeta)\right] d\zeta , \tag{4.14.27}$$

and, in fact, a further integration reveals that

$$\int_0^1 \exp\left[-R(\zeta)\right]d\zeta = \frac{e^{5PeZ_{p\infty}/8}}{PeZ_{p\infty}} + O\left(\frac{1}{Pe^3 Z_{p\infty}^3}\right) . \qquad (4.14.28)$$

Substituting this expression into equation (4.14.19) then gives us

$$\frac{B_r}{PeZ_{p\infty}} + O\left[\frac{B_r}{(PeZ_{p\infty})^3}\right] = PeZ_{p\infty} \qquad (4.14.29)$$

From this equation we deduce that

$$Z_p = \sqrt{\frac{Br}{Pe}} + O(Br^{-\frac{1}{2}}) \qquad (4.14.30)$$

Comparison of this expression with equation (4.11.12) reveals that the approximate solution is far less accurate for larger values of Br, however, as can be seen from Figure 4.23, the discrepancy is still very small for values in the range $0 \leq B_r \leq 10$.

4.14.1 Results and Discussion

In this section various results for the steady state are compared and discussed.

Using the numerical solutions of equations (4.12.29) and (4.12.61), plots of $Z_{p\infty}$ against Br, for various values of Pe, are given in Figure 4.24, for the cases $\mu = 1/\theta$ and $\mu = (\partial V/\partial Z)^{1/n-1}$. We notice by comparing these curves with those in Figure 4.23 that values of $Z_{p\infty}$ predicted by the models $\mu = 1$ and $\mu = 1/\theta$ are quite close whereas those predicted by the model $\mu = (\partial V/\partial Z)^{1/n-1}$ differ vastly from the other two. However it seemslikely that if the exponential

term, $\exp\left\{Q/R\left[T_{AM}+ (T_c-T_{AM})\right]\right\}$, were included in the latter model then the values of $z_{p\infty}$ predicted would be reduced.

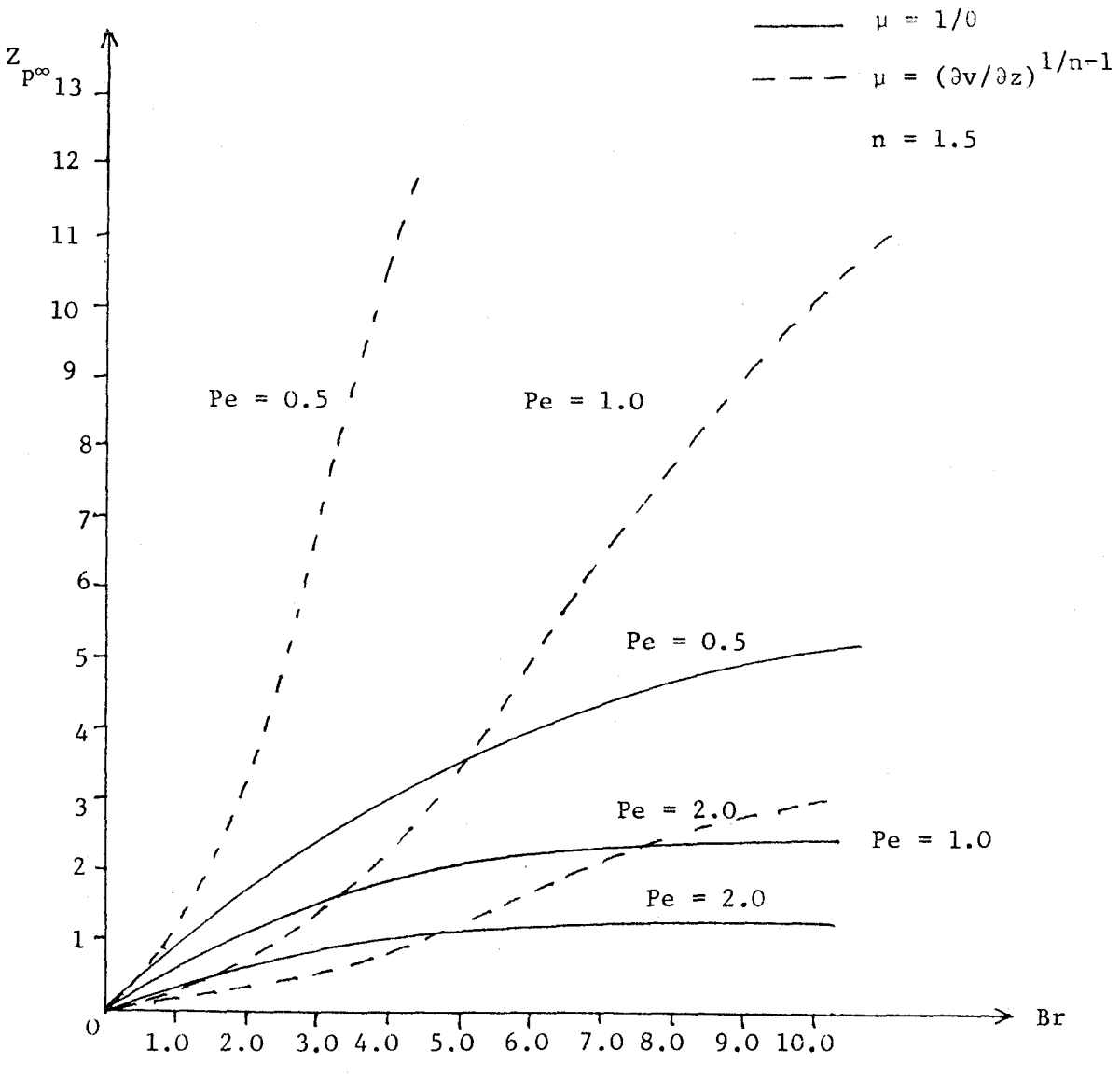

Figure 4.24 Plots of $Z_{p\infty}$ against Br for the models $\mu = 1/\theta$ and $\mu = (\partial v/\partial z)^{1-1/n}$

In Figure 4.25 the interface temperature $\theta_\infty(0)$ is plotted against Br for the models $\mu = 1$, $\mu = 1/\theta$ and $\mu = (\partial v/\partial z)^{1/n-1}$. We note in all cases that a value of Br exists, Br_c , at which

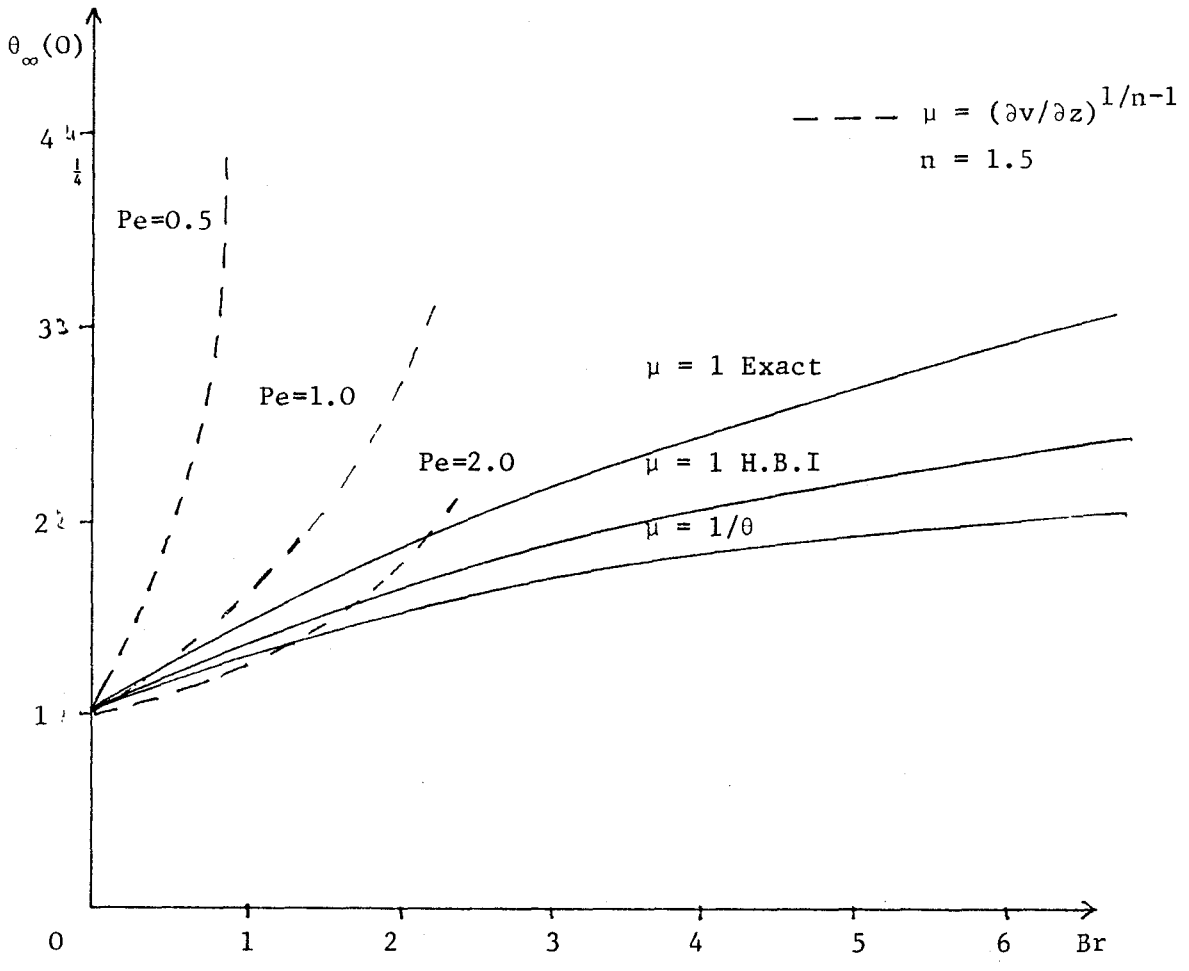

Figure 4.25 Plots of $\theta_\infty(0)$ against Br for the models $\mu = 1$, $\mu = 1/\theta$ and $\mu = (\partial v/\partial z)^{1/n-1}$

melting is attained. It is seen that in the case $\mu = 1/\theta$ the value of Br_c is greater than for $\mu = 1$ whereas taking $\mu = (\partial v/\partial z)^{1/n-1}$ leads to smaller values of Br_c. It thus seems likely that it is the decay of viscosity with increasing temperature that prevents melting from being achieved. In fact a suitable model for the viscosity would be one which obeys law (4.12.32) for temperatures less than the melting temperature and falls very rapidly to zero in the close proximity of the melting temperature. In this case

the heat generation term would fall to zero as melting temperature was approached and consequently melting would never be reached.

4.15 The Deceleration Phase

So far in this thesis the final phase in the frictioning stage, the deceleration phase, has not been discussed.

At the start of the deceleration phase a friction brake is applied to the head stock chuck and the rotating component is rapidly brought to rest. The manner in which the rotation is halted can significantly effect the weld quality as has been extensively studied, experimentally by Duffin and Bahrani [38] . In this section a model is developed to describe the deceleration phase and a solution valid for the early stages of this phase is obtained.

Let the angular velocity of the rotating component, during the deceleration phase be $\omega_D(t)$. In this section the time t is measured from the end of the equilibrium phase so ω must satisfy the initial condition

$$\omega_D(0) = \omega, \tag{4.15.1}$$

where ω is the angular velocity during phases II and III .

During the deceleration phase the equations governing the pressures and velocities are given by (4.2.7) to (4.2.13) and the corresponding boundary conditions are (4.2.14) to (4.2.18), with the exception that condition $(4.2.17)_2$ is replaced by

$$V(Z_p,t) = \omega_D(t)/\omega = V_D(t) \quad . \tag{4.15.2}$$

In view of (4.15.1) it follows that $V_D(0) = 1$. Retaining the assumptions of Section 4.8 (including the postulate $\mu = 1$) , the velocity components u,v and w are given by (4.7.15), (4.7.2) and (4.7.14) respectively and the pressures p_0 and p_1 by (4.7.1) and (4.7.22) respectively. However, the amended form of equation (4.4.7) obtained by applying boundary condition (4.15.2) to (4.4.6) is

$$V_D(t) = \tau(t)\ Z_p(t) \ . \tag{4.15.3}$$

On substituting equations (4.7.2) and (4.7.14) for the velocity component v and w respectively into equation (4.8.14) and expressing the shear stress τ in terms of Z_p using equation (4.15.3), the energy equation for the plastic region becomes

$$\frac{\partial^2\theta}{\partial Z^2} + \frac{B_r V_D^2}{Z_p^2} = \frac{PeZ}{2Z_p^3}(Z^2-3Z_p^2)\frac{\partial\theta}{\partial Z} + \frac{1}{F_0}\frac{\partial\theta}{\partial t} \quad , \quad 0 \leq Z \leq Z_p \ . \tag{4.15.4}$$

The corresponding equation for the solid region is unchanged from (4.8.24) and the relevant boundary conditions are given by (4.2.23),(4.2.24), (4.2.25) and (4.4.3). However the new initial conditions are

$$\theta(Z,0) = \theta_\infty(Z) \tag{4.15.5}$$

and

$$\theta_s(Z,0) = \theta_{s\infty}(Z) \ , \tag{4.15.6}$$

where θ and θ_s are the steady state temperature profiles.

We develop here a solution to the above system of partial differential equations which is valid for small times. Since at the beginning of the deceleration phase the system is in equilibrium it

seems logical to assume solutions of the form

$$\theta(Z,t) = \theta_{\infty}(Z) + \theta_1(Z,t) \ , \tag{4.15.7}$$

$$\theta_s(Z,t) = \theta_{s\infty}(Z) + \theta_{s1}(Z,t) \ , \tag{4.15.8}$$

$$Z_p(t) = Z_{p\infty} + Z_1(t) \tag{4.15.9}$$

and

$$\tau(t) = \tau_{\infty} + \tau_1(t) \ , \tag{4.15.10}$$

where the suffix (∞) denotes steady state variables. For early times it may be assumed that the transient terms are much smaller than the steady state counterpart, thus we can write

$$|\theta_{\infty}| >> |\theta_1| \ , \ |\theta_{s\infty}| >> |\theta_{s1}| \ , \ |Z_{p\infty}| >> |Z_1| \quad \text{and} \quad |\tau_{\infty}| >> |\tau_1| \ . \tag{4.15.11}$$

Let us also write

$$V_D(t) = 1 + \beta(t) \tag{4.15.12}$$

in which case

$$\beta(0) = 0 \tag{4.15.13}$$

and consistent with (4.15.11) it can be assumed that $\beta << 1$.
On substituting equations (4.15.7) to (4.15.10) and (4.15.12) into equations (4.15.4) and (4.8.24) and expanding in small quantities, the energy equations can be written

$$\frac{d^2\theta_{\infty}}{dZ^2} + \frac{\partial^2\theta_1}{\partial Z^2} + \frac{Br}{Z_{p\infty}^2}(1+2\beta(t)+\ldots)(1-2Z_1/Z_{p\infty}+\ldots) \equiv$$

$$\frac{PeZ}{2Z_{p_{\infty}}^3}(1-3Z_1/Z_{p\infty})(Z^2-3Z_{p\infty}^2-6Z_{p\infty}Z_1+\ldots)\left[\frac{d\theta_{\infty}}{dZ} + \frac{\partial\theta_1}{\partial Z}\right] + \frac{1}{F_0}\frac{\partial\theta_1}{\partial t} \tag{4.15.14}$$

and

$$\frac{d^2\theta_{s\infty}}{dZ^2} + \frac{\partial 2\theta_1}{\partial Z^2} = - Pe\left[\frac{d\theta_{s\infty}}{dZ} + \frac{\partial\theta_{s1}}{\partial Z} + \frac{1}{F_0}\frac{\partial\theta_{s1}}{\partial t}\right]. \qquad (4.15.15)$$

Similarly using equations (4.15.7), (4.15.8) and (4.15.9) in the boundary conditions (4.2.23), (4.2.24), (4.2.25) and (4.4.3) and expanding in small quantities using Taylor's theorem, one obtains

$$\frac{d\theta_\infty}{dZ}(0) + \frac{\partial\theta_1}{\partial Z}(0,t) = 0 , \qquad (4.15.16)$$

$$\theta_\infty(Z_{p\infty}) + \theta_1(Z_{p\infty},t) + Z_1\frac{d\theta_\infty}{dz}(Z_{p\infty}) + O(Z_1^2) = 1 , \qquad (4.15.17)$$

$$\theta_{s\infty}(Z_{p\infty}) + \theta_{s1}(Z_{p\infty},t) + Z_1\frac{d\theta_{s\infty}}{dZ}(Z_{p\infty}) + O(Z_1^2) = 1 , \qquad (4.15.18)$$

$$\frac{d\theta_\infty}{dZ}(Z_{p\infty}) + \frac{\partial\theta_1}{\partial Z}(Z_{p\infty},t) + Z_1\frac{d^2\theta_\infty}{dZ^2}(Z_{p\infty}) + O(Z_1^2) =$$

$$= \frac{d\theta_{s\infty}}{dZ}(Z_{p\infty}) + \frac{\partial\theta_{s1}}{\partial Z}(Z_{p\infty},t) + Z_1\frac{d^2\theta_{s\infty}}{dZ^2}(Z_{p\infty}) + O(Z_1^2)$$

$$(4.15.19)$$

and

$$\theta_{s\infty}(Z) + \theta_{s1}(Z,t) \to 0 \quad \text{as} \quad Z \to \infty \quad . \qquad (4.15.20)$$

Finally the initial conditions (4.15.5) and (4.15.6) reduce to

$$\theta_1(Z,0) = 0 \quad \text{and} \quad \theta_{s1}(Z,0) = 0 \qquad (4.15.21)$$

4.15.1 The Steady State System

The steady state terms in the above identities yield the pair of ordinary differential equations (4.14.1) and (4.14.2) with the boundary conditions (4.14.3), (4.14.4), (4.14.5) and (4.14.6). The solution to this system has been given in Section 4.11 and requires no further discussion here.

4.15.2 The Transient System

Equating the time dependent terms in the identities (4.15.14) and (4.15.15) and neglecting terms $O(Z_1^2)$ yields, after some rearrangement, the following pair of partial differential equations

$$\frac{\partial^2\theta_1}{\partial Z^2} - \frac{PeZ}{2Z_{p\infty}^3}(Z^2-3Z_{p\infty}^2)\frac{\partial\theta_1}{\partial Z} - \frac{1}{F_O}\frac{\partial\theta_1}{\partial t} = \frac{2Br}{Z_{p\infty}^3}(Z_1-Z_{p\infty}\beta) + \frac{3Pe\ Z_1 Z}{2Z_{p\infty}^4}(Z_{p\infty}^2-Z^2)\frac{d\theta_\infty}{dZ} \tag{4.15.22}$$

and

$$\frac{\partial^2\theta_{s1}}{\partial Z^2} = -Pe\frac{\partial\theta_{s1}}{\partial Z} + \frac{1}{F_O}\frac{\partial\theta_{s1}}{\partial t} \tag{4.15.23}$$

Similarly the boundary conditions (4.15.16) to (4.15.20) reduce to

$$\frac{\partial\theta_1}{\partial Z}(0,t) = 0 \quad , \tag{4.15.24}$$

$$\theta_1(Z_{p\infty},t) = -Z_1\frac{d\theta_\infty}{dZ}(Z_{p\infty}) \quad , \tag{4.15.25}$$

$$\theta_{s1}(Z_{p\infty},t) = -Z_1\frac{d\theta_{s\infty}}{dZ}(Z_{p\infty}) \quad , \tag{4.15.26}$$

$$\frac{\partial \theta_1}{\partial Z} + Z_1 \frac{d^2\theta_\infty}{dZ^2}(Z_{p\infty}) = \frac{\partial \theta_{s1}}{\partial Z} + Z_1 \frac{d^2\theta_{s\infty}}{dZ^2}(Z_{p\infty}) \tag{4.15.27}$$

and

$$\theta_{s1}(Z,t) \to 0 \quad \text{as} \quad Z \to \infty \quad , \tag{4.15.28}$$

and the initial conditions are given by (4.15.21).

Introducing the variable ζ, defined by (4.14.7), into the above system, the latter can be written

$$\frac{\partial^2\theta_1}{\partial\zeta^2} - \frac{PeZ_{p\infty}}{2}\zeta(\zeta^2-3)\frac{\partial\theta_1}{\partial\zeta} - \frac{Z_{p\infty}^2}{F_0}\frac{\partial\theta_1}{\partial t} = \frac{2Br}{Z_{p\infty}}(Z_1 - Z_{p\infty}\beta) + \frac{3PeZ_1}{2}\zeta(1-\zeta^2)\frac{d\theta_\infty}{d\zeta} \quad , \tag{4.15.29}$$

$$\frac{\partial^2\theta_{s1}}{\partial\zeta^2} + PeZ_{p\infty}\frac{\partial\theta_{s1}}{\partial\zeta} - \frac{Z_{p\infty}^2}{F_0}\frac{\partial\theta_{s1}}{\partial t} = 0 \quad , \tag{4.15.30}$$

$$\frac{\partial\theta_1}{\partial\zeta}(0,t) = 0 \quad , \tag{4.15.31}$$

$$\theta_1(1,t) = -\frac{Z_1}{Z_{p\infty}}\frac{d\theta_\infty}{d\zeta}(1) \quad , \tag{4.15.32}$$

$$\theta_{s1}(1,t) = -\frac{Z_1}{Z_{p\infty}}\frac{d\theta_{s\infty}}{d\zeta}(1) \quad , \tag{4.15.33}$$

$$\frac{\partial\theta_1}{\partial\zeta}(1,t) + \frac{Z_1}{Z_{p\infty}}\frac{d^2\theta_\infty}{d\zeta^2}(1) = \frac{\partial\theta_{s1}}{\partial\zeta}(1,t) + \frac{Z_1}{Z_{p\infty}}\frac{d^2\theta_{s\infty}}{d\zeta^2}(1) \tag{4.15.34}$$

$$\theta_{s1}(\zeta,t) \to 0 \quad \text{as} \quad \zeta \to \infty \tag{4.15.35}$$

and

$$\theta_1(\zeta,0) = 0, \quad \theta_{s1}(\zeta,0) = 0 \quad . \tag{4.15.36}$$

There does not appear to be an exact solution to this system of equations. However, by assuming that the Brinkman number is small a series solution can be developed.

Let us assume, therefore, that Br is small and write:

$$\theta_1(\zeta,t,B_r) = \psi_0(\zeta,t) + Br\,\psi_1(\zeta,t) + Br^2\psi_2(\zeta,t) + \ldots \qquad (4.15.37)$$

and

$$Z_1(t,Br) = Br\,h_1(t) + Br^2 h_2(t) + \ldots \qquad (4.15.38)$$

Substituting the series (4.14.23), (4.14.24), (4.15.37) and (4.15.38) into equation (4.15.29) and the boundary conditions (4.15.31) and (4.15.32) results in:

$$\frac{\partial^2\psi_0}{\partial\zeta^2} + Br\,\frac{\partial^2\psi_1}{\partial\zeta^2} + Br^2\,\frac{\partial^2\psi_2}{\partial\zeta^2} + \ldots - \frac{1}{2}Br\left(1-\frac{2}{5}Br+\ldots\right)\zeta(\zeta^2-3)\left[\frac{\partial\psi_0}{\partial\zeta} + Br\,\frac{\partial\psi_1}{\partial\zeta} + \ldots\right]$$

$$- \left[\frac{Br}{F_0\,Pe^2}+\ldots\right]\left[\frac{\partial\psi_0}{\partial t} + B_r\,\frac{\partial\psi_1}{\partial t} + \ldots\right] \equiv 2Br\left(1+\frac{2}{5}Br+\ldots\right)\left[(Pe\,h_1-\beta) + Br\left(Pe\,h_2+\frac{2}{5}\beta\right)\right.$$

$$\left. + \ldots\right] + \frac{3Br^2Pe}{2}(h_1+Br\,h_2+\ldots)\zeta^2(\zeta^2-1)\left[1-Br\,\zeta^2(5-\zeta^2)/10+\ldots\right], \qquad (4.15.39)$$

$$\frac{\partial\psi_o}{\partial\zeta}(0,t) + Br\,\frac{\partial\psi_1}{\partial\zeta}(0,t) + Br^2\frac{\partial\psi_2}{\partial\zeta}(0,t)+\ldots \equiv 0 \qquad (4.15.40)$$

and

$$\psi_0(1,t) + Br\,\psi_1(1,t) + Br^2\psi_2(1,t)+\ldots = BrPe(h_1+Br\,h_2+\ldots)\left(1+\frac{2}{5}Br+\ldots\right)$$

$$\left(1-\frac{2}{5}Br+\ldots\right) \qquad (4.15.41)$$

The terms independent of Br in the above expressions lead to the equation

$$\frac{\partial^2 \psi_0}{\partial \zeta^2} = 0 \ , \tag{4.15.42}$$

which must be solved subject to

$$\frac{\partial \psi_0}{\partial \zeta}(0,t) = 0 \quad \text{and} \quad \psi_0(1,t) = 0 \tag{4.15.43}$$

It is immediately obvious from the above that

$$\psi_0 = 0 \ . \tag{4.15.44}$$

The terms in (4.15.39) to (4.15.41) which are linear in Br give the equation

$$\frac{\partial^2 \psi_1}{\partial \zeta^2} = 2(Peh_1 - \beta) \tag{4.15.45}$$

with the boundary conditions

$$\frac{\partial \psi_1}{\partial \zeta}(0,t) = 0 \quad \text{and} \quad \psi_1(1,t) = Peh_1 \ . \tag{4.15.46}$$

Integrating both sides of (4.15.45) twice with respect to ζ and applying the boundary conditions $(4.15.46)_{1,2}$ yields

$$\psi_1 = \beta(1-\zeta^2) + Pe\ h_1 \zeta^2 \ . \tag{4.15.47}$$

From the coefficient of Br^2 in the system (4.15.39) to (4.15.41) there results, with the aid of (4.15.44) and (4.15.47), and after some rearrangement, the equation

$$\frac{\partial^2\psi_2}{\partial\zeta^2} = \frac{Peh_1}{2}\left[5\zeta^4 - 9\zeta^2 + \frac{8}{5}\right] - \zeta^2(\zeta^2-3)\beta + 2Peh_2 \qquad (4.15.48)$$

and the boundary conditions

$$\frac{\partial\psi_2}{\partial\zeta}(0,t) = 0 \quad \text{and} \quad \psi_2(1,t) = Peh_2 \ . \qquad (4.15.49)$$

Integrating equation (4.15.48) with respect to ζ and applying the boundary condition $(4.15.49)_1$ gives us

$$\frac{\partial\psi_2}{\partial\zeta} = \frac{Peh_1}{2}\left[\zeta^5-3\zeta^3 + \frac{8\zeta}{5}\right] - \frac{\zeta^3}{5}(\zeta^2-5)\beta + 2Peh_2\zeta \qquad (4.15.50)$$

and integrating again and making use of condition $(4.15.49)_2$ yields

$$\psi_2 = \frac{Peh_1}{120}\left[10(\zeta^6-1)-45(\zeta^4-1) + 48(\zeta^2-1)\right] - \frac{\beta}{60}\left[2(\zeta^6-1)-15(\zeta^4-1)\right] + Peh_2\zeta^2 \ . \qquad (4.15.51)$$

Thus from equations (4.15.37), (4.15.44), (4.15.47) and (4.15.51) the solution for θ_1 may be expressed as

$$\theta_1 = Br\left[Peh_1\zeta^2+\beta(1-\zeta^2)\right] + Br^2\left\{Peh_2\zeta^2 - \frac{\beta}{60}\left[2(\zeta^6-1) - 15(\zeta^4-1)\right] + \frac{Peh_1}{120}\left[10(\zeta^6-1) - 45(\zeta^4-1) + 48(\zeta^2-1)\right]\right\} + O(Br^3) \qquad (4.15.52)$$

Higher order terms could be obtained in a similar manner but since the task is lengthy, the series is now terminated.

Let us now turn our attention to the solid region. Since equation (4.15.30) is linear in t and has constant coefficients it may be solved analytically using Laplace transforms.

Taking the transform of equation (4.15.30) we obtain, on making use of the initial condition $(4.15.36)_2$, the equation

$$\frac{d^2\bar{\theta}_{s1}}{d\zeta^2} + PeZ_{p_\infty} \frac{d\bar{\theta}_{s1}}{d\zeta} - \frac{Z_{p\infty}^2}{F_0} S\bar{\theta}_{s1} = 0 \ , \qquad (4.15.53)$$

whilst the appropriate boundary conditions (4.15.33) and (4.15.35) transform to

$$\bar{\theta}_{s1}(1,\S) = - \frac{\bar{Z}_1}{Z_{p\infty}} \frac{d\theta_{s\infty}}{d\zeta} (1) \qquad (4.15.54)$$

and

$$\bar{\theta}_{s1}(\zeta,\S) \to 0 \quad \text{as} \quad \zeta \to \infty \qquad (4.15.55)$$

Following standard notation the superposed bar denotes a transformed quantity and $\S$ is the transformation variable. Equation (4.15.53) is now a simple second order ordinary differential equation with constant coefficients for which the general solution is readily found to be

$$\bar{\theta}_{s1} = exP(-PeZ_{p\infty}\ \zeta/2)\Big[A(S)\exp(\tfrac{1}{2} Z_{p\infty}\ \zeta\sqrt{Pe^2+4S/F_0}) + \\ + B(S)\exp(-\tfrac{1}{2} Z_{p\infty}\ \zeta\sqrt{Pe^2+ 4S/F_0})\Big] \ , \qquad (4.15.56)$$

where A and B are arbitrary functions of $\S$ introduced through the integration. This expression satisfies the boundary condition (4.15.55) only if $A(\S)$ is identically zero. Thus putting $A(\S) = 0$ in equation (4.15.56) and using the boundary condition (4.15.54) we deduce that:

$$\bar{\theta}_{s1} = Pe\,\bar{Z}_1 \exp\left[\frac{1}{2} Z_{p\infty}(1-\zeta)(Pe + \sqrt{Pe^2 + 4S/F_0})\right] \qquad (4.15.57)$$

Before we can apply the final boundary condition (4.15.34) we must expand the above in small Br . Thus making use of (4.14.23) and (4.15.38) and expanding we obtain, after some rearrangement

$$\bar{\theta}_{s1} = Br Pe\,\bar{h}_1 + Br^2\left[Pe\bar{h}_2 + \frac{1}{2}\bar{h}_1(1-\zeta)(Pe + \sqrt{Pe^2 + 4S/F_0})\right] \qquad (4.15.58)$$

Taking the Laplace transform of expression (4.15.52) and substituting the resulting expression and equations (4.14.24), (4.14.25) and (4.15.58) for $\bar{\theta}_1$, θ_∞, $\theta_{s\infty}$ and $\bar{\theta}_{s1}$ respectively, into the Laplace transform of boundary condition (4.15.34), leads to the identity

$$2Br(Pe\bar{h}_1 - \bar{\beta}) + \frac{Br^2}{5}(10Pe\,\bar{h}_2 + 4\bar{\beta} - Pe\bar{h}_1) + \ldots - PeBr(\bar{h}_1 + Br\bar{h}_2 + \ldots)$$

$$(1 + \frac{2}{5}Br + \ldots)(1 - Br + \ldots) \equiv -\frac{1}{2} Br^2 \bar{h}_1 (Pe + \sqrt{Pe^2 + 4S/F_0})$$

$$+ PeBr^2(\bar{h}_1 + Br\bar{h}_2 + \ldots)(1 + \frac{2}{5}Br + \ldots)(1 + \ldots) \; . \qquad (4.15.59)$$

Equating the coefficient of Br in this identity yields

$$2(Pe\bar{h}_1 - \bar{\beta}) - Pe\bar{h}_1 = 0 \; , \qquad (4.15.60)$$

from which we deduce

$$\bar{h}_1 = 2\bar{\beta}/Pe \; . \qquad (4.15.61)$$

It immediately follows from inverting this result that

$$h_1 = 2\beta/Pe \; . \qquad (4.15.62)$$

From equating the coefficient of Br^2 in (4.15.59) we obtain

$$\frac{2}{5}\,(5Pe\bar{h}_2 + 4\bar{\beta} - 3Pe\bar{h}_1) = -\,\bar{h}_1(Pe + \sqrt{Pe^2 + 4S/F_0})\ , \tag{4.15.63}$$

and with the use of (4.15.61) it follows that

$$\bar{h}_2 = -\,\frac{3\bar{\beta}}{5Pe} - \frac{\bar{\beta}}{Pe^2}\sqrt{Pe^2 + 4S/F_0} \tag{4.15.64}$$

which becomes after inverting

$$h_2 = -\,\frac{3\beta}{5Pe} - \frac{1}{Pe^2}\,L^{-1}\left[\bar{\beta}\ \sqrt{Pe^2 + 4S/F_0}\right]\ . \tag{4.15.65}$$

Inverting the term in square brackets is not possible until β is specified. The form of β depends upon the manner in which the rotation is brought to a halt and must thus be determined experimentally. However, we shall suppose here, for illustration, that β is a linear function in t and write

$$\beta = -\delta t \tag{4.15.66}$$

where δ is a constant. The expression for h_1 then becomes

$$h_1 = -\,2\delta t/Pe \tag{4.15.67}$$

and for h_2 we have

$$h_2 = \frac{3\delta t}{5Pe} + \frac{\delta}{Pe^2}\,L^{-1}\left[\frac{1}{s^2}\ \sqrt{Pe^2 + 4S/F_0}\right]\ . \tag{4.15.68}$$

Since equation (4.15.18) is only valid for small time it may be expanded for large S leading to

$$h_2 = \frac{3\delta t}{5Pe} + \frac{2\delta}{Pe^2\sqrt{F_0}} L^{-1}\left[\frac{1}{S^{3/2}} + \frac{Pe^2 F_0}{8S^{5/2}} + \ldots\right] \qquad (4.15.69)$$

This expression can be easily inverted to yield

$$h_2 = \frac{4\delta}{Pe^2\sqrt{F_0}}\sqrt{\frac{t}{\pi}} + \frac{3\delta t}{5Pe} + \frac{\pi}{3}\ \delta\sqrt{F_0}\left(\frac{t}{\pi}\right)^{3/2} + \ldots(\qquad (4.15.70)$$

Thus using equations (4.15.38), (4.15.67) and (4.15.70) the expression for Z_1 can be written

$$Z_1 = -\frac{2\delta t}{Pe} Br + \delta\left[\frac{4}{Pe^2\sqrt{F_0}}\sqrt{\frac{t}{\pi}} + \frac{3t}{5Pe} + \frac{\pi\sqrt{F_0}}{3}\left(\frac{t}{\pi}\right)^{3/2} + \ldots\right] Br^2 + O(B_r^3) \qquad (4.15.71)$$

The solution for θ_1 is given by (4.15.52) with the aid of (4.15.66), (4.15.67) and (4.15.70) and the solution for θ_{s1} is obtained by inverting (4.15.58). On doing this we obtain

$$\theta_{s1} = PeBrh_1 + Br^2\left\{Peh_2 + \frac{Pe}{2}(1-\zeta)h_1 + \frac{1}{2}(1-\zeta)L^{-1}\left[h_1\sqrt{Pe^2 + 4S/F_0}\right]\right\} \qquad (4.15.72)$$

With the aid of (4.15.61) and (4.15.65) the term in the square brackets can be expressed in terms of h_2 and β and we have finally

$$\theta_{s1} = BrPeh_1 + Br^2\left\{Peh_2 + Pe\,(1-\zeta)h_1/2 - (1-\zeta)\left[3\beta/5 + Peh_2\right]\right\} + O(Br^3)\ ,\ [1-\zeta] \ll 1\ . \qquad (4.15.73)$$

Substituting equations (4.15.9), (4.15.10) and (4.15.12) into (4.15.3) leads to the expression

$$\tau_\infty Z_{p\infty} + \tau_\infty Z_1 + Z_{p\infty}\tau_1 + Z_1\tau_1 = 1 + \beta \qquad (4.15.74)$$

from which the shear stresses τ_∞ and τ_1 can be obtained. Equating the terms independent of time in the above, we deduce that

$$\tau_\infty = 1/Z_{p\infty} \quad , \qquad (4.15.75)$$

where $Z_{p\infty}$ is the solution of (4.14.19). Then neglecting term $O(Z_1\tau_1)$ and equating the remaining transient terms results in

$$\tau_1 = \frac{\beta - \tau_\infty Z_1}{Z_{p\infty}} \qquad (4.15.76)$$

The temperature profiles for the deceleration phase can now be determined in full, with the aid of (4.15.66), (4.15.67) and (4.15.70), for the plastic region by equations (4.15.7), (4.14.24) and (4.15.52) and for the solid region by (4.15.8), (4.14.25) and (4.15.73). Also the thickness of the plastic region Z_p and the shear stress τ are determined by (4.15.9), (4.14.23) and (4.15.71) and (4.15.10), (4.15.75) and (4.15.76) respectively.

4.15.3 Results and Discussion

The above series solution is of limited value since it is only valid for small values of both **Br** and **t** . However, the model does demonstrate the effect of slowing down the rotating component and in particular the increase in torque which is observed in practice. plots of τ, Z_p and V_D against time for the conditions Br=0 (0.1), Pe = 1.0 and ζ = 1.0 are given in Figures 4.26(a), (b), (c) and (d) respectively.

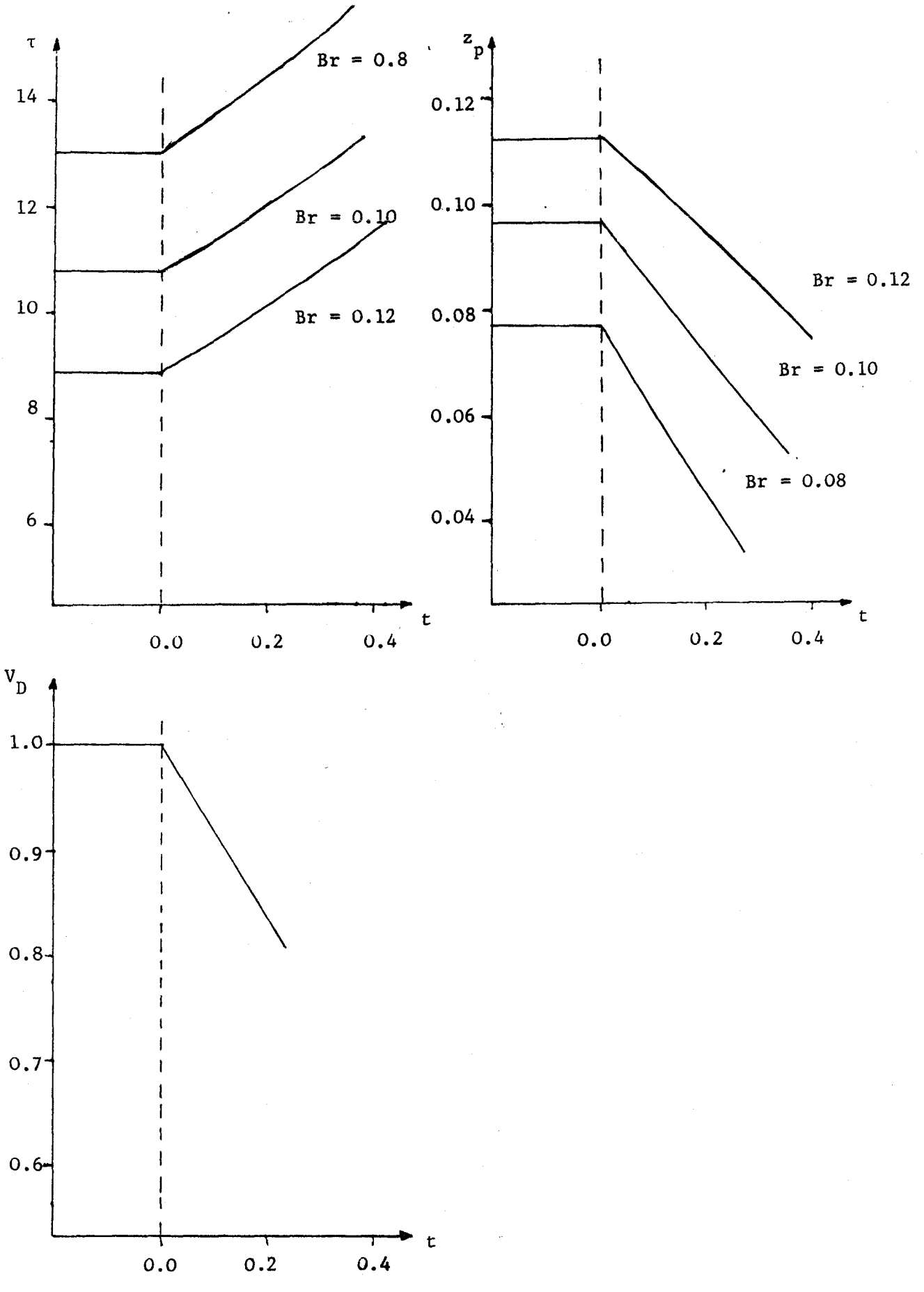

Figure 4.26 Graphs of (a) τ , (b) z_p and (c) V_D for the deceleration phase.

4.16 Inertia-Welding

So far in this chapter we have considered phases II, III and IV of the conventional friction welding process. In this section we consider the inertial friction welding process in which phases II, III and IV are consolidated into one phase [See Figure 1.4].

In the inertia welding process one of the components is held in the stationary tailstock chuck while the other is held in the headstock chuck which is attached to a flywheel. The flywheel is given a known rotational speed thus storing a predetermined amount of energy. The drive to the flywheel is then disengaged and the two components brought together under an applied axial load, as in the conventional process. Rubbing at the weld interface then begins to take place. The energy stored in the flywheel is subsequently used to generate heat and a softened layer of material develops close to the weld interface as in the continuous drive process. As rubbing proceeds the speed of rotation decreases until eventually the rotating component comes to rest. The applied force is maintained until the weld is consolidated.

In this section a simple model is developed to describe this process and appropriate solutions are given.

4.16.1 Governing Equations and Boundary Conditions

Making all the assumptions of section 4.8 the governing equations of motion in the plastic region are given by (4.2.7) to (4.2.13), and the energy equations for the plastic and solid regions by (4.8.14) and (4.8.15), respectively. The boundary conditions on the pressures and velocities are given by (4.2.14) to (4.2.18) apart from $(4.2.17)_2$

which must be amended since the velocity V on the interface $Z = Z_p(t)$ is now dependent on time. The manner in which this velocity varies is discussed in the following paragraph. The thermal boundary conditions are given by (4.2.23), (4.2.24), (4.2.25), (4.4.3) and (4.4.4).

Let the moment of inertia of the flywheel about the Z axis be I_f then the equation of motion governing this flywheel is

$$I_f \frac{d\omega_f}{d\bar{t}} = - T_q \tag{4.16.1}$$

where ω_f is the angular velocity of the flywheel and T_q is the resisted torque. Initially ω_f must have some prescribed value so we write

$$\omega_f(0) = \omega \tag{4.16.2}$$

For our 2-dimensional model the torque can be expressed in the form (see Chapter 3):

$$T_q = A\bar{R}\bar{\tau}(\bar{t}) \tag{4.16.3}$$

where A is the cross-sectional area of the tubes, $\bar{R}$ is the mean radius and $\bar{\tau}$ is the shear stress acting on the face $\bar{x}_3 = \bar{z}_p(\bar{t})$ in the $\bar{x}_2$ direction. i.e. $\bar{\tau} = \sigma_{yz}\big|_{\bar{x}_3=\bar{z}_p(\bar{t})}$ (see Chapter 3). Multiplying equation (4.16.3) by $\bar{R}$ and substituting (4.16.1) for T_q yields

$$I_f \frac{d\bar{V}_f}{d\bar{t}} = - A\bar{R}^2 \bar{\tau}(\bar{t}) \tag{4.16.4}$$

where V_f is the velocity component of the solid region in the y-direction given by

$$\bar{V}_f = \omega_f \bar{R} \quad . \tag{4.16.5}$$

Expressing (4.16.4) in terms of dimensionless variables we have

$$\frac{dV_f}{dt} = - \Delta\tau(t) \tag{4.16.6}$$

where t, V_f, Δ and τ are defined by

$$t = \frac{\bar{t}}{t_o} \ , \ V_f = \bar{V}_f/\omega\bar{R} \ , \ \Delta = \frac{A\bar{R}^2\mu_o t_o}{I_f Z_{po}} \quad , \quad \tau = \frac{\bar{\tau}}{(\mu_o \omega \bar{R}/Z_{po})} \tag{4.16.7}$$

where t_o is a typical weld time and μ_o and Z_{po} are defined as in Chpater 3. The dimensionless form of the initial condition (4.16.2) is

$$V_f(0) = 1 \tag{4.16.8}$$

Integrating equation (4.16.6) with respect to t and making use of condition (4.16.8) leads to the expression

$$V_f = 1 - \Delta \int_0^t \tau \, dt \tag{4.16.9}$$

Hence, the boundary condition $(4.2.17)_2$ must, for the case of inertial welding, be replaced by

$$V_f = 1 - \Delta \int_0^t \tau \, dt \quad \text{on} \quad Z = Z_p \tag{4.16.10}$$

We shall now determine a simple solution for inertia welding through the heat balance integral method, which was used extensively in Section 4.8.

4.16.2 Pressure, Velocity and Temperature Profiles

The equations and boundary conditions governing the pressures are identical to those in Section 4.7 the solutions are thus given by (4.7.1) and (4.7.22) and need no further discussion. Similarly the velocity components U,V and W are given by (4.7.15),(4.7.2) and (4.7.14) respectively. However, the amended form of equation (4.7.3) obtained by using boundary condition (4.16.10) in (4.7.2) is

$$\tau Z_p = 1 - \Delta \int_0^t \tau \, dt \qquad (4.16.11)$$

Differentiating this equation with respect to t results in the ordinary differential equation

$$\tau \frac{dZ_p}{dt} + Z_p \frac{d\tau}{dt} = - \Delta\tau \; ; \qquad (4.16.12)$$

an equation connecting Z_p and τ .

Using the heat balance integral method to solve equations (4.8.14) and (4.8.15), as in Section 4.8, we obtain a further two ordinary differential equations connecting a_2, Z_p and τ , namely

$$2a_2 + Br\tau^2 Z_p^2 = - \frac{2}{3F_0} Z_p^2 \frac{da_2}{dt} - \frac{2a_2}{3F_0} Z_p \frac{dZ_p}{dt} - \frac{4}{5} Pe Z_p a_2 \qquad (4.16.13)$$

and

$$-2a_2 = Pe Z_p - \frac{Z_p^2}{3F_0} \frac{d}{dt}\left(\frac{1}{a_2}\right) + \frac{Z_p}{F_0}\left(1 - \frac{1}{3a_2}\right) \frac{dZ_p}{dt} \quad , \qquad (4.16.14)$$

where it has again been assumed that the temperature profiles for θ and θ_s are given by (4.8.35) and (4.8.47) respectively. Equation (4.16.14) is, of course, identical to (4.8.48) and (4.16.13) is obtained from (4.8.36) by replacing Br by $BrZ_p^2\tau^2$. Again a numerical solution to equations (4.16.12), (4.16.13) and (4.16.14) for Z_p a_2 and τ is sought, and a small time series is required to obtain starting values. For the starting values it proves sufficient to use the representations

$$a_2 = a_{20} , \tag{4.16.15}$$

$$Z_p = 2\, Z_1 \sqrt{F_0 t} , \tag{4.16.16}$$

$$\tau = 1/Z_p . \tag{4.16.17}$$

and a sufficiently small value of t, where a_{20} is the -ve solution of (4.8.63) and Z_1 is given by (4.8.62).

The solutions must be terminated after a time t_f when V_f has reached zero - no steady state solution to the set (4.16.12), (4.16.13) and (4.16.14) exists. With the aid of (4.16. 9) and (4.16.11) we see that t_f is given by

$$Z_p(t_f)\, \tau(t_f) = 0 . \tag{4.16.18}$$

4.16.3 Results and Discussion

Equations (4.16.12), (4.16.13) and (4.16.14) were solved using the Runge-Kutta process. Using these results the interface temperature $\theta(0,t)$ and the rubbing velocity V_f were obtained using the relationships

$$\theta(0,t) = 1 - a_2 \qquad (4.16.19)$$

and

$$V_f = \tau Z_p \qquad (4.16.20)$$

respectively. These results are illustrated for the case $\Delta = 0.2$ in Figures 4.27 to 4.30.

Comparing the plots of shear stress τ given in Figures 4.27(a) and 4.29(a) with the idealised torque trace in Figure 1.4. we note that the main qualitative feature of this trace, the two torque peaks, is predicted by our model. However comparison of the plots in Figures 4.28(b) and 4.30(b) for the rubbing speed V_f with the corresponding idealised trace in Figure 1.4 indicates that for small times a much faster decay of V_f is predicted by our model than is found in practice. This is felt to be a consequence of the initial singularity in the shear stress τ which leads to a much higher resistive force to the rubbing motion during the early moments of the weld time.
For later times it is noted that the qualitative agreement between the two decay rates of V_f is much improved. Examination of the plots of interface temperature against t shown in Figures 4.27(b) and 4.29(b) reveals that this temperature has its maximum at $t = 0$ and then decays until it reaches the conditioning temperature at time t_f. In practice, however, the interface temperature rises rapidly during the initial stages of the process until it attains its maximum, after which it decreases as the speed of rotation reduces to zero. Moreover in reality the temperature does not fall to the conditioning temperature; if this were so there would be no plastic region at the end of the frictioning stage and the specimens could not be forged together.

The error in the interface temperature for the early stages of the process predicted by our model is due to the omission of the conditioning phase as was pointed out in Section 4.13 for the continuous drive process. The reason our model predicts a lower than expected temperature at the end of the frictioning stage is felt to be due to our definition of the plastic region. The position of the plastic region is governed by the condition $\theta = 1$ on $Z = Z_p(t)$. As the rotation slows down the rate of heat generation falls and consequently the thickness of the plastic region decreases. This process continues until eventually at $t = t_f$ Z_p reaches 0 and then, by definition, the interface assumes the temperature $\theta = 1$.

4.17 Comparison with Experimental Results

The main purpose of this thesis has been to produce simple mathematical models which describe the friction welding process qualitatively. However, in this section we present, for completeness, a quantitative comparison between experimental data and the theory.

At Marchwood Engineering Laboratories a series of friction welds were made using tubes of 12 mm outer radius and 3 mm wall thickness. In Figure 4.31 a typical trace of the output, from one of these welds, of torque, applied load, speed and axial shortening is given.

In order to make a comparison between the models and experimental data the mean line from the torque trace is taken and compared with torques from the constant viscosity model of Section 4.8. Results for the case $Pe = 0.6$ and several values of Br are presented in Figure 4.32.

This brief comparison demonstrates that the agreement between the theoretical solutions and experimental results is quite good. However, before any comparison is made in depth it is felt that a much sounder knowledge of material properties, particularly viscosity, in the range $700^{o}C < T < 1300^{o}C$ is required.

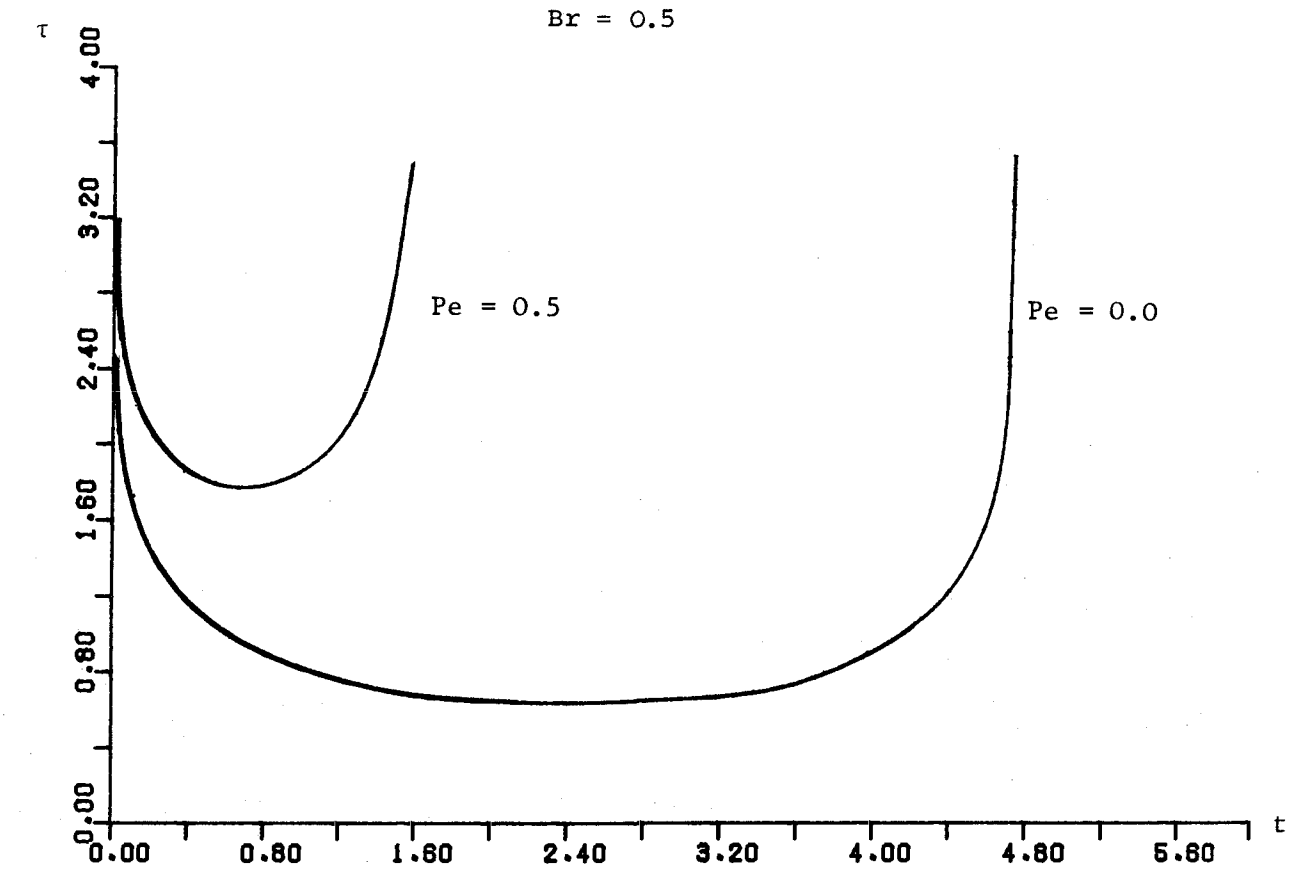

(a)

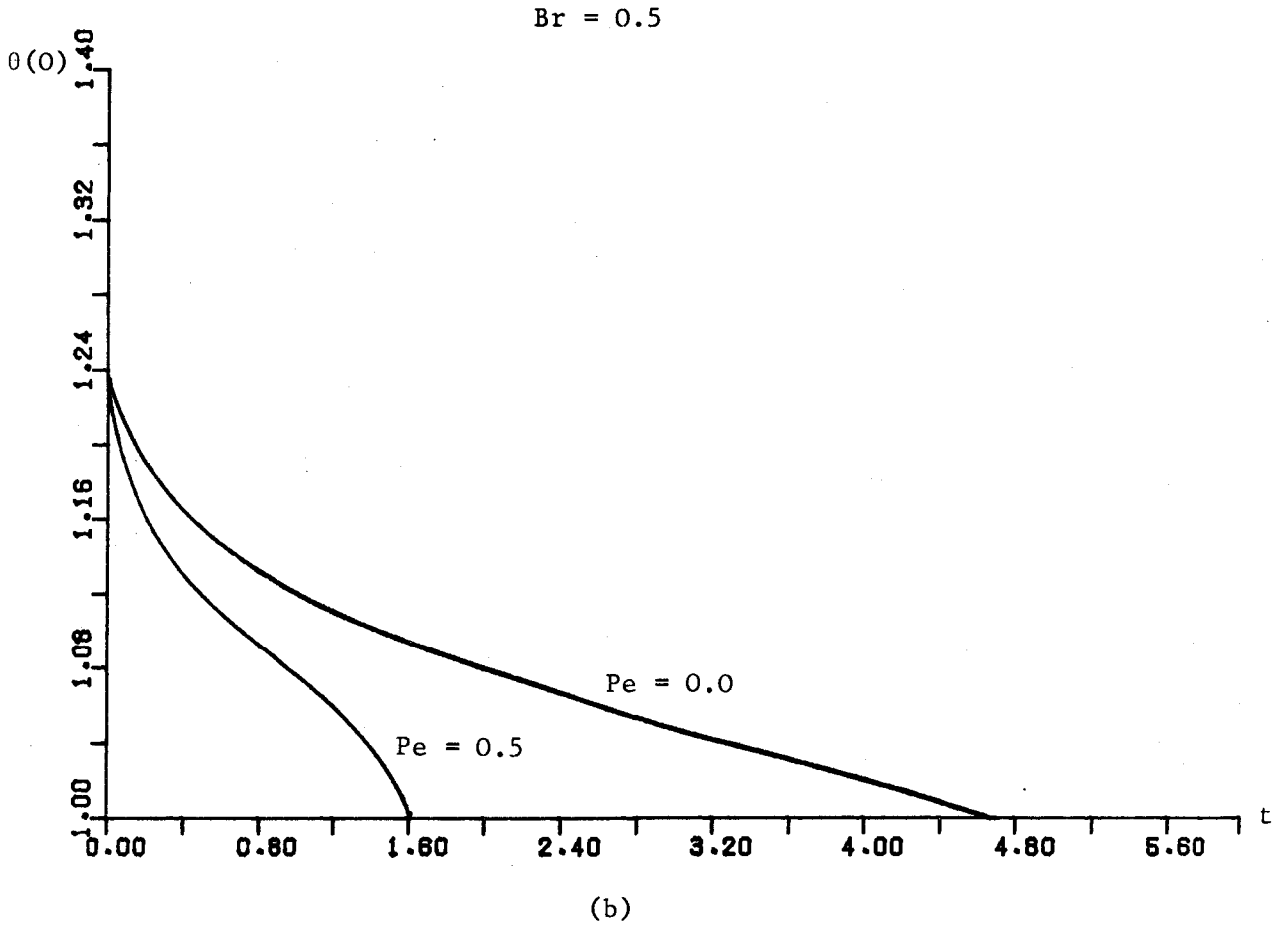

(b)

Figure 4.27 Graphs of τ and $\theta(0)$ against t for the inertial welding process.

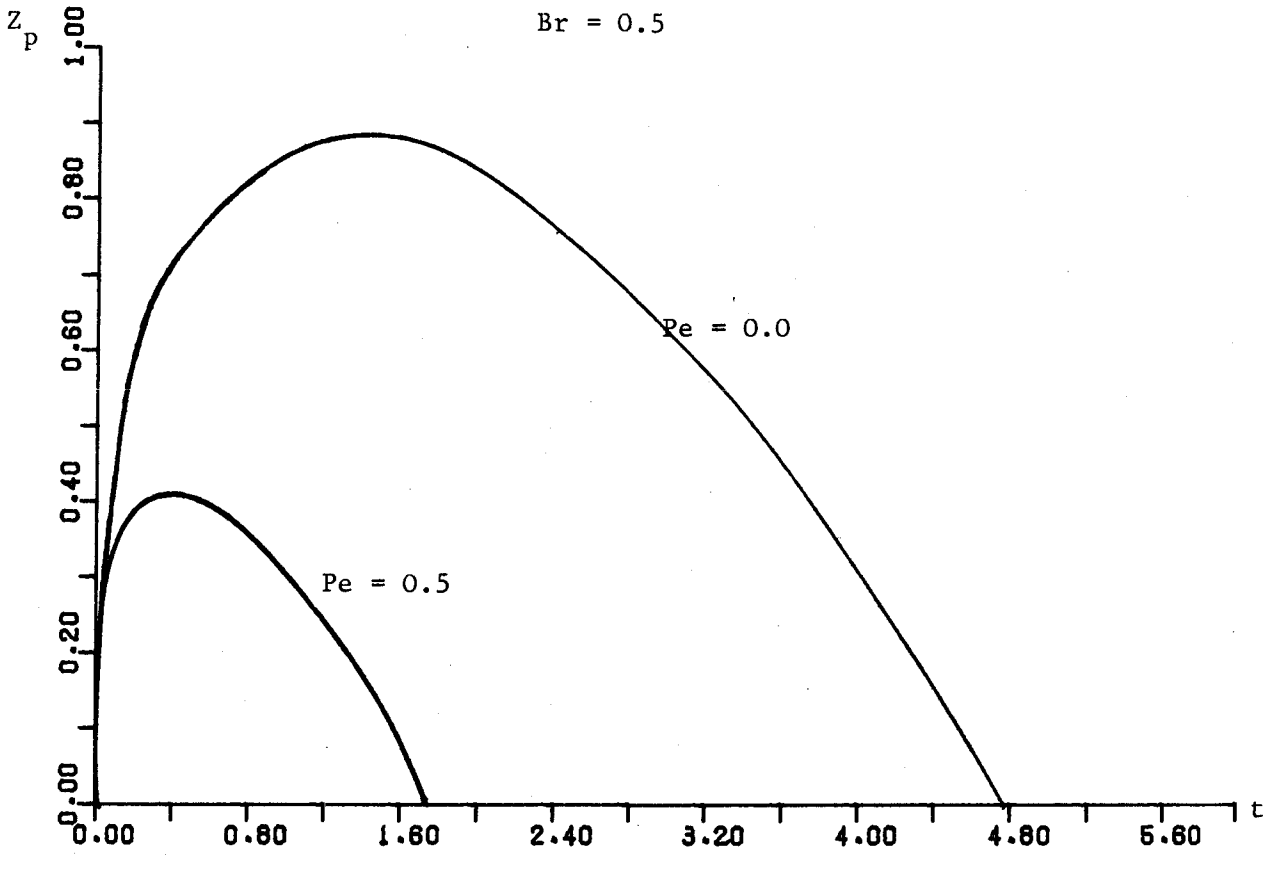

(a)

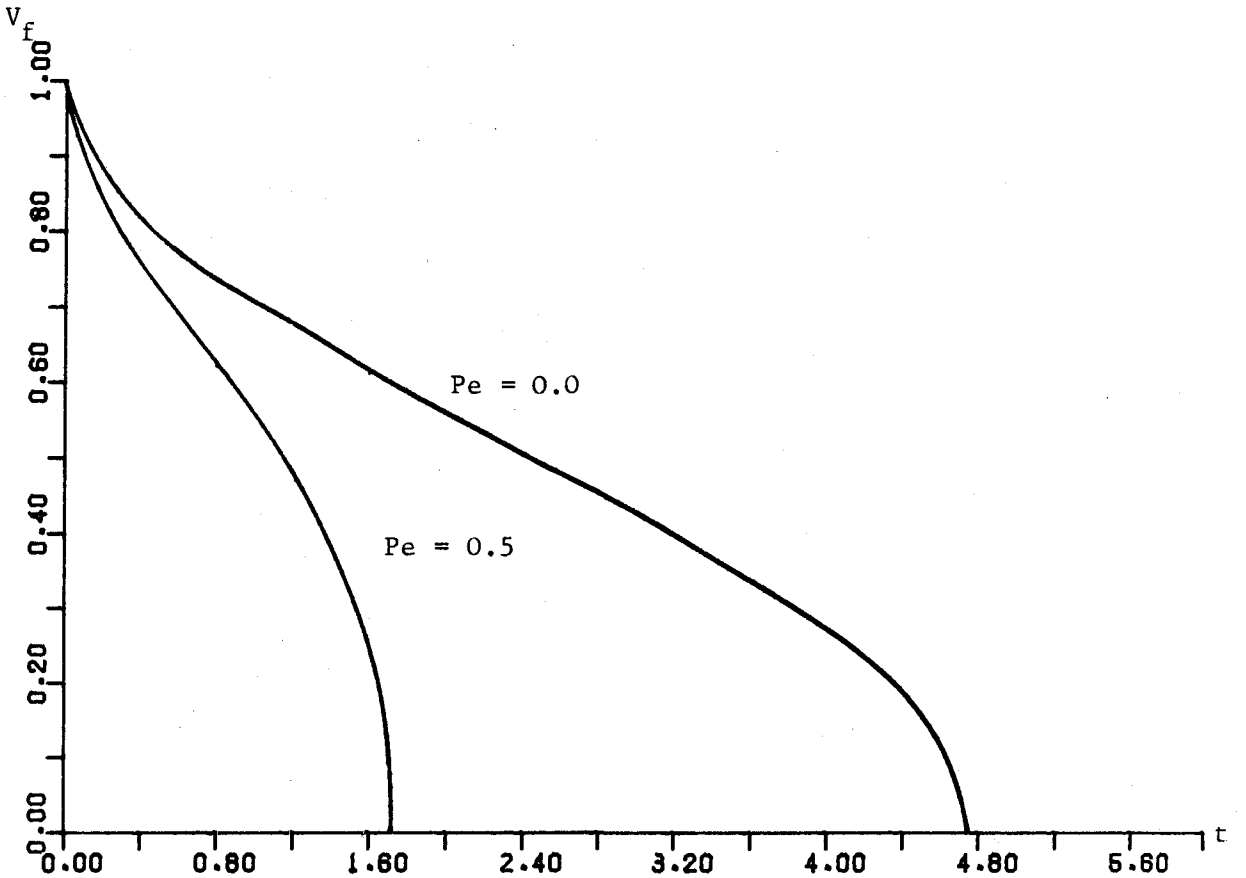

(b)

Figure 4.28 Graphs of Z_p and V_f against t for the inertial welding process.

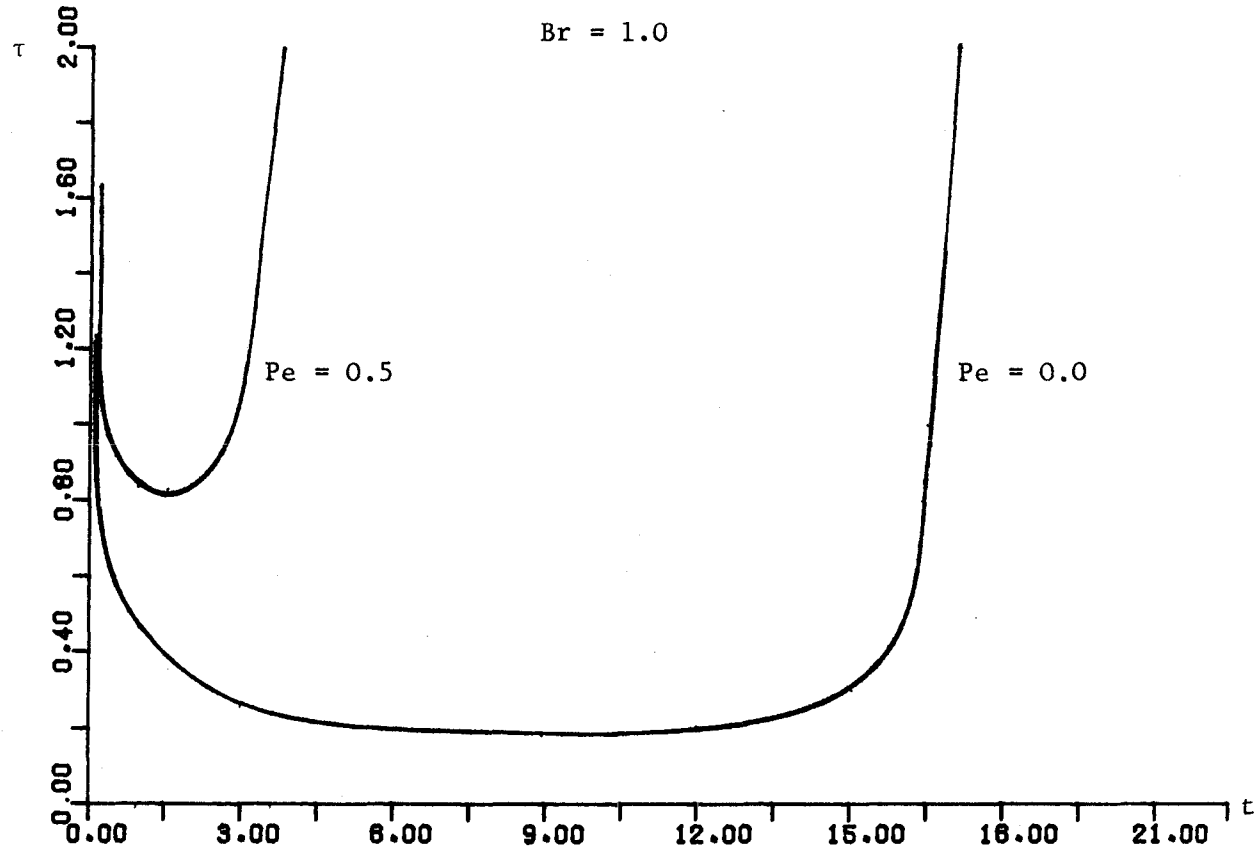

(a)

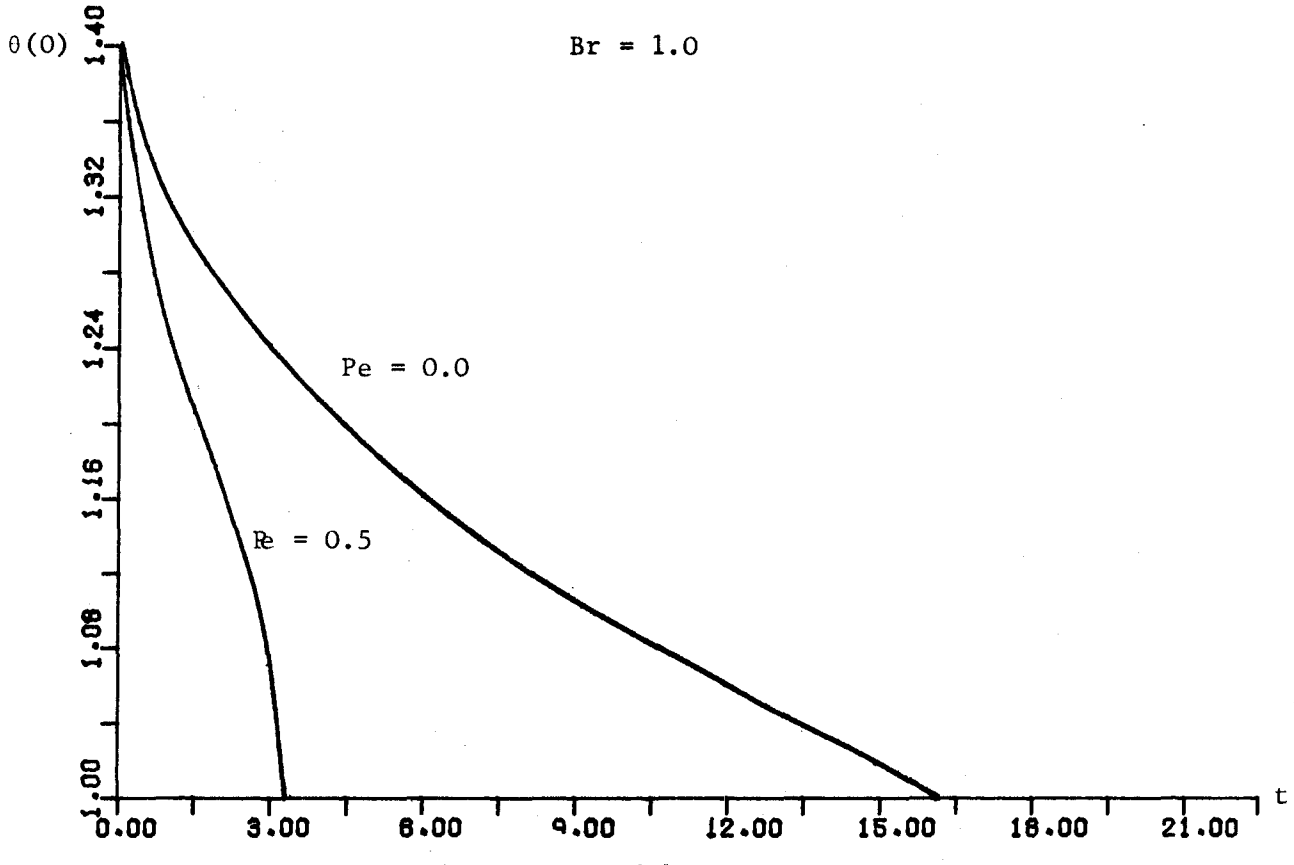

(b)

Figure 4.29 Graphs of τ and $\theta(0)$ against t for the inertial welding process.

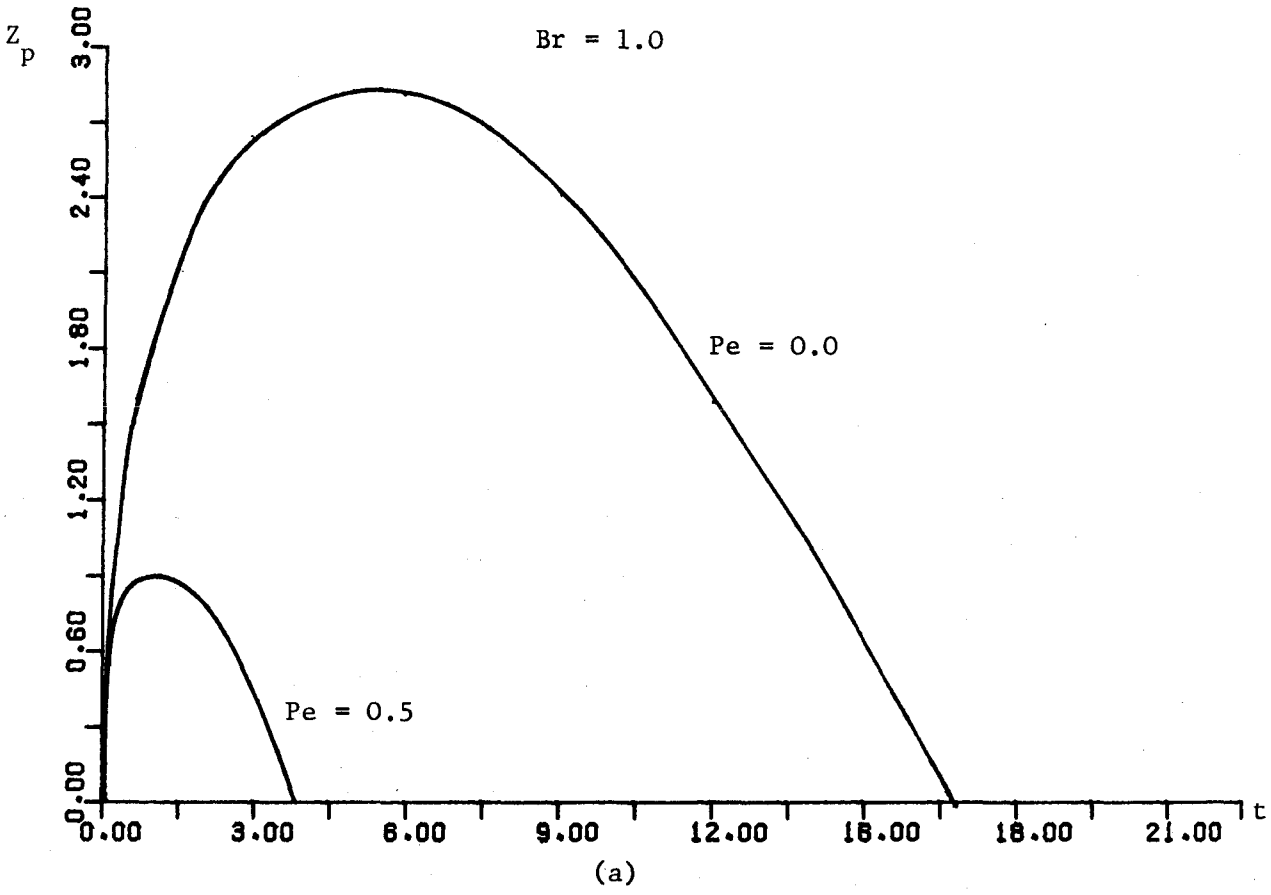

(a)

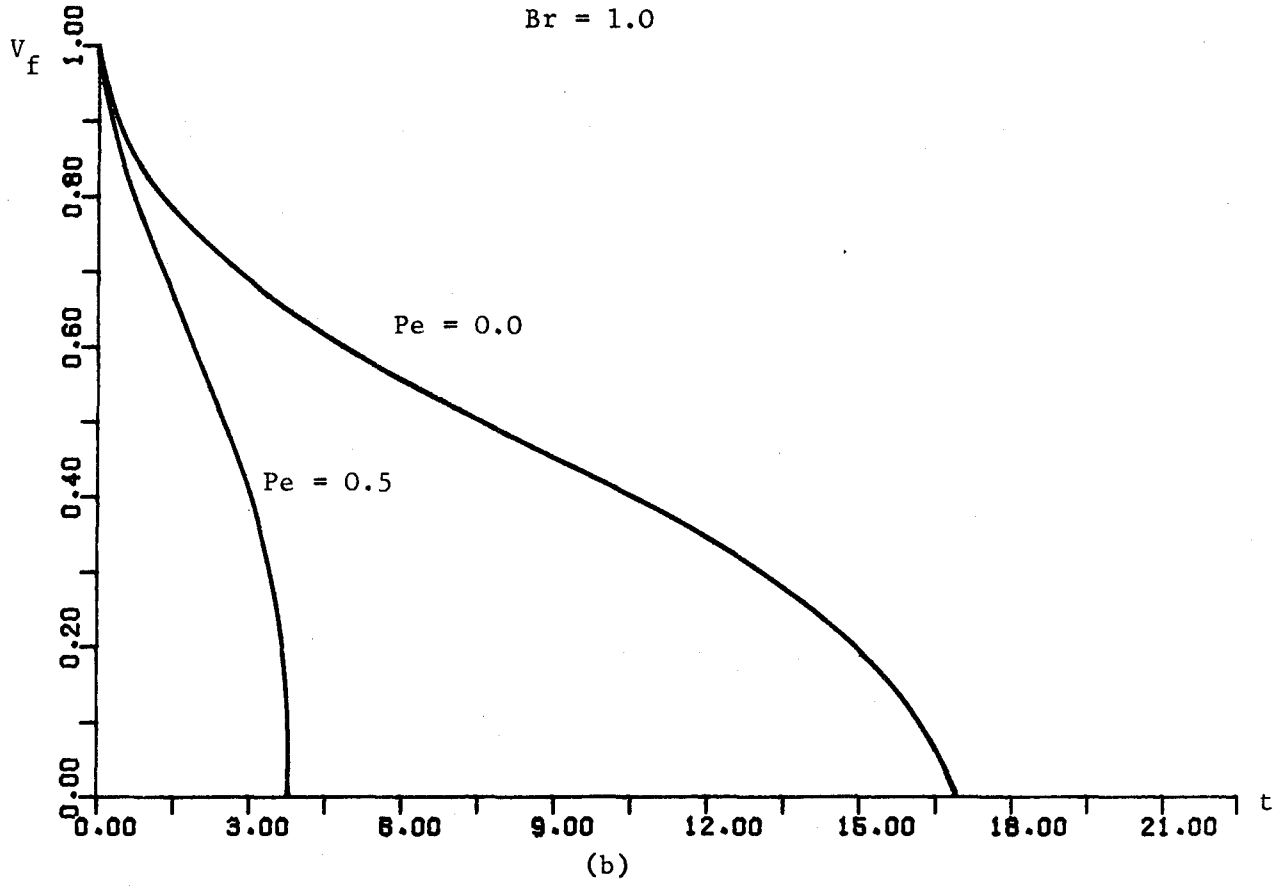

(b)

Figure 4.30 Graphs of Z_p and V_f against t for the inertial welding process.

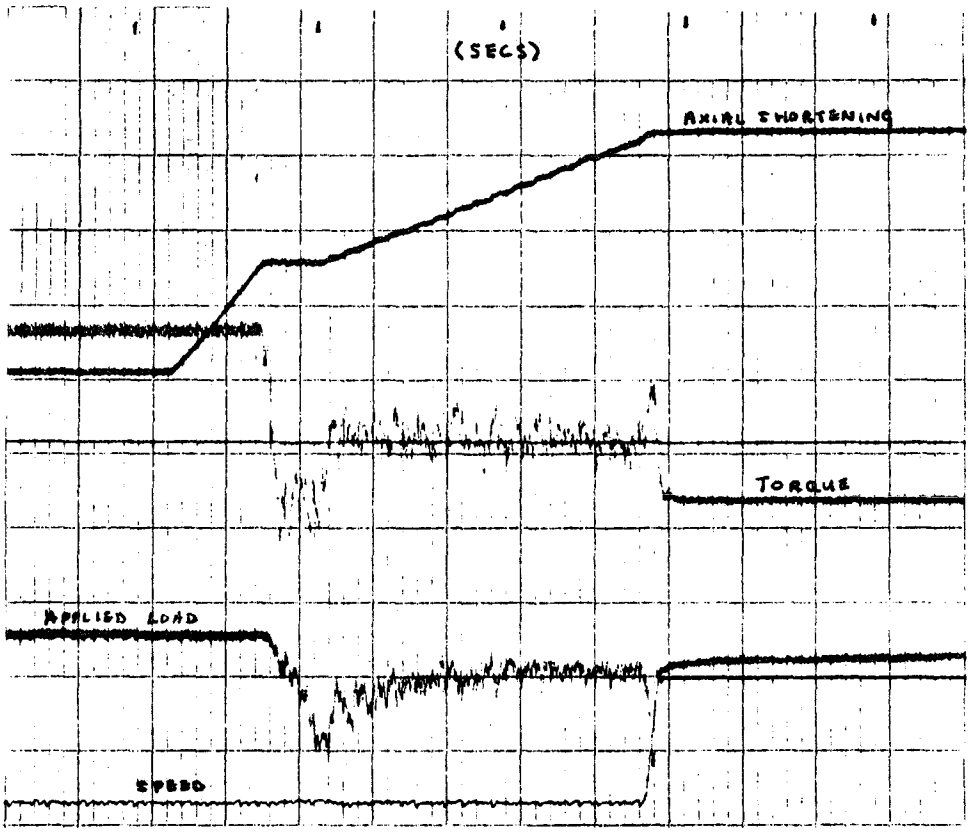

Figure 4.31 Experimental traces of torque, applied load and axial shortening.

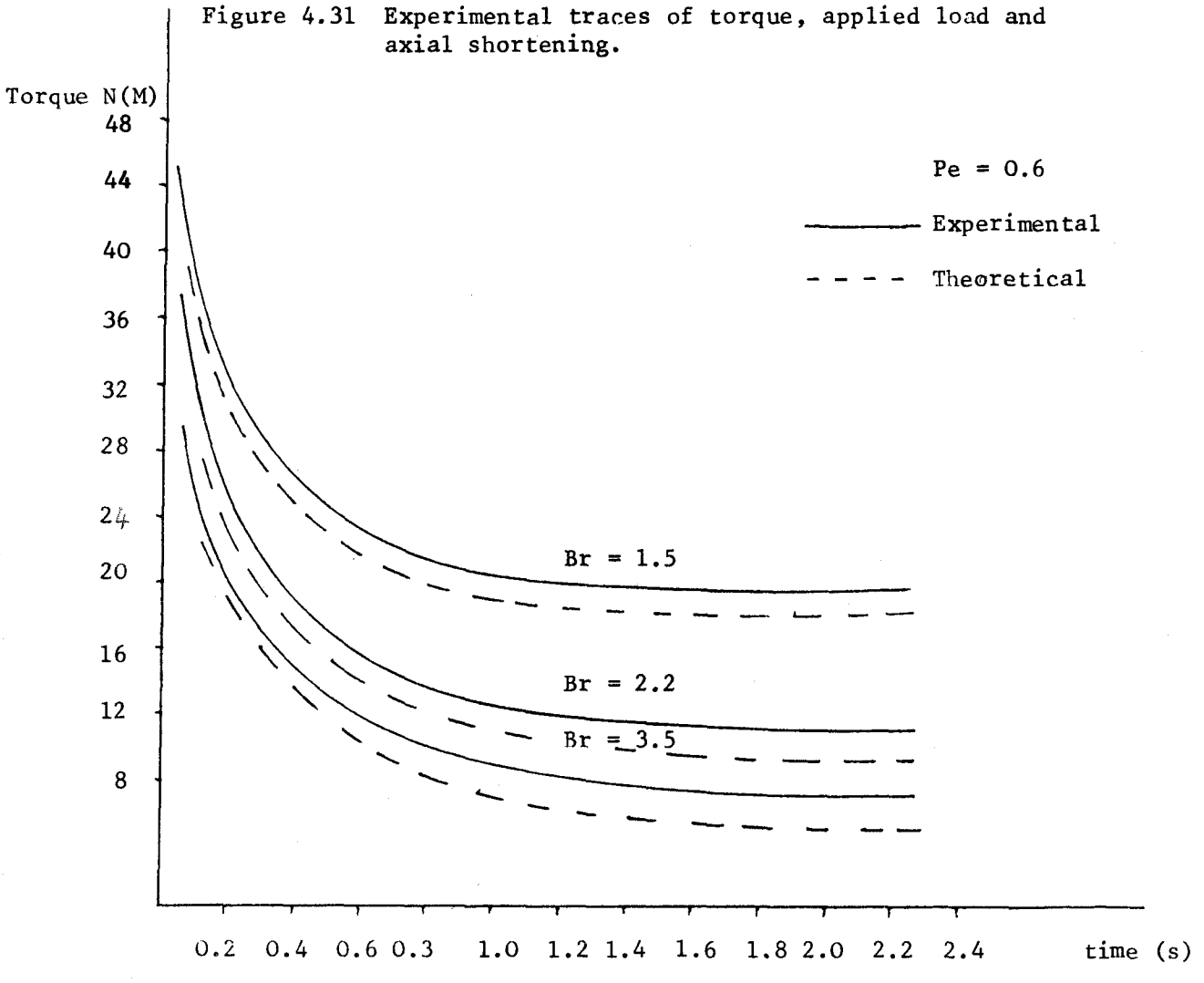

Figure 4.32 Comparison between experiment and theory.

CHAPTER 5

BINGHAM SUBSTANCE MODELS

In this chapter some of the simpler models of Chapter 4 are reconsidered when the plastic region is modelled by a Bingham substance. Here it is again assumed that the temperature profiles θ and θ_s and the velocity components V and W are independent of x. It is also assumed throughout this chapter that the viscosity μ is constant and taken to be unity for convenience. Both phase II and the equilibrium phase are considered here and we again neglect the effect of the conditioning phase.

5.1 Governing equations and boundary conditions

Making use of the above assumptions and splitting the governing equations of motion (3.4.28) to (3.4.30) into two subsystems, one of $O(CpRe)$ and the other of $O(1)$, the latter become

$$O(CpRe) \quad \frac{\partial P_o}{\partial x} = 0 , \tag{5.1.1}$$

$$\frac{\partial P_o}{\partial z} = 0 , \tag{5.1.2}$$

$$O(1) \quad \frac{1}{2}\frac{\partial P_1}{\partial x} = \beta^2 \frac{\partial}{\partial z}\left[\left(1 + \frac{B\sigma_o}{2\sqrt{I}}\right)\frac{\partial u}{\partial z}\right] + 2\frac{\partial}{\partial x}\left[\left(1 + \frac{B\sigma_o}{2\sqrt{I}}\right)\frac{\partial u}{\partial x}\right] , \tag{5.1.3}$$

$$\frac{\partial}{\partial z}\left[\left(1 + \frac{B\sigma_o}{2\sqrt{I}}\right)\frac{\partial V}{\partial z}\right] = 0 , \tag{5.1.4}$$

$$\frac{1}{2}\frac{\partial P_1}{\partial z} = 2\frac{\partial}{\partial z}\left[\left(1 + \frac{B\sigma_o}{2\sqrt{I}}\right)\frac{\partial w}{\partial z}\right] + \frac{\partial}{\partial x}\left[\left(1 + \frac{B\sigma_o}{2\sqrt{I}}\right)\frac{\partial u}{\partial z}\right] , \qquad (5.1.5)$$

where the second invariant of the rate of strain tensor I is given by

$$I = \left(\frac{\partial V}{\partial z}\right)^2 \qquad (5.1.6)$$

The equation of incompressibility (3.4.31), rewritten here for convenience is

$$\frac{\partial u}{\partial x} + \frac{\partial w}{\partial z} = 0 \qquad (5.1.7)$$

Again making the further assumption that the thermal properties k, k_s, C_v and C_{vs} are constant and conveniently taken to be unity and that superficial heat loss may be neglected, the energy equations for the plastic and solid regions, (3.4.37) and (3.4.40) respectively, reduce to

$$\frac{\partial^2\theta}{\partial z^2} + Br\left[1 + \frac{B\sigma_o}{2\sqrt{I}}\right]\left(\frac{\partial V}{\partial z}\right)^2 = Pew\frac{\partial\theta}{\partial z} + \frac{1}{Fo}\frac{\partial\theta}{\partial t} , \quad 0 \leq z \leq z_p(t) , \qquad (5.1.8)$$

and

$$\frac{\partial^2\theta_s}{\partial z^2} = -PeWo(t)\frac{\partial\theta_s}{\partial z} + \frac{1}{Fo}\frac{\partial\theta_s}{\partial t} , \quad z \geq z_p(t) . \qquad (5.1.9)$$

On splitting the condition (3.5.18) into two subsystems one $O(CpRe)$ and the other $O(1)$, the pressures P_o and P_1 must satisfy the pair of conditions

$$O(CpRe) \int_{-\frac{1}{2}}^{\frac{1}{2}} P_o(x, z_p, t)dx = 1 , \qquad (5.1.10)$$

and

$$O(1) \int_{-\frac{1}{2}}^{\frac{1}{2}} P_1(x, z_p, t) - 4\left(1 + \frac{B\sigma_o}{2\sqrt{I}}\right)\left.\frac{\partial w}{\partial z}\right|_{z=z_p(t)} dx = 0 . \qquad (5.1.11)$$

The conditions on the velocity component are given by (4.2.16) to (4.2.18) and are rewritten here

$$\frac{\partial u}{\partial z}(x,0,t) = 0, \; -\frac{1}{2} \leq x \leq \frac{1}{2} \; ; \; v(0,t) = 0 \; , \; w(0,t) = 0 \; , \qquad (5.1.12)$$

$$u(x,z_p,t) = 0, \; -\frac{1}{2} \leq x \leq \frac{1}{2} \; ; \; v(z_p,t) = 1, \; w(z_p,t) = -w_o(t), \qquad (5.1.13)$$

and

$$u(0,z,t) = 0 \; , \quad 0 \leq z \leq z_p(t) \qquad (5.1.14)$$

Under the present assumptions the thermal boundary conditions are

$$\frac{\partial \theta}{\partial z}(0,t) = 0 \; , \qquad (5.1.15)$$

$$\theta(z_p,t) = \theta_s(z_p,t) \; , \qquad (5.1.16)$$

$$\frac{\partial \theta}{\partial z}(z_p,t) = \frac{\partial \theta_s}{\partial z}(z_p, t) \qquad (5.1.17)$$

and

$$\theta_s(z,t) \to 0 \quad \text{as} \quad z \to \infty \; , \qquad (5.1.18)$$

and remembering that the conditioning phase is again neglected, the initial condition is

$$\theta_s(z,0) = 0 \ . \tag{5.1.19}$$

These conditions are identical to those for the viscous fluid model (4.2.23), (4.2.24), (4.2.25), (4.4.3) and (4.4.4) apart from the temperatures on the plastic/solid interface is no longer specified as unity. The position of z_p must now be defined by the Bingham yield criterion (3.5.7) which is rewritten here for convenience

$$\left[1 + \frac{B\sigma_o}{2\sqrt{I}}(\theta,t)\right]^2 I = \frac{\sigma_o^2 B^2}{4} \quad \text{on} \quad z = z_p(t) \ . \tag{5.1.20}$$

With the aid of (5.1.6) the above can be expressed in the form

$$\frac{\partial v}{\partial z}\left[\frac{\partial v}{\partial z} + B\sigma_o\right] = 0 \quad \text{on} \quad z = z_p(t) \tag{5.1.21}$$

Noting that the velocity gradient $\frac{\partial v}{\partial z}$ cannot be negative, this condition reduces to

$$\frac{\partial v}{\partial z} = 0 \quad \text{on} \quad z = z_p(t) \tag{5.1.22}$$

Having now obtained this simplified form of the basic equations a few of the models considered in Chapter 4 are now examined for the case with the plastic region modelled by a Bingham Substance.

5.2 Velocity and pressure profiles

The solution to (5.1.1) and (5.1.2) subject to (5.1.10) was as given in Section 4.3 and requires no further discussion.

Substituting (5.1.6) into (5.1.4) gives us

$$\frac{\partial}{\partial z}\left[\frac{\partial v}{\partial z} + \frac{B\sigma_o}{2}\right] = 0 \qquad (5.2.1)$$

Integrating this equation with respect to z yields

$$\frac{\partial v}{\partial z} = \tau(t) - \frac{B\sigma_o}{2} \qquad (5.2.2)$$

where τ is the dimensionless shear stress, and a further integration with respect to z results in

$$v = \tau(t)z - \int_o^z \frac{B\sigma_o}{2}(\theta,t)dz \ , \qquad (5.2.3)$$

which satisfies the condition $(5.1.12)_2$. In order that the condition $(5.1.13)_2$ is satisifed, z_p must be related to τ through

$$1 = z_p\tau - \frac{B}{2}\int_o^{z_p} \sigma_o(\theta,t)dz \ . \qquad (5.2.4)$$

With the aid of equations (5.1.6) and (5.2.2), the pair of partial differential equations (5.1.3) and (5.1.5) can be expressed in the forms

$$\frac{1}{2}\frac{\partial P_1}{\partial x} = 2\tau\beta^2 \frac{\partial}{\partial z}\left(\frac{1}{\tau^*}\frac{\partial u}{\partial z}\right) + 4\tau \frac{\partial}{\partial x}\left(\frac{1}{\tau^*}\frac{\partial u}{\partial x}\right) \qquad (5.2.5)$$

and

$$\frac{1}{2}\frac{\partial P_1}{\partial z} = 4\tau\,\frac{\partial}{\partial z}\left(\frac{1}{\tau^*}\frac{\partial w}{\partial z}\right) + 2\tau\,\frac{\partial}{\partial x}\left(\frac{1}{\tau^*}\frac{\partial u}{\partial z}\right), \tag{5.2.6}$$

where the quantity τ^* is defined by

$$\tau^*(\theta,t) = 2\tau(t) - B\sigma_o(\theta,t) . \tag{5.2.7}$$

Integrating the equation of incompressibility (5.1.7) with respect to x yields

$$u = -x\,\frac{\partial w}{\partial z} + f(z,\,t) \tag{5.2.8}$$

where f is an arbitrary function of z and t and on using the boundary condition (5.1.14) it is obvious that this function must be identically zero and we write

$$u = -x\,\frac{\partial w}{\partial z} . \tag{5.2.9}$$

Substituting this expression into (5.2.5) and (5.2.6) leads to, after some rearrangement

$$\frac{1}{4}\frac{\partial P_1}{\partial x} = -\beta^2 x\tau\,\frac{\partial}{\partial z}\left(\frac{1}{\tau^*}\frac{\partial^2 w}{\partial z^2}\right) \tag{5.2.10}$$

and

$$\frac{1}{4}\frac{\partial P_1}{\partial z} = \frac{\tau}{\tau^*}\frac{\partial^2 w}{\partial z^2} + 2\tau\,\frac{\partial w}{\partial z}\,\frac{\partial}{\partial z}\left(\frac{1}{\tau^*}\right) . \tag{5.2.11}$$

Integrating (5.2.10) with respect to x yields

$$\frac{P_1}{2} = -\beta^2 x^2 \tau\,\frac{\partial}{\partial z}\left(\frac{1}{\tau^*}\frac{\partial^2 w}{\partial z^2}\right) + g(z,t) \tag{5.2.12}$$

where g is an arbitrary function of z and t.

On differentiating both sides of this expression with respect to z and using (5.2.12) to eliminate $\partial P_1/\partial z$ from the resulting equation leads to, after some rearrangement, the identity

$$\frac{2\tau}{\tau^*}\frac{\partial^2 w}{\partial z^2} + 4\tau\frac{\partial w}{\partial z}\frac{\partial}{\partial z}\left(\frac{1}{\tau^*}\right) \equiv -\tau\beta^2 x^2\frac{\partial^2}{\partial z^2}\left(\frac{1}{\tau^*}\frac{\partial^2 w}{\partial z^2}\right) + \frac{\partial g}{\partial z} \qquad (5.2.13)$$

Since the above holds for all x in $\left(-\frac{1}{2}, \frac{1}{2}\right)$ the functions w, σ_o and g, which are all independent of x must necessarily satisfy the equations

$$\frac{\partial^2}{\partial z^2}\left(\frac{1}{\tau^*}\frac{\partial^2 w}{\partial z^2}\right) = 0 \qquad (5.2.14)$$

and

$$\frac{2\tau}{\tau^*}\frac{\partial^2 w}{\partial z^2} + 4\tau\frac{\partial w}{\partial z}\frac{\partial}{\partial z}\left(\frac{1}{\tau^*}\right) = \frac{\partial g}{\partial z} \quad . \qquad (5.2.15)$$

Repeated integration of equation (5.2.14) with respect to z yields

$$W = \int_o^z\int_o^\ell \tau^*\left(\theta(k,t),t\right)\left[C_o(t)k + C_1(t)\right]dkd\ell + C_2(t)z + C_3(t) \quad , \qquad (5.2.16)$$

where C_o, C_1, C_2 and C_3 are arbitrary functions of t only. The velocity component u is now obtained by substituting the above expression for w into (5.2.9) yielding

$$u = -x\left[\int_o^z \tau^*\left(\theta(k,t),t\right)\left[C_o(t)k + C_1(t)\right]dk + C_2(t)z\right] \qquad (5.2.17)$$

Using the boundary conditions $(5.1.12)_{1\ 3}$ and $(5.1.13)_1$ the functions C_1, C_2 and C_3 are readily expressed in terms of C_o leading to the expressions

$$W = C_o \int_o^z \int_{z_p}^{\ell} \tau^*\left(\theta(k,t),t\right) k dk d\ell \qquad (5..218)$$

and

$$u = - C_o x \int_{z_p}^{z} \tau^*\left(\theta(k,t),t\right) k dk \ . \qquad (5.2.19)$$

Again the assumption is made that the upset velocity w_o is constant and taken to be unity for convenience, thus we write

$$w_o = 1 \ . \qquad (5.2.20)$$

On using condition $(5.1.13)_3$ in expression (5.2.13) C_o is found to be, in view of (5.2.20)

$$C_o = -1 \Big/ \int_o^{z_p} \int_{z_p}^{\ell} \tau^*\left(\theta(k,t),t\right) k dk d\ell \ . \qquad (5.2.21)$$

Having determined the velocity component u,v and w we turn our attention to the pressure component p_1 . Substituting (5.2.18) into (5.2.15) gives us

$$\frac{\partial g}{\partial z} = 2\tau C_o z + 4\tau C_o \frac{\partial}{\partial z}\left(\frac{1}{\tau^*}\right) \int_{z_p}^{z} \tau^*\left(\theta(k,t),t\right) k dk \ . \qquad (5.2.22)$$

Integrating the above with respect to z yields

$$g = \tau C_o z^2 + 4\tau C_o \int_o^z \int_{z_p}^{\ell} \tau^* k dk \frac{\partial}{\partial \ell}\left(\frac{1}{\tau^*}\right) d\ell + e(t) \qquad (5.2.23)$$

where e is an arbitrary function of t introduced through the integration. On substituting equation (5.2.23) into (5.2.12) the function $e(t)$ is obtained by using the boundary condition (5.1.12), the resulting expression for P_1 is then given by

$$P_1 = 2\tau C_o\left[(z^2 - z_p^2) + \beta^2\left(\frac{1}{12} - x^2\right)\right] + 8C_o\tau \int_o^z \int_{z_p}^{\ell} \tau^* k dk \frac{\partial}{\partial \ell}\left(\frac{1}{\tau^*}\right) d\ell \; . \qquad (5.2.24)$$

Thus for our Bingham substance model the velocity component u, v and w are given by equations (5.2.19), (5.2.3) and (5.2.18) respectively and the pressure P_1 by (5.2.24). However, the integrals which appear in these equations cannot be evaluated until σ_o and hence τ^* are known as functions of z and t. As we have stated σ_o is in general a function of the temperature θ and t, thus it will be again necessary to solve the above mentioned equations simultaneously with the energy equations.

5.3 The energy equations and thermal boundary conditions

On substituting equations (5.2.3), and (5.2.18), for the velocity components v and w respectively, into equation (5.1.8), the energy equation for the plastic region becomes, with the aid of (5.1.6) and (5.2.7)

$$\frac{\partial^2\theta}{\partial z^2} + \frac{Br}{2}\tau\tau^* = PeC_o \int_o^z \int_{z_p}^{\ell} \tau^*\big(\theta(k,t),t\big)\,k\,dk\,d\ell \,\frac{\partial\theta}{\partial z} + \frac{1}{Fo}\frac{\partial\theta}{\partial t}\ ,\quad 0 \leq z \leq z_p \tag{5.3.1}$$

Making use of assumption (5.2.20) the energy equation for the solid region (5.1.9) is again expressed in the form

$$\frac{\partial^2\theta_s}{\partial z^2} = -\,Pe\,\frac{\partial\theta_s}{\partial z} + \frac{1}{Fo}\frac{\partial\theta_s}{\partial t}\ ,\quad z \geq z_p(t) \tag{5.3.2}$$

The thermal boundary and initial conditions are given by (5.1.15) to (5.1.19) and on substituting the equation (5.2.2) into (5.1.21), the Bingham yield criterion which specifies the position of z_p may be expressed, recalling definition (5.2.7), as

$$\tau^* = 0 \quad \text{on} \quad z = z_p(t) \tag{5.3.3}$$

Before we can proceed any further, the yield stress σ_o must be expressed as a function of temperature θ and time t. During the equilibrium phase we shall follow Bahrani et al [18] and assume a linear relationship between σ_o and θ of the form

$$\sigma_{o\infty}(\theta) = (1-\varepsilon\theta)/(1-\varepsilon)\ , \tag{5.3.4}$$

where ε is a constant obtained from experimental data. However the above expression cannot be used during phase II since, as is seen from equation (5.3.3), with the aid of definition (5.2.7), the asymptotic behaviour of σ_o for both large and small values of time must be proportional to that of the shear stress τ. It thus seems logical to assume a relationship between σ_o, θ and t of the form

$$\sigma_o = \frac{(1-\varepsilon\theta)}{(1-\varepsilon)}\,G(t)\ , \tag{5.3.5}$$

where the asymptotic behaviour of the function G is proportional to that of τ for both small and large values of time. In the following section a solution to the above system of equations is obtained using the heat balance method. Asymptotic solutions for small and large values of t are derived first from which a form for G is deduced. This form for G is then used throughout the chapter.

5.4 Heat balance integral solution

In this section a heat balance integral solution is given, similar to that of Section (4.8), which describes the phase II portion of the welding cycle, the plastic region being modelled by a Bingham substance.

Introducing the variable η defined by equation (4.8.25) into equations (5.3.1) and (5.3.2) leads to

$$\frac{\partial^2\theta}{\partial\eta^2} + \frac{Br}{2}\tau\tau^* z_p^2 = PeC_o z_p^4 \int_o^\eta \int_1^{\ell'} \tau^*\left(\theta(k',t),t\right)k'dk'd\ell'\frac{\partial\theta}{\partial\eta} + \frac{z_p^2}{Fo}\frac{\partial\theta}{\partial t} - \frac{z_p}{Fo}\frac{dz_p}{dt}\eta\frac{\partial\theta}{\partial\eta}\ ,\ 0 \leq \eta \leq 1 \qquad (5.4.1)$$

and

$$\frac{\partial^2\theta_s}{\partial\eta^2} = -Pez_p\frac{\partial\theta_s}{\partial\eta} + \frac{z_p^2}{Fo}\frac{\partial\theta_s}{\partial t} - \frac{z_p}{Fo}\frac{dz_p}{dt}\eta\frac{\partial\theta_s}{\partial\eta}\ ,\ \eta \geq 1 \qquad (5.4.2)$$

and the function $C_o(t)$ given by (5.2.21) may be expressed in terms of η

$$C_o = -1\Big/ z_p^3 \int_o^1 \int_1^{\ell'} \tau^*\left(\theta(k',t),t\right)k'dk'd\ell' \ . \qquad (5.4.3)$$

The equation connecting z_p and τ (5.2.4) becomes with the aid of (5.2.7)

$$2 = z_p \int_o^1 \tau^*\left(\theta(\eta,t),t\right)d\eta \tag{5.4.4}$$

and the boundary conditions transform to

$$\frac{\partial\theta}{\partial\eta}(0,t) = 0 \tag{5.4.5}$$

$$\theta(1,t) = \theta_s(1,t) \tag{5.4.6}$$

$$\frac{\partial\theta}{\partial\eta}(1,t) = \frac{\partial\theta_s}{\partial\eta}(1,t) \tag{5.4.7}$$

$$\theta_s(\eta,t) \to 0 \quad \text{as} \quad \eta \to \infty \tag{5.4.8}$$

and

$$\tau^* = 0 \quad \text{on} \quad \eta = 1 \tag{5.4.9}$$

Making use of definition (5.2.7) and substituting equation (5.3.5) into equation (5.4.1) and integrating the latter with respect to η between the limits $\eta = 0$ and $\eta = 1$, the heat balance integral for the plastic region is

$$\frac{\partial\theta}{\partial\eta}(1,t) - \frac{\partial\theta}{\partial\eta}(0,t) + \frac{Br\tau z_p^2}{2}\left[2\tau - \frac{BG}{(1-\varepsilon)}\int_o^1 (1-\varepsilon\theta)d\eta\right]$$

$$= PeC_o z_p^4 \int_o^1\int_o^\eta\int_1^{\ell'}\left[2\tau - \frac{BG}{(1-\varepsilon)}\left(1-\varepsilon\theta(k',t)\right)\right]k'dk'd\ell'\,\frac{\partial\theta}{\partial\eta}\,d\eta$$

$$+ \frac{z_p^2}{Fo}\frac{d}{dt}\int_o^1 \theta d\eta - \frac{z_p}{Fo}\frac{dz_p}{dt}\int_o^1 \eta\,\frac{\partial\theta}{\partial\eta}\,d\eta\ . \tag{5.4.10}$$

Again a quadratic temperature profile in the plastic region in the form

$$\theta = a_o(t) + a_1(t)\eta + a_2(t)\eta^2, \quad 0 < \eta < 1 \tag{5.4.11}$$

is assumed, where a_o, a_1 and a_2 are functions of t only. Using condition (5.4.5) we deduce that a_1 must be identically zero. The remaining two functions are determined in terms of z_p τ and G, with the aid of (5.2.7) by substituting (5.4.11) into (5.4.4) and (5.4.9) giving us the equations

$$2 = 2\tau z_p - \frac{BGz_p}{(1-\varepsilon)}\left[1-\varepsilon(a_o + \frac{1}{3}a_2)\right], \tag{5.4.12}$$

and

$$2\tau = \frac{BG}{(1-\varepsilon)}\left[1-\varepsilon(a_o+a_2)\right], \tag{5.4.13}$$

respectively. This pair of linear simultaneous equations is readily solved yielding

$$a_o = \frac{1}{\varepsilon} + \frac{(3-2\tau z_p)(1-\varepsilon)}{\varepsilon BGz_p} \tag{5.4.14}$$

and

$$a_2 = -\frac{3(1-\varepsilon)}{\varepsilon BGz_p} \tag{5.4.15}$$

On substituting equation (5.4.11) into (5.4.10), there results the ordinary differential equation

$$2a_2 + \frac{Br\tau z_p^2}{2}\left[2\tau - \frac{BG}{(1-\varepsilon)}(1-\varepsilon a_o - \frac{1}{3}\varepsilon a_2)\right] = -\frac{4PeC_o z_p^4 a_2}{105}\left\{7\left[2\tau - \frac{BG}{(1-\varepsilon)}(1-\varepsilon a_o)\right] + \frac{4BG}{(1-\varepsilon)}\varepsilon a_2\right\} + \frac{z_p^2}{Fo}\frac{d}{dt}\left[a_o + \frac{1}{3}a_2\right] - \frac{2z_p a_2}{3Fo}\frac{dz_p}{dt}, \tag{5.4.16}$$

and using (5.2.7) and substituting (5.4.11) into (5.4.3) the expression for C_o is

$$C_o = \frac{15(1-\varepsilon)}{z_p^3\left\{5\left[2\tau(1-\varepsilon)-BG(1-\varepsilon a_o)\right]+3BG\varepsilon a_2\right\}} \tag{5.4.17}$$

Finally substituting this equation into (5.4.16) and making use of (5.4.14) and (5.4.15) leads, after some algebra, to the ordinary differential equation connecting τ and z_p

$$\frac{d\tau}{dt} - \frac{3Fo}{z_p^3} + \frac{Br\varepsilon FoBG\tau}{2(1-\varepsilon)z_p} = \frac{9PeFo}{7z_p^2} - \frac{(1-z_p\tau)}{Gz_p}\frac{dG}{dt} . \tag{5.4.18}$$

Our attention is now turned to the solid region. Again in order to use the heat balance integral method we could define a thermal layer $z_p(t) < z < \zeta(t)$ such that all the material beyond $z = \zeta(t)$ is at ambient temperature, $\theta = 0$, and hence having zero heat flux across this surface. The procedure would then follow the lines of Section 4.8. However, the algebra becomes tedious using this method and as we are looking for a simple approximate solution an alternative method is sought.

It is well known that in most thermal problems the temperature decays exponentially over a semi-infinite domain and bearing this in mind we assume a temperature profile θ_s in the form

$$\theta_s = \left[b_o(t) + b_1(t)\eta\right]e^{-\eta^2/4Fo} , \quad \eta \geq 1 \tag{5.4.19}$$

where b_o and b_1 are functions of t only. This equation automatically satisfies boundary condition (5.4.8) and in order that conditions (5.4.6) and (5.4.7) are satisfied the functions b_o and b_1 must necessarily be given by

$$b_o = \left\{\left[BGz_p - 2\tau z_p(1-\varepsilon)\right](2Fo-1) + 12Fo(1-\varepsilon)\right\} e^{1/(4Fo)} / 2B\varepsilon FoGz_p \qquad (5.4.20)$$

and

$$b_1 = \left[BGz_p - 2(6Fo+\tau z_p)(1-\varepsilon)\right] e^{1/(4Fo)} / 2B\varepsilon FoGz_p \qquad (5.4.21)$$

The heat balance integral for the solid region is obtained by integrating equation (5.4.2) with respect to η between the limits $\eta = 1$ and $\eta \to \infty$ giving us

$$-\frac{\partial\theta_s}{\partial\eta}(1,t) = Pez_p\theta_s(1,t) + \frac{z_p^2}{Fo}\frac{d}{dt}\int_1^\infty \theta_s d\eta - \frac{z_p}{Fo}\frac{dz_p}{dt}\int_1^\infty \eta\frac{\partial\theta_s}{\partial\eta}d\eta \,, \qquad (5.4.22)$$

where use of the fact that $\theta_s \to 0$ and $\partial\theta_s/\partial\eta \to 0$ as $\eta \to \infty$ has been made in the derivation of this result. On substituting equation (5.4.19) into equation (5.4.22) there results the ordinary differential equation

$$\frac{\left[b_o - b_1(2Fo-1)\right]}{2Foe^{1/(4Fo)}} = \frac{Pez_p(b_o+b_1)}{e^{1/(4Fo)}} + \frac{z_p^2}{Fo}\frac{d}{dt}\left[\sqrt{\pi Fo}\, b_o\, erfc\frac{1}{2\sqrt{Fo}} + 2\frac{Fob_1}{e^{1/(4Fo)}}\right] +$$

$$\frac{z_p}{Fo}\frac{dz_p}{dt}\left[\frac{b_o}{e^{1/(4Fo)}} + \sqrt{\pi Fo}\, bo\, erfc\left(\frac{1}{2\sqrt{Fo}}\right) + \frac{b_1(1+2Fo)}{e^{1/(4Fo)}}\right] \qquad (5.4.23)$$

Substituting equations (5.4.20) and (5.4.21) into the above, leads, after some algebra to a second ordinary differential equation connecting z_p and τ, namely

$$\frac{6Fo}{z_p^2} + q_2 z_p\left[\frac{d\tau}{dt} - \frac{\tau}{G}\frac{dG}{dt}\right] + \left[q_1\frac{dz_p}{dt} + PeFo\right]\left[2\tau - \frac{BG}{(1-\varepsilon)}\right] - \frac{3q_3}{G}\frac{dG}{dt} = 0 \,,$$

(5.4.24)

where the constants q_1, q_2 and q_3 are defined by

$$q_1 = 2 + \frac{1}{2}(2Fo-1)\sqrt{\frac{\pi}{Fo}}\, e^{1/(4Fo)}\, \mathrm{erfc}\left(\frac{1}{2\sqrt{Fo}}\right)$$

$$q_2 = 2 + (2Fo-1)\sqrt{\frac{\pi}{Fo}}\, e^{1/(4Fo)}\, \mathrm{erfc}\left(\frac{1}{2\sqrt{Fo}}\right) \qquad (5.4.25)$$

and

$$q_3 = 4Fo - 2\sqrt{\pi Fo}\, e^{1/(4Fo)}\, \mathrm{erfc}\left(\frac{1}{2\sqrt{Fo}}\right) .$$

Since we are assuming that the thickness of the plastic region is initially zero it is evident with the aid of (5.2.4) that the initial conditions on (5.4.18) and (5.4.24) are

$$z_p(0) = 0 \quad \text{and} \quad \lim_{t\to 0} \tau \to \infty \qquad (5.4.26)$$

There is no analytical solution to this initial value problem and a numerical procedure must be adopted. Again to avoid the complication due to the singularity at $t = 0$ a series expansion, valid for small times, to equations (5.4.18) and (5.4.24) must be obtained. Before this can be done, however, a small time representation for the function $G(t)$ must be known. In view of the fact that G must be asymptotically proportional to τ for small time, if we assume a series for z_p in the form

$$z_p = z_1 t^m + z_2 t^{2m} + \ldots, \qquad (5.4.27)$$

where m is a positive real number, then from (5.4.4) and (5.4.9) it seems likely that τ and G should be expressed in the forms

$$\tau = \tau_{-1}t^{-m} + \tau_o + \tau_1 t^m + \ldots \tag{5.4.28}$$

and

$$G = g_{-1}t^{-m} + g_o + g_1 t^m + \ldots \tag{5.4.29}$$

respectively. On substituting these series into equations (5.4.18) and (5.4.24) there results the pair of identities

$$-\frac{m\tau_{-1}}{t^{m+1}} + \ldots - \frac{3Fo}{z_1^3 t^{3m}}\left[1 - \frac{3z_2}{z_1}t^m + \ldots\right] + \frac{Br\varepsilon FoB}{2(1-\varepsilon)}\left[\frac{\tau_{-1}g_{-1}}{z_1 t^{3m}} + \frac{1}{z_1 t^{2m}}\right.$$

$$\left.(\tau_{-1}g_o + \tau_o g_{-1} - \tau_{-1}g_{-1}z_2/z_1) + \ldots\right] \equiv \frac{9PeFo}{7z_1^2 t^{2m}}\left[1 - 2\frac{z_2}{z_1}t^m + \ldots\right]$$

$$+ \frac{m(1-z_1\tau_{-1})}{z_1 t^{m+1}} - \frac{m}{z_1 t}\left[(\tau_{-1}z_2 + \tau_o z_1) + (1-\tau_{-1}z_1)\left(\frac{z_2}{z_1} + \frac{g_o}{g_{-1}}\right)\right] + \ldots \tag{5.4.30}$$

and

$$\frac{6Fo}{z_1^2 t^{2m}}(1 - 2Z_2/z_1 t^m + \ldots) + q_2 z_1 t^m (1 + z_2/z_1 t^m + \ldots)\left[-m\left(\frac{\tau_{-1}g_o}{g_{-1}} - \tau_o\right)\frac{1}{t} + \ldots\right] +$$

$$\left[\frac{mq_1 z_1 t^m}{t}(1 + 2z_2/z_1 t^m + \ldots) + PeFo\right]\left[\frac{2\tau_{-1}}{t^m}(1 + \tau_o/\tau_{-1}t^m + \ldots) -\right.$$

$$\left.\frac{Bg_{-1}}{(1-\varepsilon)t^m}(1 + g_o/g_{-1}t^m + \ldots)\right] + 3q_3\left(\frac{m}{t} + \ldots\right)(1 - g_o/g_{-1}t^m + \ldots) \equiv 0\ , \tag{5.4.31}$$

respectively. A close examination of (5.4.30) reveals that for a solution to exist, m must satisfy one of the equations

$$m + 1 = 3m,\ m + 1 = 2m \quad \text{or} \quad 3m = 1\ . \tag{5.4.32}$$

If from $(5.4.32)_3$, $m = \frac{1}{3}$ then equating the coefficient of $t^{-4/3}$ in (5.4.30) yields

$$-\frac{\tau_{-1}}{3} = \frac{1}{3z_1} - \frac{\tau_{-1}}{3} \tag{5.4.33}$$

for which there is no finite solution. If, from $(5.4.32)_2$, $m = 1$ then we have on equating the coefficients of t^{-2} in (5.4.31)

$$\frac{6Fo}{z_1^2} = 0 , \tag{5.4.34}$$

which again has no finite solution. We thus deduce that $m = \frac{1}{2}$, from $(5.4.32)_1$. Using this result in (5.4.30) and (5.4.31) and equating the coefficients of $t^{-3/2}$ and t^{-1} respectively, results in a pair of equations connecting z_1 and τ_{-1}, namely

$$\frac{1}{Fo} + \frac{6}{z_1^2} = \frac{BrB\varepsilon\tau_{-1}g_{-1}}{(1-\varepsilon)} \tag{5.4.35}$$

and

$$\frac{6Fo}{z_1^2} + q_1 z_1 \tau_{-1} - \frac{q_1 z_1 B g_{-1}}{2(1-\varepsilon)} + \frac{3q_3}{2} = 0 . \tag{5.4.36}$$

Although the first terms z_1 and τ_{-1} are sufficient to determine starting values for the numerical method we also determine the next pair z_2 and τ_o. These are then compared with their counterparts obtained from the series solution obtained in Section 5.7 and some assessment of the accuracy of the approximate method is made.

On equating the coefficient of t^{-1} and t^{-2} in equations (5.4.30) and (5.4.31) respectively, recalling that $m = \frac{1}{2}$, we obtain the pair of linear algebraic equations

$$h_1 z_2 + h_2 \tau_o = h_3 \tag{5.4.37}$$

and

$$h_4 z_2 + h_5 \tau_o = h_6$$

where the constants h_1, h_2, h_3, h_4, h_5, and h_6 are defined by

$$\left.\begin{aligned} h_1 &= \frac{9Fo}{z_1^3} - \frac{BrB\varepsilon Fo\tau_{-1}g_{-1}}{2(1-\varepsilon)z_1} + \frac{1}{2z_1}\ , \\ h_2 &= \frac{BrB\varepsilon Fog_{-1}}{2(1-\varepsilon)} + \frac{z_1}{2}\ , \\ h_3 &= \frac{9PeFo}{7z_1} - \frac{(1-\tau_{-1}z_{-1})g_o}{2g_{-1}} - \frac{BrB\varepsilon Fo\tau_{-1}g_o}{2(1-\varepsilon)} \end{aligned}\right\} \qquad (5.4.39)$$

$$\left.\begin{aligned} h_4 &= q_1\left[2\tau_{-1} - \frac{Bg_{-1}}{(1-\varepsilon)}\right] - \frac{12Fo}{z_1^3}\ , \\ h_5 &= \left[\frac{q_2}{2} + q_1\right] z_1 \end{aligned}\right\} \qquad (5.4.40)$$

and

$$h_6 = \left[\frac{3q_3}{g_{-1}} + \frac{q_1 z_1 B}{(1-\varepsilon)} + \frac{q_2 z_1 \tau_{-1}}{g_{-1}}\right]\frac{g_o}{2} - PeFo\left[2\ \tau_{-1} - \frac{Bg_{-1}}{(1-\varepsilon)}\right].$$

Using (5.4.35) to eliminate τ_{-1} from (5.4.36) leads to, after some algebra,

$$\frac{q_1 B g_{-1}}{2(1-\varepsilon)}\left[1 - \frac{2(1-\varepsilon)^2}{BrB^2\varepsilon Fog_{-1}^2}\right]z_1^3 - \frac{3q_3}{2}z_1^2 - \frac{6q_1(1-\varepsilon)}{BrB\varepsilon g_{-1}}z_1 - 6Fo = 0 \qquad (5.4.41)$$

Taking $Fo = 5$ we see from (5.4.25) that q_1, q_2 and q_3 are all positive, it then follows that the coefficients of z_1^2, z_1 and unity, in the above, are all negative. It is then evident by examination of the coefficient of z_1^3 that there is no positive solution for z_1 when Br does not satisfy the inequality

$$Br > \frac{2(1-\varepsilon)^2}{B^2 g_{-1}^2 \varepsilon Fo}\ . \qquad (5.4.42)$$

Let us now examine the nature of the roots of (5.4.41) when (5.4.42) is satisfied by Br. (That is, the coefficient of z_1^3 is positive). Let us firstly assume that all three roots are real and denote them by Γ_1, Γ_2 and Γ_3. It then follows from the general theory of cubics that

$$\Gamma_1\Gamma_2\Gamma_3 = \frac{12Fo(1-\varepsilon)}{q_1 Bg_{-1}} \Bigg/ \left[1 - \frac{2(1-\varepsilon)^2}{BrB^2 g_{-1}^2 \varepsilon Fo}\right] > 0 \qquad (5.4.43)$$

and

$$\Gamma_1\Gamma_2 + \Gamma_1\Gamma_3 + \Gamma_2\Gamma_3 = -\frac{12q_1(1-\varepsilon)^2}{Brq_1\varepsilon B^2 g_{-1}^2} \Bigg/ \left[1 - \frac{2(1-\varepsilon)^2}{BrB^2\varepsilon Fog_{-1}^2}\right] < 0 \,. \qquad (5.4.44)$$

From (5.4.43) we deduce that there are one or three positive roots. However (5.4.44) reveals that there is at least one negative root. We thus conclude that if there are three real roots then only one is positive.

Let us now consider the event of there being two complex conjugate roots and one real root and denote them by C_1, $\bar{C}_1$ and Γ_1 respectively. We can then write.

$$\Gamma_1\left[R_e^2(C_1)+I_m^2(C_1)\right] = \frac{12Fo(1-\varepsilon)}{q_1 Bg_{-1}} \Bigg/ \left[1 - \frac{2(1-\varepsilon)^2}{BrB^2\varepsilon Fog_{-1}^2}\right] > 0 \qquad (5.4.45)$$

from which it is immediately obvious that Γ_1 is positive.

We finally conclude that there is no solution when the inequality (5.4.42) is violated by Br but when it is satisfied a unique solution for z_1 exists.

The coefficient τ_{-1} is readily obtained in terms of z_1 from equation (5.4.35) yielding

$$\tau_{-1} = \left(1 + \frac{6Fo}{z_1^2}\right) \frac{(1-\varepsilon)}{BrB\varepsilon Fog_{-1}} \qquad (5.4.46)$$

The solution to (5.4.37) and (5.4.38) is readily obtained by Cramer's rule [35] giving

$$z_2 = [h_3h_5 - h_2h_6]/\Delta \qquad (5.4.47)$$

and

$$\tau_o = [h_1h_6 - h_4h_3]/\Delta \qquad (5.4.48)$$

when the determinant Δ is defined by

$$\Delta = h_1h_5 - h_2h_4 \; . \qquad (5.4.49)$$

The full numerical solution to (5.4.18) and (5.4.24) is delayed until Section 5.6 since before this can be obtained it is necessary to specify explicitly the function $G(t)$ for all time. As we have already stated we must choose a form for G that is asymptotically proportional to τ for both small and large values of t. We have already obtained an asymptotic solution for τ valid for small t thus we now require a solution for large t and this is developed in the following section.

5.5 Asymptotic solution for large t.

In this section, the asymptotic solution for large t, to equations (5.4.18) and (5.4.24), is developed. This is used to determine the asymptotic behaviour of G and to give a qualitative estimate of the time taken for the system to reach steady state.

Let us assume the following forms for z_p, τ and G

$$z_p = z_{p\infty} + z_T(t) \ , \tag{5.5.1}$$

$$\tau = \tau_\infty + \tau_T(t) \ , \tag{5.5.2}$$

and

$$G = 1 + g(t) \ , \tag{5.5.3}$$

where $z_{p\infty}$ and τ_∞ are the steady state values of z_p and τ respectively and z_T, τ_T and g are the remaining transient terms for which at large time it is appropriate to assume

$$|z_T| << |z_{p\infty}|, \ |\tau_T| << |\tau_\infty| \quad \text{and} \quad |g| << 1 \ . \tag{5.5.4}$$

Substituting (5.5.1), (5.5.2) and (5.5.3) into (5.4.18) and (5.4.24) and expanding the resulting equations in small quantities, results in the identities

$$\frac{d\tau_T}{dt} - \frac{3Fo}{z_{p\infty}^3}(1-3z_T/z_{p\infty}+\ldots) + \frac{BrB\varepsilon Fo\tau_\infty}{2(1-\varepsilon)z_p}(1+\tau_T/\tau_\infty)(1+g)(1-z_T/z_{p\infty}+\ldots) =$$

$$\frac{9PeFo}{7z_{p\infty}^2}(1-2z_T/z_{p\infty}+\ldots) - \frac{1}{z_{p\infty}}\left[(1-\tau_\infty z_{p\infty}) - \tau_T z_{p\infty} - z_T\tau_\infty - \ldots\right](1-z_T/z_{p\infty}+\ldots)$$

$$(1-g+\ldots)\frac{dg}{dt}$$

(5.5.5)

and

$$\frac{6Fo}{z_{p\infty}^2}(1-2z_T/z_{p\infty}+\ldots) - 3q_3(1-g-\ldots)\frac{dg}{dt} + q_2 z_{p\infty}(1+z_T/z_{p\infty})$$

$$\left[\frac{d\tau_T}{dt} - \tau_\infty(1+\tau_T/\tau_\infty)(1-g-\ldots)\frac{dg}{dt}\right] + \left[q_1\frac{dz_T}{dt} + PeFo\right]\left[2\tau_\infty(1+\tau_T/\tau_\infty) - \frac{B(1+g)}{(1-\varepsilon)}\right] = 0 \ .$$

(5.5.6)

5.5.1 Steady State Solution

Equating the steady state terms in the identities (5.5.5) and (5.5.6) leads to the pair of algebraic equations

$$-\frac{3}{z_{p\infty}^3}+\frac{BrB\varepsilon\tau_\infty}{2(1-\varepsilon)z_{p\infty}}=\frac{9Pe}{7z_{p\infty}^2} \tag{5.5.7}$$

and

$$\frac{6}{z_{p\infty}^2}+2Pe\left[\tau_\infty-\frac{B}{2(1-\varepsilon)}\right]=0 \tag{5.5.8}$$

respectively. Using (5.5.8) to eliminate τ_∞ from (5.5.7) results, after a little algebra, in the quadratic

$$B_r\varepsilon\left(\frac{B}{2(1-\varepsilon)}\right)^2 z_{p\infty}^2-\frac{9Pe}{7}z_{p\infty}-3\left[\frac{Br\varepsilon}{Pe}\left(\frac{B}{2(1-\varepsilon)}\right)+1\right] \tag{5.5.9}$$

This quadratic is readily solved yielding the solution

$$z_{p\infty}=\frac{18Pe(1-\varepsilon)^2}{7BrB^2\varepsilon}+2\sqrt{\left[\frac{81Pe^2(1-\varepsilon)^4}{49Br^2B^4\varepsilon^2}+\frac{3(1-\varepsilon)}{2B}\left(\frac{1}{Pe}+\frac{2(1-\varepsilon)}{BrB\varepsilon}\right)\right]} \tag{5.5.10}$$

where the positive square root is taken since $z_{p\infty}$ must, of course, be positive. The expression for τ_∞ is then obtained in terms of $z_{p\infty}$ from (5.5.8) giving

$$\tau_\infty=\frac{B}{2(1-\varepsilon)}-\frac{3}{PeZ_{p\infty}^2} \tag{5.5.11}$$

In Section (5.8) an exact solution to the steady state problem is derived which is valid for small values of Pe only. It is thus thought useful to give here an expansion of (5.5.10) for small Pe,

for later comparison with its exact steady state counterpart.

On expanding (5.5.10) for small Pe one obtains

$$z_{p\infty} \sim 2\sqrt{\frac{3(1-\varepsilon)}{2B}}\left[\frac{1}{\sqrt{Pe}} + \frac{\sqrt{Pe}\,(1-\varepsilon)}{BrB\varepsilon} + \ldots\right] \qquad (5.5.12)$$

and substituting this expansion into equation (5.5.11) we obtain

$$\tau_{\infty} \sim Pe/Br\varepsilon + \ldots \qquad (5.5.13)$$

We also present here for comparison with equations (4.11.11) and (4.11.12) for the viscous fluid model, the asymptotic expansions of (5.5.10) for small and large values of Br. For small values of Br we have

$$z_{p\infty} \sim \frac{36Pe(1-\varepsilon)^2}{7BrB^2\varepsilon} + \frac{7}{3Pe} + \ldots, \qquad (5.5.14)$$

and the result for large Br is

$$z_{p\infty} \sim 2\sqrt{\frac{3(1-\varepsilon)}{2BPe}} + \frac{2(1-\varepsilon)}{BrB\varepsilon}\left[\sqrt{\frac{3Pe(1-\varepsilon)}{2B}} + \frac{9Pe(1-\varepsilon)}{7B}\right] + \ldots \qquad (5.5.15)$$

5.5.2 First Order Transient Solution

From the remaining time dependent terms in (5.5.5) and (5.5.6) we have, on neglecting terms $O(z_T^2/z_{p\infty}^2)$, a pair of linear, first order, ordinary differential equations, namely

$$\frac{d\tau_T}{dt} + e_0\tau_T + e_1 z_T = f_0 g + f_1 \frac{dg}{dt} \qquad (5.5.16)$$

and

$$\frac{d\tau_T}{dt} + e_2\tau_T + e_3 z_T + e_4 \frac{dz_T}{dt} = f_2 g + f_3 \frac{dg}{dt} \qquad (5.5.17)$$

where the constants e_0, e_1, e_2, e_3 and e_4 are defined by

$$\left.\begin{aligned} e_0 &= \frac{BrB\varepsilon Fo}{2(1-\varepsilon)z_{p\infty}}, \quad e_1 = \frac{9Fo}{z_{p\infty}^4} + \frac{18PeFo}{7z_{p\infty}^3} - \frac{e_0\tau_\infty}{z_{p\infty}} \\ e_2 &= \frac{2PeFo}{q_2 z_{p\infty}}, \quad e_3 = -\frac{12Fo}{q_2 z_{p\infty}^4} \end{aligned}\right\} \qquad (5.5.18)$$

and

$$e_4 = \frac{2q_1}{q_2 z_{p\infty}}\left[\tau_\infty - \frac{B}{2(1-\varepsilon)}\right]$$

and the constants f_0, f_1, f_2 and f_3 are defined by

$$\left.\begin{aligned} f_0 &= -e_0\tau_\infty, \quad f_1 = (z_{p\infty}\tau_\infty - 1)/z_{p\infty} \\ f_2 &= \frac{PeFoB}{(1-\varepsilon)q_2 z_{p\infty}} \text{ and } f_3 = \frac{(q_2 z_{p\infty}\tau_\infty + 3q_3)}{q_2 z_{p\infty}} \end{aligned}\right\} \qquad (5.5.19)$$

We recall here that we are seeking a form for G that is asymptotically proportional to τ for large t, hence we require a form for g that behaves like τ_T for large t. It thus seems logical with reference to equations (5.5.16) and (5.5.19) to choose g to have the same functional form as the complementary function of τ_T.

Following standard procedure we assume complementary functions to τ and z_p of the forms

$$z_T = \gamma e^{-nt} \quad \text{and} \quad \tau_T = \zeta e^{-nt} \qquad (5.5.20)$$

Substituting these two expressions into equations (5.5.16) and (5.5.17) leads, after a little algebra to the pair of homogeneous linear simultaneous equations

$$(e_0-n)\zeta + e_1\gamma = 0 \qquad (5.5.21)$$

and

$$(e_2-n)\zeta + (e_3-e_4 n)\gamma = 0 \qquad (5.5.22)$$

Clearly the above equations have a non-trivial solution only if the determinant of the system is zero. Thus n must satisfy the quadratic

$$e_4 n^2 + (e_1-e_3-e_0e_4)n + e_0e_3-e_1e_2 = 0 \ . \qquad (5.5.23)$$

This quadratic is readily solved yielding the pair of solutions

$$n_1 = N_1 - N_2 \qquad (5.5.24)$$

and

$$n_2 = N_1 + N_2 \ , \qquad (5.5.25)$$

where N_1 and N_2 are defined by

$$\left.\begin{aligned} N_1 &= \left[e_4e_0+e_3-e_1\right]/2e_4 \\ \text{and} \quad N_2 &= \sqrt{N_1^2 - \frac{(e_0e_3-e_1e_2)}{e_4}} \end{aligned}\right\} \ . \qquad (5.5.26)$$

Using computed values of τ_∞ and $z_{p\infty}$ numerical values of n_1 and n_2 were calculated, for various values of Pe and Br, using equations (5.5.24) and (5.5.25) with the aid of (5.5.18) and (5.5.26). The Bingham number was taken as $B = 5.0$ and following Bahrani [18] we chose ε to give zero yield stress at melting temperature

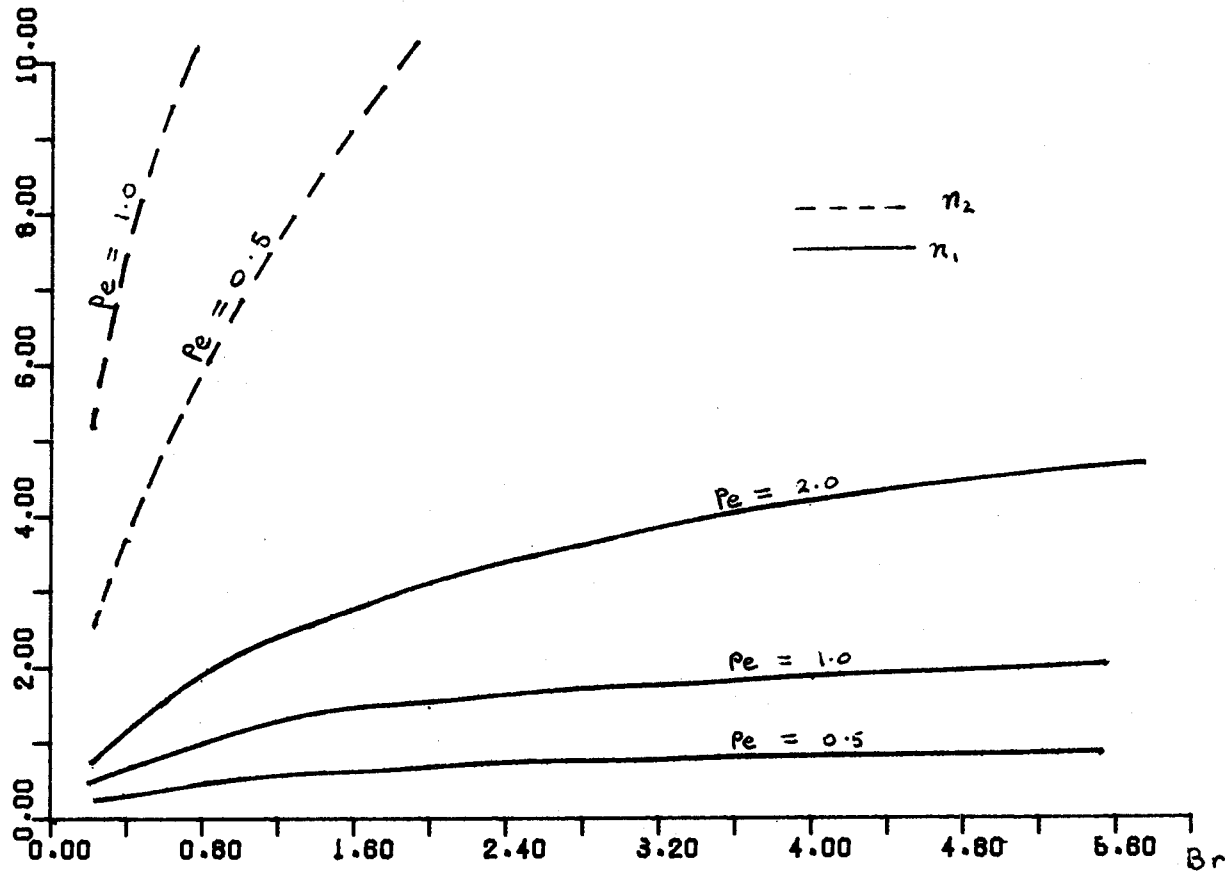

Figure 5.1 Plots of n_1 and n_2 against Br .

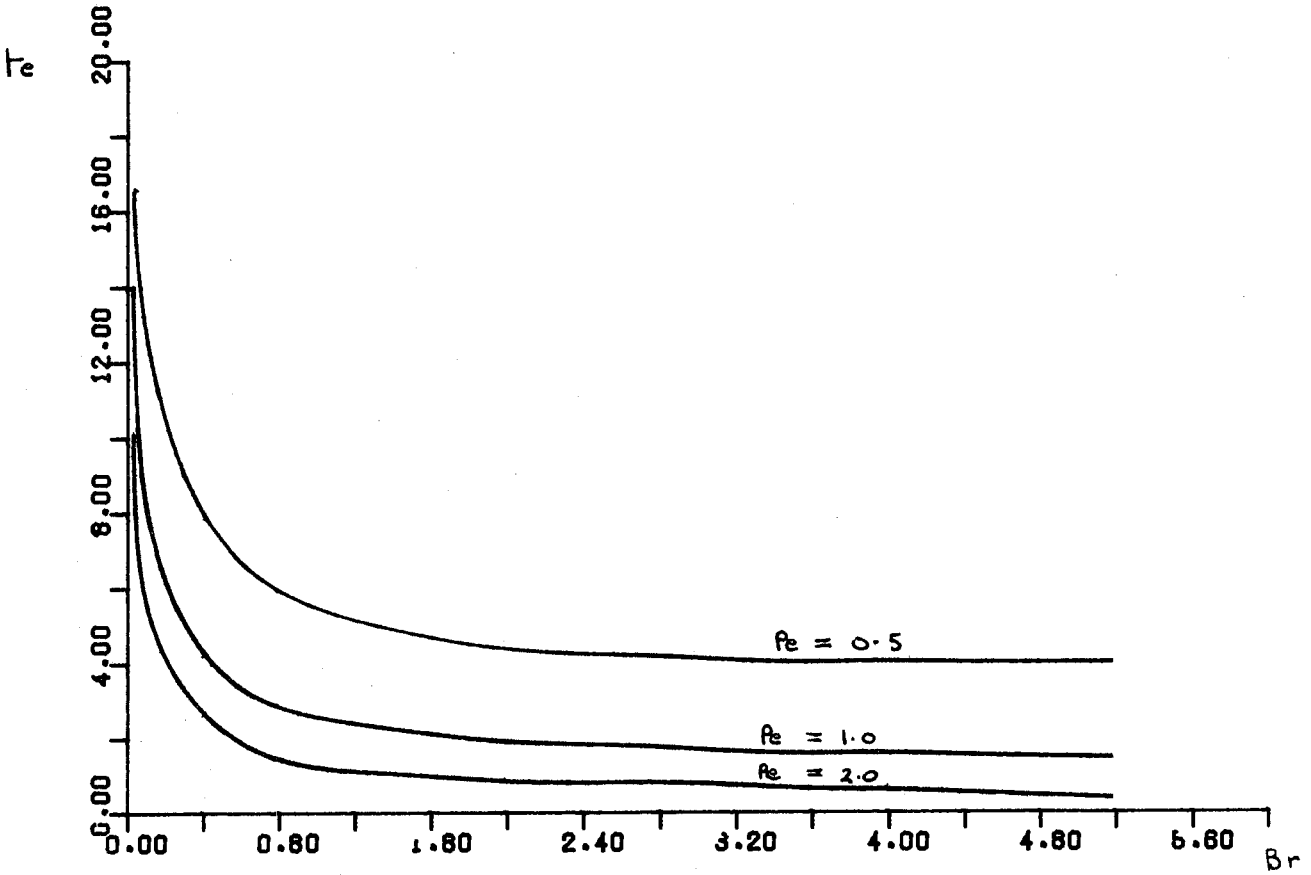

Figure 5.2 Plots of te against Br .

resulting in $\varepsilon \approx 0.4$.

It is found that n_1 and n_2 are both real and positive for all values of Br and Pe and n_1 is obviously always smaller than n_2. A plot of these quantities against Br for various values of Pe is given in Figure 5.1.

Since n_1 is in most cases much smaller than n_2 we deduce that z_T and τ_T are asymptotically proportional to $\exp[-n_1 t]$ for large time. Hence assuming g to have the same functional form as τ_T we now write

$$g \propto e^{-n_1 t} . \tag{5.5.27}$$

Furthermore, recalling equation (5.4.29) we see that for small t

$$G \propto 1/\sqrt{t} \tag{5.5.28}$$

Thus on recalling definition (5.5.3) one deduces that a suitable form for G satisfying both (5.5.27) and (5.5.28) is

$$G = (1-e^{-n_1 t})^{-\frac{1}{2}} \tag{5.5.29}$$

Although there may be other representations for G equation (5.5.29) is simple and possesses the right asymptotic properties for small and large time. Expanding (5.5.29) for small t the comparison of the resulting expression with the series (5.4.29) reveals that

$$g_{-1} = 1/\sqrt{n_1} \quad \text{and} \quad g_o = 0 . \tag{5.5.30}$$

Also on expanding (5.5.29) for large t and using the definition (5.5.3) it is seen that

$$g = \frac{1}{2} e^{-n_1 t} . \qquad (5.5.31)$$

Having now established a suitable form for G we could go on and calculate the particular integrals to equations (5.5.16) and (5.5.17). However, since these particular integrals are not really required, and even if we obtained them we could not give a complete solution, since we have no conditions from which to determine the unknown constant in the complementary functions, it is thus pointless taking this solution any further.

Although the main objective of this section (that is to obtain a form for G) has been achieved, it is thought useful to give with the aid of the above results, a simple model from which the duration of phase II can be obtained and this is done in the following subsection.

5.5.3 Estimate of time taken to reach steady state

In this section we present a simple model to illustrate the qualitative effect of the only two control parameters, Br and Pe, on the time taken to reach equilibrium. Although the exact form for z_T is not known, its functional form is known and as in Section 4.11 we assume

$$z_T = - Z_{p\infty} e^{-n_1 t} \qquad (5.5.32)$$

Following Section (4.11) we shall assume here that equilibrium has been reached

when the thickness of the plastic region has reached 95% of its asymptotic steady value. The time taken to reach equilibrium te, is thus given by

$$te = \frac{1}{n_1} \ln 20 , \qquad (5.5.33)$$

and a plot of this quantity against Br for various values of Pe is presented on Figure 5.2.

Comparison of the results in Figure 5.2 with those in Figure 4.10 reveals that the models are very different for small values of Br. In the case of the viscous fluid model the time taken to reach equilibrium approaches zero as $Br \to 0$ whereas for the Bingham substance $te \to \infty$ as $Br \to 0$. However for larger values of Br we notice that the difference is much smaller.

5.6 Results and Discussion

In this section the plots of z_p and τ against time are given for various values of Pe and Br.

Using the computed values of n_1 and n_2 and equation (5.5.30) in (5.4.42) it is found that this inequality is satisifed for all Pe and Br used. We thus deduce that there is a unique solution to (5.4.37). This is readily calculated using the Newton-Raphson method and presented together with the corresponding values of τ_{-1}, given by (5.4.43), in table 5.1. Using these values and a suitably small starting value for t the pair of ordinary differential equations (5.4.18) and (5.4.24) were readily solved using the

Br	Pe = 0.1		Pe = 0.5	
	z_1	$\tau-1$	z_1	$\tau-1$
0.1	0.915	5.908	1.572	4.479
0.2	0.902	3.415	1.553	2.796
0.3	0.897	2.421	1.554	2.071
0.4	0.895	1.880	1.558	1.657
0.5	0.893	1.538	1.562	1.386
0.6	0.892	1.302	1.567	1.193
0.7	0.891	1.129	1.570	1.049
0.8	0.890	0.996	1.574	0.936
0.9	0.889	0.892	1.577	0.846
1.0	0.889	0.807	1.579	0.772
2.0	0.887	0.415	1.593	0.415
5.0	0.885	0.169	1.603	0.175
Br	Pe = 1.0		Pe = 2.0	
	z_1	$\tau-1$	z_1	$\tau-1$
0.1	1.936	3.886	2.236	3.511
0.2	1.943	2.443	2.326	2.177
0.3	1.959	1.824	2.389	1.619
0.4	1.977	1.467	2.437	1.302
0.5	1.993	1.232	2.480	1.094
0.6	2.008	1.065	2.519	0.945
0.7	2.022	0.939	2.550	0.834
0.8	2.034	0.840	2.580	0.747
0.9	2.045	0.761	2.608	0.676
1.0	2.055	0.696	2.634	0.619
2.0	2.120	0.378	2.812	0.337
5.0	2.132	0.161	3.032	0.144

Table 5.1

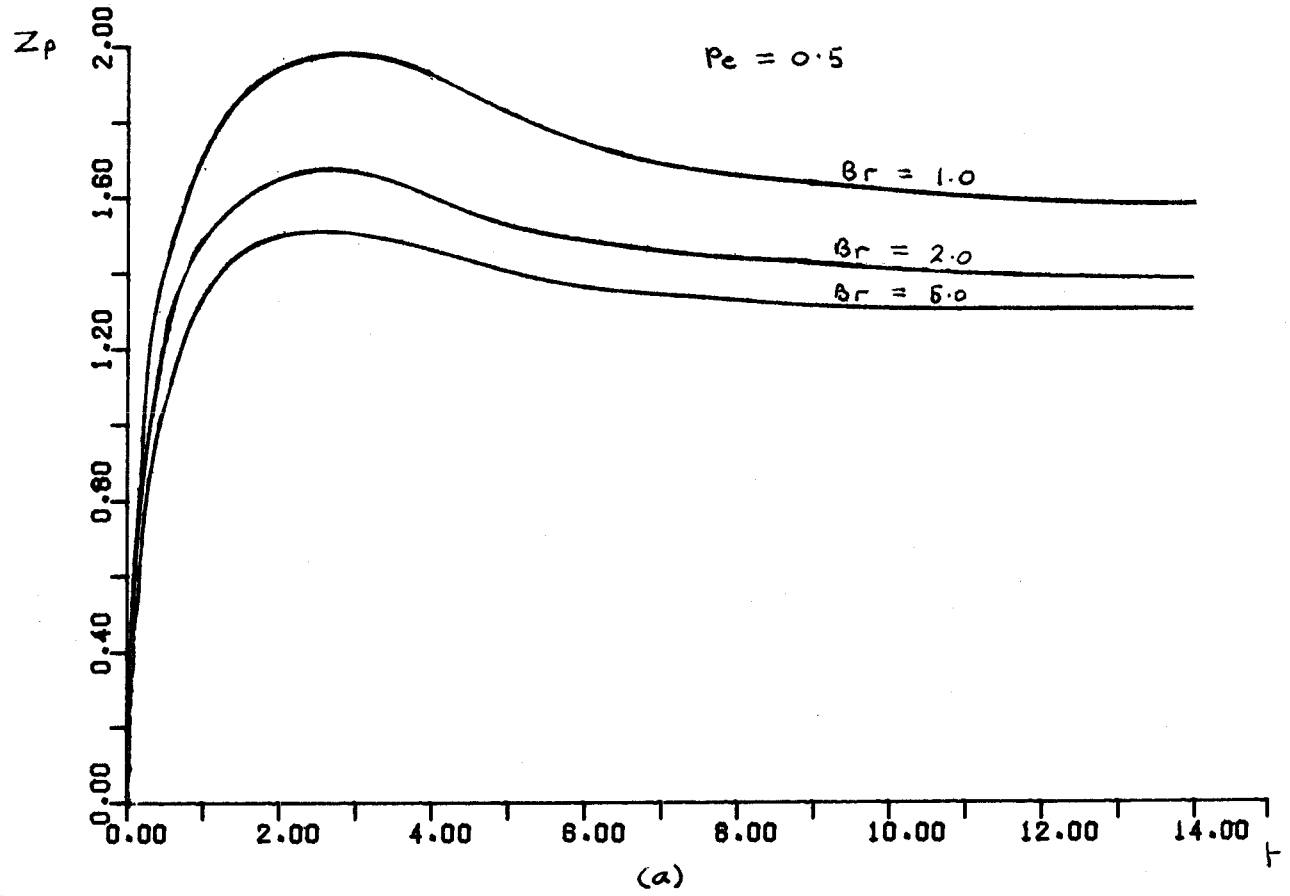

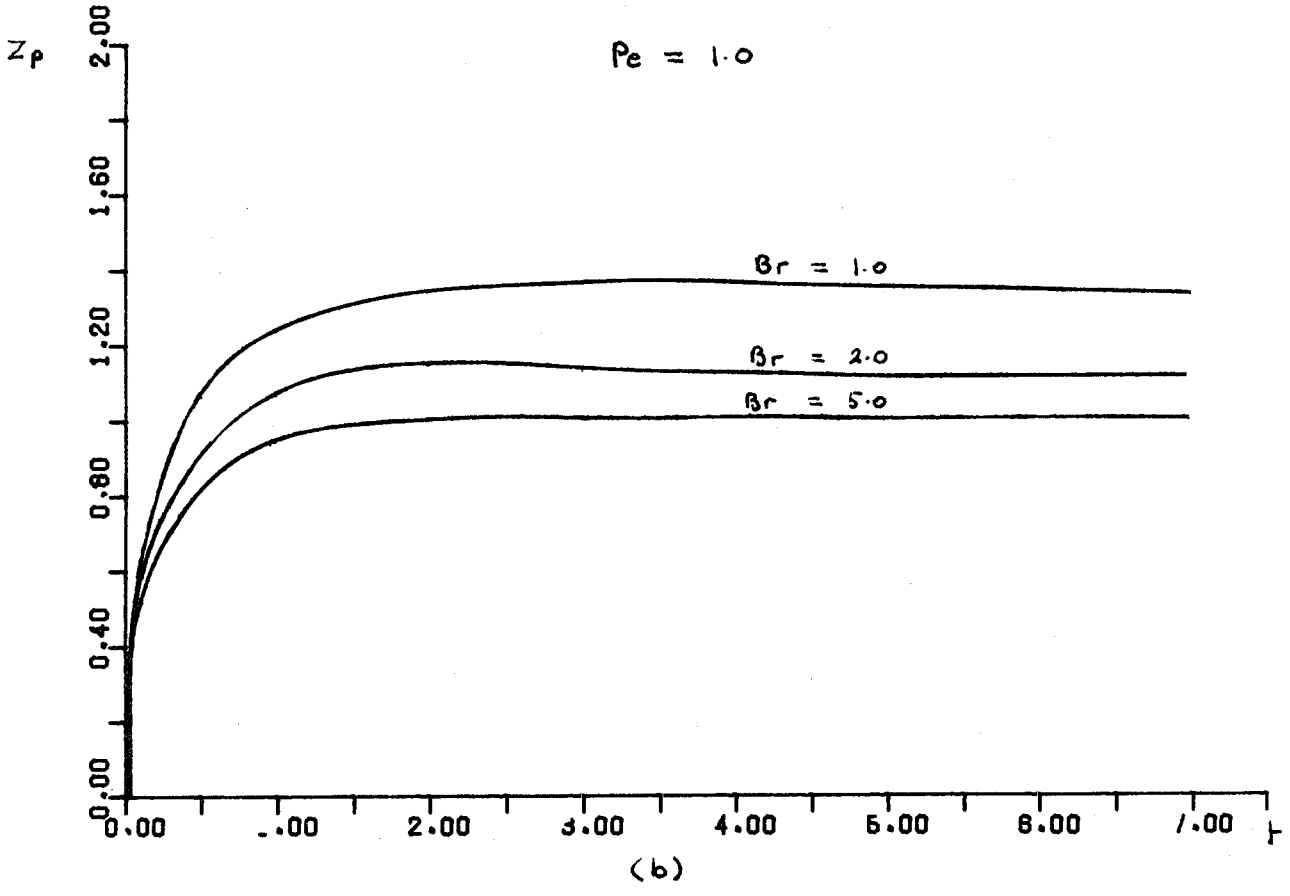

Figure 5.3 Plots of z_p against t .

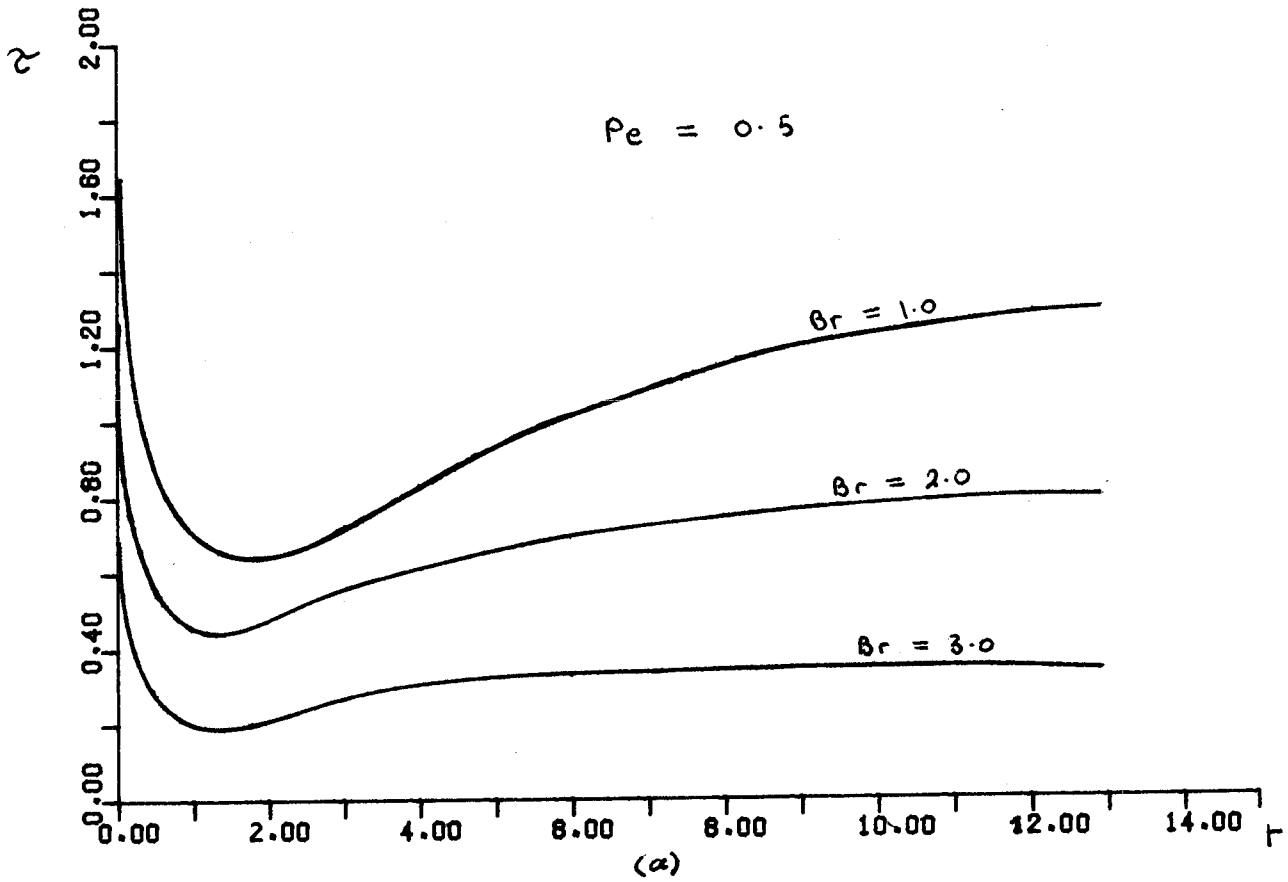

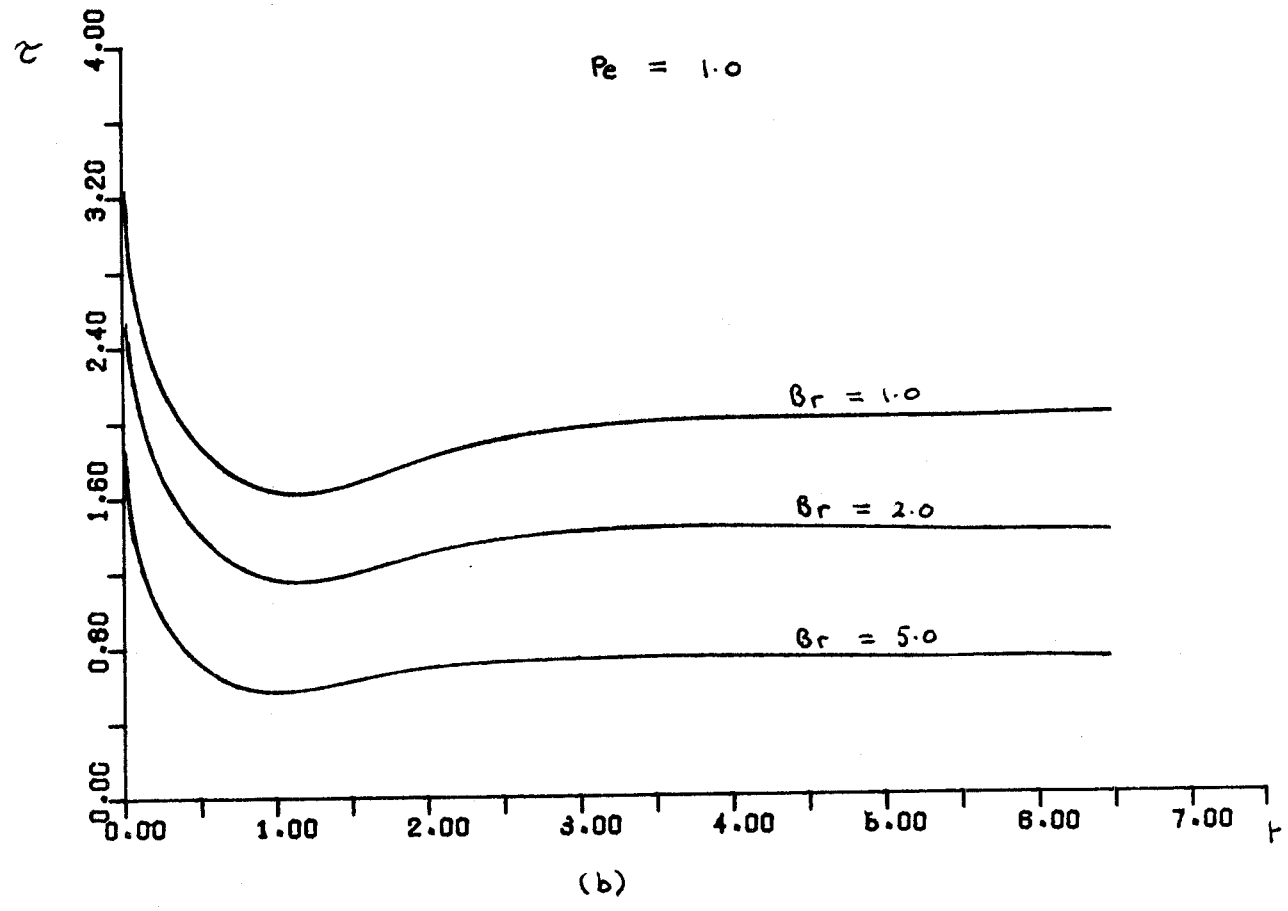

Figure 5.4 Graphs of τ against t .

Runge-Kutta method and these results are presented in Figures 5.3 and 5.4.

Comparison of the traces of τ given in Figures 5.4 (a) and (b) with the corresponding traces from the viscous fluid model, Figures 4.7(a) to (d), shows that, apart from the peculiar dip for small times, the results are qualitatively similar. ie. τ decreases with increasing values of Br and increases with increasing values of Pe. However, comparing Figures 4.6(a) to (d) we see that the plots of z_p do not agree qualitatively. Although in both cases z_p decreases with increasing Pe the effect of increasing Br leads to an increase of z_p for the viscous fluid model but has the opposite effect with the Bingham model. This difference is further illustrated by comparing the asymptotic expansions of $z_{p\infty}$ for small and large Br, (5.5.14) and (5.5.15) respectively, with their counterparts from the viscous model (4.11.11) and (4.11.12). We see that for small Br $z_{p\infty} \sim Br$ in the case of the viscous model whereas $z_{p\infty} \sim 1/Br$ for the Bingham model. Also for large Br $z_{p\infty} \sim \sqrt{Br}$ in the viscous case but $z_{p\infty} \sim$ constant in the Bingham case.

5.7 Series Solution Valid for Small Time

In this section an analytical solution, valid for small time only, to the problem of section (5.4) is developed. The governing equations and boundary conditions are given, in terms of the variable η by equations (5.4.1) to (5.4.9). The appropriate form for G should be obtained by developing an exact analytic solution for large time

and following the lines of Section 5.5. However, this would be very tedious and it is thought more desirable to use the form for G, derived from the approximate solution, given by (5.5.30). The complication of the nonlinearity of the above mentioned system is reduced, as in Section 4.9, by assuming series expansion in integral powers of $\sqrt{t}$. for θ, θs, z_p and τ in the forms

$$\theta = \theta_0(\eta) + \sqrt{t}\,\theta_1(\eta) + O(t) , \tag{5.7.1}$$

$$\theta_s = \theta_{so}(\eta) + \sqrt{t}\,\theta_{s1}(\eta) + O(t) , \tag{5.7.2}$$

$$z_p = z_1\sqrt{t} + z_2 t + O(t^{3/2}) \tag{5.7.3}$$

and

$$\tau = \tau_{-1}/\sqrt{t} + \tau_0 + O(t^{1/2}) \tag{5.7.4}$$

On substituting equations(5.5.30) and (5.2.7) into (5.4.1) and (5.4.2) and substituting the above series into the resulting expressions, and expanding in small quantities, one obtains the pair of identities

$$\frac{d_2\theta_0}{d\eta^2} + \sqrt{t}\,\frac{d^2\theta_1}{d\eta^2} + \ldots + \frac{Br}{2}\left[\tau_{-1}z_1^2\sqrt{t} + (2z_1z_2\tau_{-1} + z_1^2\tau_0)t + \ldots\right]$$

$$\times\left[\frac{2\tau_{-1}}{\sqrt{t}} + 2\tau_0 + \ldots - \frac{B}{(1-\varepsilon)n_1^{\frac{1}{2}}\sqrt{t}}(1-\varepsilon\theta_0-\varepsilon\theta_1\sqrt{t}\ \ldots)(1+n_1t/4+\ldots)\right]$$

$$= Pe(z_1^4t^2+\ldots)C_o\int_0^{\eta}\int_1^{\ell'}\left[\frac{2\tau_{-1}}{\sqrt{t}} + 2\tau_0+\ldots - \frac{B(1-\varepsilon\theta_0-\varepsilon\theta_1\sqrt{t}\ldots)}{(1-\varepsilon)n_1^{\frac{1}{2}}\sqrt{t}}\right.$$

$$\left.\times\,(1+n_1t/4)\right]\,k'dk'd\ell'\left[\frac{d\theta_0}{d\eta} + \sqrt{t}\,\frac{d\theta_1}{d\eta} + \ldots\right] + \frac{1}{F_0}\,(z_1^2t+2z_1z_2t^{3/2}+\ldots)$$

$$\times\left[\frac{\theta_1}{2\sqrt{t}} + \ldots\right] - \frac{1}{F_0}\left[\frac{z_1^2}{2} + \frac{3z_1z_2}{2}\sqrt{t} + \ldots\right]\eta\left[\frac{d\theta_0}{d\eta} + \sqrt{t}\,\frac{d\theta_1}{d\eta} + \ldots\right], \quad 0 \leq \eta \leq 1 , \tag{5.7.5}$$

and

$$\frac{d^2\theta_{s0}}{d\eta^2} + \sqrt{t}\,\frac{d^2\theta_{s1}}{d\eta^2} + \ldots = -Pe(z_1\sqrt{t} + z_2 t + \ldots)\left(\frac{d\theta_{s0}}{d\eta} + \sqrt{t}\,\frac{d\theta_{s1}}{d\eta} + \ldots\right)$$

$$+ \frac{1}{F_0}\,(z_1^2 t + 2z_1 z_2 t^{3/2} + \ldots)\left[\frac{\theta_{s1}}{2\sqrt{t}} + \ldots\right] - \frac{1}{F_0}\left[\frac{z_1^2}{2} + \frac{3z_1 z_2}{2}\sqrt{t} + \ldots\right]$$

$$\times\,\eta\left[\frac{d\theta_{s0}}{d\eta} + \sqrt{t}\,\frac{d\theta_{s1}}{d\eta} + \ldots\right], \quad \eta \geq 1\,. \tag{5.7.6}$$

Similarly, the expression for C_o, equation (5.4.3), and equation (5.4.4) are expanded, resulting in

$$C_o = -\left(\frac{1}{z_1^3 t^{3/2}} + \ldots\right)\Bigg/\int_0^1\int_1^{\ell'}\left[\frac{2}{\sqrt{t}}\,\tau_{-1} + 2\tau_0 + \ldots - \right.$$

$$\left.\frac{B(1-\varepsilon\theta_0 - \varepsilon\theta_1\sqrt{t} - \ldots)}{2(1-\varepsilon)n_1^{\frac{1}{2}}\sqrt{t}}\,(1 + n_1 t/4)\right]k'\,dk'\,d\ell' \tag{5.7.7}$$

and $$\tau_{-1} Z_1 + (\tau_0 Z_1 + \tau_{-1} Z_2)\sqrt{t} + \cdots$$

$$-\frac{B(z_1\sqrt{t} + z_2 t + \ldots)}{2(1-\varepsilon)n_1^{\frac{1}{2}}\sqrt{t}}\int_0^1 (1-\varepsilon\theta_0 - \varepsilon\theta_1\sqrt{t} - \ldots)(1 + n_1 t/4 + \ldots)\,d\eta = 1 \tag{5.7.8}$$

and the boundary conditions (5.4.5) to (5.4.9) expand to

$$\frac{d\theta_0}{d\eta}(0) + \sqrt{t}\,\frac{d\theta_1}{d\eta}(0) + \ldots \equiv 0\,, \tag{5.7.9}$$

$$\theta_0(1) + \sqrt{t}\,\theta_1(1) + \ldots \equiv \theta_{s0}(1) + \sqrt{t}\,\theta_{s1}(1) + \ldots, \tag{5.7.10}$$

$$\frac{d\theta_0}{d\eta}(1) + \sqrt{t}\,\frac{d\theta_1}{d\eta}(1) + \ldots = \frac{d\theta_{s0}}{d\eta}(1) + \sqrt{t}\,\frac{d\theta_{s1}}{d\eta}(1) + \ldots, \tag{5.7.11}$$

$$\theta_{s0}(\eta) + \sqrt{t}\,\theta_{s1}(\eta) + \ldots \to 0 \quad \text{as} \quad \eta \to \infty \tag{5.7.12}$$

and

$$\frac{2\tau_{-1}}{\sqrt{t}} + 2\tau_0 + \ldots \equiv \frac{B}{(1-\varepsilon)n_1^{\frac{1}{2}}\sqrt{t}}\,(1-\varepsilon\theta_0(1)-\varepsilon\theta_1(1)\sqrt{t}-\ldots)(1+n_1\,t/4+\ldots). \tag{5.7.13}$$

Equating the coefficient of like powers of t in the above identities leads to a set of subsystems of ordinary differential equations, the first two of which are given and solved here.

5.7.1 First Order Subsystems

On equating the coefficients of the lowest order non-zero terms in t, in the above system of identities, one obtains after some rearrangement

$$\frac{d^2\theta_0}{d\eta^2} + \frac{z_1^2\eta}{2F_0}\frac{d\theta_0}{d\eta} + Br\Gamma_2\tau_{-1}z_1^2\theta_0 = Br\tau_{-1}z_1^2\left[\frac{\Gamma_2}{\varepsilon} - \tau_{-1}\right], \quad 0 \leq \eta \leq 1 \tag{5.7.14}$$

and

$$\frac{d^2\theta_{s0}}{d\eta^2} + \frac{z_1^2}{2F_0}\,\eta\,\frac{d\theta_{s0}}{d\eta} = 0, \quad \eta \geq 1 \tag{5.7.15}$$

where z_1 and τ_{-1} are related through

$$z_1\tau_{-1} - \frac{\Gamma_2 z_1}{\varepsilon}\int_0^1 (1-\varepsilon\theta_0)d\eta = 1 \qquad (5.7.16)$$

and the boundary conditions are

$$\frac{d\theta_0}{d\eta}(0) = 0 , \qquad (5.7.17)$$

$$\theta_0(1) = \theta_{s0}(1) , \qquad (5.7.18)$$

$$\frac{d\theta_0}{d\eta}(1) = \frac{d\theta_{s0}}{d\eta}(1) , \qquad (5.7.19)$$

$$\theta_{s0}(\eta) \to 0 \quad \text{as} \quad \eta \to \infty \qquad (5.7.20)$$

and

$$\tau_{-1} = \frac{\Gamma_2}{\varepsilon}\left[1-\varepsilon\theta_0(1)\right] . \qquad (5.7.21)$$

In the above the constant Γ_2 is defined by

$$\Gamma_2 = \frac{B\varepsilon}{2(1-\varepsilon)n_1^{\frac{1}{2}}} . \qquad (5.7.22)$$

Following standard procedure we split the solution for θ_0 into two parts; the complementary function θ_{0_c} and the particular integral θ_{0_p} and write

$$\theta_0 = \theta_{0_c} + \theta_{0_p} . \qquad (5.7.23)$$

By inspection of equation (5.7.14) the particular integral is readily seen to be

$$\theta_{0_p} = 1/\varepsilon - \tau_{-1}/\Gamma_2 . \qquad (5.7.24)$$

As there appears to be no closed form analytic solution to the complementary function of (5.7.14) a series solution in integral powers of η of the form

$$\theta_{0_c} = \chi_0 \sum_{n=0}^{\infty} a_n \eta^n \ , \quad \text{with} \quad a_0 = 1 \ , \tag{5.7.25}$$

is sought, where the a_n's and χ_0 are constants. On substituting (5.7.25) into (5.7.14) and equating the left hand side of the latter to zero, there results the identity

$$\chi_0 \sum_{n=0}^{\infty} a_n \left[n(n-1)\eta^{n-2} + \frac{z_1^2}{2F_0} n\eta^n + Br\Gamma_2 \tau_{-1} z_1^2 \eta^n \right] \equiv 0 \tag{5.7.26}$$

On equating the coefficient of η^n in the above identity we deduce that the a_n's are connected by the difference equation

$$a_{n+2} = - \frac{\left[\frac{nz_1^2}{2F_0} + Br\Gamma_2 \tau_{-1} z_1^2 \right]}{(n+2)(n+1)} \ a_n, \ n \geq 0 \tag{5.7.27}$$

with

$$a_0 = 1$$

Using boundary condition (5.7.17) we deduce that

$$a_1 = 0 \ , \tag{5.7.28}$$

which reveals by way of equation (5.7.27), that the a_n's are zero for all odd values of n . Thus the general solution for θ_0 may be written with the aid of (5.7.23), (5.7.24) and (5.7.25) as

$$\theta_0 = \chi_0 \sum_{n=0}^{\infty} a_{2n} \eta^{2n} + \frac{1}{\varepsilon} - \frac{\tau_{-1}}{\Gamma_2} \ , \ 0 \leq \eta \leq 1 \tag{5.7.29}$$

where the a_{2n}'s are generated by

$$a_{2n+2} = -\frac{\left[\frac{nz_1^2}{F_0} + Br\Gamma_2\tau_{-1}z_1^2\right]}{2(n+1)(2n+1)}\, a_{2n} \quad , \; n \geq 0 \tag{5.7.30}$$

with $a_0 = 1$. Using conditions (5.7.16) and (5.7.21) we obtain the two equations connecting χ_0, z_1 and τ_{-1}

$$\Gamma_2 z_1 \chi_0 \sum_{n=0}^{\infty} \frac{a_{2n}}{2n+1} = 1 \tag{5.7.31}$$

and

$$\chi_0 \sum_{n=0}^{\infty} a_{2n} = 0 \tag{5.7.32}$$

respectively.

From (5.7.31) it is clear that $\chi_0 \neq 0$ thus we deduce from (5.7.32) that

$$\sum_{n=0}^{\infty} a_{2n} = 0 \tag{5.7.33}$$

It is seen from equation (4.4.19) in Section 4.4 that the general solution of (5.7.15) satisfying condition (5.6.20) is

$$\theta_{s0} = D \operatorname{erfc}\left(\frac{z_1\eta}{2\sqrt{F_0}}\right) \tag{5.7.34}$$

The constant D is obtained by substituting (5.7.29) and (5.7.34) into condition (5.7.18) and making use of (5.7.30) which results in the expression for θ_{s0}

$$\theta_{s0} = \left[\frac{1}{\varepsilon} - \frac{\tau_{-1}}{\Gamma_2}\right] \operatorname{erfc}\left(\frac{z_1\eta}{2\sqrt{F_0}}\right) \Big/ \operatorname{erfc}\left(\frac{z_1}{2\sqrt{F_0}}\right), \quad \eta \geq 1 \qquad (5.7.35)$$

On using the boundary condition (5.7.19) we have a further condition connecting θ_0, z_1 and τ_{-1}, namely

$$\chi_0 \sum_{n=0}^{\infty} na_{2n} = -\frac{z_1}{2\sqrt{\pi F_0}}\left[\frac{1}{\varepsilon} - \frac{\tau_{-1}}{\Gamma_2}\right] e^{-z_1^2/4F_0} \Big/ \operatorname{erfc}\left(\frac{z}{2\sqrt{F_0}}\right) \qquad (5.7.36)$$

Using equation (5.7.31) to eliminate χ_0 from (5.7.36) we have

$$\frac{1}{z_1^2\Gamma_2} \sum_{n=0}^{\infty} na_{2n} \Big/ \sum_{n=0}^{\infty} \frac{a_{2n}}{(2n+1)} = -\frac{1}{2\sqrt{\pi F_0}}\left[\frac{1}{\varepsilon} - \frac{\tau_{-1}}{\Gamma_2}\right] e^{-z_1^2/4F_0} / \operatorname{erfc}(z_1/2\sqrt{F_0}) \qquad (5.7.37)$$

The two transcendental equations (5.7.33) and (5.7.37) can now be solved numerically for τ_{-1} and z_1 using a similar method to that of Section 4.5. It was found that about the first fifteen terms were required in the sumations to obtain accuracy to four decimal places. The results for z_1 and τ_{-1} are presented for various values of Pe and Br in Table 5.2. By comparing these figures with the corresponding figures obtained by the heat balance method which are presented in Table 5.1, the accuracy of the approximate method can be assessed. It is noticed that the error increases as both Br and Pe become larger. The smallest error in the figures presented is about 5%, ocurring when Pe = 0.1 and Br = 0.1 but for Pe = 2.0 and Br = 5.0 the error is as large as 55%.

Br	Pe=0.1		Pe=0.5	
	z_1	τ_{-1}	z_1	τ_{-1}
0.1	0.800	6.258	1.334	4.900
0.2	0.785	3.653	1.306	3.114
0.3	0.779	2.602	1.299	2.333
0.4	0.776	2.026	1.297	1.882
0.5	0.774	1.660	1.292	1.584
0.7	0.771	1.221	1.297	1.210
1.0	0.769	0.875	1.298	0.899
2.0	0.766	0.451	1.299	0.489
5.0	0.764	0.184	1.300	0.208
Br	Pe=1.0		Pe=2.0	
	z_1	τ_{-1}	z_1	τ_{-1}
0.1	1.594	4.407	1.798	4.084
0.2	1.573	2.861	1.816	2.659
0.3	1.568	2.181	1.827	2.044
0.4	1.568	1.783	1.836	1.686
0.5	1.569	1.517	1.844	1.445
0.7	1.574	1.=79	1.858	1.138
1.0	1.581	0.892	1.874	0.875
2.0	1.595	0.502	1.911	0.510
5.0	1.608	0.222	1.952	0.236

Table 5.2

Having now obtained values for z_1 and τ_{-1} the constant χ_0 can be obtained using equation (5.7.31). The temperature profiles can then be obtained using (5.7.29) and (5.7.33) for the plastic and solid regions respectively.

In the following subsection, the solution to the second order subsystem is developed.

5.7.2 Second Order Subsystem

Substituting equation (5.7.7) into equation (5.7.5) and equating the terms in $\sqrt{t}$ results in the ordinary differential equation

$$\frac{d^2\theta_1}{d\eta^2} + \frac{z_1^2}{2F_0}\frac{d\theta_1}{d\eta} + z_1^2\left[Br\tau_{-1}\Gamma_2 - \frac{1}{2F_0}\right]\theta_1 =$$

$$Brz_1\left[\frac{\Gamma_2}{\varepsilon}(1-\varepsilon\theta_0)(2z_2\tau_{-1}+z_1\tau_0)-2\tau_{-1}(z_2\tau_{-1}+z_1\tau_0)\right] - Pez_1\int_0^\eta\int_1^\ell \left[\tau_{-1} - \frac{\Gamma_2}{\varepsilon}(1-\varepsilon\theta_0)\right]kdkd\ell\ \frac{d\theta_0}{d\eta}\Big/\int_0^1\int_1^\ell\left[\tau_{-1} - \frac{\Gamma_2}{\varepsilon}(1-\varepsilon\theta_0)\right]kdkd\ell - \frac{3z_1z_2}{F_0}\eta\frac{d\theta_0}{d\eta}, \tag{5.7.38}$$

where the constant Γ_2 is defined by equation (5.7.22).

Similarly equating the coefficient of $\sqrt{t}$ in equations (5.7.6) and (5.7.8) yields

$$\frac{d^2\theta_{s1}}{d\eta^2} + \frac{z_1^2}{2F_0}\eta\frac{d\theta_{s1}}{d\eta} - \frac{z_1^2}{2F_0}\theta_{s1} = -z_1\left[Pe + \frac{3z_2}{2F_0}\eta\right]\frac{d\theta_{s0}}{d\eta} \tag{5.7.39}$$

and

$$(z_1\tau_0 + \tau_{-1}z_2) - \Gamma_2\left[\frac{z_2}{\varepsilon}\int_0^1 (1-\varepsilon\theta_0)d\eta - z_1\int_0^1 \theta_1 d\eta\right] = 0 \ . \quad (5.7.40)$$

The boundary conditions obtained from the coefficient of $\sqrt{t}$ in (5.7.9) to (5.7.13) are

$$\frac{d\theta_1}{d\eta}(0) = 0 \ , \quad (5.7.41)$$

$$\theta_1(1) = \theta_{s1}(1) \ , \quad (5.7.42)$$

$$\frac{d\theta_1}{d\eta}(1) = \frac{d\theta_{s1}}{d\eta}(1) \ , \quad (5.7.43)$$

$$\theta_{s1}(\eta) \to 0 \quad \text{as} \quad \eta \to \infty \quad (5.7.44)$$

and

$$\tau_0 = -\Gamma_2\theta_1(1) \ . \quad (5.7.45)$$

On substituting the expressions for θ_0 and θ_{s0}, given by equations (5.7.29) and (5.7.35) respectively, into equations (5.7.38) and (5.7.39) respectively the latter become;

$$\frac{d^2\theta_1}{d\eta^2} + \frac{z_1^2}{2Fo}\eta\frac{d\theta_1}{d\eta} + z_1^2\left[Br\tau_{-1}\Gamma_2 - \frac{1}{2Fo}\right]\theta_1 =$$

$$Brz_1\left\{\left[\tau_{-1} - \Gamma_2\chi_0\sum_{n=0}^{\infty} a_{2n}\eta^{2n}\right](2z_2\tau_{-1} + z_1\tau_0) - 2\tau_{-1}(z_2\tau_{-1}+z_1\tau_0)\right\} +$$

$$2Pez_1\chi_0\left[\sum_{m=0}^{\infty}\frac{a_{2m}\eta^{2m+2}}{(2m+2)(2m+3)} - \sum_{m=0}^{\infty}\frac{a_{2m}}{(2m+2)}\right]\sum_{n=0}^{\infty} na_{2n}\eta^{2n} \Big/ \sum_{n=0}^{\infty}\frac{a_{2n}}{2n+3}$$

$$- \frac{3z_1z_2\chi_0}{Fo}\sum_{n=0}^{\infty} na_{2n}\eta^{2n} \quad (5.7.46)$$

and

$$\frac{d^2\theta_{s1}}{d\eta^2} + \frac{z_1^2}{2Fo}\,\eta\,\frac{d\theta_{s1}}{d\eta} - \frac{z_1^2}{2Fo}\,\theta_{s1} = \Gamma_1\left[Pe + \frac{3z_2}{2Fo}\,\eta\right]e^{-z_1^2\eta^2/4Fo}\ , \tag{5.7.47}$$

where the constant Γ_1 is defined by

$$\Gamma_1 = \frac{z_1^2}{\varepsilon\sqrt{\pi Fo}}\left[1 - \frac{\varepsilon\tau - 1}{\Gamma_2}\right]\Bigg/\,\mathrm{erfc}(z_1/2\sqrt{Fo})\ . \tag{5.7.48}$$

Similarly substituting (5.7.29) into (5.7.40) yields

$$z_1\tau_0 + z_2/z_1 = z_1\Gamma_2\int_0^1 \theta_1 d\eta\ . \tag{5.7.49}$$

Defining the constant Γ_0 by

$$\Gamma_0 = \sum_{n=0}^{\infty}\frac{a_{2n}}{(2n+3)}\ , \tag{5.7.50}$$

and noting that

$$\sum_{m=0}^{\infty}\frac{a_{2m}\eta^{2m+2}}{(2m+2)(2m+3)}\sum_{n=0}^{\infty}na_{2n}\eta^{2n} = \sum_{n=0}^{\infty}d_{2n}\eta^{2n+2} \tag{5.7.51}$$

provided that the coefficients d_{2n} are given by

$$d_{2n} = \sum_{j=0}^{n}\frac{(n-j)a_{2j}a_{2(n-j)}}{(2j+2)(2j+3)}\ ,\ n \geq 0\ , \tag{5.7.52}$$

equation (5.7.46) may be reduced to

$$\frac{d^2\theta_1}{d\eta^2} + \frac{z_1^2}{2Fo}\,\eta\,\frac{d\theta_1}{d\eta} + m_1\theta_1 = -\tau_0\left[m_2 + m_5\sum_{n=0}^{\infty} a_{2n}\eta^{2n}\right]$$

$$- z_2\sum_{n=0}^{\infty}(m_3+nm_4)a_{2n}\eta^{2n} + \sum_{n=0}^{\infty}\left[m_6 d_{2n}\eta^2 - m_7 n a_{2n}\right]\eta^{2n} \qquad (5.7.53)$$

where the constants m_1, m_2, m_3, m_4, m_5, m_6 and m_7 are defined by

$$\left.\begin{aligned} m_1 &= z_1^2\left[Br\tau_{-1}\Gamma_2 - \frac{1}{2Fo}\right], \quad m_2 = Brz_1^2\tau_{-1}, \\ m_3 &= 2Brz_1\chi_0\tau_{-1}\Gamma_2, \qquad m_4 = \frac{3z_1\chi_0}{Fo}, \\ m_5 &= Brz_1^2\chi_0\Gamma_2, \qquad m_6 = \frac{2Pez_1\chi_0}{\Gamma_0} \end{aligned}\right\} \qquad (5.7.54)$$

and

$$m_7 = \frac{2Pez_1\chi_0}{\Gamma_0}\sum_{m=0}^{\infty}\frac{a_{2m}}{2m+2}.$$

Denoting the complementary function and particular integral by θ_{1c} and θ_{1p} respectively we write

$$\theta_1 = \theta_{1c} + \theta_{1p}. \qquad (5.7.55)$$

The form of the left hand side of equation (5.7.53) differs from the left hand side of (5.7.14) in that the term $Br\tau_{-1}z_1^2\Gamma_2$ in the latter is replaced by m_1, thus the form of the complementary function to (5.7.53) can be obtained from (5.7.25) and (5.7.27) by replacing $Br\tau_{-1}z_1^2\Gamma_2$ by m_1 giving us

$$\theta_{1c} = \psi_0\sum_{n=0}^{\infty} e_n\eta^n \quad \text{with} \quad e_0 = 1, \qquad (5.7.56)$$

where the e_n's are generated by the recurrence relation

$$e_{n+2} = -\left[\frac{z_1^2 n/2Fo+m_1}{(n+1)(n+2)}\right] e_n, \quad n \geq 0 , \tag{5.7.57}$$

and ψ_0 is a constant. It is convenient to divide the solution to the particular integral into three parts, thus

$$\theta_{1p} = \tau_0 \sum_{n=1}^{\infty} p_{2n}\eta^{2n} + z_2 \sum_{n=1}^{\infty} q_{2n}\eta^{2n} + \sum_{n=1}^{\infty} r_{2n}\eta^{2n} . \tag{5.7.58}$$

On substituting this expression into equation (5.7.53) we obtain the identity

$$\tau_0 \sum_{n=1}^{\infty} \left[2n(2n-1)\eta^{-2} + \frac{nz_1^2}{Fo} + m_1\right] p_{2n}\eta^{2n} +$$

$$z_2 \sum_{n=1}^{\infty} \left[2n(2n-1)\eta^{-2} + \frac{nz_1^2}{Fo} + m_1\right] q_{2n}\eta^{2n} +$$

$$\sum_{n=1}^{\infty} \left[2n(2n-1)\eta^{-2} + \frac{nz_1^2}{Fo} + m_1\right] r_{2n}\eta^{2n} \equiv$$

$$-\tau_0 \left[m_2+m_5 \sum_{n=0}^{\infty} a_{2n}\eta^{2n}\right] - z_2 \sum_{n=0}^{\infty} (m_3+nm_4) a_{2n}\eta^{2n} + \sum_{n=0}^{\infty} \left[m_6 d_{2n}\eta^2 - m_7 n a_{2n}\right]\eta^{2n} . \tag{5.7.59}$$

It is now easily deduced from the above that the coefficients p_{2n}, q_{2n} and r_{2n} can be generated by the difference equations

$$\left.\begin{aligned} p_{2n+2} &= -\frac{\left[(z_1^2 n/Fo+m_1)p_{2n}+m_5 a_{2n}\right]}{(2n+1)(2n+2)}\ ,\ n \geq 1 \\ p_2 &= -(m_2+m_5)/2\ , \end{aligned}\right\} \qquad (5.7.60)$$

$$\left.\begin{aligned} q_{2n+2} &= -\frac{\left[(z_1^2 n/Fo+m_1)q_{2n}+(m_3+m_{4n})a_{2n}\right]}{(2n+1)(2n+2)}\ ,\ n \geq 1 \\ q_2 &= -\,m_3/2 \end{aligned}\right\} \qquad (5.7.61)$$

and

$$\left.\begin{aligned} r_{2n+2} &= -\frac{\left[(z_1^2 n/Fo+m_1)r_{2n}-m_6 d_{2n-2}+m_7 n a_{2n}\right]}{(2n+2)(2n+1)}\ ,\ n \geq 1 \\ r_2 &= 0 \end{aligned}\right\} \qquad (5.7.62)$$

Substituting equations (5.7.56) and (5.7.58) into equation (5.7.55) and applying the boundary condition (5.7.41) to the resulting expression it is clear that the coefficient e_1 is zero. It then follows from the recurrence relation (5.7.57) that

$$e_{2n+1} = 0\ ,\ n \geq 0\ . \qquad (5.7.63)$$

In view of this result the general solution for θ_1 may then be expressed, with the aid of (5.7.56), (5.7.58) and (5.7.55), in the form

$$\theta_1 = \psi_0 \sum_{n=0}^{\infty} e_{2n}\eta^{2n} + \tau_0 \sum_{n=1}^{\infty} p_{2n}\eta^{2n} + z_2 \sum_{n=1}^{\infty} q_{2n}\eta^{2n} + \sum_{n=1}^{\infty} r_{2n}\eta^{2n}\ ,\ 0 \leq \eta \leq 1\ , \qquad (5.7.64)$$

where the e_{2n}'s are generated by

$$\left.\begin{aligned} e_{2n+2} &= -\frac{\left[z_1^2 n/Fo+m_1\right]e_{2n}}{(2n+1)(2n+2)},\ n \geq 0 \\ e_0 &= 1 \end{aligned}\right\}. \qquad (5.7.65)$$

Substituting equation (5.7.64) into conditions (5.7.40) and (5.7.45) leads, after some algebra, to a pair of linear equations connecting τ_0, z_2 and ψ_0, namely

$$k_1\tau_0 + k_2 z_2 + k_3\psi_0 = k_4 \tag{5.7.66}$$

and

$$k_5\tau_0 + k_6 z_2 + k_7\psi_0 = k_8 , \tag{5.7.67}$$

where the constants k_1, k_2, k_3, k_4, k_5, k_6, k_7 and k_8 are defined by

$$k_1 = z_1\left[1 + \Gamma_2 \sum_{n=1}^{\infty} \frac{p_{2n}}{2n+1}\right] , \tag{5.7.68}$$

$$k_2 = \left[\frac{1}{z_1} + z_1\Gamma_2 \sum_{n=1}^{\infty} \frac{q_{2n}}{2n+1}\right] , \tag{5.7.69}$$

$$k_3 = \Gamma_2 z_1 \sum_{n=0}^{\infty} \frac{e_{2n}}{2n+1} , \quad k_4 = -\Gamma_2 z_1 \sum_{n=1}^{\infty} \frac{r_{2n}}{2n+1} , \tag{5.7.70}$$

$$k_5 = 2 + 2\Gamma_2 \sum_{n=1}^{\infty} p_{2n}, \quad k_6 = 2\Gamma_2 \sum_{n=1}^{\infty} q_{2n}, \tag{5.7.71}$$

$$k_7 = 2\Gamma_2 \sum_{n=0}^{\infty} e_{2n} \quad \text{and} \quad k_8 = -2\Gamma_2 \sum_{n=1}^{\infty} r_{2n} \tag{5.7.72}$$

The solution to equation (5.7.47) satisfying the boundary condition (5.6.43) is readily seen to be

$$\theta_{s1} = A_{s1}\left[\frac{z_1\eta}{2\sqrt{Fo}}\,\mathrm{erfc}\left(\frac{z_1\eta}{2\sqrt{Fo}}\right) - \frac{1}{\sqrt{\pi}}\,e^{-z_1^2\eta^2/4Fo}\right] - \frac{\Gamma_1}{z_1^2}\left[PeFo + z_2\eta\right]e^{-z_1^2\eta^2/4Fo} \tag{5.7.73}$$

On substituting equations (5.7.64) and (5.7.73) into the condition (5.7.42) we deduce after some algebra that the constant A_{s1} is given by

$$A_{s1} = \frac{1}{\ell_1}\left\{\psi_0 \sum_{n=0}^{\infty} e_{2n} + \tau_0 \sum_{n=1}^{\infty} p_{2n} + z_2\left[\sum_{n=1}^{\infty} q_{2n} + \frac{\Gamma_1}{z_1^2}\,e^{-z_1^2/4Fo}\right]\right.$$

$$\left. + \left[\sum_{n=1}^{\infty} r_{2n} + \frac{\Gamma_1}{z_1^2}\,PeFo\,e^{-z_1^2/4Fo}\right]\right\} \tag{5.7.74}$$

where the constant ℓ_1 is given by

$$\ell_1 = \frac{z_1}{2\sqrt{Fo}}\,\mathrm{erfc}(z_1/2\sqrt{Fo}) - \frac{1}{\sqrt{\pi}}\,e^{-z_1^2/4Fo} \tag{5.7.75}$$

Finally making use of the condition (5.7.43) we obtain, with the aid of equations (5.7.64), (5.7.73) and (5.7.74), after some algebra, a further linear equation in z_2, τ_0 and ψ_0, namely

$$k_9\tau_0 + k_{10}z_2 + k_{11}\psi_0 = k_{12}\ , \tag{5.7.76}$$

where the constants k_9, k_{10}, k_{11} and k_{12} are defined by

$$k_9 = 2\sum_{n=1}^{\infty} np_{2n} - \frac{z_1}{2\ell_1\sqrt{Fo}}\,\mathrm{erfc}(z_1/2\sqrt{Fo})\sum_{n=1}^{\infty} p_{2n}\ , \tag{5.7.77}$$

$$k_{10} = 2\sum_{n=1}^{\infty} nq_{2n} - \frac{z_1}{2\ell_1\sqrt{Fo}}\,\mathrm{erfc}(z_1/2\sqrt{Fo})\left[\sum_{n=1}^{\infty} q_{2n} + \frac{\Gamma_1}{z_1^2}\,e^{-z_1^2/4Fo}\right] -$$

$$\Gamma_1\left(\frac{1}{2Fo} - \frac{1}{z_1^2}\right)e^{-z_1^2/4Fo}\ , \tag{5.7.78}$$

$$k_{11} = 2 \sum_{n=0}^{\infty} n e_{2n} - \frac{z_1}{2\ell_1\sqrt{F_0}} \operatorname{erfc}(z_1/2\sqrt{F_0}) \sum_{n=0}^{\infty} e_{2n} \qquad (5.7.79)$$

and

$$k_{12} = -2 \sum_{n=1}^{\infty} n r_{2n} + \frac{z_1}{2\ell_1\sqrt{Fo}} \operatorname{erfc}(z_1/2\sqrt{Fo}) \left[\sum_{n=1}^{\infty} r_{2n} + \frac{\Gamma_1 PeFo}{z_1^2} e^{-z_1^2/4Fo} \right] + \frac{\Gamma_1 Pe}{2} e^{-z_1^2/4Fo} \qquad (5.7.80)$$

Using Cramer's rule we deduce from equations (5.7.66), (5.7.67) and (5.7.76) that z_2, τ_0 and ψ_0 are given by

$$z_2 = \frac{1}{\Delta} \left[k_1(k_8k_{11} - k_{12}k_7) - k_4(k_5k_{11} - k_9k_7) + k_3(k_5k_{12} - k_9k_8) \right], \qquad (5.7.81)$$

$$\tau_0 = \frac{1}{\Delta} \left[k_4(k_6k_{11} - k_{10}k_7) - k_2(k_8k_{11} - k_{12}k_7) + k_3(k_8k_{10} - k_{12}k_6) \right], \qquad (5.7.82)$$

and

$$\psi_0 = \frac{1}{\Delta} \left[k_1(k_6k_{12} - k_{10}k_8) - k_2(k_5k_{12} - k_9k_8) + k_4(k_5k_{10} - k_9k_6) \right] \qquad (5.7.83)$$

where the determinant Δ is given by

$$\Delta = k_1(k_6k_{11} - k_{10}k_7) - k_2(k_5k_{11} - k_9k_7) + k_3(k_5k_{10} - k_9k_6) \qquad (5.7.84)$$

Values of z_2 and τ_0 computed from equations (5.7.81) and (5.7.82) respectively are presented and compared with the corresponding values from the approximate solution, given by (5.4.36a) and (5.4.36b), in Figure (5.5). It is noticed from these plots that the agreement is very poor for $Br < 1$ but for Br in the range $1.0 < Br < 3.0$ the approximate method is quite good.

The heat balance method does not seem as accurate here as for the case of the viscous fluid. This is probably due to the form shown for

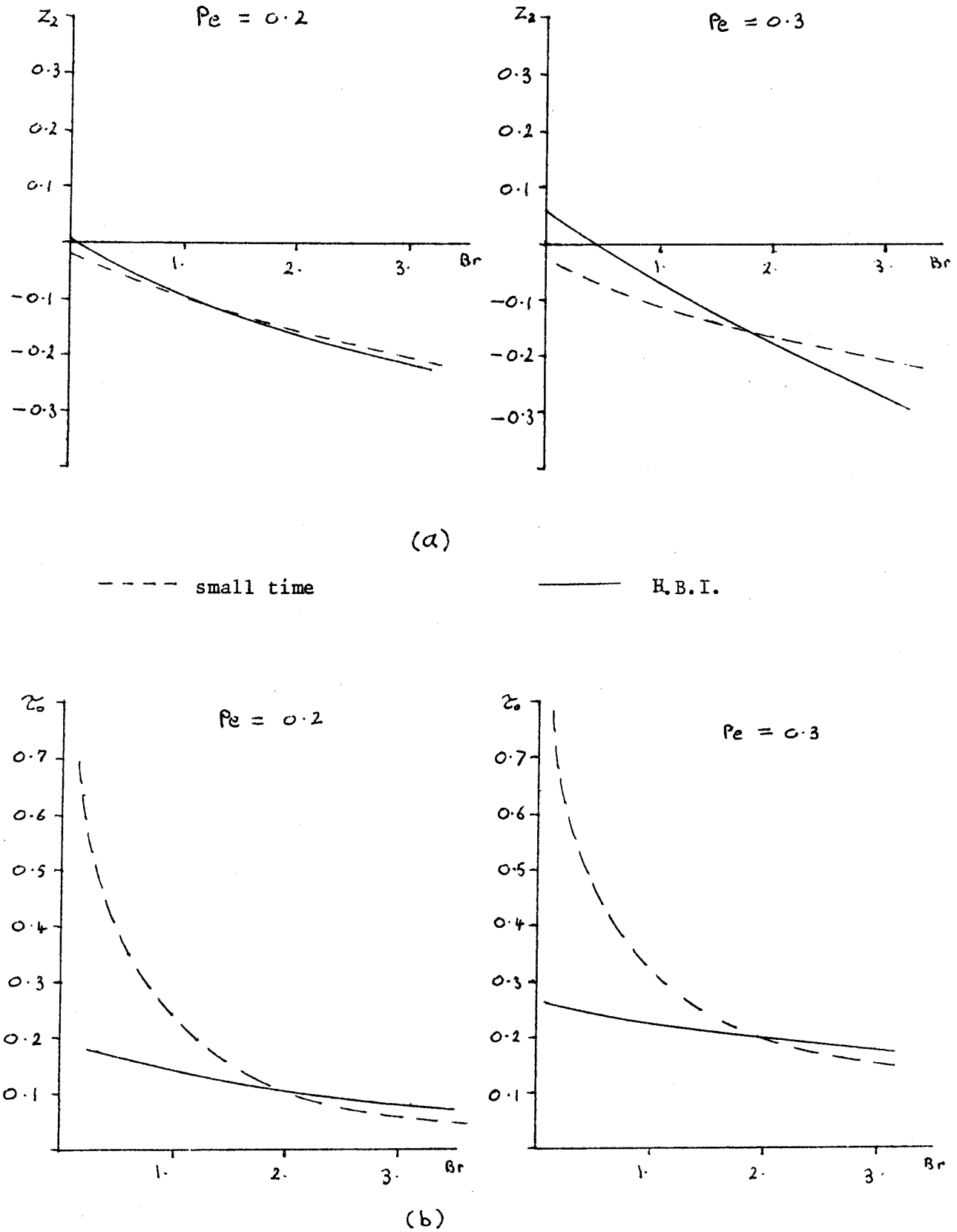

Figure 5.5 (a) Plots of z_2 against Br, (b) Plots of τ_0 against Br.

the temperature profile in the solid region and it is thus felt that the introduction of the thermal boundary layer is the more accurate approach.

5.8 Steady State Series Solution

In this section we solve the partial differential equations (5.1.8) and (5.1.9) subject to the boundary conditions (5.1.15) to (5.1.18), (5.2.4) and (5.3.4) for the steady state case. Firstly we derive the steady state form, of the above mentioned system, which is obtained by taking all quantities to be independent of time; consequently all derivatives with respect to t vanish leaving us with a system of ordinary differential equations.

Denoting steady state quantities by a suffix, ∞ , the steady state form of equation (5.1.8) may be expressed, with the aid of equations (5.2.7), (5.2.18) and (5.3.5) in the form;

$$\frac{d^2\theta_\infty}{dz^2} + \frac{Br\tau_\infty}{2}\left[2\tau_\infty - \frac{B(1-\varepsilon\theta_\infty)}{(1-\varepsilon)}\right] = PeCo_\infty \int_0^z \int_{zp_\infty}^{\ell} \left[2\tau_\infty - \frac{B\left[1-\varepsilon\theta_\infty(k)\right]}{(1-\varepsilon)}\right] kdkd\ell \frac{d\theta_\infty}{dz} , \quad 0 \leq z \leq zp_\infty \tag{5.8.1}$$

where the constant Co_∞ , obtained from equation (5.2.21) with the aid of (5.2.7) and (5.3.5), is given by

$$C_{O\infty} = -1 \Big/ \int_0^{zp_\infty} \int_{zp_\infty}^{\ell} \left[2\tau_\infty - \frac{B\left[1-\varepsilon\theta_\infty(k)\right]}{(1-\varepsilon)}\right] kdkd\ell \ . \tag{5.8.2}$$

Similarly the steady state form of equation (5.1.9), again assuming that equation (5.2.20) holds, is readily seen to be

$$\frac{d^2\theta_s}{dz^2} = - Pe \frac{d\theta_{s\infty}}{dz} , \quad z \geq z_{p\infty} \tag{5.8.3}$$

Likewise, with the aid of (5.2.7) and (5.3.5), the steady state forms of the boundary conditions (5.1.15), to (5.1.18), (5.2.4) and (5.3.3) are seen to be

$$\frac{d\theta_\infty}{dz}(0) = 0 , \tag{5.8.4}$$

$$\theta_\infty(z_{p\infty}) = \theta_{s\infty}(z_{p\infty}) , \tag{5.8.5}$$

$$\frac{d\theta_\infty}{dz}(z_{p\infty}) = \frac{d\theta_{s\infty}}{dz}(z_{p\infty}) , \tag{5.8.6}$$

$$\theta_{s\infty}(z) \to 0 \quad \text{as} \quad z \to \infty , \tag{5.8.7}$$

$$\tau_\infty z_{p\infty} - \frac{B}{2} \int_0^{z_{p\infty}} \frac{\left[1-\varepsilon\theta_\infty(z)\right]}{(1-\varepsilon)} dz = 1 \tag{5.8.8}$$

and

$$2\tau_\infty = \frac{B\left[1-\varepsilon\theta_\infty(z_{p\infty})\right]}{(1-\varepsilon)} . \tag{5.8.9}$$

There appears to be no analytical solution to equation (5.8.1), unfortunately, but a series solution may be obtained when the Peclet number Pe is assumed to be small and this solution is given in the following subsection. However, it is a trivial matter to solve (5.8.3) and the solution satisfying condition (5.8.7) is given by

$$\theta_{s\infty} = A_\infty e^{-Pez} , \tag{5.8.10}$$

where A is a constant of integration.

5.8.1 Series solution for small Pe .

Recalling the series approximation, valid for small Pe , to $z_{p\infty}$ obtained from the heat balance integral solution, and given by equation (5.5.14) we note that

$$z_{p\infty} \sim 1/\sqrt{Pe} \quad , \tag{5.8.11}$$

for small Pe . This result and a close inspection of the system of equations (5.8.1) to (5.8.9) leads us to seek series solutions in the form

$$\theta_{\infty}(\zeta, Pe) = \phi_0(\zeta) + \sqrt{Pe}\ \phi_1(\zeta) + Pe\phi_2(\zeta) + \ldots, \tag{5.8.12}$$

$$\zeta_{p\infty}(Pe) = \zeta_0 + \sqrt{Pe}\ \zeta_1 + Pe\zeta_2 + \ldots, \tag{5.8.13}$$

and

$$\tau_{\infty}(Pe) = Pe\tau_2 + Pe^{3/2}\tau_3 + \ldots \ , \tag{5.8.14}$$

where the new variable ζ is defined by

$$\zeta = \sqrt{Pe}\ z \tag{5.8.15}$$

and the quantity ζ_p , following from this definition is given by

$$\zeta_{p\infty} = \sqrt{Pe}\ z_{p\infty}. \tag{5.8.16}$$

Expressing $\theta_{s\infty}$ by equation (5.8.10) and introducing the variable ζ , given by (5.8.15) into equations (5.8.1), (5.8.2), (5.8.4) to (5.8.6), (5.8.8) and (5.8.9) yields, with the aid of (5.8.16),

$$Pe \frac{d^2\theta_\infty}{d\zeta^2} + \frac{Br\tau_\infty}{2}\left[2\tau_\infty - \frac{B(1-\varepsilon\theta_\infty)}{(1-\varepsilon)}\right] =$$

$$C_{o\infty} \int_0^{\zeta} \int_{\zeta_{p\infty}}^{\ell'} \left[2\tau_\infty - \frac{B\left[1-\varepsilon\theta_\infty(k')\right]}{(1-\varepsilon)} k'dk'd\ell' \frac{d\theta_\infty}{d\zeta}\right], \quad 0 \leq \zeta \leq \zeta_{p\infty} \qquad (5.8.17)$$

where the constant $C_{o\infty}$ is given by

$$C_{o\infty} = -Pe^{3/2} \Big/ \int_0^{\zeta_{p\infty}} \int_{\zeta_{p\infty}}^{\ell'} \left[2\tau_\infty - \frac{B\left[1-\varepsilon\theta_\infty(k')\right]}{(1-\varepsilon)} k'dk'd\ell'\right], \qquad (5.8.18)$$

and the boundary conditions

$$\frac{d\theta_\infty}{d\zeta}(0) = 0, \qquad (5.8.19)$$

$$\theta_\infty(\zeta_{p\infty}) = A_\infty e^{-\sqrt{Pe}\,\zeta_{p\infty}} \qquad (5.8.20)$$

$$\frac{d\theta_\infty}{d\zeta}(\zeta_{p\infty}) = -A_\infty\sqrt{Pe}\, e^{-\sqrt{Pe}\,\zeta_p}, \qquad (5.8.21)$$

$$\tau_{\infty p\infty} - \frac{B}{2}\int_0^{\zeta_{p\infty}} \frac{\left[1-\varepsilon\theta_\infty(\zeta)\right]}{(1-\varepsilon)} d\zeta = \sqrt{Pe} \qquad (5.8.22)$$

and

$$2\tau_\infty = \frac{B}{(1-\varepsilon)}\left[1-\varepsilon\theta_\infty(\zeta_{p\infty})\right], \qquad (5.8.23)$$

respectively. Substituting the series (5.8.12), (5.8.13) and (5.8.14) into equations (5.8.17) and (5.8.18) we obtain the identities

$$Pe\frac{d^2\phi_0}{d\zeta^2} + Pe^{3/2}\frac{d^2\phi_1}{d\zeta^2} + Pe^2\frac{d^2\phi_2}{d\zeta^2} + \ldots +$$

$$\frac{BrPe}{2}(\tau_2 + \sqrt{Pe}\,\tau_3 + \ldots)\left[2Pe\tau_2 + \ldots - \frac{B}{(1-\varepsilon)}(1-\varepsilon\phi_0 - \varepsilon\sqrt{Pe}\,\phi_1 - \varepsilon Pe\phi_2 - \ldots)\right]$$

$$\equiv C_{0\infty}\int_0^{\zeta}\int_{\zeta_0+\sqrt{Pe}}^{\ell'}\int_{\zeta_1+Pe\zeta_2+}\left[2Pe\tau_2+\ldots-\frac{B}{(1-\varepsilon)}\left[1-\varepsilon\phi_0(k')-\varepsilon\sqrt{Pe}\,\phi_1(k')-\right.\right.$$

$$\left.\left.-\varepsilon Pe\phi_2(k')\right]\right]k'dk'd\ell'\left[\frac{d\phi_0}{d\zeta} + \sqrt{Pe}\frac{d\phi_1}{d\zeta} + Pe\frac{d\phi_2}{d\zeta} + \ldots\right] , \qquad (5.8.24)$$

and

$$C_{0\infty} = -Pe^{3/2}\Big/\int_0^{\zeta_0+\sqrt{Pe}\,\zeta_1+Pe\zeta_2+\ldots}\int_{\zeta_0+\sqrt{Pe}\,\zeta_1+Pe\zeta_2+\ldots}^{\ell'}\left[2Pe\tau_2+\ldots-\frac{B}{(1-\varepsilon)}\right.$$

$$\left.\left[1-\varepsilon\phi_0(k') - \varepsilon\sqrt{Pe}\,\phi_1(k') - Pe\phi_2(k')-\ldots\right]\right]k'dk'd\ell' . \qquad (5.8.25)$$

Expanding the integral, which appears in equations (5.8.24), by Taylors theorem we can write

$$\int_{\zeta_0+\sqrt{Pe}\,\zeta_1+Pe\zeta_2+\ldots}^{\ell'}\left[2Pe\tau_2+\ldots-\frac{B}{(1-\varepsilon)}\left[1-\varepsilon\theta_0(k') - \varepsilon\sqrt{Pe}\,\phi_1(k') - \varepsilon Pe\phi_2(k')-\ldots\right]\right]$$

$$k'dk' = \int_{\zeta}^{\ell'}\left[2Pe\tau_2+\ldots-\frac{B}{(1-\varepsilon)}\left[1-\varepsilon\phi_0(k')-\varepsilon\sqrt{Pe}\,\phi_1(k')-\varepsilon Pe\phi_2(k')-\ldots\right]\right]k'dk'$$

$$-\sqrt{Pe}\,\zeta_1\zeta_0\left[2Pe\tau_2+\ldots-\frac{B}{(1-\varepsilon)}\left[1-\varepsilon\phi_0(\zeta_0)-\varepsilon\sqrt{Pe}\,\phi_1(\zeta_0)-\varepsilon Pe\phi_2(\zeta_0)-\ldots\right]\right]+\ldots$$

(5.8.26)

Substituting this expansion back into equation (5.8.24), we obtain, after a little regrouping of terms;

$$\frac{Pe\,d^2\phi_0}{d\zeta^2} + Pe^{3/2}\frac{d^2\phi_1}{d\zeta^2} + Pe^2\frac{d^2\phi_2}{d\zeta^2} + \ldots + \frac{BrPe}{2}(\tau_2 + \sqrt{Pe}\,\tau_3 + \ldots)$$

$$\left[2Pe\tau_2 + \ldots - \frac{B}{(1-\varepsilon)}(1-\varepsilon\phi_0 - \varepsilon\sqrt{Pe}\,\phi_1 - \varepsilon Pe\phi_2 - \ldots)\right]$$

$$= -\frac{C_{0\infty}B}{(1-\varepsilon)}\left\{\int_0^{\zeta}\int_{\zeta_0}^{\ell'}\left[1-\varepsilon\phi_0(k')\right]k'dk'd\ell' - \sqrt{Pe}\left[\varepsilon\int_0^{\zeta}\int_{\zeta}^{\ell'}\phi_1(k')k'dk'd\ell' + \right.\right.$$

$$\left.\left.\zeta_1\zeta_0\zeta\left[1-\varepsilon\phi_0(\zeta_0)\right]\right] + \ldots\right\}\left[\frac{d\phi_0}{d\zeta} + \sqrt{Pe}\,\frac{d\phi_1}{d\zeta} + \ldots\right] . \qquad (5.8.27)$$

Expanding the integral in equation (5.8.25) in a similar manner to the above results in the expressions for $C_{0\infty}$,

$$C_0 = \frac{Pe^{3/2}(1-\varepsilon)}{B}\Bigg/\left\{\int_0^{\zeta_0}\int_{\zeta_0}^{\ell'}\left[1-\varepsilon\phi_0(k')\right]k'dk'd\ell' - \right.$$

$$\left.\sqrt{Pe}\left[\varepsilon\int_0^{\zeta_0}\int_{\zeta_0}^{\ell'}\phi_1(k')k'dk'\,d\ell' + \zeta_1\zeta_0^2\left[1-\varepsilon\phi_0(\zeta_0)\right]\right] + \ldots\right\} \qquad (5.8.28)$$

On substituting this expression into equation (5.8.27) and dividing both sides of the resulting expression by Pe results in

$$\frac{d^2\phi_0}{d\zeta^2} + \sqrt{Pe}\,\frac{d^2\phi_1}{d\zeta^2} + Pe\,\frac{d^2\phi_2}{d\zeta^2} + \ldots +$$

$$\frac{Br}{2}\,(\tau_2+\sqrt{Pe}\,\tau_3+\ldots)\left[2Pe\tau_2+\ldots-\frac{B}{(1-\varepsilon)}\,(1-\varepsilon\phi_0-\varepsilon\sqrt{Pe}\,\phi_1-\varepsilon Pe\phi_2\ldots)\right] = -\sqrt{Pe}$$

$$\left\{\int_0^{\zeta}\int_{\zeta_0}^{\ell'}\left[1-\varepsilon\phi_0(k')\right]k'dk'd\ell'-\sqrt{Pe}\left[\varepsilon\int_0^{\zeta}\int_{\zeta_0}^{\ell'}\phi_1(k')k'dk'd\ell' + \zeta\zeta_1\zeta_0\left[1-\varepsilon\phi_0(\zeta_0)\right]\right]\right.$$

$$\left.+\ldots\right\}\left\{1 + \sqrt{Pe}\left[\varepsilon\int_0^{\zeta_0}\int_{\zeta_0}^{\ell'}\phi_1(k')k'dk'd\ell' + \zeta_1\zeta_0^2\left[1-\varepsilon\phi_0(\zeta_0)\right]\right]\Big/\int_0^{\zeta_0}\int_{\zeta_0}^{\ell'}\right.$$

$$\left[1-\varepsilon\phi_0(k')\right]k'dk'd\ell' + \ldots\left.\right\}\left[\frac{d\phi_0}{d\zeta} + \sqrt{Pe}\,\frac{d\phi_1}{d\zeta} + \ldots\right]\Big/\int_0^{\zeta_0}\int_{\zeta_0}^{\ell'}\left[1-\varepsilon\phi_0(k')\right]k'dk'd\ell'+\ldots$$

(5.8.29)

Expressing the constant A_∞ by the series

$$A_\infty = a_0 + \sqrt{Pe}\,a_1 + Pea_2+\ldots \qquad (5.8.30)$$

and substituting this and the series (5.8.12), (5.8.13) and (5.8.14) into the equations (5.8.19) to (5.8.23) and expanding where necessary using Taylors theorem the corresponding forms for the b.c's are

$$\frac{d\phi_0}{d\zeta}(0) + \sqrt{Pe}\,\frac{d\phi_1}{d\zeta}(0) + Pe\,\frac{d\phi_2}{d\zeta}(0) + \ldots = 0 \qquad (5.8.31)$$

$$\phi_0(\zeta_0) + \sqrt{Pe}\left[\phi_1(\zeta_0) + \zeta_1\,\frac{d\phi_0}{d\zeta}(\zeta_0)\right] + Pe\left[\phi_2(\zeta_0) + \zeta_1\,\frac{d\phi_1}{d\zeta}(\zeta_0)\right.$$

$$\left.+\,\zeta_2\,\frac{d\phi_0}{d\zeta} + \frac{\zeta_1^2}{2}\,\frac{d^2\phi_0}{d\zeta^2}(\zeta_0)\right]+\ldots = a_o + (a_1-a_0\zeta_0)\sqrt{Pe}$$

$$+\left[a_2-a_1\zeta_0+a_0(\zeta_0^2/2-\zeta_1)\right]Pe+\ldots, \qquad (5.8.32)$$

$$\frac{d\phi_0}{d\zeta}(\zeta_0) + \sqrt{Pe}\left[\frac{d\phi_1}{d\zeta}(\zeta_0) + \zeta_1 \frac{d^2\phi_0}{d\zeta^2}(\zeta_0)\right] + Pe\left[\frac{d\phi_2}{d\zeta}(\zeta_0) + \zeta_1 \frac{d^2\phi_1}{d\zeta^2}(\zeta_0)\right.$$

$$\left. + \zeta_2 \frac{d^2\phi_0}{d\zeta^2}(\zeta_0) + \frac{\zeta_1^2}{2}\frac{d^3\phi_0}{d\zeta^3}(\zeta_0)\right] + \ldots = -\sqrt{Pe}\, a_0 - (a_1 - a_0\zeta_0)Pe + \ldots, \tag{5.8.33}$$

$$Pe\zeta_0\tau_2 - \frac{B}{2(1-\varepsilon)}\left\{\int_0^{\zeta_0}\left(1-\varepsilon\phi_0(k')\right)dk - \sqrt{Pe}\left[\varepsilon\int_0^{\zeta_0}\phi_1(k')dk' - \zeta_1\right.\right.$$

$$\left.\left[1-\varepsilon\phi_0(\zeta_0)\right]\right] - Pe\left[\varepsilon\int_0^{\zeta_0}\phi_2 d\zeta + \varepsilon\zeta_1\phi_1(\zeta_0) - \zeta_2\left[1-\varepsilon\phi_0(\zeta_0)\right] + \varepsilon\frac{\zeta_1^2}{2}\frac{d\phi_0}{d\zeta}(\zeta_0)\right]$$

$$\left. + \ldots\right\} = \sqrt{Pe}\,. \tag{5.8.34}$$

and

$$2Pe\tau_2 + \ldots = \frac{B}{(1-\varepsilon)}\left\{1-\varepsilon\phi_0(\zeta_0) - \varepsilon\sqrt{Pe}\left[\phi_1(\zeta_0) + \zeta_1\frac{d\phi_0}{d\zeta}(\zeta_0)\right]\right.$$

$$\left. - \varepsilon Pe\left[\phi_2(\zeta_0) + \zeta_1\frac{d\phi_1}{d\zeta}(\zeta_0) + \zeta_2\frac{d\phi_0}{d\zeta}(\zeta_0) + \frac{\zeta_1^2}{2}\frac{d^2\phi_0}{d\zeta^2}(\zeta_0)\right] + \ldots\right\}. \tag{5.8.35}$$

Having now derived the expanded forms of the governing equations and boundary conditions, valid for small Pe, by equating the coefficients of like powers of Pe in the expansions we can obtain a set of subsystems of ordinary differential equations the first two of which are given and solved here.

(i) First order subsystem.

Equating the coefficients of unity in the system of identities (5.8.29) to (5.8.35) results in the equation

$$\frac{d^2\phi_0}{d\zeta^2} + \frac{BrB\tau_2\varepsilon\phi_0}{2(1-\varepsilon)} = \frac{BrB\tau_2}{2(1-\varepsilon)} \tag{5.8.36}$$

and the boundary conditions

$$\frac{d\phi_0}{d\zeta}(0) = 0 , \tag{5.8.37}$$

$$\phi_0(\zeta_0) = a_0 , \tag{5.8.38}$$

$$\frac{d\phi_0}{d\zeta}(\zeta_0) = 0 , \tag{5.8.39}$$

$$\int_0^{\zeta_0} \left[1-\varepsilon\phi_0(k')\right] dk' = 0 \tag{5.8.40}$$

and

$$1 - \varepsilon\phi_0(\zeta_0) = 0 . \tag{5.8.41}$$

The general solution of (5.8.36) which satisfies condition (5.8.37) is readily seen to be

$$\phi_0 = B_0 \cos\zeta\sqrt{\frac{BrB\varepsilon\tau_2}{2(1-\varepsilon)}} + \frac{1}{\varepsilon} \tag{5.8.42}$$

where B_0 is a constant of integration. This expression satisfies the three conditions (5.8.39), (5.8.40) and (5.8.41) only if B_0 is equal to zero, thus the solution for ϕ_0 is

$$\phi_0 = \frac{1}{\varepsilon} \tag{5.8.43}$$

Finally from condition (5.8.38) we deduce that

$$a_0 = \frac{1}{\varepsilon} \tag{5.8.44}$$

(ii) Second order subsystem.

Owing to the simple expression for ϕ_0 given by (5.8.43) the identities (5.8.29) and (5.8.31) to (5.8.35) are greatly simplified and rewritten here for convenience

$$\sqrt{Pe}\,\frac{d^2\phi_1}{d\zeta^2} + Pe\,\frac{d^2\phi_2}{d\zeta^2} + \ldots + \frac{Br}{2}\,(\tau_2+\sqrt{Pe}\,\tau_3+\ldots)\left[2Pe\tau_2 + \frac{B\varepsilon\sqrt{Pe}}{(1-\varepsilon)}\,\phi_1 + \right.$$

$$\left.\frac{B\varepsilon Pe\phi_2}{(1-\varepsilon)} + \ldots\right] = -\,Pe\left[\int_0^{\zeta}\int_{\zeta_0}^{\ell'} \phi_1(k')k'dk'd\ell' \quad \int_0^{\zeta_0}\int_{\zeta_0}^{\ell'} \phi_1(k')k'dk'd\ell'\right]\frac{d\phi_1}{d\zeta} + \ldots$$

(5.8.45)

$$\sqrt{Pe}\,\frac{d\phi_1}{d\zeta}\,(0) + Pe\,\frac{d\phi_2}{d\zeta}\,(0) + \ldots = 0$$

$$\sqrt{Pe}\,\phi_1(\zeta_0) + Pe\left[\phi_2(\zeta_0) + \zeta_1\,\frac{d\phi_1}{d\zeta}(\zeta_0)\right] + \ldots = \sqrt{Pe}\,(a_1-\zeta_0/\varepsilon)$$

$$+ \left[a_2-a_1\zeta_0+(\zeta_0^2/2-\zeta_1)/\varepsilon\right]Pe+\ldots, \qquad (5.8.46)$$

$$\sqrt{Pe}\,\frac{d\phi_1}{d\zeta}\,(\zeta_0) + Pe\left[\frac{d\phi_2}{d\zeta}\,(\zeta_0) + \zeta_1\,\frac{d^2\phi_1}{d\zeta^2}\,(\zeta_0)\right]+\ldots = -\,\frac{1}{\varepsilon}\,\sqrt{Pe} - (a_1-\zeta_0/\varepsilon)Pe+\ldots,$$

(5.8.47)

$$Pe\zeta_0\tau_2 + \frac{B}{2(1-\varepsilon)}\left\{\varepsilon\sqrt{Pe}\int_0^{\zeta_0}\phi_1(k')dk' + Pe\varepsilon\left[\int_0^{\zeta_0}\phi_2(k')dk' + \zeta_1\phi_1(\zeta_0)\right]\right\}$$

$$+ \ldots = \sqrt{Pe} \qquad (5.8.48)$$

and

$$2Pe\tau_2+\ldots = -\,\frac{B}{(1-\varepsilon)}\left\{\varepsilon\sqrt{Pe}\,\phi_1(\zeta_0) + \varepsilon Pe\left[\phi_2(\zeta_0)+\zeta_1\,\frac{d\phi_1}{d\zeta}\,(\zeta_0)\right]\right\} \qquad (5.8.48)$$

Equating the coefficients of $\sqrt{Pe}$ in this system results in the equations

$$\frac{d^2\phi_1}{d\zeta^2} + \frac{BrB\varepsilon\tau_2}{2(1-\varepsilon)}\phi_1 = 0 \tag{5.8.50}$$

with the boundary conditions

$$\frac{d\phi_1}{d\zeta}(0) = 0 \tag{5.8.51}$$

$$\phi_1(\zeta_0) = a_1 - \zeta_0/\varepsilon \tag{5.8.52}$$

$$\frac{d\phi_1}{d\zeta}(\zeta_0) = -\frac{1}{\varepsilon} \tag{5.8.53}$$

$$\frac{B\varepsilon}{2(1-\varepsilon)}\int_0^{\zeta_0} \phi_1(k')dk' = 1 \tag{5.8.54}$$

and

$$\phi_1(\zeta_0) = 0 \tag{5.8.55}$$

The general solution to (5.8.50) satisfying (5.8.51) is obviously

$$\phi_1 = B_1 \cos \zeta\sqrt{\frac{BrB\varepsilon\tau_2}{2(1-\varepsilon)}} \tag{5.8.56}$$

where B_1 is a constant of integration. Substituting this expression into (5.8.54) we obtain the equation

$$\frac{B\epsilon B_1}{2(1-\epsilon)} \operatorname{Sin}\zeta_0 \sqrt{\frac{BrB\epsilon\tau_2}{2(1-\epsilon)}} = \sqrt{\frac{BrB\epsilon\tau_2}{2(1-\epsilon)}}, \tag{5.8.57}$$

and making use of equations (5.8.53) and (5.8.55) results in

$$\operatorname{Cos}\zeta_0 \sqrt{\frac{BrB\epsilon\tau_2}{2(1-\epsilon)}} = 0 \tag{5.8.58}$$

and

$$B_1 \sqrt{\frac{BrB\epsilon\tau_2}{2(1-\epsilon)}} \operatorname{Sin}\zeta_0 \sqrt{\frac{BrB\epsilon\tau_2}{2(1-\epsilon)}} = \frac{1}{\epsilon} \tag{5.8.59}$$

It is now easily deduced from these three equations that B_1, ζ_0 and τ_2 are given by

$$B_1 = \frac{1}{\epsilon}\sqrt{\frac{2(1-\epsilon)}{B}}, \tag{5.8.60}$$

$$\zeta_0 = \frac{\pi}{2}\sqrt{\frac{2(1-\epsilon)}{B}} \tag{5.8.61}$$

and

$$\tau_2 = \frac{1}{Br\epsilon} \tag{5.8.62}$$

Finally condition (5.8.52) and equation (5.8.61) reveal that

$$a_1 = \frac{\pi}{2\epsilon}\sqrt{\frac{2(1-\epsilon)}{B}} \tag{5.8.63}$$

The third order subsystem has been solved but the solution is lengthy and since the first two are adequate to make a useful comparison with the heat balance integral solution it is decided to terminate the series here. Thus with the aid of (5.8.13), (5.8.14), (5.8.16), (5.8.61) and (5.8.62) the expression for $z_{p\infty}$ and τ_∞ may be approximated by

$$z_{p\infty} = \frac{\pi}{2}\sqrt{\frac{2(1-\varepsilon)}{BPe}} + \ldots \qquad (5.8.64)$$

and

$$\tau_{\infty} = \frac{Pe}{Br\varepsilon} + \ldots \qquad (5.8.65)$$

respectively.

5.8.2 Results and Discussion

Comparison of (5.8.64) with the leading term in the corresponding expression for the approximate solution (5.5.12) reveals that they differ only by a numerical factor. Since $\pi/\sqrt{2} \approx 2.222$ and $\sqrt{6} \approx 2.449$ the error is about 10%. However, comparing (5.8.65) with (5.5.13) we see that to a first approximation the shear stresses are identical. This gives us further indication that the errors in heat balance method for earlier times are probably due to the form of the temperature profile assumed in the solid region.

Finally we make a brief comparison of the solution with Bahrani et al. [18]. They solved the steady state problem again assuming that Pe is small and consequently reglecting the effect of convection in the plastic region altogether. A temperature dependent yield stress of the form

$$\bar{\sigma}_0(\theta) = \bar{G}_0 + \bar{\varepsilon}(\bar{\theta}_0 - \bar{\theta}) \qquad (5.8.66)$$

was assumed whe $\bar{\theta}_0$ is the interface temperature. Assuming $\bar{\sigma}_0$ falls to zero at melting temperature $\bar{\theta}_m$ the above is expressed as

$$\bar{\sigma}_0(\theta) = \bar{\varepsilon}(\bar{\theta}_m - \bar{\theta}) \ . \qquad (5.8.67)$$

Non-dimensionalising this expression gives

$$\sigma_0 = \varepsilon(\theta_m - \theta) \ . \tag{5.8.68}$$

where

$$\varepsilon = \bar{\varepsilon} T_B / \sigma_B \ , \tag{5.8.69}$$

T_B and σ_B being typical values of temperature and yield stress respectively. With (5.8.69) it is easy to see that equations (23) and (26) of [18] can be expressed in dimensionless forms

$$\tau = 2\theta_m \frac{Pe}{B\bar{\varepsilon}} \left[1 + \frac{2Pe}{\varepsilon BBr} \right]^{-1} \tag{5.8.70}$$

and

$$z^* = \frac{\pi}{2} \sqrt{\frac{1}{2\theta_m PeB \left[\varepsilon + 2Pe/BrB \right]}} \tag{5.8.71}$$

respectively. Comparing these expressions with (5.8.64) and (5.8.65) we note that the leading terms differ only by numerical constants. This is due to slight differences in definition of σ_0 and scaling. Thus this solution is a first order approximation to the exact solution. The following terms in the expansion for small Pe will be error due to the neglect of convection.

Bahrani used equation (27) to determine an upper bound on the thickness of the plastic region. It must be remembered that this expression is valid for small Pe only. Let us briefly examine the implications of small Pe . Using definition (3.4.38) we see that a small value of Pe implies either z_{p_o} is small or W_∞ is small.

Bahrani et al. assumed z_{p_o} to be small and confined to zone A [5]. Hence expression (27) in [18] could be assumed to be valid for larger values of W_∞ leading to the small values of z^* and consequently lower values of μ through (26) which is compatible with definition (3.4.21). However, it is felt that the region of plastic flow extends through zone B and into zone C where temperatures O (700^oc) have been reported [5]. In this case (27) is only valid for small W_∞ in which case the small values of z^* will not be observed.

CHAPTER 6

THE UPSET COLLAR

6.0 Introduction

So far in this thesis we have examined the mechanisms that are present within the confinement of the tube walls (that is, with respect to the 2-dimensional model between the limits $-\frac{1}{2} \leq x \leq \frac{1}{2}$). However, on all friction welds an upset collar is formed by the material that is expelled from the plastic region across the surfaces $x = \pm \frac{1}{2}$. It is of interest to examine the motion in the regions $|x| > \frac{1}{2}$ in order to predict the shape of the collar.

In this chapter a simple fluid model, compatable with the model in Chapter 4, is developed in order to gain insight into the mechanisms involved.

Again we consider only thin walled tubes and all the assumptions of Section 4.8 are made. With the assumption of symmetry about $x = 0$ we need only consider the extruded zone, $x \geq \frac{1}{2}$, and we are thus confronted with the problem of a viscous fluid bounded by the surfaces $x = \frac{1}{2}$, $L_I(x,z,t)$ and $L_0(x,z,t)$. (See Figure 6.1).

Recalling the equations governing the motion in the domain $0 \leq \bar{x} \leq \frac{1}{2} h$, $0 \leq \bar{z} \leq \bar{z}_p$, (4.2.7) to (4.2.11), we note that the dominant terms are the hydrostatic pressure terms. We shall assume here that the same equations can be applied in the extruded region. Then to a first approximation, neglecting the effect of any motion in this region, P_A, is balanced by the surface forces in L_0 and L_I.

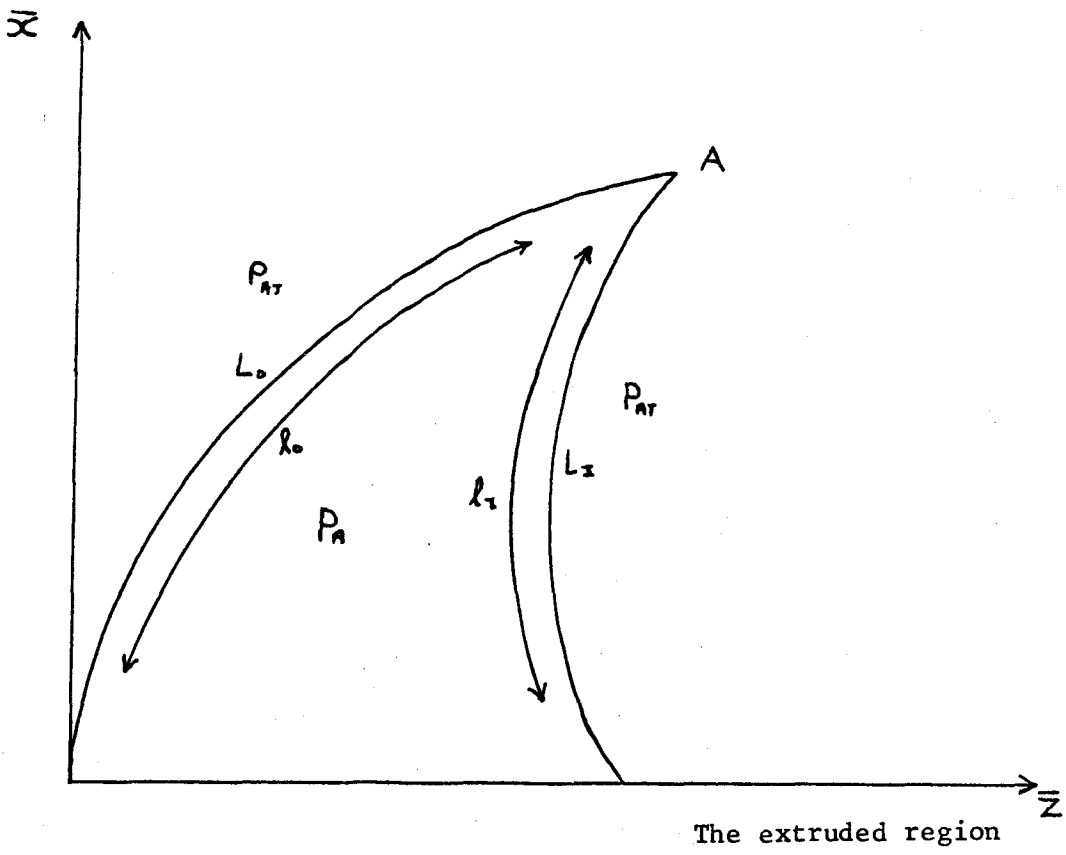

Figure 6.1

Thus the problem can therefore be assumed to be quasi-steady; that is, although the problem is overall time dependent we assume that at any given time the system is in a state of static equilibrium.

Before we can proceed further the nature of the surface forces on L_0 and L_I must be established. It is usually appropriate in this sort of problem to assume that the surface forces are due to surface tension. However, when a surface is constrained by surface tension, the pressure on the concave side must exceed that on the convex side of the surface. Clearly this is true in the case of surface L_0 but unfortunately the converse is true for surface L_I. By comparing the orders of magnitude of the pressure P_A with the atmospheric pressure P_{AT}, clearly the pressure on the convex side of L_I is far greater than that on the concave side, and it therefore seems necessary for the surface

L_I to possess a certain amount of stiffness.

The simplest way to model this stiffness is to assume that L_I behaves as an elastic beam. The surface forces are then easily calculated and the stiffness is given by the product $E_I I_I$ where E_I is Youngs modulus and I_I is the second moment of area of the surface L_I. We shall assume the beam is inextensible but has temperature dependent stiffness. The forces in the surface L_0 could be modelled by surface tension, however, the analysis is simplified if we model this surface as another elastic beam, with a different stiffness $E_0 I_0$.

The lengths of L_0 and L_I are denoted by $\ell_0(t)$ and $\ell_I(t)$ respectively and are determined with the aid of the model presented in Section 4.8. The cusp, that is the point A at which the surfaces L_0 and L_I are joined (see Figure 6.1) appears to come from the original 'corner' $z = 0$, $x = \frac{1}{2}$. Thus the length ℓ_I will be approximately the amount of axial shortening that has taken place, or mathematically

$$\ell_I = W_\infty \bar{t} \ . \qquad (6.0.1)$$

The length ℓ_0 is obtained indirectly from the condition of mass conservation, that is the amount of material which crosses the interface $z = z_p$ between the limits $x = 0$ and $x = \frac{1}{2}$ must equal the amount of material that is bounded by the surfaces L_0, L_I and $x = \frac{1}{2}$, $0 \leq z \leq z_p$. This condition leads to an equation which completes a set and allows ℓ_0 to be calculated along with other quantities.

6. Derivation of the Governing Equations and Boundary Conditions

In this section the equations governing the bounding surfaces L_O and L_I, and the boundary conditions to be applied to each surface are derived. Both surfaces are assumed to behave as inextensible perfectly elastic beams of variable thicknesses with temperature dependent stiffnesses. A point P on a beam is identified by four quantities of which only one is independent. These four quantities are the two rectangular coordinates x and z, the arc length s and the deflection angle θ which is the angle between the tangent to the beam at the given point and the x-axis. We shall denote the point P by the symbol $(\bar{x}, \bar{z}, \theta, \bar{s})$. Before we start the analysis let us state the sign conventions that we shall use throughout this chapter. Consider an element of beam of length ds, then with s measured from left to right we take downward loadings w, clockwise acting shear forces F_s and sagging bending moment M as being positive. (See Figure 6.2)

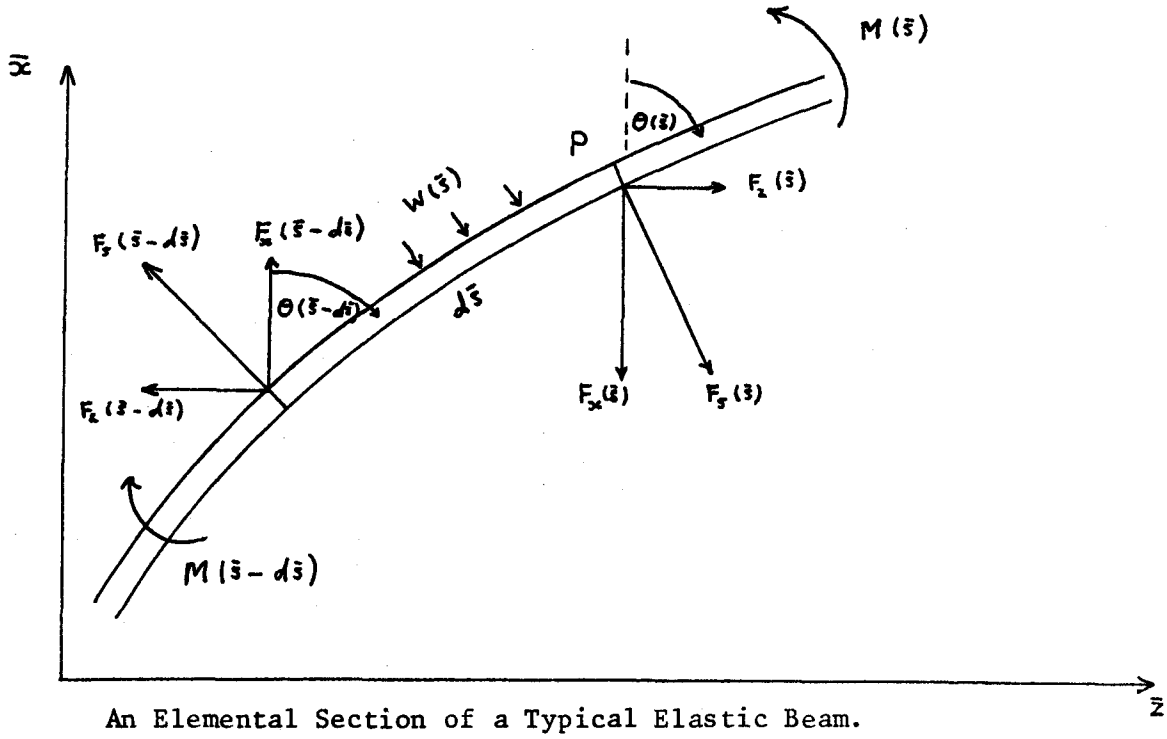

An Elemental Section of a Typical Elastic Beam.

Figure 6.2

Let us now determine the relationships between the quantities W, F_s and M. Suppose that thecomponents of the total force acting parallel to the $\bar{x}$ and $\bar{z}$ directions, at the point $P(\bar{x}, \bar{z}, \theta, \bar{s})$ are F_x and F_z respectively, the positive senses of which are taken to be consistent with our sign conventions (See Figure 6.2). On resolving this pair of force components in the normal direction to the beam at the point $(\bar{x}, \bar{z}, \theta, \bar{s})$ the shear force F_s can be expressed as

$$F_s = F_x \, \mathrm{Sin}\theta + F_z \, \mathrm{Cos}\theta \qquad (6.1.1)$$

In addition on resolving F_x and F_z in the tangential direction at $P(\bar{x}, \bar{z}, \theta, \bar{s})$ one could obtain an expression for the tensile force F_T. However, since we are assuming that the beams are inextensible this force is not required.

Considering the equilibrium of forces in the $\bar{x}$ direction we obtain

$$F_x(\bar{s}-d\bar{s}) - W(\bar{s}) \, \mathrm{Sin}\theta \, d\bar{s} - F_x(\bar{s}) = 0 \qquad (6.1.2)$$

On expanding this equation for small $d\bar{s}$ using Taylor's theorem, dividing by $d\bar{s}$ and taking the limit as $d\bar{s} \to 0$ of the resulting expression, we obtain

$$\frac{dF_x}{d\bar{s}} = - W \, \mathrm{Sin}\theta \quad . \qquad (6.1.3)$$

Similarly from the balance of forces in the $\bar{z}$ direction we have

$$\frac{dF_z}{d\bar{s}} = - W \, \mathrm{Cos}\theta \quad , \qquad (6.1.4)$$

and from the equilibrium of moments we obtain

$$\frac{dM}{d\bar{s}} = F_s \qquad (6.1.5)$$

Having established these basic results, we can now derive the equations governing our system.

Let us firstly describe the system. The beam L_0, which has length $\bar{\ell}_0$, is assumed fixed at the point (0, 0, 0, 0) with the gradient $d\bar{z}_0/d\bar{x}_0$ being zero at this point. The other end of the beam $(\bar{x}_{\ell 0}, \bar{z}_{\ell 0}, \theta_{\ell 0}, \bar{\ell}_0)$ is held by a force of magnitude F_0 whose line of action makes an angle α_0 to the tangent of the curve at the point under discussion. Similarly the beam L_I, which has length ℓ_I, is assumed fixed at the point $(0, \bar{z}_p, -\pi/2, 0)$ with its gradient $d\bar{z}_I/d\bar{x}_I$ becoming infinite on approach to this point. The other end of $L_I(\bar{x}_{\ell I}, \bar{z}_{\ell I}, \theta_{\ell I}, \bar{\ell}_I)$, is held by a force of magnitude F_I whose direction makes an angle α_I to the tangent to the curve at the point under discussion. [See Figure 6.3]. We shall assume that the internal pressure acting on L_0 is $\bar{p}_0$ and that the pressure on L_I is $\bar{p}_I$ where $\bar{p}_0$ and $\bar{p}_I$ are of the same order of magnitude but not necessarily equal.

6.1.1 The Governing Equations

Considering the beam L_0 we shall obtain an expression for the shear force acting at any point. On resolving the force acting at the point $(\bar{x}_{\ell 0}, \bar{z}_{\ell 0}, \theta_{\ell 0}, \bar{\ell}_0)$ into component parallel to $\bar{x}$ and $\bar{z}$ axes, F_{x0} and F_{z0} respectively, we obtain [See Figure 6.3].

$$F_{x0} = - F_0 \, \mathrm{Cos}(\alpha_0 + \theta_{\ell 0}) \tag{6.1.6}$$

and

$$F_{z0} = F_0 \, \mathrm{Sin}(\alpha_0 + \theta_{\ell 0}) \, . \tag{6.1.7}$$

Replacing W by $-\bar{p}_0$ the appropriate forms of (6.1.3) and (6.1.4) are

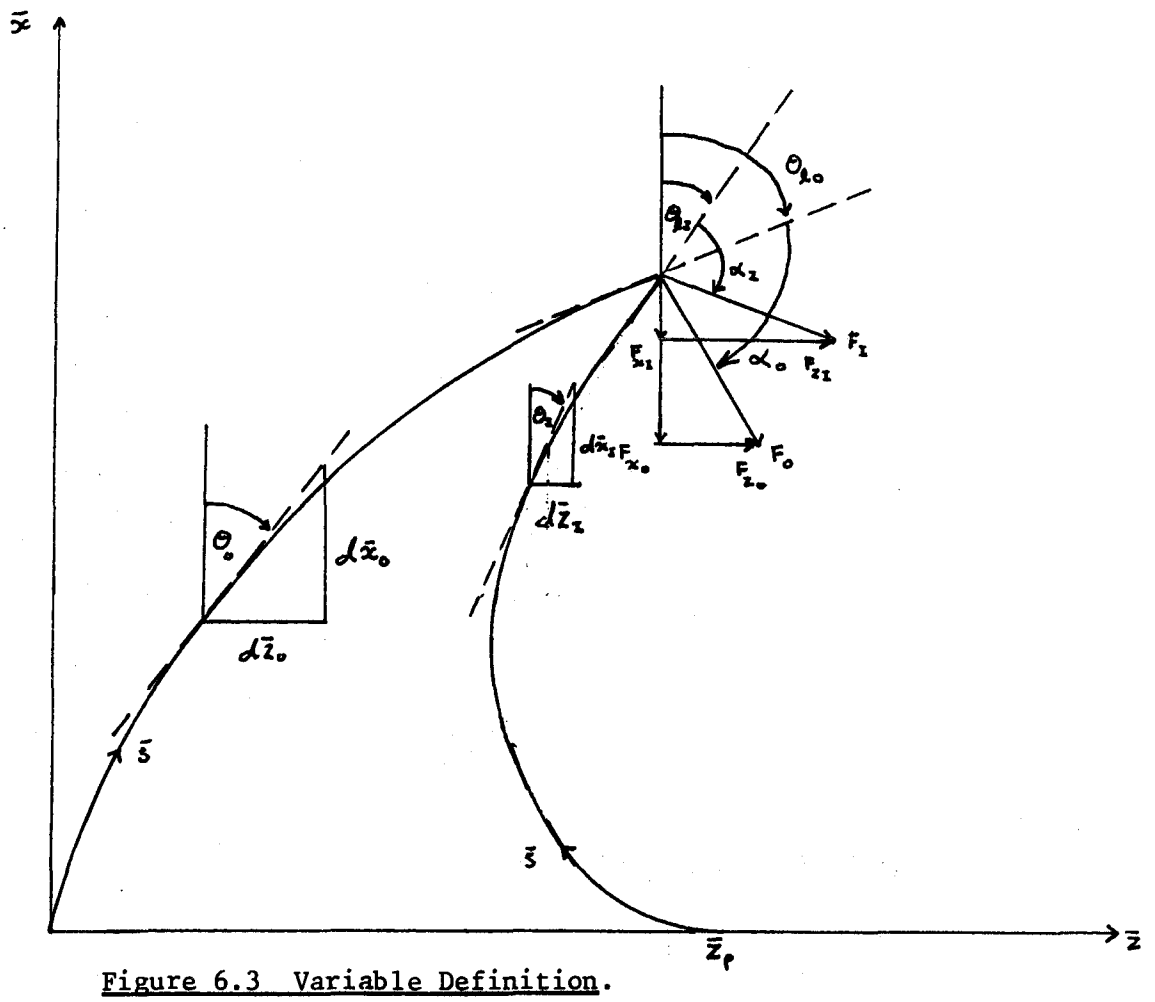

Figure 6.3 Variable Definition.

$$\frac{dF_x}{d\bar{s}} = \bar{p}_0 \text{ Sin } \theta_0 \qquad (6.1.8)$$

and

$$\frac{dF_z}{d\bar{s}} = \bar{p}_0 \text{ Cos } \theta_0 \ . \qquad (6.1.9)$$

The boundary conditions to these equations are

$$F_x(\bar{x}_{\ell 0}, \bar{z}_{\ell 0}, \theta_{\ell 0}, \bar{\ell}_0) = F_{x0} \quad \text{and} \quad F_z(\bar{x}_{\ell 0}, \bar{z}_{\ell 0}, \theta_{\ell 0}, \bar{\ell}_0) = F_{z0} \qquad (6.1.10)$$

respectively where F_{x0} and F_{z0} are given by (6.1.6) and (6.1.7) respectively. Integrating equation (6.1.8) with respect to $\bar{s}$ and applying the boundary condition $(6.1.10)_1$, results, with the aid of (6.1.6), in

$$F_x = - \int_{\bar{s}}^{\bar{\ell}_0} \bar{p}_0 \, \mathrm{Sin}\, \theta_0 d\bar{s} - F_0 \, \mathrm{Cos}(\alpha_0 + \theta_{\ell 0}) \, . \qquad (6.1.11)$$

The corresponding result for force F_z obtained using (6.1.9), $(6.1.10)_2$ and (6.1.7) is

$$F_z = - \int_{\bar{s}}^{\bar{\ell}_0} \bar{p}_0 \, \mathrm{Cos}\theta_0 d\bar{s} + F_0 \, \mathrm{Sin}(\alpha_0 + \theta_{\ell 0}) \qquad (6.1.12)$$

Substituting equations (6.1.11) and (6.1.12) into (6.1.1) yields

$$F_s = -\left[F_0 \mathrm{Cos}(\alpha_0 + \theta_{\ell 0}) + \int_{\bar{s}}^{\bar{\ell}_0} \bar{p}_0 \, \mathrm{Sin}\theta_0 d\bar{s}\right] \mathrm{Sin}\,\theta_0 + \left[F_0 \mathrm{Sin}(\alpha_0 + \theta_{\ell 0}) - \int_{\bar{s}}^{\bar{\ell}_0} \bar{p}_0 \, \mathrm{Cos}\theta_0 d\bar{s}\right] \mathrm{Cos}\theta_0 \, , \qquad (6.1.13)$$

which is an expression for the shear force F_s at the point (x, z, θ, s).

At this stage we make use of the Euler-Bernoulli theorem [37] which states that the bending moment at a given point on a beam is proportional to the curvature at that point. Mathematically the theorem is expressed

$$\bar{E}_0 \bar{I}_0 \frac{d\theta_0}{d\bar{s}} = - M \, , \qquad (6.1.14)$$

where the constant of proportionality is the product of the Youngs modulus, $\bar{E}_0$, and the second moment of area, $\bar{I}_0$, and is called the stiffness. Differentiating both sides of (6.1.14) with respect to $\bar{s}$ and making use of equations (6.1.5) and (6.1.3) gives, after some rearrangement, the ordinary differential equation

$$\frac{d}{d\bar{s}}\left[\bar{E}_O\bar{I}_O\frac{d\theta_O}{d\bar{s}}\right] = -F_O\sin(\alpha_O+\theta_{\ell O}-\theta_O) + \int_{\bar{s}}^{\bar{\ell}_O}\bar{p}_O\cos\theta_O d\bar{s}\cos\theta_O + \int_{\bar{s}}^{\bar{\ell}_O}\bar{p}_O\sin\theta_O d\bar{s}\sin\theta_O,\ 0 \leq \bar{s} \leq \bar{\ell}_O \qquad (6.1.15)$$

Applying a similar analysis to the surface, L_I, one obtains the equation

$$\frac{d}{d\bar{s}}\left[\bar{E}_I\bar{I}_I\frac{d\theta_I}{d\bar{s}}\right] = -F_I\sin(\alpha_I+\theta_{\ell I}-\theta_I) - \int_{\bar{s}}^{\bar{\ell}_I}\bar{p}_I\cos\theta_I d\bar{s}\cos\theta_I - \int_{\bar{s}}^{\bar{\ell}_I}\bar{p}_I\sin\theta_I d\bar{s}\sin\theta_I\ ,\ 0 \leq \bar{s} \leq \bar{\ell}_I \qquad (6.1.16)$$

in the derivation of which the positive sign of p_I was taken since this quantity respresents a downwards loading.

The coordinates $\bar{x}$ and $\bar{z}$ are easily seen to relate to $\bar{s}$ and θ through the equations

$$\frac{d\bar{x}_O}{d\bar{s}} = \cos\theta_O \quad \text{and} \quad \frac{d\bar{z}_O}{d\bar{s}} = \sin\theta_O \qquad (6.1.17)$$

and

$$\frac{d\bar{x}_I}{d\bar{s}} = \cos\theta_I \quad \text{and} \quad \frac{d\bar{z}_I}{d\bar{s}} = \sin\theta_I \qquad (6.1.18)$$

At this stage it is convenient to int roduce the new dimensionless variables

$$\left.\begin{aligned} &s = \bar{s}/\bar{z}_p,\ \ell_O = \bar{\ell}_O/\bar{z}_p,\ \ell_I = \bar{\ell}_I/\bar{z}_p,\ x_O = \bar{x}_O/\bar{z}_p,\ z_O = \bar{z}_O/\bar{z}_p \\ &x_I = \bar{x}_I/\bar{z}_p,\ z_I = \bar{z}_I/\bar{z}_p,\ x_{\ell O} = \bar{x}_{\ell O}/\bar{z}_p,\ z_{\ell O} = \bar{z}_{\ell O}/\bar{z}_p \\ &x_{\ell I} = \bar{x}_{\ell I}/\bar{z}_p,\ z_{\ell I} = \bar{z}_{\ell I}/\bar{z}_p,\ B_O = \bar{E}_O\bar{I}_O/EI,\ B_I = \bar{E}_I\bar{I}_I/EI \\ &f_O = \frac{F_O\bar{z}_p^2}{EI},\ f_I = \frac{F_I\bar{z}_p^2}{EI},\ p_O = \frac{\bar{p}_O\bar{z}_p^3}{EI}\ p_I = \frac{\bar{p}_I\bar{z}_p^3}{EI} \end{aligned}\right\} \qquad (6.1.19)$$

where E and I are typical values of Youngs modulus and the second moment of area respectively. Using these variables the dimension less forms of equations (6.1.15) and (6.1.16) are

$$\frac{d}{ds}\left[B_0 \frac{d\theta_0}{ds}\right] = - f_0 \mathrm{Sin}(\alpha_0+\theta_{\ell 0}-\theta_0) + \int_s^{\ell_0} p_0 \mathrm{Cos}\theta_0 ds \, \mathrm{Cos}\theta_0 + \int_s^{\ell_0} p_0 \mathrm{Sin}\theta_0 ds \mathrm{Sin}\theta_0 , \quad 0 \leq s \leq \ell_0 \tag{6.1.20}$$

and

$$\frac{d}{ds}\left[B_I \frac{d\theta_I}{ds}\right] = - f_I \mathrm{Sin}(\alpha_I+\theta_{\ell I}-\theta_I) - \int_s^{\ell_I} p_I \mathrm{Cos}\theta_I ds \mathrm{Cos}\theta_I - \int_s^{\ell_I} p_I \mathrm{Sin}\theta_I ds \mathrm{Sin}\theta_I , \; 0 \leq s \leq \ell_I \tag{6.1.21}$$

respectively. Similarly equations $(6.1.17)_{1,2}$ and $(6.1.18)_{1,2}$ become

$$\frac{dx_0}{ds} = \mathrm{Cos}\theta_0 \quad \text{and} \quad \frac{dz_0}{ds} = \mathrm{Sin}\theta_0 \tag{6.1.22}$$

and

$$\frac{dx_I}{ds} = \mathrm{Cos}\theta_I \quad \text{and} \quad \frac{dz_I}{ds} = \mathrm{Sin}\theta_I . \tag{6.1.23}$$

6.1.2 The Boundary Conditions

From the condition of attachment at the end $\bar{s} = 0$ of the surface L_0 we can write

$$\bar{x}_0 = 0 \quad \text{and} \quad \bar{z}_0 = 0 \text{ on } \bar{s} = 0 \tag{6.1.24}$$

The slope of the curve at $\bar{s} = 0$ is zero, thus we have

$$\frac{d\bar{z}_0}{d\bar{x}_0} = 0 \quad \text{on} \quad \bar{s} = 0 \ . \tag{6.1.25}$$

From equation $(6.1.17)_{1,2}$ it is easily verified that

$$\frac{d\bar{z}_0}{d\bar{x}_0} = \tan\theta_0 \ , \tag{6.1.26}$$

and hence conditions (6.1.25) can be expressed

$$\theta_0 = 0 \quad \text{on} \quad \bar{s} = 0 \ . \tag{6.1.27}$$

At the other end, $\bar{s} = \bar{\theta}_0$, of the surface L_0 we can write

$$\bar{x}_0 = \bar{x}_{\ell 0}, \ \bar{z}_0 = \bar{z}_{\ell 0} \quad \text{and} \quad \theta_0 = \theta_{\ell 0} \quad \text{on} \quad \bar{s} = \bar{\ell}_0 \tag{6.1.28}$$

and since there is no bending moment at this point we have

$$\frac{d\theta_0}{d\bar{s}} = 0 \quad \text{on} \quad \bar{s} = \bar{\ell}_0 \ . \tag{6.1.29}$$

For the surface L_I the attachment condition at $\bar{s} = 0$ is

$$\bar{x}_I = 0 \quad \text{and} \quad \bar{z}_I = \bar{z}_p \quad \text{on} \quad \bar{s} = 0 \tag{6.1.30}$$

and from consideration of the slope at this point we write

$$\lim_{s \to 0} \frac{d\bar{z}_I}{d\bar{x}_I} \to -\infty \tag{6.1.31}$$

which with the aid of (6.1.26) can be expressed in the form

$$\theta_I = -\pi/2 \quad \text{on} \quad \bar{s} = 0 \tag{6.1.32}$$

At the end $s = \ell_I$ of the surface L_I the conditions are

$$\bar{x}_I = \bar{x}_{\ell I},\ \bar{z}_I = \bar{z}_{\ell I},\ \theta_I = \theta_{\ell I} \quad \text{on} \quad \bar{s} = \bar{\ell}_I \tag{6.1.33}$$

and the zero bending moment implies

$$\frac{d\theta_I}{d\bar{s}} = 0 \quad \text{on} \quad \bar{s} = \bar{\ell}_I \tag{6.1.34}$$

Since the ends $\bar{s} = \bar{\ell}_0$ and $\bar{s} = \bar{\ell}_I$, of the two surfaces L_0 and L_I respectively are coincident we can write

$$\bar{x}_{\ell 0} = \bar{x}_{\ell I} \quad \text{and} \quad \bar{z}_{\ell 0} = \bar{z}_{\ell I}\ , \tag{6.1.35}$$

and as the system is in a state of equilibrium the magnitude of the forces acting at the points $(\bar{x}_{\ell 0},\ \bar{z}_{\ell 0},\ \theta_{\ell 0},\ \bar{\ell}_0)$ and $(\bar{x}_{\ell I},\ \bar{z}_{\ell I},\ \theta_{\ell I},\ \bar{\ell}_I)$ must be equal and act in opposite senses. Thus we can write

$$F_0 = F_I \quad \text{and} \quad \alpha_0 + \theta_{\ell 0} = \alpha_I + \theta_{\ell I} + \pi \tag{6.1.36}$$

Finally we require a condition expressing the conservation of mass. Assuming that all the material that flows over the surface $\bar{z} = \bar{z}_p$ between the limits $\bar{x} = 0$ and $\bar{x} = \frac{1}{2}h$ is expelled into the extruded region we can write

$$\frac{W_\infty \bar{h}t}{2} = \int_0^{\theta_{\ell 0}} \bar{x}_0 \frac{d\bar{z}_0}{d\theta_0}\, d\theta_0 - \int_{-\pi/2}^{\theta_{\ell I}} \bar{x}_I \frac{d\bar{z}_I}{d\theta_I}\, d\theta_I \tag{6.1.37}$$

With the aid of (6.1.19) these conditions can be expressed in the dimensionless form

$$x_0 = 0,\ z_0 = 0,\ \theta_0 = 0 \quad \text{on} \quad s = 0 \tag{6.1.38}$$

$$x_0 = x_{\ell 0},\ z_0 = z_{\ell 0},\ \theta_0 = \theta_{\ell 0},\ d\theta_0/ds = 0 \text{ on } s = \ell_0 \tag{6.1.39}$$

$$x_I = 0,\ z_I = 1,\ \theta_I = -\pi/2 \quad \text{on} \quad s = 0 \tag{6.1.40}$$

$$x_I = x_{\ell I},\ z_I = z_{\ell I},\ \theta_I = \theta_{\ell I},\ d\theta_I/ds = 0 \quad \text{on} \quad s = \ell_I \tag{6.1.41}$$

$$x_{\ell 0} = x_{\ell I},\ z_{\ell 0} = z_{\ell I} \tag{6.1.42}$$

$$f_0 = f_I,\ \alpha_0 + \theta_{\ell 0} = \alpha_I + \theta_{\ell I} + \pi \tag{6.1.43}$$

and

$$\frac{V_m t}{z_p^2\,(t)} = \int_0^{\theta_{\ell 0}} x_0 \frac{dz_0}{d\theta_0}\, d\theta_0 - \int_{-\pi/2}^{\theta_{\ell I}} x_I \frac{dz_I}{d\theta_I}\, d\theta_I \tag{6.1.44}$$

where the constant V_m is defined by

$$V_m = \frac{W_\infty h t_0}{2z_{p0}^2} \ . \tag{6.1.45}$$

and z_p and z_{p0} are defined in chapter 3. (See page 40).

6.2 Solution with Zero Hydrostatic Pressure ($P_0 = P_I = 0$)

There appears to be no analytic solution to the above system of equations and further simplifications must be made if one is to be obtained. In this section we shall neglect the effect of the hydrostatic pressure and assume that

$$P_0 = P_I = 0 \ . \tag{6.2.1}$$

We shall also assume that the stiffnesses B_0 and B_I are both constant but not necessarily equal. In view of (6.1.19) we may therefore take, without loss of generality,

$$B_0 = 1 \quad \text{and} \quad B_I = 1/\delta \tag{6.2.2}$$

where the quantity δ is defined by

$$\delta = E_0 I_0 / E_I I_I \tag{6.2.3}$$

These assumptions simplify our equations considerably and allow an analytic solution to be obtained.

Using assumptions (6.2.1) and (6.2.2) in (6.1.20) and (6.1.21) and making use of condition $(6.1.43)_1$ leads to

$$\frac{d^2\theta_0}{ds^2} = - f_0 \, \text{Sin}(\alpha_0 + \theta_{\ell 0} - \theta_0) \qquad 0 \leq s \leq \ell_0 \tag{6.2.4}$$

and

$$\frac{1}{\delta} \frac{d^2\theta_I}{ds^2} = - f_0 \, \text{Sin}(\alpha_I + \theta_{\ell I} - \theta_I) \, , \qquad 0 \leq s \leq \ell_I \tag{6.2.5}$$

Multiplying equation (6.2.4) by $2d\theta_0/ds$ and integrating the resulting expression with respect to s yields

$$\left(\frac{d\theta_0}{ds}\right)^2 = C_0 - 2f_0 \, \text{Cos}(\alpha_0 + \theta_{\ell 0} - \theta_0) \, , \tag{6.2.6}$$

where C_0 is a constant introduced through the integration. Using condition $(6.1.39)_4$ to determine C_0 and taking the square root of (6.2.6) results in

$$\frac{d\theta_0}{ds} = \sqrt{2f_0} \left[\text{Cos}\alpha_0 - \text{Cos}(\alpha_0 + \theta_{\ell 0} - \theta_0)\right]^{\frac{1}{2}} \, , \qquad 0 \leq s \leq \ell_0 \tag{6.2.7}$$

where it has been assumed that the curvature $d\theta/ds$ remains positive in the region $0 \leq s \leq \ell_0$. Integrating equation (6.2.5) in a similar manner and using condition $(6.1.41)_4$ to determine the constant of integration gives

$$\frac{d\theta_I}{ds} = \sqrt{2f_0\delta}\left[\mathrm{Cos}\alpha_I - \mathrm{Cos}(\alpha_1+\theta_{\ell I}-\theta_I)\right]^{\frac{1}{2}}, \quad 0 \leq s \leq \ell_I \qquad (6.2.8)$$

where it has again been assumed that the curvature $d\theta_I/ds$ remains positive in the region $0 \leq s \leq \ell_I$. Using the method of separation of variables to integrate equations (6.2.7) and (6.2.8) and using conditions $(6.1.38)_3$ and $(6.1.40)_3$ to determine the constants of integration leads to

$$s\sqrt{2f_0} = \int_0^{\theta_0} \frac{d\theta_0}{\left[\mathrm{Cos}\alpha_0 - \mathrm{Cos}(\alpha_0+\theta_{\ell 0}-\theta_0)\right]^{\frac{1}{2}}} \qquad (6.2.9)$$

and

$$s\sqrt{2f_0\delta} = \int_{-\pi/2}^{\theta} \frac{d\theta_I}{\left[\mathrm{Cos}\alpha_I - \mathrm{Cos}(\alpha_I+\theta_{\ell I}-\theta_I)\right]^{\frac{1}{2}}} \qquad (6.2.10)$$

On making the change of variable through the equation

$$\mathrm{Cos}(\alpha_0+\theta_{\ell 0}-\theta_0) = 2k_0^2\,\mathrm{Sin}^2\phi_0 - 1 , \qquad (6.2.11)$$

where k_0^2 is defined by

$$2k_0^2 = 1 + \mathrm{Cos}\alpha_0 \qquad (6.2.12)$$

it is seen that (See Appendix 1) the integral on the right hand-side of equation (6.2.9) can be transformed into the well known elliptic integral of the first kind $F[31]$ in which case (6.2.) becomes

$$s\sqrt{f_0} = F(\phi_0, k_0) - F(\phi_{\ell 0}, k_0) , \quad \phi_{\ell 0} \leq \phi_0 \leq \pi/2 . \qquad (6.2.13)$$

In the above the elliptic integral F is defined by

$$F(u,\ k) = \int_0^u \frac{dv}{\sqrt{1-k^2 \mathrm{Sin}^2 v}} \tag{6.2.14}$$

and $\phi_{\ell 0}$ is given by the equation

$$\mathrm{Cos}(\alpha_0+\theta_{\ell 0}) = 2k_0^2 \mathrm{Sin}^2 \phi_{\ell 0} - 1 \ . \tag{6.2.15}$$

The equation derived from (6.2.10) and similar to (6.2.13) is

$$s\sqrt{f_0 \delta} = F(\phi_I,\ k_I) - F(\phi_{\ell I},\ k_I) \ , \quad \phi_{\ell I} \leq \phi_I \leq \pi/2 \tag{6.2.16}$$

where k_I, ϕ_I and $\phi_{\ell I}$ are defined by

$$2k_I^2 = 1 + \mathrm{Cos}\alpha_I \ , \tag{6.2.17}$$

$$\mathrm{Cos}(\alpha_I+\theta_{\ell I}-\theta_I) = 2k_I^2 \ \mathrm{Sin}^2 \phi_I - 1 \tag{6.2.18}$$

and

$$\mathrm{Cos}(\alpha_I+\theta_{\ell I}+\pi/2) = 2k_I^2 \ \mathrm{Sin}^2 \phi_{\ell I} - 1 \ . \tag{6.2.19}$$

Using the condition $(6.1.39)_3$ in equation (6.2.13) yields, with the aid of definitions (6.2.11) and (6.2.12),

$$\ell_0 \sqrt{f_0} = F(\pi/2,\ k_0) - F(\phi_{\ell 0},\ k_0) \tag{6.2.20}$$

Similarly, using condition $(6.1.41)_3$ in equation (6.2.16) gives, with the aid of definitions (6.2.17) and (6.2.18),

$$\ell_I \sqrt{f_0 \delta} = F(\pi/2,\ k_I) - F(\phi_{\ell I},\ k_I) \tag{6.2.21}$$

Eliminating the unknown force f_0 from the latter two equations results in

$$F(\pi/2,\ k_0) - F(\phi_{\ell 0},\ k_0) = \frac{\ell_0}{\ell_I \sqrt{\delta}} \left[F(\pi/2,\ k_I) - F(\phi_{\ell I},\ k_I) \right] . \tag{6.2.22}$$

Using the chain rule, equations $(6.1.22)_{1,2}$ and $(6.1.23)_{1,2}$ can be written

$$\frac{dx_0}{d\theta_0} = \cos\theta_0 \Big/ \frac{d\theta_0}{ds} \quad \text{and} \quad \frac{dz_0}{d\theta_0} = \sin\theta_0 \Big/ \frac{d\theta_0}{ds} \tag{6.2.23}$$

and

$$\frac{dx_I}{d\theta_I} = \cos\theta_I \Big/ \frac{d\theta_s}{ds} \quad \text{and} \quad \frac{dz_I}{d\theta_I} = \sin\theta_I \Big/ \frac{d\theta_I}{ds} \tag{6.2.24}$$

respectively. Substituting equations (6.2.7) into $(6.2.23)_{1,2}$ we obtain

$$\frac{dx_0}{d\theta_0} = \frac{\cos\theta_0}{\sqrt{2f_0}\left[\cos\alpha_0 - \cos(\alpha_0+\theta_{\ell 0}-\theta_0)\right]^{\frac{1}{2}}} \tag{6.2.25}$$

and

$$\frac{dz_0}{d\theta_0} = \frac{\sin\theta_0}{\sqrt{2f_0}\left[\cos\alpha_0 - \cos(\alpha_0+\theta_{\ell 0}-\theta_0)\right]^{\frac{1}{2}}}$$

Separating variables and integrating this pair of ordinary differential equations yields with the aid of conditions (6.1.38)

$$x_0 = \frac{1}{\sqrt{2f_0}} \int_0^{\theta_0} \frac{\cos\theta_0 d\theta_0}{\left[\cos\alpha_0 - \cos(\alpha_0+\theta_{\ell 0}-\theta_0)\right]^{\frac{1}{2}}} \tag{6.2.27}$$

and

$$z_0 = \frac{1}{\sqrt{2f_0}} \int_0^{\theta_0} \frac{\sin\theta_0 d\theta_0}{\left[\cos\alpha_0 - \cos(\alpha_0+\theta_{\ell 0}-\theta_0)\right]^{\frac{1}{2}}} \tag{6.2.28}$$

Similarly from (6.2.8), $(6.2.24)_{1,2}$ and $(6.1.40)_3$ we obtain

$$x_I = \frac{1}{\sqrt{2f_0\delta}} \int_{-\pi/2}^{\theta_I} \frac{\cos\theta_I d\theta_I}{\left[\cos\alpha_I - \cos(\alpha_I+\theta_{\ell I}-\theta_I)\right]^{\frac{1}{2}}} \tag{6.2.29}$$

and

$$z_I = \frac{1}{\sqrt{2f_0\delta}} \int_{-\pi/2}^{\theta_I} \frac{\mathrm{Sin}\theta_I d\theta_I}{\left[\mathrm{Cos}\alpha_I - \mathrm{Cos}(\alpha_I + \theta_{\ell I} - \theta_I)\right]^{\frac{1}{2}}} + 1 \qquad (6.2.30)$$

Making the change of variable, given by (6.2.11), in equations (6.2.27) and (6.2.28), the latter can be reduced to

$$x_0 = \left\{(2k_0^2\mathrm{Sin}^2\phi_{\ell 0} - 1)\left[F(\phi_0,k_0) - F(\phi_{\ell 0},k_0) - 2E(\phi_0,k_0) + 2E(\phi_{\ell 0},k_0)\right]\right.$$

$$\left. + 4k_0^2\mathrm{Sin}\phi_{\ell 0}(\mathrm{Cos}\phi_{\ell 0} - \mathrm{Cos}\phi_0)\sqrt{1-k_0^2\mathrm{Sin}^2\phi_{\ell 0}}\right\}/\sqrt{f_0}, \phi_{\ell 0} \leq \phi_0 \leq \pi/2 \quad (6.2.31)$$

and

$$z_0 = \left\{2k_0\mathrm{Sin}\phi_{\ell 0}\sqrt{1-k_0^2\mathrm{Sin}^2\phi_{\ell 0}}\left[F(\phi_0,k_0) - F(\phi_{\ell 0},k_0) - 2E(\phi_0,k_0) + 2E(\phi_{\ell 0},k_0)\right]\right.$$

$$\left. - 2k_0(2k_0^2\mathrm{Sin}^2\phi_{\ell 0} - 1)(\mathrm{Cos}\phi_{\ell 0} - \mathrm{Cos}\phi_0)\right\}/\sqrt{f_0}, \phi_{\ell 0} \leq \phi_{\ell 0} \leq \pi/2 \qquad (6.2.32)$$

where E is in the elliptic integral of the second kind defined by

$$E(u, k) = \int_0^u \sqrt{1-k^2\mathrm{Sin}^2 v}\, dv \qquad (6.2.33)$$

See Appendix for details. Similarly equations (6.2.29) and (6.3.30) reduce to

$$x_I = \left\{2k_I\mathrm{Sin}\phi_{\ell I}\sqrt{1-k_I^2\mathrm{Sin}^2\phi_{\ell I}}\left[F(\phi_I,k_I) - F(\phi_{\ell I},k_I) - 2E(\phi_I,k_I) + 2E(\phi_{\ell I},k_I)\right]\right.$$

$$\left. + 2k_I(1-2k_I^2\mathrm{Sin}^2\phi_{\ell I})(\mathrm{Cos}\phi_{\ell I} - \mathrm{Cos}\phi_I)\right\}/\sqrt{f_0\delta}, \ \phi_{\ell I} \leq \phi_I \leq \pi/2 \quad (6.2.34)$$

and

$$z_I = \left\{(1-2k_I^2\mathrm{Sin}^2\phi_{\ell I})\left[F(\phi_I,k_I) - F(\phi_{\ell I},k_I) - 2E(\phi_I,k_I) + 2E(\phi_{\ell I},k_I)\right]\right.$$

$$\left. - 4k_I^2\mathrm{Sin}\phi_{\ell I}(\mathrm{Cos}\phi_{\ell I} - \mathrm{Cos}\phi_I)\sqrt{1-k_I^2\mathrm{Sin}^2\phi_{\ell I}}\right\}/\sqrt{f_0\delta} + 1, \ \phi_{\ell I} \leq \phi_I \leq \pi/2$$

(6.2.35)

Applying the boundary conditions $(6.1.39)_1$, and $(6.1.39)_2$ to the equations (6.2.31) and (6.2.32) respectively yields with the aid of condition $(6.1.39)_3$ and definitions (6.2.10) and (6.2.12)

$$x_{\ell O} = \left\{ (2k_O^2\mathrm{Sin}^2\phi_{\ell O}-1)\left[F(\pi/2,k_O)-F(\phi_{\ell O},k_O)-2E(\pi/2,k_O)+2E(\phi_{\ell O},k_O)\right] \right.$$
$$\left. + 4k_O^2\mathrm{Sin}\phi_{\ell O}\mathrm{Cos}\phi_{\ell O}\sqrt{1-k_O^2\mathrm{Sin}^2\phi_{\ell O}}\right\}/\sqrt{f_O} \qquad (6.2.36)$$

and

$$z_{\ell O} = \left\{ 2k_O\mathrm{Sin}\phi_{\ell O}\sqrt{1-k_O^2\mathrm{Sin}^2\phi_{\ell O}}\left[F(\pi/2,k_O)-F(\phi_{\ell O},k_O)-2E(\pi/2,k_O)\right.\right.$$
$$\left.\left. + 2E(\phi_{\ell O},k_O)\right] -2k_O(2k_O^2\mathrm{Sin}^2\phi_{\ell O}-1)\mathrm{Cos}\phi_{\ell O}\right\}/\sqrt{f_O} \qquad (6.2.37)$$

Similarly applying the conditions $(6.1.41)_1$ and $(6.1.41)_2$ to the equations (6.2.34) and (6.2.35) respectively gives us with the aid of condition $(6.1.40)_3$ and definition (6.2.17) and (6.2.18)

$$x_{\ell I} = \left\{2k_I\mathrm{Sin}\phi_{\ell I}\sqrt{1-k_I^2\mathrm{Sin}^2\phi_{\ell I}}\left[F(\pi/2,k_I)-F(\phi_{\ell I},k_I)-2E(\pi/2,k_I)\right.\right.$$
$$\left.\left. + 2E(\phi_{\ell I},k_I)\right] + 2k_I(1-2k_I^2\mathrm{Sin}^2\phi_{\ell I})\mathrm{Cos}\phi_{\ell I}\right\}/\sqrt{f_O\delta} \qquad (6.2.38)$$

and

$$z_{\ell I} = \left\{(1-2k_I^2\mathrm{Sin}^2\phi_{\ell I})\left[F(\pi/2,k_I)-F(\phi_{\ell I},k_I)-2E(\pi/2,k_I)+2E(\phi_{\ell I},k_I)\right]\right.$$
$$\left. -4k_I^2\mathrm{Sin}\phi_{\ell I}\mathrm{Cos}\phi_{\ell I}\sqrt{1-k_I^2\mathrm{Sin}^2\phi_{\ell I}}\right\}/\sqrt{f_O\delta} + 1 \qquad (6.2.39)$$

Now substituting equations (6.2.36) and (6.2.38) into conditions $(6.1.42)_1$ and equation (6.2.37) and (6.2.39) into condition $(6.1.42)_2$ results in the pair of equations

$$(2k_0^2\mathrm{Sin}^2\phi_{\ell O}-1)\left[F(\pi/2,k_0)-F(\phi_{\ell O},k_0)-2E(\pi/2,k_0)+2E(\phi_{\ell O},k_0)\right] +$$

$$4k_0^2\mathrm{Sin}\phi_{\ell O}\mathrm{Cos}\phi_{\ell O}\sqrt{1-k_0^2\mathrm{Sin}^2\phi_{\ell O}} = \left\{2k_I\mathrm{Sin}\phi_{\ell I}\sqrt{1-k_I^2\mathrm{Sin}^2\phi_{\ell I}}\left[F(\pi/2,k_I)\right.\right.$$

$$\left.\left.-F(\phi_{\ell I},k_I)-2E(\pi/2,k_I)+2E(\phi_{\ell I},k_I)\right] + 2k_I(1-2k_I^2\mathrm{Sin}^2\phi_{\ell I})\mathrm{Cos}\phi_{\ell I}\right\}\sqrt{\delta} \tag{6.2.40}$$

and

$$2k_0\mathrm{Sin}\phi_{\ell O}\sqrt{1-k_0^2\mathrm{Sin}^2\phi_{\ell O}}\left[F(\pi/2,k_0)-F(\phi_{\ell O},k_0)-2E(\pi/2,k_0)+2E(\phi_{\ell O},k_0)\right]$$

$$- 2k_0(2k_0^2\mathrm{Sin}^2\phi_{\ell O}-1)\mathrm{Cos}\phi_{\ell O} = \left\{(1-2k_I^2\mathrm{Sin}^2\phi_{\ell I})\left[F(\pi/2,k_I)-F(\phi_{\ell I},k_I)\right.\right. -$$

$$\left.\left.2E(\pi/2,k_I)+2E(\phi_{\ell I},k_I)\right]-4k_I^2\mathrm{Sin}\phi_{\ell I}\mathrm{Cos}\phi_{\ell I}\sqrt{1-k_I^2\mathrm{Sin}^2\phi_{\ell I}}\right\}/\sqrt{\delta} + \sqrt{f_0} \tag{6.2.41}$$

The condition $(6.1.43)_2$ may be expressed in the form

$$\tan(\alpha_0+\theta_{\ell O}) = \tan(\alpha_I+\theta_{\ell I}) \tag{6.2.42}$$

and with the aid of equations (6.2.15) and (6.2.19) this may be rewritten as

$$\frac{2k_I^2\mathrm{Sin}^2\phi_{\ell I}-1}{2k_I\mathrm{Sin}\phi_{\ell I}\sqrt{1-k_I^2\mathrm{Sin}^2\phi_{\ell I}}} + \frac{2k_0\mathrm{Sin}\phi_{\ell O}\sqrt{1-k_0^2\mathrm{Sin}^2\phi_{\ell O}}}{2k_0^2\mathrm{Sin}^2\phi_{\ell O}-1} = 0 \tag{6.2.43}$$

The conditions of mass conservation (6.1.44) can be expressed in terms of the new variables as

$$V_m\left\{\frac{t}{z_p^2(t)}\right\} = \int_{\phi_{\ell O}}^{\pi/2} x_0\,\frac{dz_0}{d\phi_0}\,d\phi_0 - \int_{\phi_{\ell I}}^{\pi/2} x_I\,\frac{dz_I}{d\phi_I}\,d\phi_I \tag{6.2.44}$$

where x_0 and x_I are given by (6.2.31) and (6.2.34) respectively and the expressions for $dz_0/d\phi_0$ and $dz_I/d\phi_I$, obtained by differentiating (6.2.32) and (6.2.35) with respect to ϕ_0 and ϕ_I respectively, are

$$\frac{dz_0}{d\phi_0} = \left[(2k_0^2\sin^2\phi_0 - 1)(2k_0\sin\phi_{\ell 0}\sqrt{1-k_0^2\sin^2\phi_{\ell 0}}) - \right.$$

$$\left.(2k_0^2\sin^2\phi_{\ell 0} - 1)(2k_0\sin\phi_0\sqrt{1-k_0^2\sin^2\phi_0})\right] / (\sqrt{f_0}\sqrt{1-k_0^2\sin^2\phi_0}) \qquad (6.2.45)$$

and

$$\frac{dz_I}{d\phi_I} = -\left[(2k_I\sin\phi_{\ell I}\sqrt{1-k_I^2\sin^2\phi_{\ell I}})(2k_I\sin\phi_I\sqrt{1-k_I^2\sin^2\phi_I}) + \right.$$

$$\left.(2k_I^2\sin^2\phi_{\ell I} - 1)(2k_I^2\sin^2\phi_I - 1)\right] / (\sqrt{f_0\delta}\sqrt{1-k_I^2\sin^2\phi_I}) \qquad (6.2.46)$$

Equations (6.2.22), (6.2.40), (6.2.41), (6.2.43) and (6.2.44) can now be solved numerically. With z_p and ℓ_I determined by the model of Section 4.8 this set of equations were solved numerically using Powell's method and results for the case $B_r = 1.0$, $Pe = 0.5$, $\delta = 1.0$ and $h = 0.75$ mm are presented in Table 6.1.

$Pe = 0.5$, $Br = 1.0$, $\delta = 1.0$, $h = 0.75$ mm

t	z_p	ℓ_I	$V_m t/z_p^2$	ℓ_0	$\phi_{\ell 0}$	$\phi_{\ell I}$	k_0	k_I
0.2	0.777	0.644	0.311	0.941	-0.952	0.477	0.431	0.902
0.3	0.901	0.833	0.347	0.961	-0.726	0.566	0.369	0.956
0.4	0.993	1.007	0.384	1.017	-0.655	0.616	0.306	0.974
0.5	1.065	1.173	0.413	1.103	-0.673	0.643	0.248	0.983
0.6	1.124	1.334	0.445	1.210	-0.751	0.656	0.201	0.989
0.7	1.173	1.492	0.477	1.333	-0.869	0.663	0.168	0.992
0.8	1.215	1.646	0.508	1.466	-1.014	0.666	0.145	0.994
0.9	1.250	1.800	0.540	1.605	-1.174	0.667	0.131	0.996
1.0	1.281	1.952	0.572	1.747	-1.339	0.667	0.123	0.997
1.1	1.307	2.103	0.603	1.891	-1.502	0.667	0.120	0.998

Table 6.1

The corresponding values for $\theta_{\ell O}$, $\theta_{\ell I}$, α_O and α_I , obtained using the above values and equations (6.2.12), (6.2.15), (6.2.17) and (6.2.19) are presented in Table 6.2.

Pe = 0.5, Br = 1.0, δ = 1.0, h = 0.75 mm.

t	$\theta_{\ell O}$	$\theta_{\ell I}$	α_O	α_I
0.2	92.232	-10.045	128.896	51.174
0.3	71.639	-5.974	136.717	34.329
0.4	57.086	-4.515	144.394	25.994
0.5	46.481	-3.191	151.299	20.971
0.6	39.028	-1.601	156.762	17.391
0.7	34.031	0.192	160.687	14.526
0.8	30.844	2.034	163.369	12.120
0.9	28.941	3.800	164.941	10.082
1.0	27.914	5.393	165.853	8.375
1.1	27.434	6.731	166.267	6.970

Table 6.2

The coordinates x_O, x_I, z_O and z_I can now be obtained using equations (6.2.31), (6.2.34), (6.2.32) and (6.2.35) respectively, with the aid of the results presented in Table 6.1. The plots of the profiles obtained are presented in Section 6.4.

Inspection of the results in Table 6.1 reveals that as time t increases $\phi_{\ell O}$ approaches the critical value of $-\pi/2$. Referring to equations (6.2.12) and (6.2.15) it is seen that at $\phi_{\ell O} = -\pi/2$ we can write

$$\text{Cos}\alpha_O = \text{Cos}(\alpha_O + \theta_{\ell O}) \qquad (6.2.47)$$

and substituting this result into equation (6.2.7) we deduce that

$$\frac{d\theta_O}{ds} = 0 \quad \text{at} \quad s = 0 \, . \qquad (6.2.48)$$

Hence the curvature is zero at the end $s = 0$ of the beam L_0. As t increases further the curvature will become negative at $s = 0$. However, from the symmetry condition of $z = 0$ the curvature must be positive definite and consequently our model must be modified to obtain results for larger times. A simple way to avoid negative curvature at the end $s = 0$ is to allow a region of the beam L_0, $0 \leq s \leq x_p$, to be along the x axis. The beam L_0 can then be regarded as a beam of length $\ell_0 - x_p$, having zero curvature at the end $(x_p, 0, 0, 0)$ and this model is considered in the following subsection.

6.2.1 Solution with Zero Curvature at Point $(x_p, 0, 0, 0)$

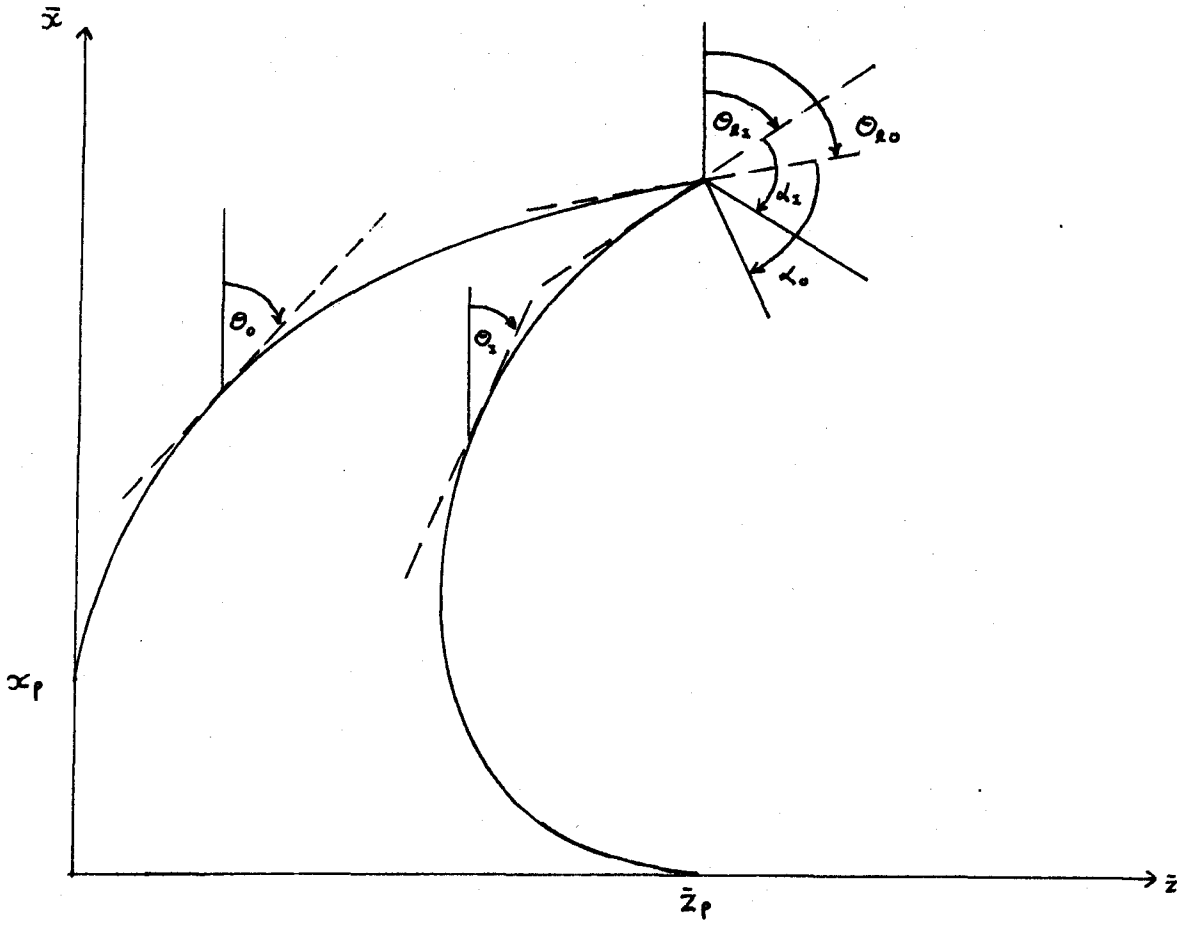

Variable Definition

Figure 6.4

The model is this section differs from the previous one in that the length of the beam L_0 is now $\ell_0 - x_o$ and the end that was attained at the point $(x = 0, z = 0)$ is now attached at the point $(x = x_p, z = 0)$ where the curvature is taken to be zero. Thus the governing equations can be obtained from those in the previous section by replacing ℓ_0 by $\ell_0 - x_p$, the point $(0, 0, 0, 0)$ by the point $(x_p, 0, 0, 0)$ and $\phi_{\ell 0}$ by $-\pi/2$. On doing this, equations (6.2.22), (6.2.40), (6.2.41), (6.2.43) and (6.2.44) became

$$2F(\pi/2,k_0) = \frac{(\ell_0-x_p)}{\ell_I\sqrt{\delta}}\left[F(\pi/2,k_I)-F(\phi_{\ell I},k_I)\right], \tag{6.2.49}$$

$$(2k_0^2-1)\left[2F(\pi/2,k_0)-4E(\pi/2,k_0)\right] + x_p\sqrt{f_0} = \left\{2k_I\sin\phi_{\ell I}\sqrt{1-k_I^2\sin^2\phi_{\ell I}}\right.$$

$$\left.\left[F(\pi/2,k_I)-F(\phi_{\ell I},k_I)-2E(\pi/2,k_I)+2E(\phi_{\ell I},k_I)\right]+2k_I(1-2k_I^2\sin^2\phi_{\ell I})\cos\phi_{\ell I}\right\}/\sqrt{\delta}\,, \tag{6.2.50}$$

$$-2k_0\sqrt{1-k_0^2}\left[2F(\pi/2,k_0)-4E(\pi/2,k_0)\right] = \left\{(1-2k_I^2\sin^2\phi_{\ell I})\left[F(\pi/2,k_I)-F(\phi_{\ell I},k_I)\right.\right.$$

$$\left.\left.-2E(\pi/2,k_I) + 2E(\phi_{\ell I},k_I)\right]-4k_I^2\sin\phi_{\ell I}\cos\phi_{\ell I}\sqrt{1-k_I^2\sin^2\phi_{\ell I}}\right\}/\sqrt{\delta} + \sqrt{f_0}\,, \tag{6.2.51}$$

$$\frac{2k_I^2\sin^2\phi_{\ell I}-1}{2k_I\sin\phi_{\ell I}\sqrt{1-k_I^2\sin^2\phi_{\ell I}}} - \frac{2k_0\sqrt{1-k_0^2}}{2k_0^2-1} = 0 \tag{6.2.52}$$

and

$$\frac{V_m t}{z_p^2} = \int_{-\pi/2}^{\pi/2} x_0\,\frac{dz_0}{d\phi_0}\,d\phi_0 - \int_{\phi_{\ell I}}^{\pi/2} x_I\,\frac{dz_I}{d\phi_I}\,d\phi_I\,. \tag{6.2.53}$$

respectively. Also the expressions for $\sqrt{f_0}$, x_0, z_0 and $dz_0/d\phi_0$ (6.2.20), (6.2.31), (6.2.32) and (6.2.45) become

$$\sqrt{f_0} = 2F(\pi/2, k_0)/(\ell_0 - x_p) , \tag{6.2.54}$$

$$x_0 = \left\{(2k_0^2-1)\left[F(\phi_0, k_0) + F(\pi/2, k_0) - 2E(\phi_0, k_0) - 2E(\pi/2, k_0)\right]\right.$$
$$\left. + 4k_0^2 \cos\phi_0 \sqrt{1-k_0^2}\right\}/\sqrt{f_0} + x_p, \; -\pi/2 \leq \phi_0 \leq \pi/2 , \tag{6.2.55}$$

$$z_0 = \left\{-2k_0\sqrt{1-k_0^2}\left[F(\phi_0,k_0)+F(\pi/2,k_0)-2E(\phi_0,k_0)-2E(\pi/2,k_0)\right]+2k_0(2k_0^2-1)\right.$$
$$\left.\cos\phi_0\right\}/\sqrt{f_0} \quad , -\pi/2 \leq \phi_0 \leq \pi/2 \tag{6.2.56}$$

and

$$\frac{dz_0}{d\phi_0} = -\left[(2k_0^2\sin^2\phi_0-1)(2k_0\sqrt{1-k_0^2}) + (2k_0^2-1)(2k_0\sin\phi_0\sqrt{1-k_0^2\sin^2\phi_0})\right]$$
$$/(\sqrt{f_0}\sqrt{1-k_0^2\sin^2\phi_0}) . \tag{6.2.57}$$

In the derivation of the above set of equations use has been made of the fact that F and E are odd functions. The expressions for x_I, z_I and $dz_I/d\phi_z$ remain unchanged and are given by (6.2.34), (6.2.35) and (6.2.46) respectively. Equations (6.2.49), (6.2.50), (6.2.51), (6.2.52) and (6.2.53) are now solved numerically and the result corresponding to Br = 1.0, Pe = 0.5, δ = 1.0 and h = 0.75 mm are presented in Table 6.3.

Using the results in Table 6.3 and equation (6.2.12), (6.2.15) (6.2.17) and (6.2.19) the values of $\theta_{\ell O}$, $\theta_{\ell I}$, α_0 and α_I are then obtained and these results are presented in Table 6.4. Also, using the figures in Table 6.3 and equations (6.2.55), (6.2.56), (6.2.34) and (6.2.35) the coordinate values x_0, z_0, x_I and z_I respectively are obtained and the corresponding profiles are presented in Section 6.4.

Pe = 0.5, Br = 1.0, δ = 1.0, h = 0.75 mm

t	z_p	ℓ_I	Vol	ℓ_O	x_p	ϕ_I	k_O	k_I
1.2	1.331	2.254	0.635	2.035	0.055	0.667	0.119	0.999
1.3	1.351	2.405	0.667	2.180	0.155	0.667	0.119	0.999
1.4	1.370	2.555	0.699	2.323	0.254	0.666	0.120	0.999
1.5	1.386	2.706	0.732	2.470	0.354	0.665	0.121	0.999
1.6	1.400	2.857	0.765	2.615	0.453	0.664	0.122	0.999
1.7	1.413	3.008	0.798	2.759	0.550	0.663	0.122	0.999
1.8	1.424	3.160	0.832	2.905	0.649	0.663	0.123	0.999
1.9	1.435	3.310	0.865	3.048	0.745	0.662	0.123	0.999
2.0	1.444	3.463	0.900	3.194	0.843	0.661	0.124	0.999

Table 6.3

Pe = 0.5 Br = 1.0, δ = 1.0, h = 0.75 mm

t	$\theta_{\ell O}$	$\theta_{\ell I}$	α_O	α_I
1.2	27.26	7.80	166.37	5.84
1.3	27.36	8.75	166.32	4.93
1.4		9.54	166.24	4.22
1.5	27.75	10.21	166.13	3.67
1.6	27.91	10.72	166.04	3.23
1.7	28.04	11.13	165.98	2.89
1.8	28.19	11.48	165.98	2.61
1.9	28.29	11.75	165.85	2.39
2.0	28.48	12.03	165.76	2.21

Table 6.4

6.3 Solution With Non-Zero Hydrostatic Pressure, ($P_o \neq 0$, $P_I \neq 0$).

In Section 6.2 we obtained an numerical solution to the system of ordinary differential equations (6.1.20) to (6.1.23) subject

to the boundary conditions (6.1.38) to (6.1.44) by making the assumption that the hydrostatic pressures p_0 and p_I were both zero. In reality these pressures are non-zero, so in this section we obtain an approximate solution for the case of non-zero p_0 and p_I. The accuracy of the approximate method, used here, is assessed by putting $p_0 = p_I = 0$ in the solution and comparing the results with those obtained in Section 6.2.

The approximate solution is obtained with an integral technique similar to the heat balance integral method which was discussed in Section 4.8. The governing equations (6.1.20) and (6.1.21) are each integrated along their lengths between the limits $0 \leqslant s \leqslant \ell_0$ and $0 \leqslant s \leqslant \ell_I$ respectively.The solutions to the resulting averaged equations for θ_0 and θ_I are then approximated by polynomial expressions in s.

It is convenient at this stage to introduce the new variable as defined by

$$u = s/\ell_0 \tag{6.3.1}$$

Again assuming that the dimensionless stiffness, B_θ, is equal to unity, and introducing the variable u into equations (6.1.20) and $(6.1.22)_{1,2}$ and the boundary conditions (6.1.38) and (6.1.39), yields

$$\frac{d^2\theta_0}{du^2} = - f_0\ell_0^2 \mathrm{Sin}(\alpha_0+\theta_{\ell 0}-\theta_0) + p_0\ell_0^3 \int_u^1 \mathrm{Cos}\theta_0 du \mathrm{Cos}\theta_0 + p_0\ell_0^3 \int_u^1 \mathrm{Sin}\theta_0 du \mathrm{Sin}\theta_0 \ , \ 0 \leqslant u \leqslant 1 \ , \tag{6.3.2}$$

$$\frac{dx_0}{du} = \ell_0 \mathrm{Cos}\theta_0, \quad \frac{dz_0}{du} = \ell_0 \mathrm{Sin}\theta_0 , \tag{6.3.3}$$

$$x_0 = 0, \quad z_0 = 0, \quad \theta_0 = 0 \quad \text{on} \quad u = 0 \tag{6.3.4}$$

and

$$x_0 = x_{\ell 0}, \; z_0 = z_{\ell 0}, \quad \theta_0 = \theta_{\ell 0}, \; \frac{d\theta_0}{du} = 0 \quad \text{on} \quad u = 1 \tag{6.3.5}$$

respectively. Averaging equation (6.3.2) by integrating both sides with respect to u between the limits $u = 0$ and $u = 1$ we obtain

$$\left.\frac{d\theta_0}{du}\right|_{u=1} - \left.\frac{d\theta_0}{du}\right|_{u=0} = -f_0 \ell_0^2 \int_0^1 \mathrm{Sin}(\alpha_0 + \theta_{\ell 0} - \theta_0)\,du$$

$$+ p_0 \ell_0^3 \int_0^1 \int_u^1 \mathrm{Cos}\theta_0 d\mu \; \mathrm{Cos}\theta_0 du + p_0 \ell_0^3 \int_0^1 \int_u^1 \mathrm{Sin}\theta_0 d\mu \mathrm{Sin}\theta_0 du \tag{6.3.6}$$

In this section it is sufficient to take θ_0 as a quadratic in u. However in the following section we require the curvature to be zero at $u = 0$ and in order to apply this condition the polynomial approximation to θ_0 must be of degree 3 or more. It proves convenient therefore to assume a cubic profile in this section, in which case the solution in the following section can be found as a simple deduction. Consequently we assume

$$\theta_0 = a_0 + a_1 u + a_2 u^2 + a_3 u^3 , \tag{6.3.7}$$

where a_0, a_1, a_2 are functions of t only. Equation (6.3.7) must satisfy the three boundary conditions $(6.3.4)_3$, $(6.3.5)_3$ and $(6.3.5)_4$. However there are four uknowns in equation (6.3.7) so one extra condition is required. By putting $u = 1$ in equation (6.3.2) we deduce, with the aid of condition $(6.3.5)_3$, that

$$\frac{d^2\theta_0}{du^2} = - f_0 \ell_0^2 \mathrm{Sin}\alpha_0 \quad \text{on} \quad u = 1 \ . \tag{6.3.8}$$

Applying conditions $(6.3.4)_3$, $(6.3.5)_3$, $(6.3.5)_4$ and (6.3.8) to equation (6.3.7) leads to

$$a_0 = 0 \ , \tag{6.3.9}$$

$$a_1 = 3\theta_{\ell 0} - \frac{1}{2} f_0 \ell_0^2 \mathrm{Sin}\alpha_0 \ , \tag{6.3.10}$$

$$a_2 = -3\theta_{\ell 0} + f_0 \ell_0^2 \mathrm{Sin}\alpha_0 \tag{6.3.11}$$

and

$$a_3 = \theta_{\ell 0} - \frac{1}{2} f_0 \ell_0^2 \mathrm{Sin}\alpha_0 \ . \tag{6.3.12}$$

On substituting equation (6.3.7) into (6.3.6) there results the integral equation

$$a_1 = f_0 \ell_0^2 \int_0^1 \mathrm{Sin}\left[\alpha_0 + \theta_{\ell 0} - a_1 u - a_2 u^2 - a_3 u^3\right] du - p_0 \ell_0^3 \int_0^1 \int_u^1 \mathrm{Cos}\left[a_1 \mu + a_2 \mu^2 + a_3 \mu^3\right] d\mu \mathrm{Cos}\left[a_1 u + a_2 u^2 + a_3 u^3\right] du - p_0 \ell_0^3 \int_0^1 \int_u^1 \mathrm{Sin}\left[a_1 \mu + a_2 \mu^2 + a_3 \mu^3\right] d\mu \ \mathrm{Sin}\left[a_1 u + a_2 u^2 + a_3 u^3\right] du \tag{6.3.13}$$

where a_1, a_2 and a_3 are given by (6.3.10), (6.3.11) and (6.3.12) respectively.

Let us now turn our attention to equation (6.1.21). On introducing the new variable V, defined by

$$V = S/\ell_I \ , \tag{6.3.14}$$

again assuming that $B_I = 1/8$ and making use of condition $(6.1.43)_1$

equation (6.1.21) becomes

$$\frac{1}{\delta}\frac{d^2\theta_I}{dv^2} = -f_0\ell_I^2 \mathrm{Sin}(\alpha_I+\theta_{\ell I}-\theta_I) - p_I\ell_I^3 \int_v^1 \mathrm{Cos}\theta_I dv \mathrm{Cos}\theta_I - p_I\ell_I^3 \int_v^1 \mathrm{Sin}\theta_I dv\, \mathrm{Sin}\theta_I, \quad 0 \leqslant v \leqslant 1 . \tag{6.3.15}$$

The corresponding forms of the equations (6.1.23) and the boundary conditions (6.1.40) and (6.1.41) are

$$\frac{dx_I}{dv} = \ell_I \mathrm{Cos}\theta_I \quad \text{and} \quad \frac{dz_I}{dv} = \ell_I \mathrm{Sin}\theta_I , \tag{6.3.16}$$

$$x_I = 0,\ z_I = 1 ,\ \theta_I = -\pi/2 \quad \text{on} \quad V = 0 \tag{6.3.17}$$

and

$$x_I = x_{\ell I}\ z_I = z_{\ell I},\ \theta_I = \theta_{\ell I} \quad \text{and} \quad \frac{d\theta_I}{dv} = 0 \quad \text{on} \quad V = 1 \tag{6.3.18}$$

respectively.

Again we obtain the averaged form of equation (6.3.15) by integrating the latter with respect to V between the limits $V = 0$ and $V = 1$ giving

$$\frac{1}{\delta}\frac{d\theta_I}{dv}\bigg|_{v=1} - \frac{1}{\delta}\frac{d\theta_I}{dv}\bigg|_{v=0} = -f_0\ell_I^2 \int_0^1 \mathrm{Sin}(\alpha_I+\theta_{\ell I}-\theta_I)dv - p_I\ell_I^3 \int_0^1\int_v^1 \mathrm{Cos}\theta_I dv \mathrm{Cos}\theta_I dv - p_I\ell_I^3 \int_0^1\int_v^1 \mathrm{Sin}\theta_I dv \mathrm{Sin}\theta_I dv . \tag{6.3.19}$$

We assume a quadratic profile for θ_I in the form

$$\theta_I = b_0 + b_1 v + b_2 v^2 \tag{6.3.20}$$

where b_0, b_1 and b_2 are functions of t only. Equation (6.3.20) must satisfy the conditions $(6.3.17)_3$, $(6.3.18)_3$ and $(6.3.18)_4$, and hence we deduce that

$$b_0 = -\pi/2 \ , \tag{6.3.21}$$

$$b_1 = 2(\theta_{\ell I}+\pi/2) \tag{6.3.22}$$

and

$$b_2 = -(\theta_{\ell I}+\pi/2) \ . \tag{6.3.23}$$

Substituting equation (6.3.20) into (6.3.19) leads to the integral equation

$$b_1/\delta = f_0\ell_I^2 \int_0^1 \mathrm{Sin}\left[\alpha_I+\theta_{\ell I}+\pi/2-b_1 v-b_2 v^2\right]dv + p_I\ell_I^3 \int_0^1\int_v^1 \mathrm{Cos}\left[-\pi/2+b_1 v+b_2 v^2\right]dv\,\mathrm{Cos}\left[-\pi/2+b_1 v+b_2 v^2\right]dv + p_I\ell_I^3 \int_0^1\int_v^1 \mathrm{Sin}\left[-\pi/2+b_1 v+b_2 v^2\right]dv\,\mathrm{Sin}\left[-\pi/2+b_1 v+b_2 v^2\right]dv \ , \tag{6.3.24}$$

where b_1 and b_2 are given by (6.3.22) and (6.3.23) respectively.

Integrating equations $(6.3.3)_1$ and $(6.3.3)_2$ with respect to u and making use of the conditions $(6.3.4)_1$ and $(6.3.4)_2$ results in the expressions

$$x_0 = \ell_0 \int_0^u \mathrm{Cos}\theta_0 du \tag{6.3.25}$$

and

$$z_0 = \ell_0 \int_0^u \mathrm{Sin}\theta_0 du \tag{6.3.26}$$

Substituting equation (6.3.7) into these equations then yields

$$x_0 = \ell_0 \int_0^u \text{Cos}\left[a_1u+a_2u^2+a_3u^3\right]du \qquad (6.3.27)$$

and

$$z_0 = \ell_0 \int_0^u \text{Sin}\left[a_1u+a_2u^2+a_3u^3\right]du \ . \qquad (6.3.28)$$

Similarly from equations $(6.3.16)_1$, $(6.3.16)_2$, $(6.3.17)_1$, $(6.3.17)_2$ and (6.3.20) we deduce

$$x_I = \ell_I \int_0^v \text{Cos}\left[b_0+b_1v+b_2v^2\right]dv \qquad (6.3.29)$$

and

$$z_I = \ell_I \int_0^v \text{Sin}\left[b_0+b_1v+b_2v^2\right]dv + 1 \qquad (6.3.30)$$

Applying the boundary conditions $(6.3.5)_1$ and $(6.3.5)_2$ to the equations (6.3.27) and (6.3.28) respectively leads to

$$x_{\ell 0} = \ell_0 \int_0^1 \text{Cos}\left[a_1u+a_2u^2+a_3u^3\right]du \qquad (6.3.31)$$

and

$$z_{\ell 0} = \ell_0 \int_0^1 \text{Sin}\left[a_1u+a_2u^2+a_3u^3\right]du \ , \qquad (6.3.32)$$

whereas applying $(6.3.18)_1$ and $(6.3.18)_2$ to the equations (6.3.29) and (6.3.30) yields

$$x_{\ell I} = \ell_I \int_0^1 \text{Cos}\left[b_0+b_1v+b_2v^2\right]dv \qquad (6.3.33)$$

and

$$z_{\ell I} = \ell_I \int_0^1 \mathrm{Sin}\left[b_0+b_1 v+b_2 v^2\right] dv + 1 \ . \qquad (6.3.34)$$

On substituting equations (6.3.31) and (6.3.33) into the condition $(6.1.42)_1$ and putting equations (6.3.32) and (6.3.34) into $(6.1.42)_2$ we obtain the pair of integral equations

$$\ell_0 \int_0^1 \mathrm{Cos}\left[a_1 u+a_2 u^2+a_3 u^3\right] du = \ell_I \int_0^1 \mathrm{Cos}\left[b_0+b_1 v+b_2 v^2\right] dv \qquad (6.3.35)$$

and

$$\ell_0 \int_0^1 \mathrm{Sin}\left[a_1 u+a_2 u^2+a_3 u^3\right] du = \ell_I \int_0^1 \mathrm{Sin}\left[b_0+b_1 v+b_2 v^2\right] dv + 1 \ . \qquad (6.3.36)$$

It is convenient here to express condition (6.1.44) in the form

$$\frac{V_m t}{z_p^2} = \int_0^{\ell_I} x_0 \frac{dz_0}{ds} ds - \int_0^{\ell_I} x_I \frac{dz_I}{ds} ds \ , \qquad (6.3.37)$$

which in terms of the variables u and v becomes

$$\frac{V_m t}{z_p^2} = \int_0^1 x_0 \frac{dz_0}{du} du - \int_0^1 x_I \frac{dz_I}{dv} dv \qquad (6.3.38)$$

Differentiating equations (6.3.28) and (6.3.30) with respect to u and v respectively gives

$$\frac{dz_0}{du} = \ell_0 \mathrm{Sin}\left[a_1 u+a_2 u^2+a_3 u^3\right] \qquad (6.3.39)$$

and

$$\frac{dz_I}{dv} = \ell_I \mathrm{Sin}\left[b_0+b_1 v+b_2 v^2\right] \ , \qquad (6.3.40)$$

and substituting the above equations and (6.3.27) and (6.3.29) into condition (6.3.38) yields the integral equations

$$\frac{V_m t}{z_p^2} = \ell_0^2 \int_0^1 \int_0^u \text{Cos}\left[a_1\mu+a_2\mu^2+a_3\mu^3\right]d\mu \text{Sin}\left[a_1 u+a_2 u^2+a_3 u^3\right]du$$

$$- \ell_1^2 \int_0^1 \int_0^v \text{Cos}\left[b_0+b_1\nu+b_2\nu^2\right]d\nu \text{Sin}\left[b_0+b_1 v+b_2 v^2\right]dv \ . \qquad (6.3.41)$$

Equations (6.3.13), (6.3.24), (6.3.35), (6.3.36) and (6.3.41) together with conditions $(6.1.43)_2$, which is rewritten here for convenience

$$\theta_{\ell O} + \alpha_O = \theta_{\ell I} + \alpha_I + \pi \ , \qquad (6.3.42)$$

gives us six equations from which to determine the unknowns $\theta_{\ell O}$, $\theta_{\ell I}$, α_O, α_I, f_O and ℓ_O. This set of six equations are easily solved numerically and results for the case $P_I = P_O = 0$, Br = 1.0, Pe = 0.5, δ = 1.0 and h = 0.75 mm are presented in Table 6.5.

Br = 1.0, Pe = 0.5, δ = 1.0, h = 0.75 mm.

t	$\theta_{\ell O}$	$\theta_{\ell I}$	α_O	α_I	f_O	ℓ_O
0.2	90.67	-5.73	127.78	44.19	8.113	0.957
0.3	72.70	0.53	134.40	26.57	6.150	0.989
0.4	60.91	4.89	141.04	17.06	4.982	1.064
0.5	53.62	9.55	146.57	10.64	4.250	1.171
0.6	50.09	14.91	150.27	5.45	3.781	1.302
0.7	49.55	20.83	152.16	0.86	3.462	1.447
0.8	51.10	26.89	152.61	-3.18	3.232	1.601
0.9	53.82	32.62	152.11	-6.68	3.039	1.757
1.0	57.01	37.70	151.06	-9.62	2.860	1.911

Table 6.5

Comparison of these results with those presented in Table 6.2 reveals that for smaller times the values for $\theta_{\ell O}$, α_O and ℓ_O are in good agreement with the exact solutions but the agreement

between corresponding values of $\theta_{\ell I}$ and α_I is poorer. It is also apparent that as time increase the overall agreement between the two solutions decreases. The approximate solution can be improved by increasing the order of the polynomial but the process is lengthy and is not considered here. Our approximate solution, therefore, is thought to be useful for smaller times and consequently all the results presented are calculated for $t < 1$. It is found that although the error in α_I and $\theta_{\ell I}$ is sometimes very large, the error in the coordinates x_I and z_I remains quite small as can be seen from the profiles presented in Section 6.4.

Under certain conditions the curvature of the surface L_0, at $s = 0$, predicted by this model becomes negative. Since this is physically unacceptable we again need to modify our model in an analogous way to that of Section 6.2.12. This process is carried through the following section.

6.3.1 Solution with Zero Curvature at $s = 0$

As discussed above, this problem differs from the previous one in thatthe length of the beam L_0 is now $\ell_0 - x_p$, the end that was attached at the point $(0, 0, 0, 0)$ is now attached at $(x_p, 0, 0, 0)$ and at the latter point the curvature is necessarily zero.

Differentiating equation (6.3.7) with respect to u we obtain

$$\frac{d\theta_0}{du} = a_1 + 2a_2u + 3a_3u^2 , \qquad (6.3.43)$$

and on applying the conditions of zero curvature (6.2.48) to this equation recalling that u is defined by (6.3.1), we obtain

$$a_1 = 0 \ , \qquad (6.3.44)$$

The governing equations can therefore be obtained from those given in Section 6.3 by replacing ℓ_0 by $\ell_0 - x_p$, the point $(0, 0, 0, 0)$ by $(x_p, 0, 0, 0)$ and by putting $a_1 = 0$. Equations (6.3.13), (6.3.35), (6.3.36) and (6.3.41) then become

$$0 = f_0(\ell_0-x_p)^2 \int_0^1 \mathrm{Sin}\left[\alpha_0+\theta_{\ell 0}-a_2u^2-a_3u^3\right]du - p_0(\ell_0-x_p)^3 \int_0^1\int_u^1 \mathrm{Cos}\left[a_2\mu^2+a_3\mu^3\right]d\mu\mathrm{Cos}\left[a_2u^2+a_3u^3\right]du - p_0(\ell_0-x_p)^3 \int_0^1\int_u^1 \mathrm{Sin}\left[a_2\mu^2+a_3\mu^3\right] d\mu\mathrm{Sin}\left|a_2u^2+a_3u^3\right|du \ , \qquad (6.3.45)$$

$$(\ell_0-x_p)\int_0^1 \mathrm{Cos}\left[a_2u^2+a_3u^3\right]du + xp = \ell_I \int_0^1 \mathrm{Cos}\left[b_0+b_1v+b_2v^2\right]dv \ , \qquad (6.3.46)$$

$$(\ell_0-x_p)\int_0^1 \mathrm{Sin}\left[a_2u^2+a_3u^3\right]du = \ell_I \int_0^1 \mathrm{Sin}\left[b_0+b_1v+b_2v^2\right]dv + 1 \qquad (6.3.47)$$

and

$$\frac{V_m t}{z_p^2} = (\ell_0-x_p)^2 \int_0^1\int_0^u \mathrm{Cos}\left[a_2\mu^2+a_3\mu^3\right]d\mu\mathrm{Sin}\left[a_2u^2+a_3u^3\right]du - \ell_I^2 \int_0^1\int_0^v \mathrm{Cos}\left[b_0+b_1\nu+b_2\nu^2\right]d\nu\mathrm{Sin}\left[b_0+b_1v+b_2v^2\right]dv \ , \qquad (6.3.48)$$

whereas equations (6.3.24) and (6.3.42) remain unaltered.

6.4 Results and Discussion

In Figure 6.5 the profiles of the upset collar are illustrated for the case $Br = 1.0$, $Pe = 0.5$, $\delta = 1.0$ and $h = 0.75$ mm. The solid lines represent the exact solution. Figure 6.5(a) reveals that for small time the agreement between the two solutions is very good

whereas from Figures 6.5(b), (c) and (d) we see that the agreement becomes poorer as t increases. As we have already mentioned, the accuracy of the approximate method can be improved by increasing the order of the polynomials used. However, this process is lengthy and although the errors arising from the approximate method can in some cases be quite large, the method does illustrate the qualitative effects of varying δ and the pressure p_0 and p_I.

The choice of $\delta = 1.0$ means that both surfaces L_0 and L_I have the same stiffnesses. The temperature, and hence the stiffness, will vary, in the real situation, along both L_0 and L_I, but details of how the stiffness varies is unknown. In practice, however, L_0 is on average at a much higher temperature than L_I and we would expect the stiffness of L_0 to be smaller than that of L_I. The assumption that L_0 is formed from material expelled from the interface $z = 0$ suggests that the temperature of L_0 is 0 ($1200^{\circ}C$). Since surface L_I is attached to both L_0 and the solid region, the temperature will vary along L_I and lie between $700^{\circ}C$ and $1200^{\circ}C$. Data for Young's modulus at these elevated temperatures is thought to be very unreliable and for this reason it seems unwise to use a precise value for δ. The qualitative effects of varying δ are therefore illustrated in Figure 6.6, where results are given for $\delta = 0.5$, 0.1 and 0.05. We see that decreasing δ, that is decreasing the stiffness of L_0 relative to that of L_I, results in both an overall shift of the upset collar towards $z = 0$ and an increase in width of the plane at the interface.

In all the cases discussed above, the hydrostatic pressure has been taken to be zero, which is clearly unrealistic. It is difficult, however, to estimate the thicknesses of L_0 and L_I, the values

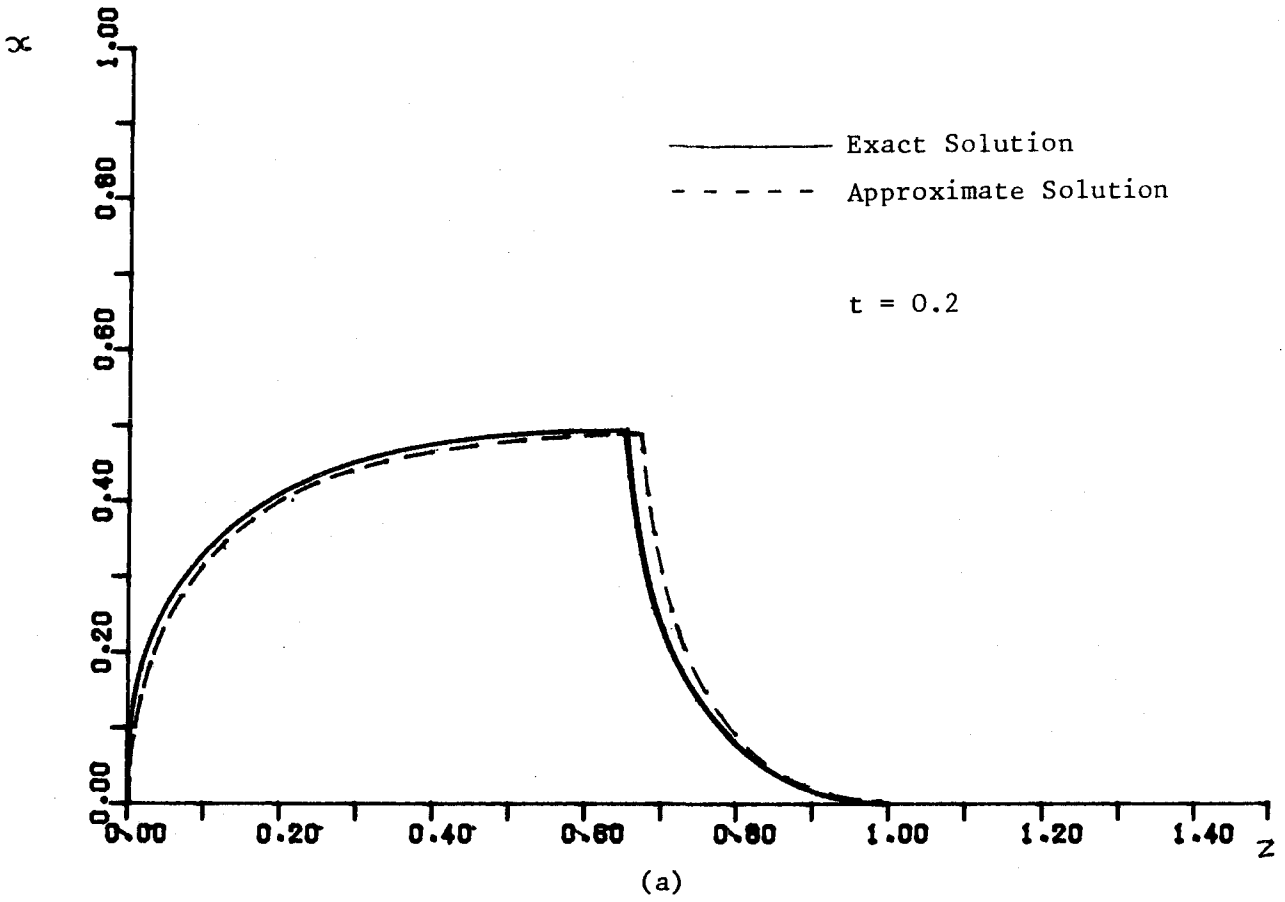

(a)

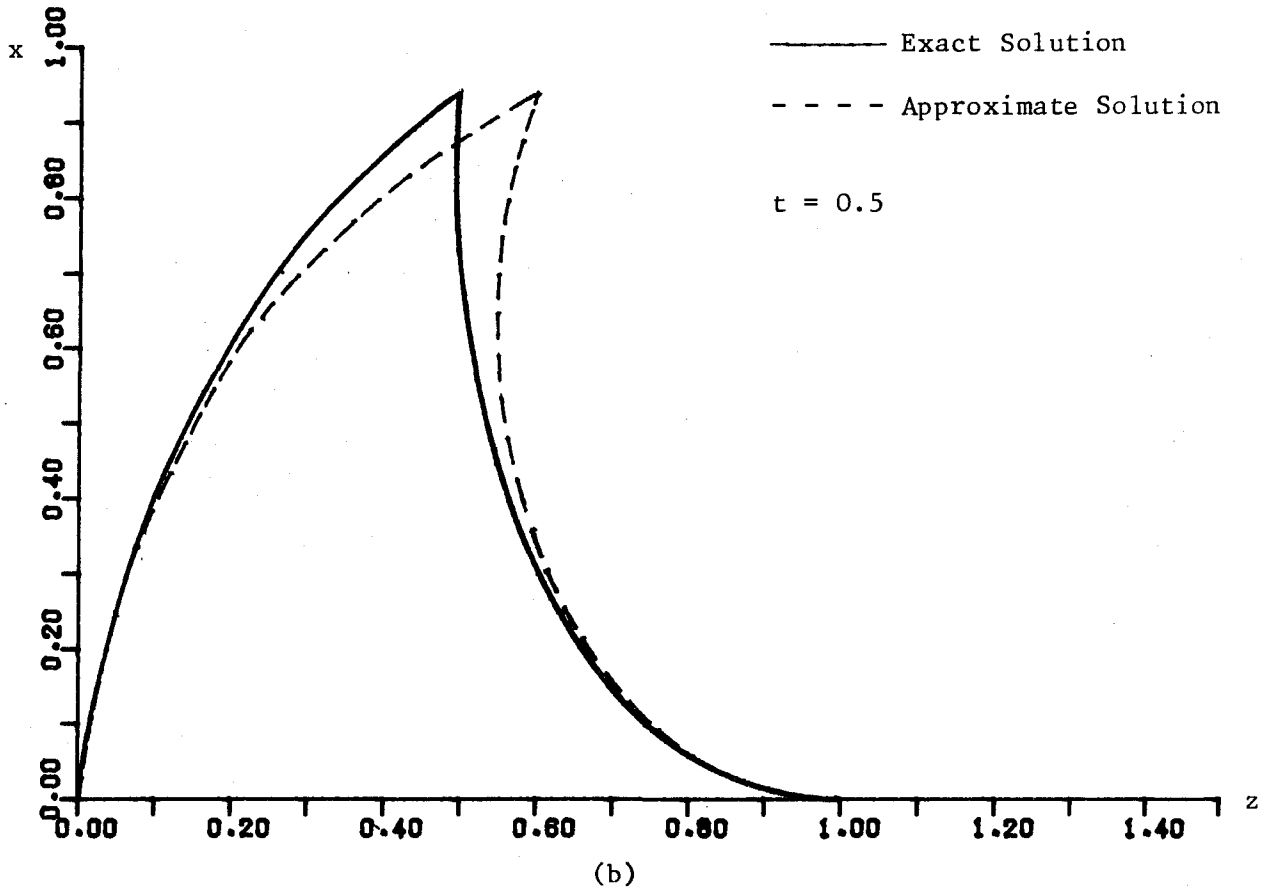

(b)

Figure 6.5 Profiles of the upset collar for the conditions

Br = 1.0, Pe = 0.5, $P_0 = P_1 = 0$, $\delta = 1.0$ and $h = 0.75$

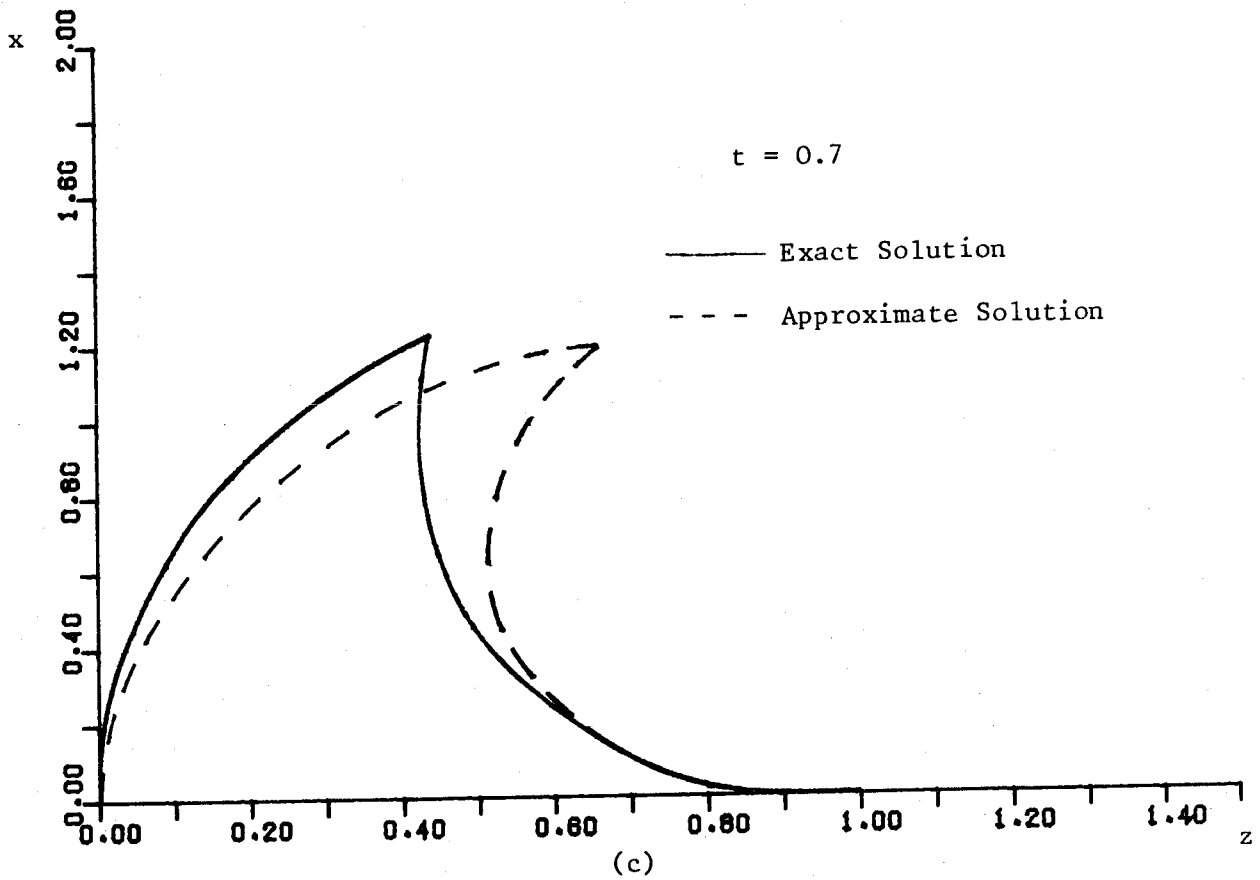

(c)

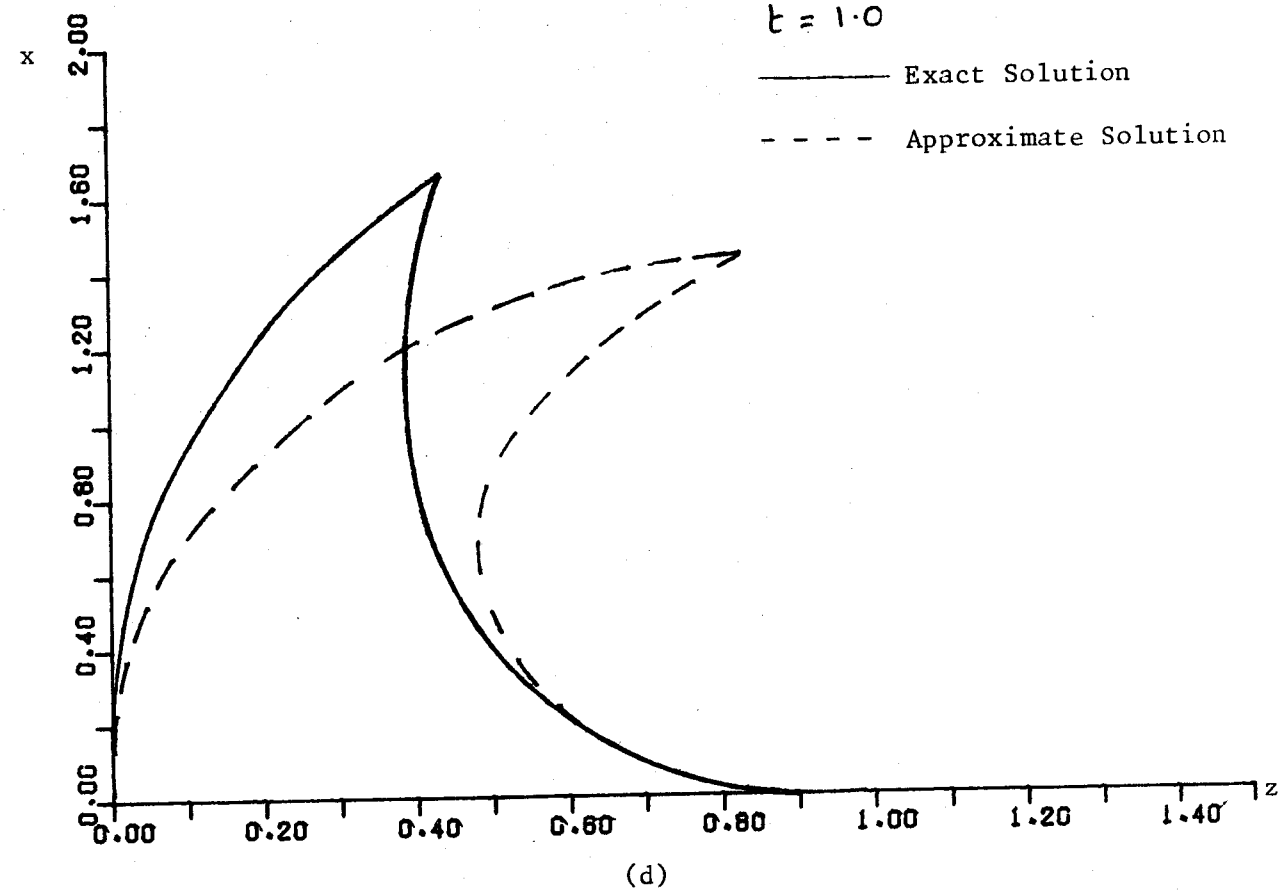

(d)

Figure 6.5 Profiles of the upset collar for the conditons Br = 1.0, Pe = 0.5, $P_0 = P_I = 0$, $\delta = 1.0$, h = 0.75.

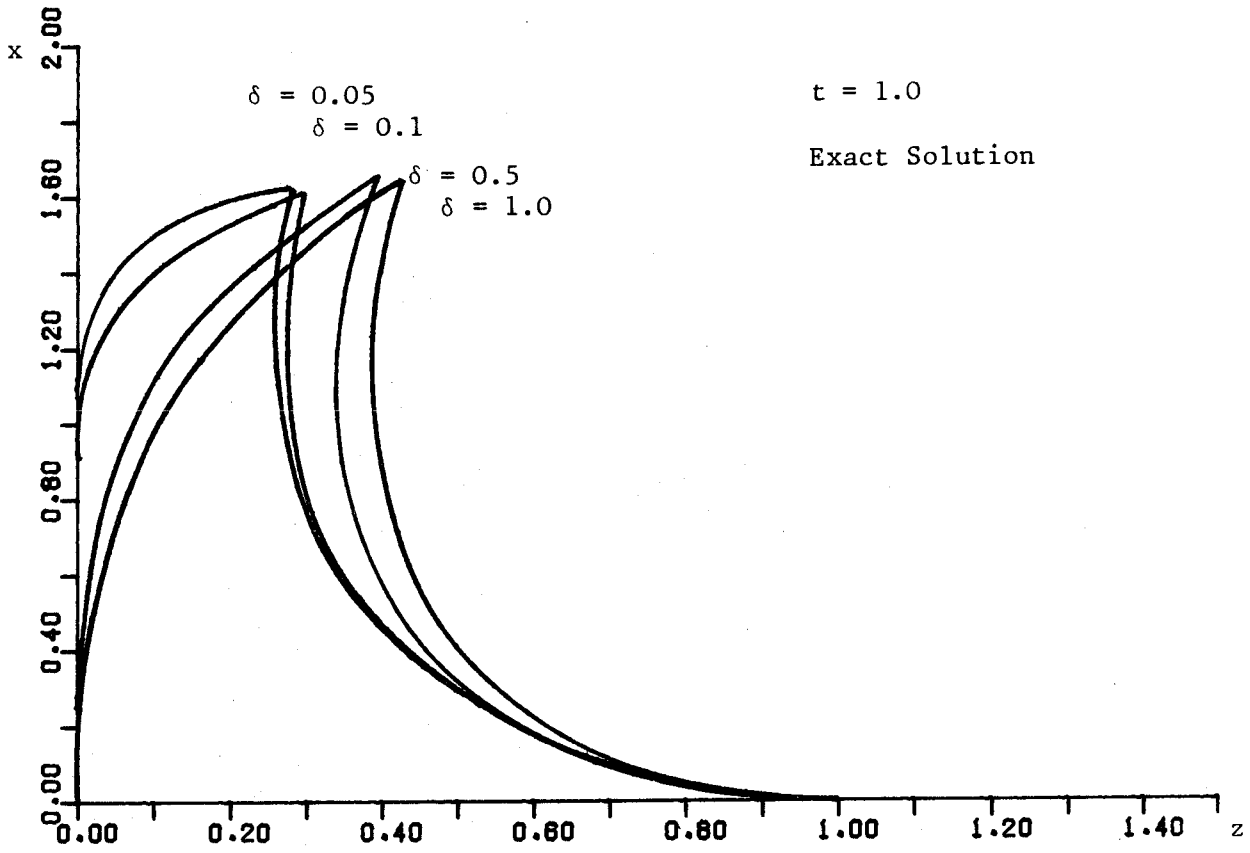

Figure 6.6 Profiles of the upset collar for the case Br = 1.0, Pe = 0.5, $P_0 = P_I$, h = 0.75 and various values of δ

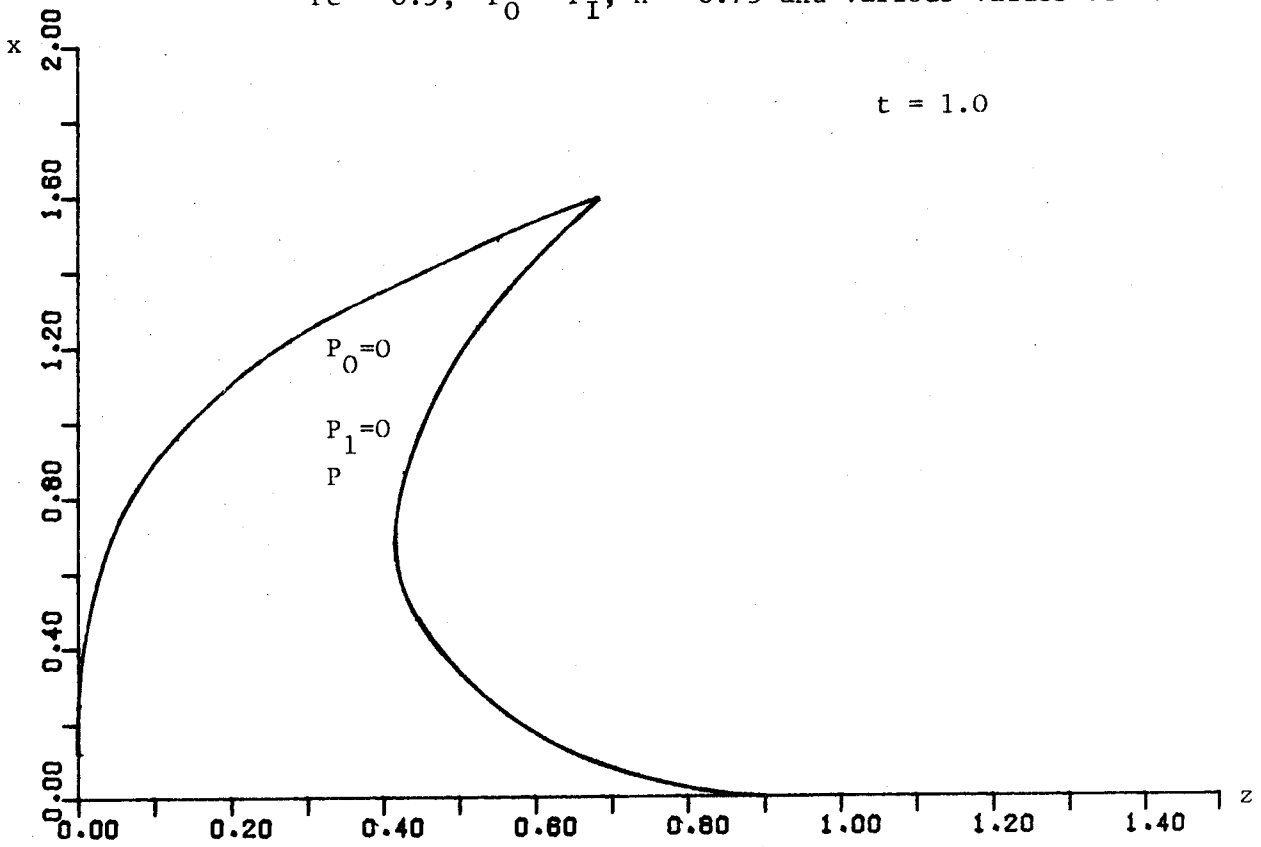

(a)

Figure 6.7 Effect of varying pressure (P_0=P_1) for case Br = 1.0, Pe = 0.5, h = 0.75, δ = 0.5

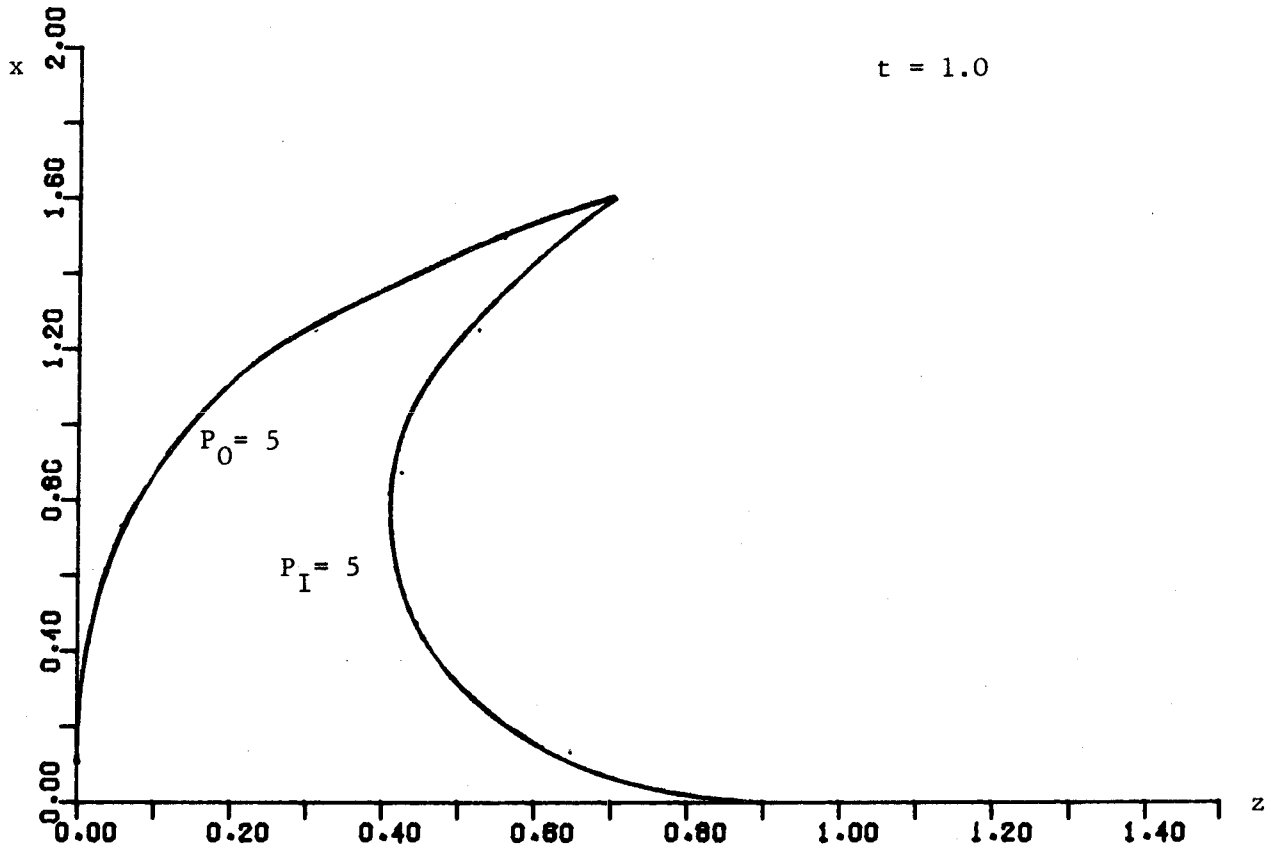

(b)

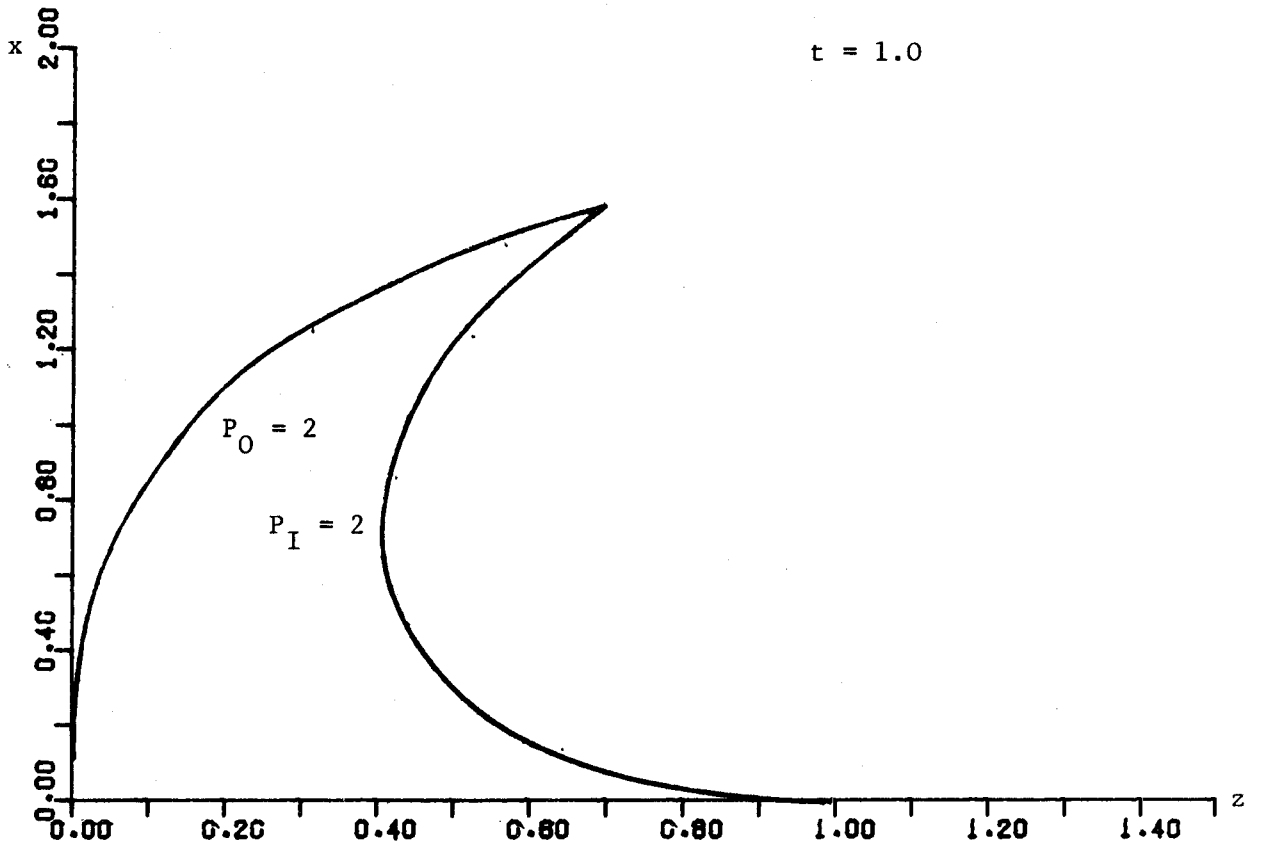

(c)

Figure 6.7 Effect of varying pressure ($P_O = P_I$) for case Br = 1.0, Pe = 0.5, h = 0.75, δ = 0.5

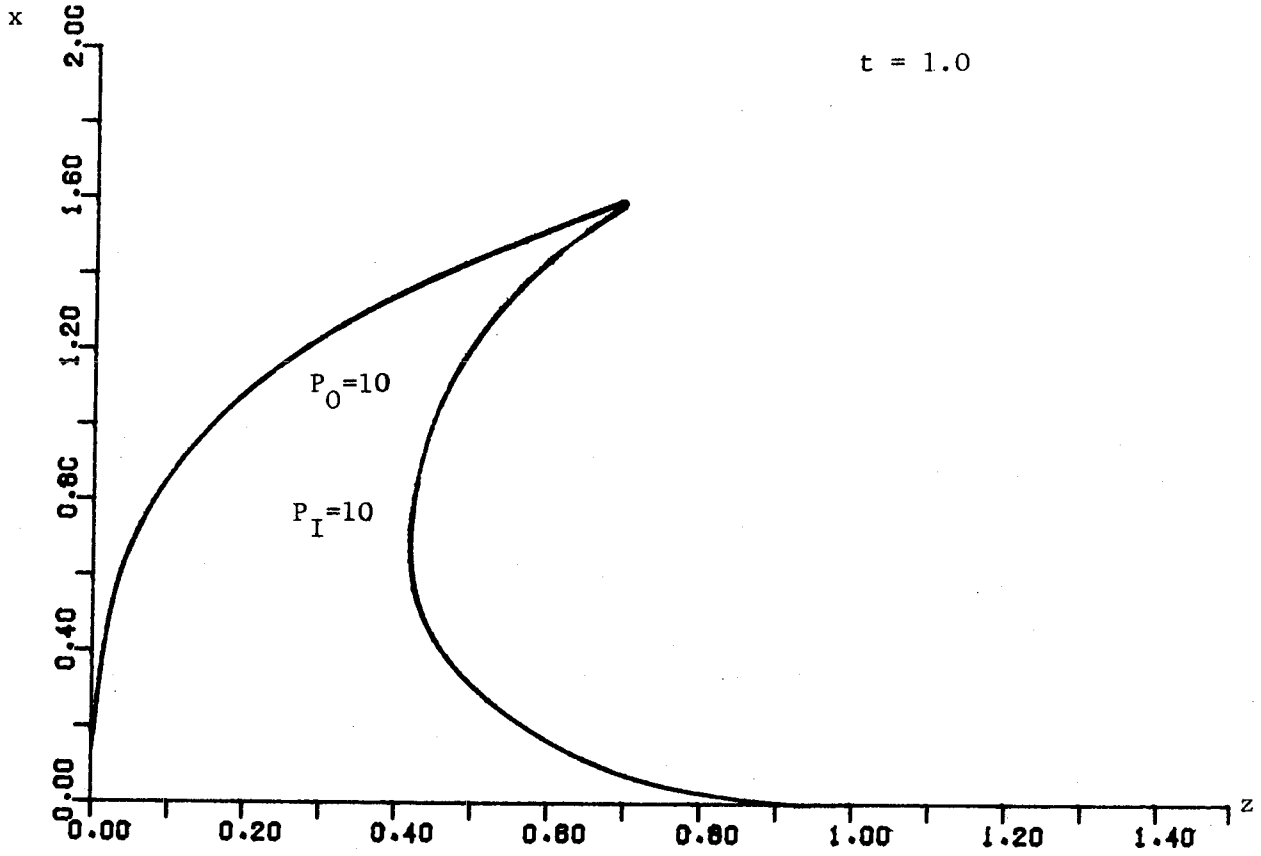

(d)

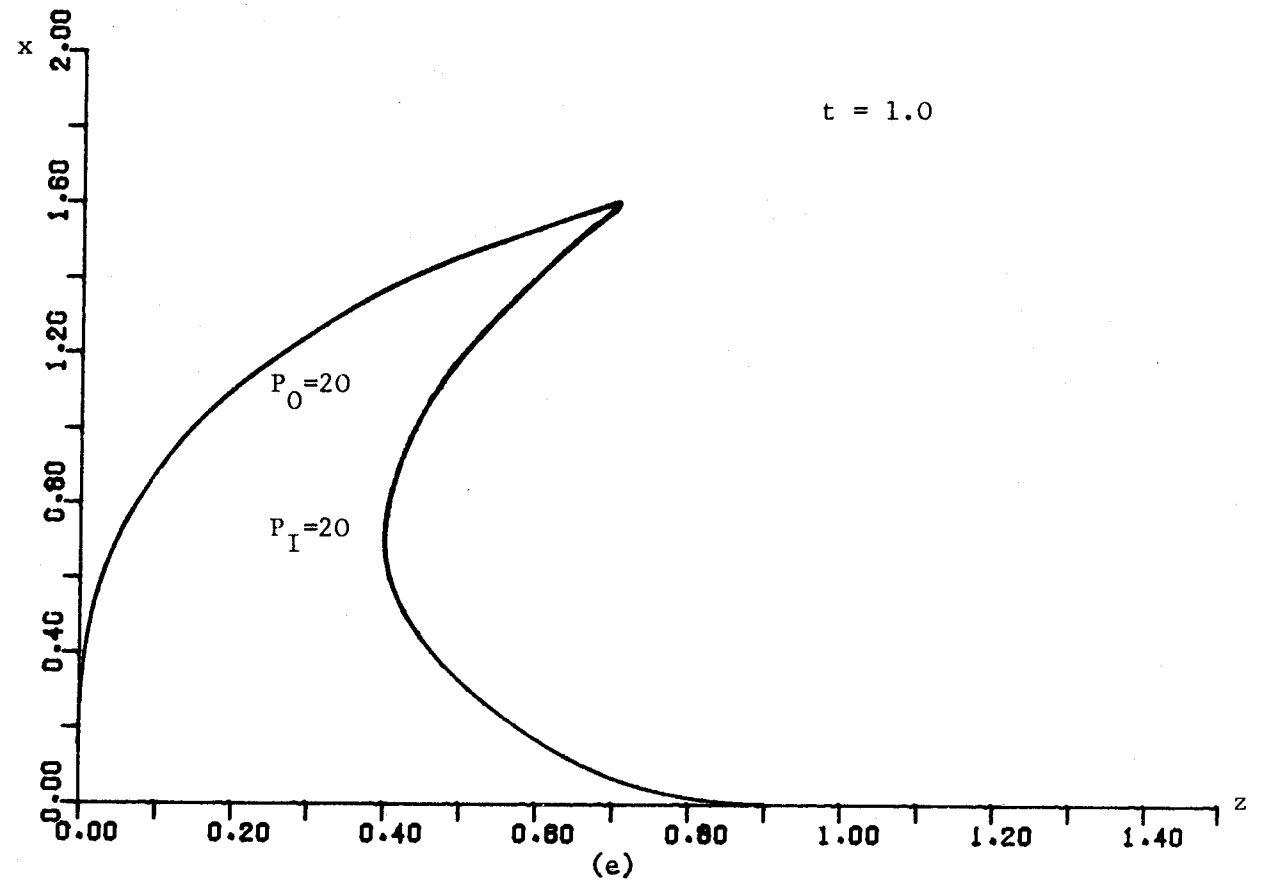

(e)

Figure 6.7 Effect of varying pressure ($P_O = P_I$) for case Br = 1.0, Pe = 0.5, h = 0.75, δ = 0.5

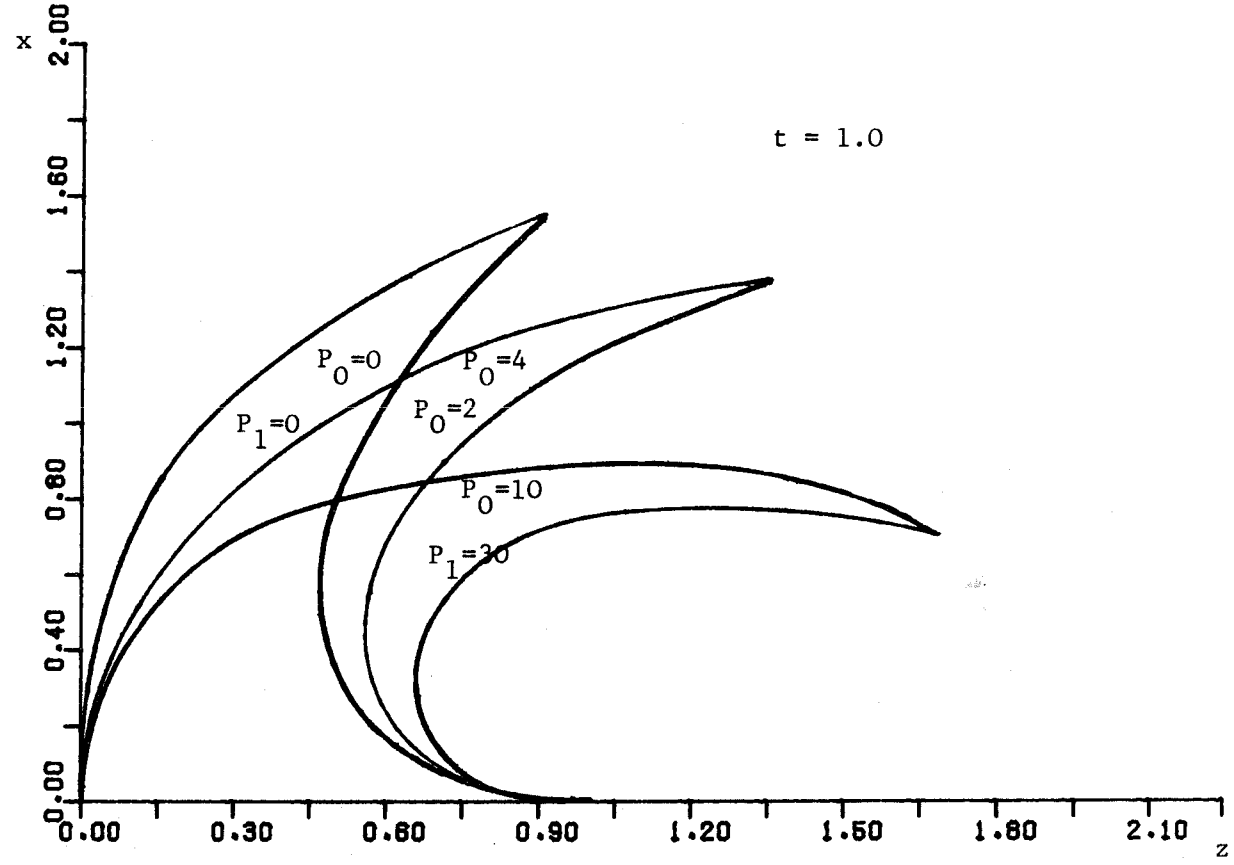

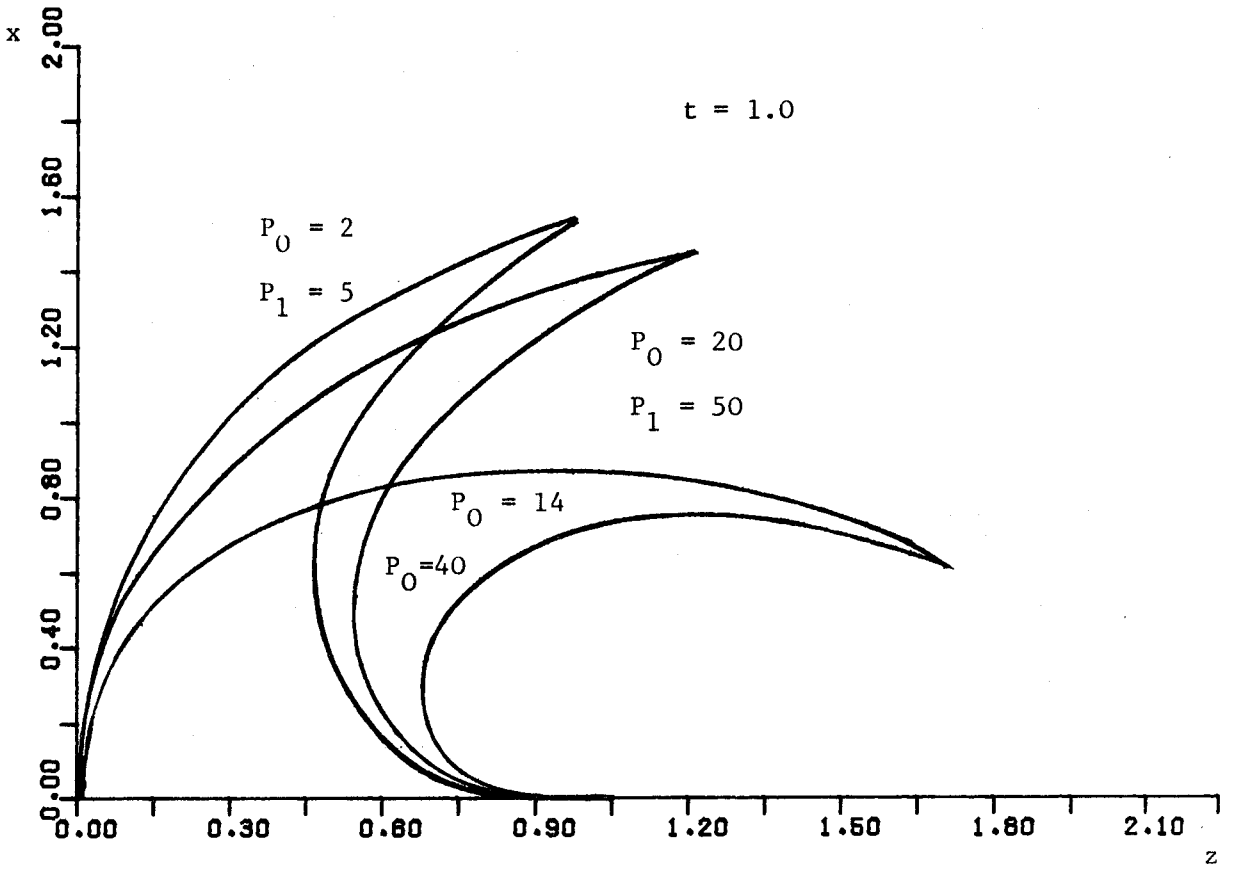

Figure 6.8 Effect of varying pressure ($P_0 \neq P_1$)

Br = 1.0, Pe = 0.5, h = 0.75, δ = 0.5.

which are necessary to calculate the second moments of area and hence p_0 and p_I. Results are presented in Figure 6.7 for the case $p_0 = p_I = p$ (say). It is easily seen from these results that varying p has little effect on the profiles, which unfortunately do not curl over as much as the collar shown in the photograph (Figure 6.9 . However by taking $p_I > p_0$ the results displayed in Figures 6.8 show that an increased curl can be achieved.

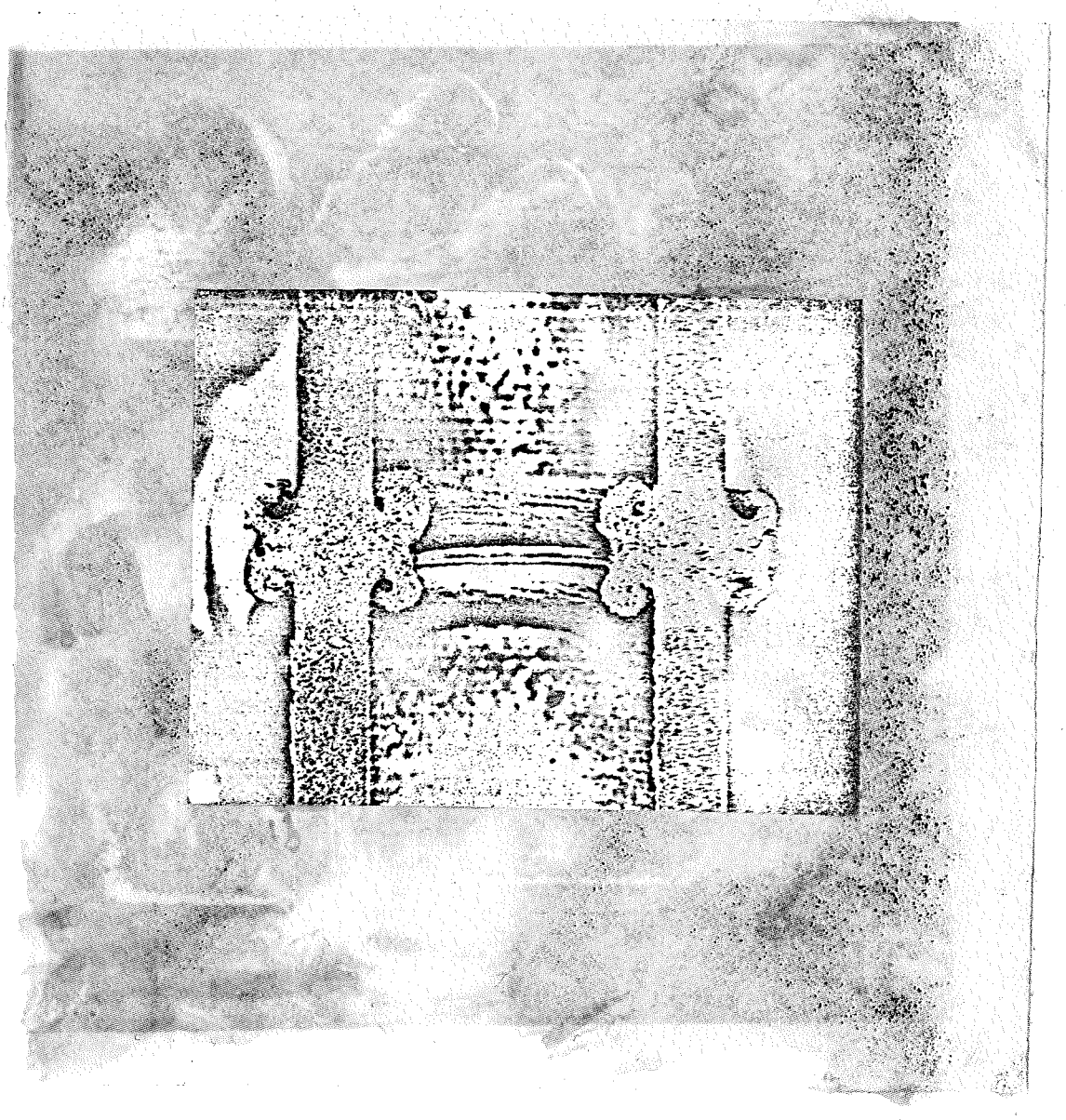

Figure 6.9 Cross-sectional view of a friction weld of a 1" diameter tube.

CHAPTER 7

CONCLUSIONS

Several models describing the frictioning stage of the friction welding process have been presented. Most attention has been focussed on phase II for which Atthey's model [22] was used as a basis. Atthey modelled the plasticised layer as a viscous fluid with constant viscosity and as a first extension to this model a series solution was developed to include the variation of viscosity with temperature. Qualitative agreement of torque traces with experimental results was observed with both these models for small times but for larger times the agreement was poorer and no equilibrium state was reached by either model. The reason for this behaviour was recognised to be the neglect of axial shortening and a solution to include the effect of the latter was subsequently developed. There was no analytical solution for the case of axial shortening and it was decided to employ the approximate heat balance integral method. With the inclusion of upset a steady state condition was achieved and the qualitative comparison of torque with experimental results was much improved. The accuracy of the heat balance integral method was assessed using a series solution valid for small times and also an exact steady state solution. For the special case $Pe = 0$ a comparison between the heat balance integral solution and the small time solution, which in this case is identical to Atthey's solution, showed the error to be less than 10% for Br in the range $0 - 10$. For non-zero Pe a comparison with the large time heat balance integral solution with the exact steady state solution revealed the error to be less than 10% for Br in the range $0 - 5$.

While z_p and τ possessed the right qualitative behaviour for small time, the interface temperature did not. This was felt to be a consequence of neglecting the conditioning phase. Without the inclusion of the conditioning phase the interface temperature actually assumed the value appropriate to $Pe = 0$ and then decayed with time to its equilibrium value, the rate of decay depending on Pe. With the conditioning phase included the interface temperature was initially the conditioning temperature and rapidly grew towards its steady state value as time increased.

Solutions were also obtained using the heat balance integral method for the case of various viscosity models. However, in all cases there was a value of the Brinkman number, Br_c, beyond which the interface temperature exceeded melting. However it was noticed when μ decreased with increasing temperature the value of Br_c was increased and it is suggested that a suitable viscosity model may be one which obeys the law given in [17] for temperatures below melting but falls rapidly to zero in the close proximity of melting, in which case interface melting should not be achieved.

A few of the simpler models had been repeated with the plasticised layer modelled as a Bingham substance. The algebra for the models is much more involved and the qualitative behaviour of the solutions does not have the agreement with experiment of the viscous fluid models, consequently the latter are felt to describe the friction welding process more aptly. In fact the most realistic model would be one incorporating the viscosity model described above and also including upset and the conditioning phase, and this could be examined in the future.

A model consistent with the viscous fluid model has been used to predict the shape of the material extruded from the plastic region. It was found that for certain variations of the hydrostatic pressure, within the extruded region, some quite good agreement between experimental observations and the theoretical predictions could be achieved.

Although extensive qualitative comparisons have been made there has been very little quantitative comparison of results with experiment. This matter could be pursued in the future but it is felt that a better knowledge of the behaviour of viscosity should be aquired beforehand.

APPENDIX

DERIVATION OF THE ELLIPTIC INTEGRALS IN CHAPTER 6

Consider the integral in equation (6.2.9) which we shall denote by I_1 and rewrite here for convenience

$$I_1 = \int_o^{\theta_o} \frac{d\theta_o}{\left[\mathrm{Cos}\alpha_o - \mathrm{Cos}(\alpha_o + \theta_{\ell o} - \theta_o)\right]^{\frac{1}{2}}} \quad . \qquad \text{(i)}$$

Changing the variable to ϕ_o through the equation

$$\mathrm{Cos}(\alpha_o + \theta_{\ell o} - \theta_o) = 2k_o^2 \mathrm{Sin}^2\phi_o - 1 \quad , \qquad \text{(ii)}$$

where k_o is defined by

$$2k_o^2 = 1 + \mathrm{Cos}\alpha_o \quad , \qquad \text{(iii)}$$

equation (i) can be expressed in the form

$$I_1 = \sqrt{2} \int_{\phi_{\ell o}}^{\phi_o} \frac{d\phi_o}{\sqrt{1 - k_o^2 \mathrm{Sin}^2\phi_o}} \quad , \qquad \text{(iv)}$$

where $\phi_{\ell o}$ is given by

$$\mathrm{Cos}(\alpha_o + \theta_{\ell o}) = 2k_o^2 \mathrm{Sin}^2\phi_{\ell o} - 1 \quad . \qquad \text{(v)}$$

Equation (iv) can be rewritten as

$$I_1 = \sqrt{2} \left[F(\phi_o, k_o) - F(\phi_{\ell o}, k_o)\right] \quad , \qquad \text{(vi)}$$

where F is the well known elliptic integral of the first kind and is defined by

$$F(u,k) = \int_{o}^{u} \frac{dV}{\sqrt{1-k^2 Sin^2 V}} \qquad \text{(vii)}$$

Let us now turn our attention to the integral in equation (6.2.28). We introduce I_2 defined by

$$I_2 = \int_{o}^{\theta_o} \frac{Sin\theta_o d\theta_o}{\left[Cos\alpha_o - Cos(\alpha_o + \theta_{\ell o} - \theta_o)\right]^{\frac{1}{2}}} .$$

It is convenient to make the change of variable given by

$$u = \alpha_o + \theta_{\ell o} - \theta_o \qquad \text{(ix)}$$

in which case I_2 can be expressed as

$$I_2 = \int_{\alpha_o+\theta_{\ell o}-\theta_o}^{\alpha_o+\theta_{\ell o}} \frac{Sin(\alpha_o+\theta_{\ell o}-u)du}{\left[Cos\alpha_o - Cosu\right]^{\frac{1}{2}}} . \qquad \text{(x)}$$

Expanding the numerator of the integral using the double angle formula we obtain

$$I_2 = J_1 Sin(\alpha_o+\theta_{\ell o}) - J_2 Cos(\alpha_o+\theta_{\ell o}) \qquad \text{(xi)}$$

where J_1 and J_2 are integrals defined by

$$J_1 = \int_{\alpha_o+\theta_{\ell o}-\theta_o}^{\alpha_o+\theta_{\ell o}} \frac{Cosu\ du}{\left[Cos\alpha_o - Cosu\right]^{\frac{1}{2}}} \qquad \text{(xii)}$$

and

$$J_2 = \int_{\alpha_o+\theta_{\ell o}-\theta_o}^{\alpha_o+\theta_{\ell o}} \frac{\mathrm{Sinu\ du}}{\left[\mathrm{Cos}\alpha_o - \mathrm{Cosu}\right]^{\frac{1}{2}}} \quad . \tag{xiii}$$

Introducing ϕ_o through the relation

$$\mathrm{Cosu} = 2k_o^2 \mathrm{Sin}^2\phi_o - 1 \ , \tag{xiv}$$

where k_o is given by (iii), equations (xii) and (xiii) become

$$J_1 = \sqrt{2} \left\{ \int_{\phi_{\ell o}}^{\phi_o} \frac{d\phi_o}{\sqrt{1-k_o^2\mathrm{Sin}^2\phi_o}} - 2 \int_{\phi_{\ell o}}^{\phi_o} \sqrt{1 - k_o^2\mathrm{Sin}^2\phi_o}\ d\phi_o \right\} \tag{xv}$$

and

$$J_2 = \sqrt{2} \int_{\phi_{\ell o}}^{\phi_o} 2k_o \mathrm{Sin}\phi_o d\phi_o \ . \tag{xvi}$$

Equation (xv) can be expressed in the form

$$J_1 = \sqrt{2} \left[F(\phi_o, k_o) - F(\phi_{\ell o}, k_o) - 2E(\phi_o, k_o) + 2E(\phi_{\ell o}, k_o) \right] \tag{xvii}$$

where E , the elliptic integral of the second kind [31], is defined by

$$E(u, k) = \int_o^u \sqrt{1-k^2\mathrm{Sin}^2 V}\ dV \ . \tag{xviii}$$

Equation (xvi) is readily integrated to yield

$$J_2 = 2\sqrt{2}\, k_o\left[\mathrm{Cos}\phi_{\ell o} - \mathrm{Cos}\phi_o\right] \quad . \tag{xix}$$

Using equation (v) it is easily deduced that

$$\mathrm{Sin}(\alpha_o+\theta_{\ell o}) = 2k_o\mathrm{Sin}\phi_{\ell o}\sqrt{1-k_o^2\mathrm{Sin}^2\phi_{\ell o}} \quad . \tag{xx}$$

Thus with the aid of (xi), (xvii), (xix), (v) and (xx) the integral I_2 can be expressed as

$$I_2 = 2\sqrt{2}\, k_o\mathrm{Sin}\phi_{\ell o}\sqrt{1-k_o^2\mathrm{Sin}^2\phi_{\ell o}}\left[F(\phi_o, k_o) - F(\phi_{\ell o}, k_o) - 2E(\phi_o,k_o) + 2E(\phi_{\ell o},k_o)\right] + 2\sqrt{2}\, k_o(2k_o^2\mathrm{Sin}^2\phi_{\ell o}-1)(\mathrm{Cos}\phi_o - \mathrm{Cos}\phi_{\ell o}) \quad . \tag{xxi}$$

We now treat the integral in equation (6.2.27) in a similar manner, we have

$$I_3 = \int_o^{\theta_o} \frac{\mathrm{Cos}\theta_o\, d\theta_o}{\left[\mathrm{Cos}\alpha_o - \mathrm{Cos}(\alpha_o+\theta_{\ell o}-\theta_o)\right]^{\frac{1}{2}}} \tag{xxii}$$

We again make the change of variable given by (ix) leading to

$$I_3 = \int_{\alpha_o+\theta_{\ell o}-\theta_o}^{\alpha_o+\theta_{\ell o}} \frac{\mathrm{Cos}(\alpha_o+\theta_{\ell o}-u)\,du}{\left[\mathrm{Cos}\alpha_o - \mathrm{Cos}u\right]^{\frac{1}{2}}} \tag{xxiii}$$

and on expanding the numerator of the integrand using the double angle formula we obtain

$$I_3 = J_1\mathrm{Cos}(\alpha_o+\theta_{\ell o}) + J_2\mathrm{Sin}(\alpha_o+\theta_{\ell o}) \quad , \tag{xxiv}$$

where the integral J_1 and J_2 have been defined by (xvii), (xix) respectively. With the aid of (xxiv), (xvii), (xx), (ix), (v) and (xx) the expression for I_3 becomes

$$I_3 = \sqrt{2}(2k_o^2\mathrm{Sin}^2\phi_{\ell o}-1)\left[F(\phi_o,k_o)-F(\phi_{\ell o},\, k_o) - 2E(\phi_o,\, k_o) + 2E(\phi_{\ell o},\, k_o)\right]$$

$$+ 4\sqrt{2}\, k_o^2\mathrm{Sin}\phi_{\ell o}\sqrt{1-k_o^2\mathrm{Sin}^2\phi_{\ell o}}\ (\mathrm{Cos}\phi_{\ell o}-\mathrm{Cos}\phi_o)$$

The integrals in equations (6.2.10), (6.2.29), (6.2.30) may be treated in exactly the same manner as the above and only the results are presented below

$$\int_{-\pi/2}^{\theta_I} \frac{d\theta_I}{\left[\mathrm{Cos}\alpha_I-\mathrm{Cos}(\alpha_I+\theta_{\ell I}-\theta_I\right]^{\frac{1}{2}}} \equiv \sqrt{2}\left[F(\theta_I,\, k_I) - F(\phi_{\ell I},\, k_I)\right] , \qquad \text{(xxvi)}$$

$$\int_{-\pi/2}^{\theta_I} \frac{\mathrm{Sin}\theta_I d\theta_I}{\left[\mathrm{Cos}\alpha_I-\mathrm{Cos}(\alpha_I+\theta_{\ell I}-\theta_I)\right]^{\frac{1}{2}}} \equiv \sqrt{2}(1-2k_I^2\mathrm{Sin}^2\phi_{\ell I})\left[F(\phi_I,\, k_I)\right.$$

$$\left. - F(\phi_{\ell I},\, k_I) - 2E(\phi_I,\, k_I) + 2E(\phi_{\ell I},\, k_I)\right] -$$

$$4\sqrt{2}\, k_I^2\mathrm{Sin}\phi_{\ell I}\sqrt{1-k_I^2\mathrm{Sin}^2\phi_{\ell I}}\ (\mathrm{Cos}\phi_{\ell I}-\mathrm{Cos}\phi_I)$$

(xxvii)

and

$$\int_{-\pi/2}^{\theta_I} \frac{\mathrm{Cos}\theta_I d\theta_I}{\left[\mathrm{Cos}\alpha_I-\mathrm{Cos}(\alpha_I+\theta_{\ell I}-\theta_I)\right]^{\frac{1}{2}}} \equiv 2\sqrt{2}\, k_I\mathrm{Sin}\phi_{\ell I}\sqrt{1-k_I^2\mathrm{Sin}^2\phi_{\ell I}}\left[F(\phi_I,k_I) -\right.$$

$$\left. F(\phi_{\ell I},k_I) - 2E(\phi_I,k_I) + 2E(\phi_{\ell I},k_I)\right] +$$

$$2\sqrt{2}\, k_I(1-2k_I^2\mathrm{Sin}^2\phi_{\ell I})(\mathrm{Cos}\phi_{\ell I}-\mathrm{Cos}\phi_I) .$$

(xxviii)

In the above ϕ_I is given by the equation

$$\mathrm{Cos}(\alpha_I+\theta_{\ell I}-\theta) = 2k_I^2\mathrm{Sin}^2\phi_I - 1 \qquad \text{(xxix)}$$

where k_I is defined by

$$\mathrm{Cos}\alpha_I = 2k_I^2 - 1 \qquad \text{(xxx)}$$

and ϕ_ℓ is given by

$$\mathrm{Sin}(\alpha_I+\theta_{\ell I}) = 1 - 2k_I^2\mathrm{Sin}^2\phi_{\ell I} \qquad \text{(xxxi)}$$

REFERENCES

1. V.I. VILL, 'Friction welding of metals', Reinhold Publishing Corporation, New York, 1962.

2. T.L. OBERLE, C.D. LLOYD and MR. CARLTON, 'Caterpillars Inertia Welding Process'.

3. C.R.G. ELLIS, 'Continuous Drive Friction Welding'.

4. F.D. DUFFIN and A.S. BAHRANI, 'The Mechanics of Friction Welding Mild Steel', Metal Construction, 1976, pp.267-271.

5. I.F. SQUIRES, 'Thermal and Mechanical Characteristics of Friction Welding Mild Steel', British Welding Journal, 1966, pp.652-657.

6. L.G. PETRUCCI, 'Temperature Distribution in Friction Welding', General Engineer', 1978, pp.179-185.

7. F.D. DUFFIN and A.S. BAHRANI, 'Frictional Behaviour of Mild Steel in Friction Welding', Wear, 1973, pp.53-74.

8. K.K. WANG and WEN LIN, 'Flywheel Friction Welding Research', Welding Journal, 1974, pp.233-s - 241 -s.

9. J. SEARLE, 'Friction Welding Non-circular Components Using Orbital Motion, Welding and Metal Fabrication', 1971, pp.294-297.

10. J. SEARLE, 'The Orbital Friction-welding Process for Non-circular Components', Engineers Digest, 1971, pp. 33-36.

11. A. ASTROP, 'Friction Welding Research Gathers Speed', Machinery and Production Engineering, 1979, pp.23-26.

12. T. RICH and R. ROBERTS, 'The Forge Phase of Friction Welding', Welding Journal, 1971, pp.137-s - 145-s.

13. N.N. RYKALIN et al., 'The Heating and Cooling of Rods Butt Welded by the Friction Process', Weld. Prod., 1959, pp.42-52.

14. V.I. VILL, 'Energy Distribution in the Friction Welding of Steel Bars', Weld. Prod., 1959, pp.31-41.

15. T. RICH and R. ROBERTS, 'Thermal Analysis for Basic Friction Welding', Metal Construction and British Welding Journal, 1971, pp.93-98.

16. Honeycombe, 'The Plastic Deformation of Metals', Arnold, 1968.

17. C.M. SELLARS and W.J. McG. TEGART, 'La relation entre la resistance et la structure dans la deformation a chaud', Mem. Sci. Rev. Met., LXII, 1966, pp.

18. A.J. BAHRANI et al., 'Analysis of Frictional Phenomena in Friction Welding of Mild Steel,' Wear, 1976, pp.265-278.

19. J.G. OLDROYD, 'A Rational Formulation of the Equations of Plastic Flow for a Bingham Solid', Proc. Camb. Phil. Soc., 1947, pp.100-105.

20. R. KUMAR and M.K. JAIN, 'Heat Transfer in Couette Flow of Bingham Material with Linearly Varying Wall Temperature', Journal of the Franklin Institute, 1967, pp.250-258.

21. N. CURLE and H.J. DAVIES, 'Modern Fluid Dynamics', Van Nastrand Reinhold, 1968.

22. D.R. ATTHEY, 'A Simple Thermal Analysis for Friction Welding', C.E.G.B. Electrical Research Memorandum No. 549, Job. No. IB 294. 1976

23. K.K. WANG and P. NAGAPPAN, 'Transient Temperature Distribution in Inertial Welding of Steels', Welding Journal, 1970, pp.419-s - 426 -s.

24. C.J. CHENG, 'Transient Temperature Distribution During Friction Welding of Two Similar Materials in Tubular Form', Welding Journal 1962, pp.542-s - 549-s.

25. A.S. GEL'DMAN and M.P. SANDER, 'Power and Heating in the Friction Welding of Thickwalled Steel Pipes', Weld. Prod., 1959, pp.53-61.

26. V.D. VOZNESENSKII, 'Power and Heat Parameters of Friction Welding', Weld Prod., 1959, pp.62-70.

27. H.S. CARSLAW and J.C. JAEGER', Conduction of Heat in Solids', Clarendon Press, 1947.

28. J.B. Hawkyard et.al., 'The Mean Dynamic Yield Strength of Copper and Low Carbon Steel at Elevated Temperatures from the Measurements of the 'mushrooming' of Flat Ended Projectiles', Int. Journ. Mech. Sci., 1968, pp.929-948.

29. V.P. VOINOV and A.F. VALIVOL, 'Friction Welding', National Lending Library for Science and Technology.

30. F.KREITH and W.Z. BLACK, 'Basic Heat Transfer', Harper and Row, 1980.

31. ABRAMOWITZ, and STEGUN, I.A. 1964. Handbook of Mathematical Functions. Washington : National Bureau of Standards.

32. RABINOWITZ, P. 'Numerical Methods for Non-Linear Algebraic Equations'. Gordon and Breach, 1970.

33. T.R. GOODMAN, 'The Heat Balance Integral and its Applications to Problems Involving a Change of Phase', Trans. A.S.M.E., 1958, pp.335-342.

34. W.J. DUNCAN, A.S. THOM and A.D. YOUNG, 'Mechanics of Fluids', Arnold, 1975.

35. R.J. GOULD , R.F. HOSKINS, J.A. MILNER and M.J. PRATT, 'Applicable Mathematics, Macmillan, 1973.

36. A.R. FORSYTH, 'A Treatise on Differential Equations', Macmillan and Co., 1951.

37. A.E.H. LOVE, 'A Treatise on the Mathematical Theory of Elasticity', Cambridge University Press, 1934.

38. F.D. DUFFIN and A.BAHRANI, 'Friction Welding of Mild Steel : the Effect of Varying the Value of Deceleration', Metal Construct., 1973 pp.125-132.